Biochemical studies to determine the role of Early Starvation 1 (ESV1) protein and its homologue Like-Early Starvation 1 (LESV) during starch degradation

---

Dissertation

zur Erlangung des akademischen Grades

"doctor rerum naturalium"

(Dr. rer. nat.)

in der Wissenschaftsdisziplin Biochemistry

eingereicht an der

Mathematisch-Naturwissenschaftlichen Fakultät

Institut für Biology/Biochemistry

der Universität Potsdam

von

Shadha Abduljaleel AL-Rawi

Potsdam. 2020

Main supervisor:	Prof Dr. habil. Joerg Fettke
Supervisors:	Prof. Dr. Alisdair Fernie
Reviewers:	Prof. Dr. Christophe D'Hulst Prof. Dr. Oluwatoyin A. Odeku

Published online on the
Publication Server of the University of Potsdam:
https://doi.org/10.25932/publishup- 48395
https://nbn-resolving.org/urn:nbn:de:kobv:517-opus4- 483956

Table of contents

Abstract

Depending on the biochemical and biotechnical approach, the aim of this work was to understand the mechanism of protein-glucan interactions in regulation and control of starch degradation. Although starch degradation starts with the phosphorylation process, the mechanisms by which this process is controlling and adjusting starch degradation are not yet fully understood. Phosphorylation is a major process performed by the two dikinases enzymes α-glucan, water dikinase (GWD) and phosphoglucan water dikinase (PWD). GWD and PWD enzymes phosphorylate the starch granule surface; thereby stimulate starch degradation by hydrolytic enzymes. Despite these important roles for GWD and PWD, so far the biochemical processes by which these enzymes are able to regulate and adjust the rate of phosphate incorporation into starch during the degradation process haven't been understood. Recently, some proteins were found associated with the starch granule. Two of these proteins are named Early Starvation Protein 1 (ESV1) and its homologue Like-Early Starvation Protein 1 (LESV). It was supposed that both are involved in the control of starch degradation, but their function has not been clearly known until now. To understand how ESV1 and LESV-glucan interactions are regulated and affect the starch breakdown, it was analyzed the influence of ESV1 and LESV proteins on the phosphorylating enzyme GWD and PWD and hydrolysing enzymes ISA, BAM, and AMY. However, the analysis determined the location of LESV and ESV1 in the chloroplast stroma of Arabidopsis. Mass spectrometry data predicted ESV1and LESV proteins as a product of the At1g42430 and At3g55760 genes with a predicted mass of ~50 kDa and ~66 kDa, respectively. The ChloroP program predicted that ESV1 lacks the chloroplast transit peptide, but it predicted the first 56 amino acids N-terminal region as a chloroplast transit peptide for LESV. Usually, the transit peptide is processed during transport of the proteins into plastids. Given that this processing is critical, two forms of each ESV1 and LESV were generated and purified, a full-length form and a truncated form that lacks the transit peptide, namely, (ESV1and tESV1) and (LESV and tLESV), respectively. Both protein forms were included in the analysis assays, but only slight differences in glucan binding and protein action between ESV1 and tESV1 were observed, while no differences in the glucan binding and effect on the GWD and PWD action were observed between LESV and tLESV. The results revealed that the presence of the N-terminal is not massively altering the action of ESV1 or LESV. Therefore, it was only used the ESV1 and tLESV forms data to explain the function of both proteins.

However, the analysis of the results revealed that LESV and ESV1 proteins bind strongly at the starch granule surface. Furthermore, not all of both proteins were released after their incubation with starches after washing the granules with 2% [w/v] SDS indicates to their binding to the deeper layers of the granule surface. Supporting of this finding comes after the binding of both proteins to starches after removing the free glucans chains from the surface by the action of ISA and BAM. Although both proteins are capable of binding to the starch structure, only LESV showed binding to amylose, while in ESV1, binding was not observed. The alteration of glucan structures at the starch granule surface is essential for the incorporation of phosphate into starch granule while the phosphorylation of starch by GWD and PWD increased after removing the free glucan chains by ISA. Furthermore, PWD showed the possibility of starch phosphorylation without prephosphorylation by GWD.

Biochemical studies on protein-glucan interactions between LESV or ESV1 with different types of starch showed a potentially important mechanism of regulating and adjusting the phosphorylation process while the binding of LESV and ESV1 leads to altering the glucan structures of starches, hence, render the effect of the action of dikinases enzymes (GWD and PWD) more able to control the rate of starch degradation. Despite the presence of ESV1 which revealed an antagonistic effect on the PWD action as the PWD action was decreased without prephosphorylation by GWD and increased after prephosphorylation by GWD (Chapter 4), PWD showed a significant reduction in its action with or without prephosphorylation by GWD in the presence of ESV1 whether separately or together with LESV (Chapter 5). However, the presence of LESV and ESV1 together revealed the same effect compared to the effect of each one alone on the phosphorylation process, therefore it is difficult to distinguish the specific function between them. However, non-interactions were detected between LESV and ESV1 or between each of them with GWD and PWD or between GWD and PWD indicating the independent work for these proteins. It was also observed that the alteration of the starch structure by LESV and ESV1 plays a role in adjusting starch degradation rates not only by affecting the dikinases but also by affecting some of the hydrolysing enzymes since it was found that the presence of LESV and ESV1leads to the reduction of the action of BAM, but does not abolish it.

Zusammenfassung

Ziel dieser Arbeit war es, den Mechanismus der Protein-Glucan-Wechselwirkungen bei der Regulation und Kontrolle des Stärkeabbaus zu verstehen. Der Stärkeabbau beginnt mit dem Phosphorylierungsprozess, der von den beiden Dikinasen, der α-Glucan, Wasserdikinase (GWD) und der Phosphoglucanwasserdikinase (PWD) durchgeführt wird. Kürzlich wurden einige Proteine gefunden, die mit dem Stärkegranulum assoziiert sind. Zwei dieser Proteine heißen Early Starvation 1 (ESV1) und das Homolog Like-Early Starvation (LESV), Es wurde vorgeschlagen, dass beide an der Kontrolle des Stärkeabbaus beteiligt sind, aber ihre Funktion ist bisher nicht bekannt.

Um zu verstehen, wie ESV1- und LESV-Glucan-Wechselwirkungen reguliert werden und den Stärkeabbau beeinflussen, wurde der Einfluss der beiden Proteine auf die Phosphorylierungsenzyme GWD und PWD, sowie die Hydrolasen isoamylase, beta-amylase, und alpha-amylase ntersucht. Dabei ergab die Analyse, dass LESV und ESV1 nicht nur stark an der Oberfläche, sondern auch in den tieferen Schichten der Stärkegranula binden. Obwohl beide Proteine in der Lage sind, an die Stärkestruktur zu binden, zeigte nur LESV eine Bindung an Amylose, während für ESV1 keine Bindung beobachtet werden konnte.

Die Veränderung der Glucanstrukturen an der Oberfläche der Stärkekörner ist für den Einbau von Phosphat wesentlich, so nahm beispielsweise die Phosphorylierung der Stärke durch GWD und PWD nach Entfernung der freien Glucanketten mittels ISA zu. Darüber hinaus konnte ebenso gezeigt werden, dass PWD auch ohne eine Präphosphorylierung durch GWD die Glucosyleinheiten innerhalb der Stärke phosphorylieren kann. Die Bindung von LESV und ESV1 führt zu einer Veränderung der Glucanstrukturen von Stärken, wodurch die Aktivität der Dikinasen (GWD und PWD) und somit die Geschwindigkeit des Stärkeabbaus wahrscheinlich besser gesteuert werden kann. Es wurden keine Wechselwirkungen zwischen LESV und ESV1 oder zwischen jedem von ihnen mit GWD und PWD oder zwischen GWD und PWD festgestellt, was auf die unabhängige Arbeit von diesen Proteinen hinweist. Es wurde auch beobachtet, dass die Modifikation der Stärkestruktur durch LESV und ESV1 eine Rolle bei der Anpassung der Stärkeabbauraten spielt, nicht nur durch Beeinflussung der Dikinasen, sondern auch durch die Beeinflussung einiger hydrolysierender Enzyme wie BAM. Den

so zeigte die Amylase eine eindeutige Reduktion ihrer katalytischen Wirkung in Präsenz von LESV und ESV1.

Daraus resumierend kann davon ausgegangen werden, dass die beiden Proteine ESV1 und LESV für die Feinregulation des Stärkeabbaus von höchster Relevanz sind.

Acknowledgement

Obtaining a PhD was not an easy goal. I am blessed to be surrounded by an inspiring person who has played a huge role in achieving this. My husband, *Mohammed* you have always encouraged me to do my best in everything, stood behind me and given me the confidence to achieve this, thank you. My daughters, *Rania, Deema, and Lara*; I hope I have made you proud. Thanks to my brother-in-law, *Jamal* for the supporting and helping in submitting all the requirements regarding the extension of my scholarship in my country, Iraq.

I would like to express my sincere appreciation to my supervisor Prof. Dr. *Joerg Fettke* for his invaluable advice, direction and supporting me during my PhD study.

I would like to thank the former members of Biopolymer Analytics Group; Dr. *Irina Malinova* and Dr. *Henrike Brust* who helped and provided me with their assistance to learn the lab techniques. Their help has been important for the starting of my PhD study as a member of the group.

I would like to thank reviewers for taking the time and effort necessary to review my thesis, especially, to Prof. Dr. *Oluwatoyin A. Odeku*. I sincerely appreciate all her valuable comments which helped me to improve my thesis.

I also would like to thank my colleagues who have provided valuable results towards my thesis; *Harendra Mahto* and *Julia Compart* for the working in the isotope laboratory and *Junio Flores Castellanos* for the helping in the analysis of LESV protein by MALDI-TOF.

Many thank also to other my colleagues in the Biopolymer Analytics Group; *Hadeel Mohammed Qasim, Abubakar Musa Ahmad, Xiaoping Li, Aakanksha Singh, Ardha Apriyanto, Qingting Liu, Sarah Mielke,* and the best friend *Sidratul Nur Muntaha* for their friendship and many happy times. I will always remember the precious time I spent with you.

I wish to thank all of the members of AG plant physiology, especially, to Dr. *Anke Koch*, for the work safety advice in laboratories and allowing me to use all her devices.

Thank you, *Kerstin Pusch* and *Carola Kuhn* for the assisting in general matters like sterilized of culture media, water, tips, and the waste of bacteria.

List of Figures

List of Tables

Abbreviation

AD	Activation domain
ADP-Glc	Adenine diphosphate glucose
AGPase	ADP-glucose pyrophosphorylase
AMY	Alpha-amylase
ATP	Adenosine triphosphate
ATPS	1, Aminopyrene-3,6,8-trisulfonic acid
BCA	Bicinchoninic acid/copper
BE	Branching enzyme
BMY	Beta-amylase
Bp	Base pairs
BSA	Bovine serum albumin
CBM	carbohydrate-binding domains
cDNA	Complementary DNA
CELIF	Capillary electrophoresis -laser-induced fluorescence
Col-0	Columbia-0
CTS	Chloroplast transit peptide
D.P	Degree of polymerisation
DBD	DNA-binding domain
DBE	Debranching enzymes
DMF	Dimethylformamide
DNA	Deoxyribonucleic acid
DPE1	Disproportionating enzyme1
DTSSP	3,3'- dithiobid(sulfosuccinimidyl propionate)
DTT	DithiothreitolEDTA Ethylenediaminetetraacetic acid
ESV1	Early Starvation 1
Fig	Figure
Fru-6P	Fructose-6-phosphate
G-1-P	Glucose-1-phosphate
GBSS	Granule-bound starch synthase
GH13	Glycoside hydrolase family 13
GN	Glycogenin
GS	Glycogen synthase
GT5	Glycosyltransferase family 5
GWD	Glucan-water dikinase
HEPES	4-(2-hydroxyethyl)-1-piperazineethanesulfonic acid
IPTG	Isopropyl β-D-1-thiogalactopyranoside
ISA	Isoamylases
kDa	Kilo Dalton
LB	Luria-Bertani

LDA	Limit-dextrinase
LESV	Like-Early Starvation 1
LS	Large subunits
LSF	Like starch excess four
MALDI-TOF	Matrix-Assisted Laser Desorption Ionization-Time-Of-Flight
MES	2-(N-morpholino) ethanesulfonic acid
min	Minutes
MEX1	Maltose excess 1
NTP	Nucleotide triphosphate
OD	Optical densit
PAGE	Polyacrylamide gel electrophoresis
PCR	Polymerase chain reaction
PGI	Phosphoglucoisomerase
pGlcT	Glucose translocator
PGM	Phosphoglucomutase
PHS1	Plastidial phosphorylase enzyme
PII1	PROTEIN INVOLVED IN STARCH INITIATION
PMSF	Phenylmethylsulfonyl fluoride
POFs	Proteins with obscure features
PTP	Protein tyrosine phosphatase
PTST	PROTEIN TARGETING TO STARCH
PUFs	Proteins with unknown functions
PUI	Pullulanase
PVDF	Polyvinylidene fluorid
PWD	Phosphoglycan, water dikinase
SBD	Starch binding domain
SDS	Sodium dodecyl sulphate
SOC	Super optimal broth
SS	Small subunits
SSs	Starch Synthases
SSV	Starch synthase 6
tLESV	Like Early Starvation 1 without transit peptide
TEMED	Tetramethylethylenediamine
TFA	Trifluoroacetic acid
UDP-Glc	Dinucleotides uridine diphosphate glucose
V/V	Volume/volume
W/V	Weight/volume
WT	Wild-type

YTH	Yeast two-hybrid

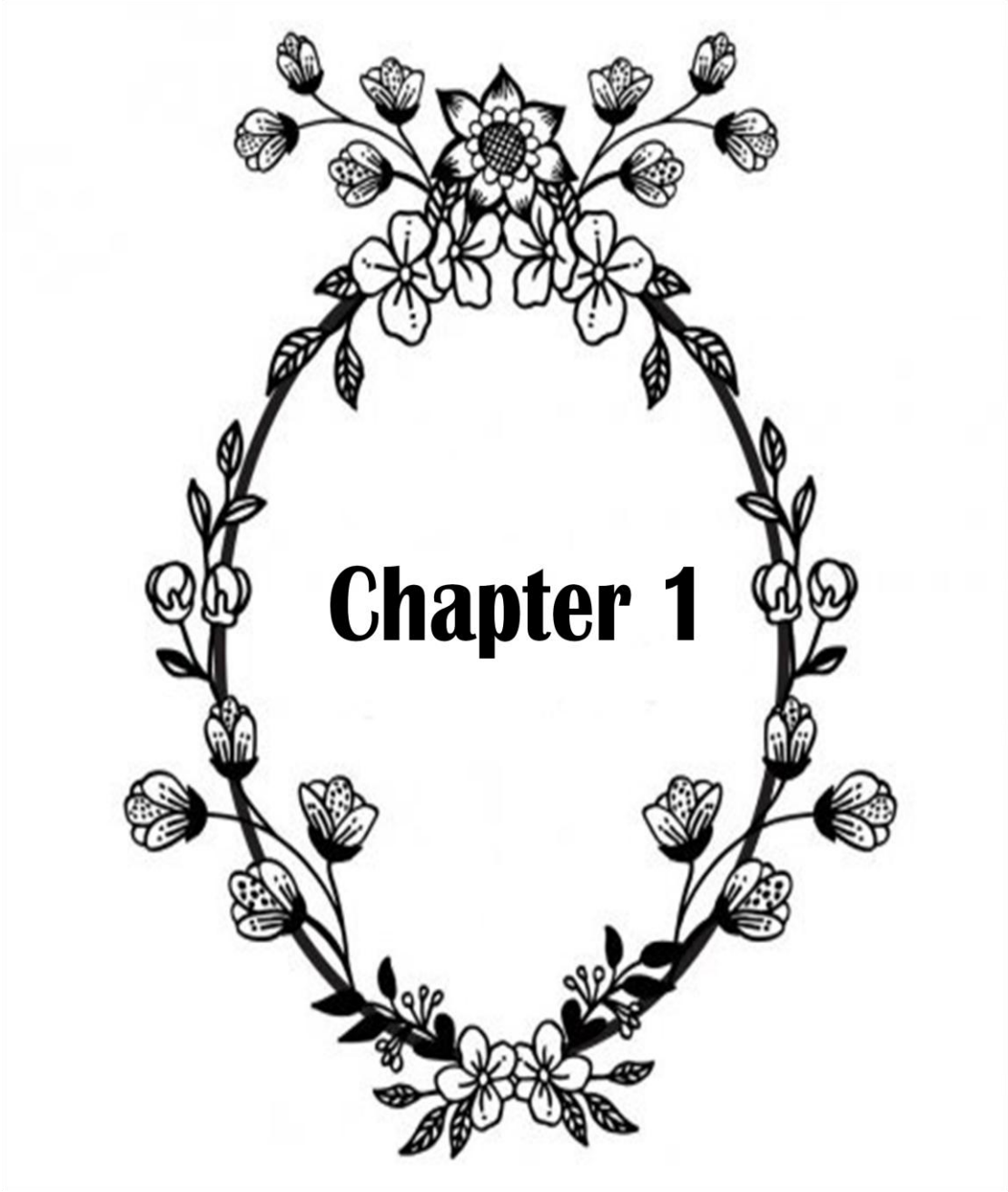
Chapter 1

1. Introduction

1.1 Carbohydrates

Along with the four main classes of biomolecules proteins, nucleic acids, lipids, and vitamins, carbohydrates are an important class of biomolecules. They are considered significant to many essential metabolic pathways in the living cells (Maughan, 2009). Chemically, carbohydrates are organic molecules consisting of carbon (C), hydrogen (H) and oxygen (O) atoms bonding together in the ratio: Cx(H2O)y. Where it depends on the numbers of *x* and *y*, the carbohydrate will be specified.

There are four important types of complex carbohydrates. Starch and glycogen serve for the storage of energy in plant and animal cells, respectively, and cellulose and chitin as structural components in plants and arthropods, respectively. Both starch and glycogen are chemically similar; they have been described as branched homoglycans including α-D glucosyl residues. However, they have two types of glycosidic bonds, α 1, 4 linked backbones and α 1, 6 linked branches. However, starch has two types of polymer. Amylose is strictly linear and water-soluble and amylopectin is highly branched and water-insoluble whereas glycogen is more similar to amylopectin. It has short and highly branched chains and soluble in the small extent.

1.2 Classification of carbohydrates

Carbohydrates are very diverse molecules and can be categorized according to the degree of polymerisation into monosaccharides (monomers), disaccharides, oligosaccharides, and polysaccharides. The simple type of carbohydrates is the monosaccharides, also called simple sugars, which have several hydroxyl groups and a carbonyl group.

1.2.1 Monosaccharides

Monosaccharides are essential metabolites widely distributed in the living cells such as glucose, fructose, and galactose (Fig. 1.1). Furthermore, ribose and deoxyribose are also considered one of the most important monosaccharides and are found in the backbone structure of RNA and DNA, respectively.

Glucose is one of the most important monosaccharides in the living cells. Both prokaryotes and eukaryotes use glucose as a source of energy in addition to its role as a metabolic intermediate. However, glucose-1-phosphate (G-1-P) is one of the most important molecules, which acts as the glycosyl donor. *In vitro* studies have found that G-

1-P can be converted to starch while acts as glycosyl donor to native starch granule (Fettke et al., 2010). Additionally, the dinucleotides uridine diphosphate glucose (UDP-Glc) and adenine diphosphate glucose (ADP-Glc) rely on G-1-P as glucosyl donor or as a substrate for their synthesis. On the other hand, it was reported that UDP-Glc plays an important role as a substrate for the synthesis of cell wall polysaccharides as the donor for glucose residue (Reiter, 2002; Verbancic et al., 2018). Whereas, ADP-Glc have a role in the synthesis of storage polysaccharides, glycogen and starch, as glucosyl donor for the elongation of α 1, 4 glucosidic chains (Ballicora et al., 2004).

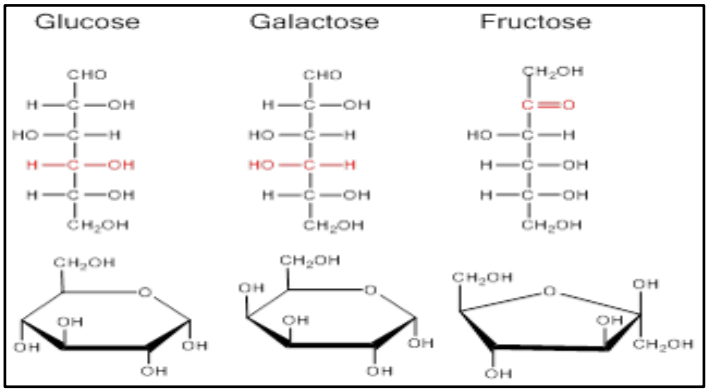

Fig.1.1: Linear and ring structures of three common monosaccharides isomers. All have the same molecular formula ($C_6H_{12}O_6$). *https://content.byui.edu/.*

1.2.2 Disaccharides

Disaccharides are sugars composed of two monosaccharides (simple sugars) that are joined by glycosidic linkage. The most common types of disaccharides are sucrose (a dimer of glucose and fructose) which is formed with a α 1, 2 glycosidic bond between carbon 1 of D-glucopyranose and carbon 2 of D-fructofuranose, maltose (a dimer of two glucose units) and is formed with a α 1, 4 glycosidic bond between carbons 1 (the anomeric carbon) and 4 of two D-glucopyranose molecules and lactose (a dimer of glucose and galactose) which is formed by connecting carbon 1 of D-galactopyranose (D-galactose) and carbon 4 of D-glucopyranose (D-glucose) with a β 1, 4 glycosidic bond (Fig. 1.2).

In plants, sucrose is the most important product of photosynthesis. It can be temporarily stored in leaves and is transported from leaves to sink tissues that do not produce this sugar (Ruan, 2014). It, in general, plays an essential role in the regulation of important metabolic processes (Tognett et al., 2013). For instance, it is considered as the main

respiratory and growth substrate (Bianco and Rieger, 2002). Furthermore, it plays pivotal roles as signalling molecules in regulated plant growth and gene expression (Loreti et al., 2005; Dahiya et al., 2017). However, the sucrose-induced expression has been reported for genes encoding UDP-glucose pyrophosphorylase (Ciereszko et al., 2001) and several anthocyanin biosynthetic genes (Solfanelli et al., 2006).

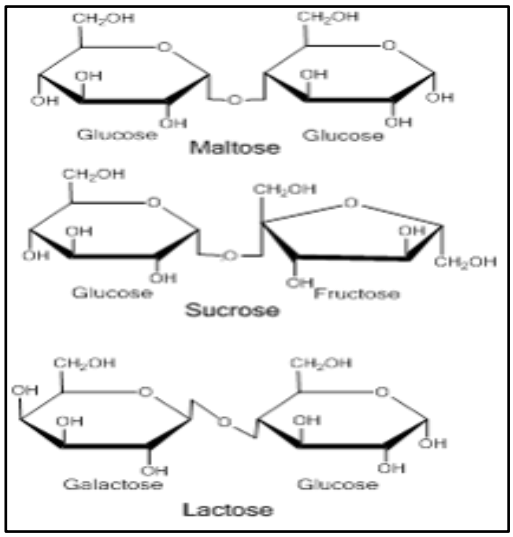

Fig.1.2: The common examples of disaccharides are maltose, sucrose, and lactose. They have the same chemical formula, $C_{12}H_{22}O_{11}$, but different structures. Lactose and maltose are reducing disaccharides, in which one monosaccharide, which is the reducing sugar of the pair, still has a free hemiacetal unit that can act as a reducing aldehyde group; Sucrose is a non-reducing disaccharide, in which the component monosaccharides bond through an acetal linkage between their anomeric centres. *https://content.byui.edu/.*

1.2.3 Oligosaccharides

Oligosaccharides are a saccharide polymer containing a small number typically (2 to 10) of monosaccharide units (the number of monosaccharide units is termed degree of polymerization or D.P) linked together with glycosidic bonds (Ibrahim, 2018). *In vivo*, oligosaccharides result from the breakdown of larger polysaccharides such as starch or cellulose or they are gradually synthesis from monosaccharides. Further, the cell wall polysaccharides of plant and microbes are considered as other sources for oligosaccharides. However, there is evidence that oligosaccharides are important regulatory molecules in which plants utilize the structural complexity of oligosaccharides to regulate important physiological processes that may help plants to resist e.g. diseases, effects on growth and development, and work as substrates for specific plant enzymes (Darvill et al., 1992; Fry et

al., 1993). Furthermore, oligosaccharides have many other functions like cell recognition and cell binding (Hayen et al., 2018; Xiao et al., 2019).

1.2.4 Polysaccharides

They range in structure from linear to highly branched (Fig. 1.3). Their sizes vary from 100 to 1,000,000 monosaccharide units, giving a different molecular weight between 16-16,000 kDa (Robyt, 2012). However, there are two types of polysaccharides. The first one consists of only one kind of monosaccharide is called homopolysaccharides (homoglycans) such as amylose, amylopectin and glycogen. The second type is called heteropolysaccharides (heteroglycans) contains two or more different monomeric units which can be both straight and branched chains. In general, polysaccharides exist in massive structural diversity as they are produced by a variety of species, including microbes, algae, plants, and animals (Posocco et al., 2015). For instance, they are found in the cell wall structure of almost all plants and in mammalian connective tissues (Meyer, 1969; Voragen et al., 2009; Espinoza et al., 2018).

However, most polysaccharides can also be classified according to their biological roles into storage polysaccharides like starch and glycogen and structural polysaccharides like cellulose and chitin.

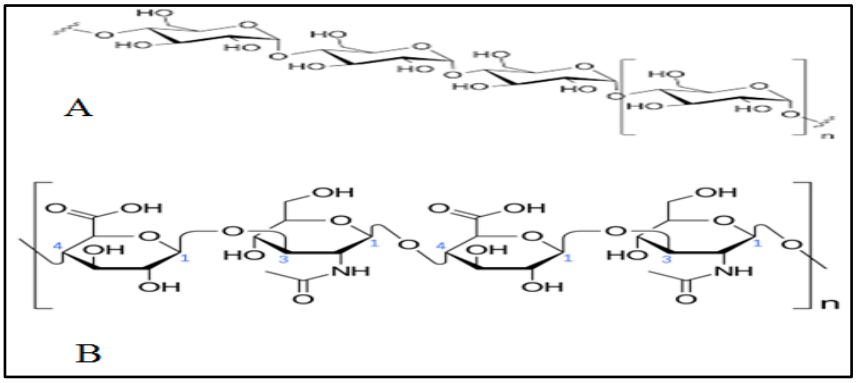

Fig.1.3: Chemical structure of polysaccharide. A: example for homoglycans: Amylose is a linear polymer composed of a long chain of glucose linked with α 1, 4 glycosidic bonds. B: example for heteroglycans: hyaluronan is an anionic, nonsulfatedglycosaminoglycan distributed widely throughout animal connective tissue. It is a polymer consisting of D-glucuronic acid and *N*-acetyl-D-glucosamine linked via alternating β1, 4 and β1, 3 glycosidic bonds. *https://en.wikipedia.org/wiki/Polysaccharide.*1.3 Starch and glycogen are the two important storage biopolymers in nature

1.3 Starch and glycogen are the two important storage biopolymers in nature

1.3.1 Glycogen

Glycogen is a branched storage polysaccharide. It exists in organisms, starting from bacteria and archaea to the higher organisms such as yeast, animals, and humans (Ball and Morell, 2003; Wilson et al., 2010; Adeva-Andany et al., 2016). Glycogen is a polymer of α 1, 4 linking glucose units having branching points with α 1, 6 glycosidic linkages occurring nearly every one in ten residues (Roach, 2002) (Fig. 1.4). Glycogen polymers are synthesised initially through the action of Glycogenin (GN) enzyme with the cooperative action of glycogen synthase (GS), and glycogen branching enzyme (Hurley, 2006; Zeqiraj et al., 2014). Glycogenin (GN) enzyme, a homodimer, has a tyrosine 194 (Tyr194) residue on each subunit. It uses UDP-glucose as a donor to transfer glucosyl residues either directly to Tyr194 or to glucose residues already attached to Tyr194 by autoglycosylation process to produce a polymer containing at least four glucose units linked by α 1, 4 glycosidic bound (Lin et al., 1999; Gibbons et al., 2002; Chaikuad et al., 2011). Once an oligosaccharide chain of glucosyl monomers is formed as glycan primer, it will elongate by glycogen synthase, but only when glycogenin and glycogen synthase are complexed together. However, during the synthesis of a glycogen molecule, glycogen synthase will dissociate from glycogenin to enable glycogen molecules to grow and reach their size (Smythe and Cohen 1991). After that, glycogen branching enzyme makes branches by transferring the end of the chain to make a α1, 6 position branch points within the same or neighbouring glucan chain in glycogen (Wang et al., 2015).

On the other hand, glycogen polymer breakdown is catalyzed by the coordinated action of two enzymes, glycogen phosphorylase and glycogen debranching enzyme. Glycogen phosphorylase releases glucose 1- phosphate from a linear glucan chain, but his action is blocked when it reaches to the last four glucosyl residues from glucan branch point. Therefore, the activity of the glycogen debranching enzyme is required, to complete the degradation and release the branch points (Burwinkel, 1998; Alonso-Casajús et al., 2006; Adeva-Andany et al., 2016). For instance, in humans, glycogen is predominantly stored in the liver which supplies glucose to the bloodstream during fasting periods. It is also stored in skeletal muscle which later provides glucose to the muscle fibres during muscle

contraction. Furthermore, it can be found in other human tissues such as the brain, heart, kidney, adipose tissue, and erythrocytes (Roach et al., 2012).

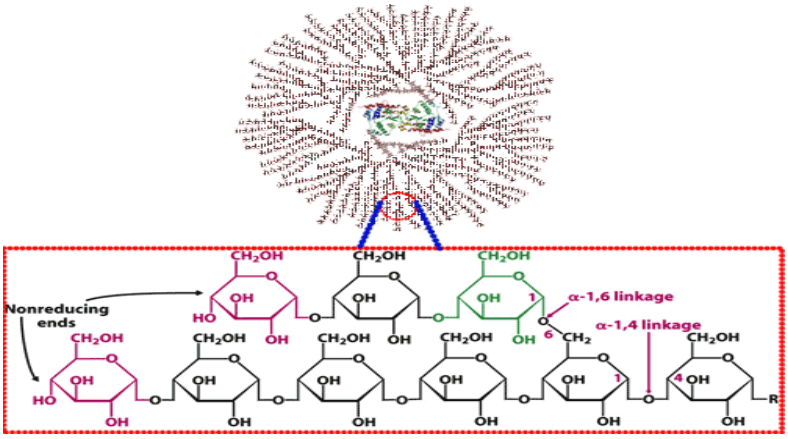

Fig.1.4: The general structure of glycogen. The linear structure is a part of a glycogen molecule; the glucose units are joined by 1, 4 glycosidic bonds and at the branching point, by α 1, 6 glycosidic bond. *https://teaching.ncl.ac.uk/*

1.3.2 Starch

Starch is an insoluble granule (Fig. 1.5). It consists of two types of glucose polymers which are amylopectin and amylose (Fig. 1.6). Both polymers are made of α 1, 4 linked glucan chains connected with a highly α 1, 6 branch point in amylopectin, compared with amylose which is slightly branched (Bertoft, 2017). It is synthesized by plants and algae. The review by Tetlow (2018) showed that starch plays a central role in human nutrition. However, there are two forms of starch synthesis in plants: transitory starch which is synthesized in the leaves directly from photosynthesis during the day and degraded in the night to produce energy in the absence of photosynthesis, and storage starch which is stored for longer periods in non-photosynthetic tissues, like seeds, stems, roots, or tubers. However, most of the starch contains about 70–80% amylopectin and 20– 30% amylose (Pe´rez and Bertof, 2010). Nevertheless, starch granules have a less organized area at their organic centre. This area is considered the starting point of starch biosynthesis, known as hilum. Therefore, the clustered branches of amylopectin chains lead to the synthesis of the double-helical semi-crystalline domains of the starch granules and rather amorphous regions (Jenkins et al., 1993; Jane et al., 2003) (Fig. 1.7). On the other hand, the distribution of branching points of amylopectin in a discontinuous manner leads to form the lamellar structure of the starch granules. It was thought that the linear chains of amylose spread randomly within the lamellar structure of amylopectin. However, the

formation of a mature starch granule occurs in the plastid under the effect of a series of enzymes synthesis activities (Zeeman et al., 2002).

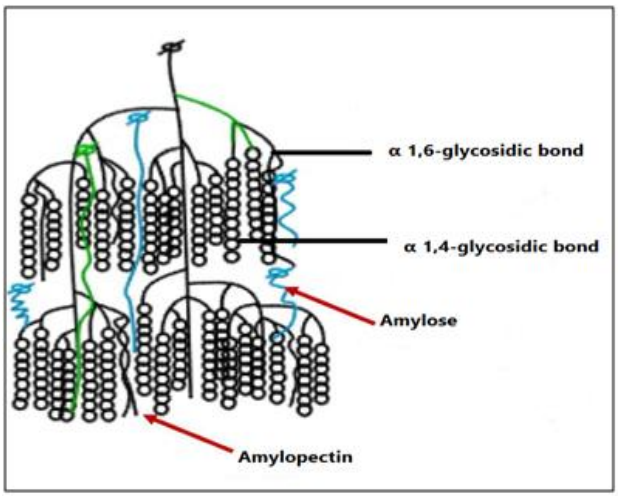

Fig.1.5: The general structure of starch. The linear structure is a part of a starch molecule; the glucose units are joined by α 1, 4 glycosidic bonds and at the branching point, by α 1, 6 glycosidic bonds, modified from (Liu et al., 2019).

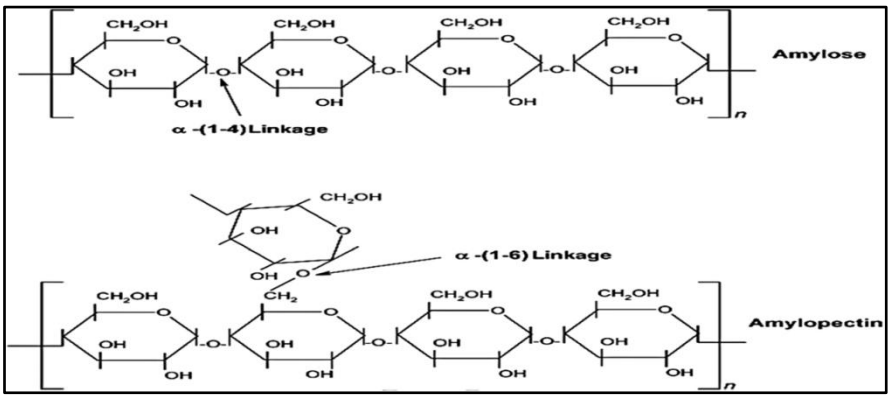

Fig.1.6: The linear structure of amylose and amylopectin. Amylose is composed of mostly linear chains of D-glucose in α 1, 4 glycosidic linkages. The linear linkages in amylopectin are α 1, 4, whereas the branch linkages are α 1, 6 glycosidic bonds (Mohammadinejad et al., 2016).

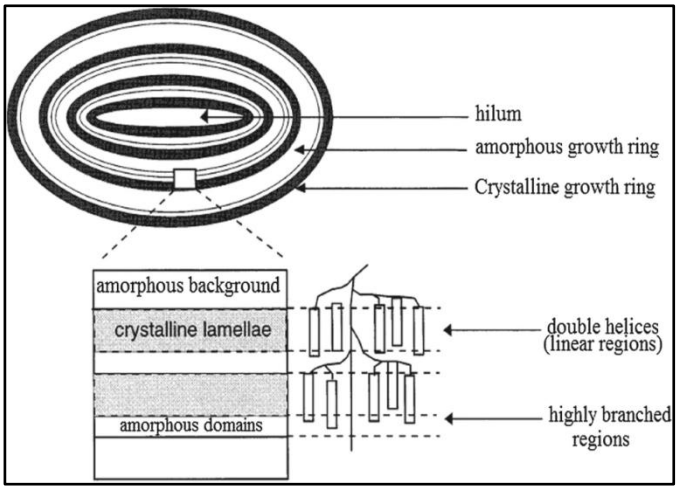

Fig.1.7: The whole starch granule structure: hilum, lamellae, and poly chains (Fasahat et al., 2014).

1.4 Starch synthesis

So far, four classes of starch metabolising enzymes are known to have main roles in starch granule synthesis:

1.4.1 Adenosine 5, diphosphate glucose pyrophosphorylase (AGPase) E.C. 2.7.7.27

Synthesis of transitory starch occur using ADP-glucose as a substrate for elongation of the non-reducing ends of glucan chain in chloroplasts during the day. The supply of ADP-glucose is catalyzed by the activity of ADP-glucose pyrophosphorylase (AGPase) (E.C 2.7.7.27) which is known as heterotetramer, two large subunits (LS) or (AGPS, 51 kDa) considered as the regulatory subunit and two small subunits (SS) or (AGPB, 50 kDa) regarded as the catalytic subunits (Okita et al., 1990; Batra et al., 2017). In chloroplasts, the generation of ADP-glucose is directly linked to the Calvin-Benson cycle by utilising the intermediate fructose-6-phosphate (Fru-6P). Fru-6P is catalysed by a series of reversible reactions of plastidial enzymes. Phosphoglucoisomerase (PGI) converts it to Glc-6P and phosphoglucomutase (PGM) converts the latter into glucose-1-phosphate (Glc-1P) (Yu et al., 2000). However, AGPase converts Glc-1P and ATP to ADP-glucose and pyrophosphate (PPi) (Emes and Neuhaus, 1997). Further, the PPi product will hydrolyse by plastidial alkaline pyrophosphatase to release two molecules of orthophosphate Pi (George et al., 2010). The formation of ADP-glucose is used as a substrate for the starch synthases E.C. 2.4.1.21 (GBSS and SSs) which binds glucose moieties to create the amylose and amylopectin (Smith et al., 1997).

1.4.2 Starch Synthases (SSs) E.C. 2.4.1.21

Starch Synthase (SS) also called (ADP-glucose: 1, 4-α-D-glucan 4-α-D-glucosyltransferases) belongs to the glycosyltransferase family 5 (GT5) (CAZy) (Coutinho et al., 2003). It has the highest number of isoforms compared with all starch biosynthesis enzymes known so far (Fujita et al., 2011). However, starch synthase (SS) can be divided into 5 subclasses, four of which are soluble (SSI, SSII, SSIII, and SSIV) in the stroma and involved in amylopectin synthesis and one is localized exclusively within the starch granule named the granule-bound starch synthase (GBSS), which is responsible for amylose synthesis (Orzechowski, 2008).

In addition to these classes, there is a putative SS class named starch synthase 6 or (SSV) that is closely similar in the sequence to SSIV, but has not yet been functionally identified in starch biosynthesis (Liu et at., 2015; Helle et al., 2018). However, starch synthase enzymes catalyze the transfer of glucosyl residues from the ADP-glucose (ADP-Glc) donor to the non-reducing end (C4) position of the acceptor to form α 1, 4 linked glucan polymer and prolong this polymer by one glucosyl residue in each reaction cycle (Keeling and Myers 2010). Furthermore, all the five starch synthase enzymes have similar C-terminal core sequence, whereas they are largely different in both N-terminal sequence and length. Close to the C-terminus, they generally consist of two conserved regions (conserved starch catalytic glucosyltransferase family 5 GT5 and GT1 domains). Both GT5 and GT1 possess conserved amino acid residues that can be involved in the binding of the ADP-glucose as glycosyl donor (Qu et al., 2018; Cuesta-Seijo et al., 2013; Brust et al., 2013).

However, GBSS enzyme has two isoforms; GBSS I and GBSS II; both with very high affinity to starch granules. Whereas it was found that GBSS I is responsible for the synthesis of amylose in the leaves and storage tissues in many species (Pfister and Zeeman 2016) , GBSS II is elongating amylose in other tissues such as pericarp (Vrinten and Nakamura, 2000). Indeed, there is no other starch synthase that can achieve this function. For instance, in Arabidopsis leaves, GBSS mutant so-called waxy mutant, typically do not produce amylose (Seung et al., 2015).

On the other hand, in the case of amylopectin production, all four SS classes appear to have a distinct role during its synthesis. They carried out this function as a group of enzymes working in concert in which SS1 prefer to elongates short A-and B-glucan chains (DP 9-10) within amylopectin clusters (Commuri and Keeling 2001; Senoura et al., 2004; Fujita et al., 2006). These effects have been characterized in Arabidopsis mutants lacking the *ss1* isoform where the transitory starch displays a reduced amount of short glucan chains (DP 8-12) (Delvallé et al., 2005). Further, this finding also suggests that SS1 prolongs the short glucan chains obtained from branching enzyme (BE). Furthermore, analyses of protein-protein interaction in Arabidopsis suggested that SS1 was able to interact with BE and then form branched glucan (Brust et al., 2014). After that, the activity of SS2 extends the short chains, produced by SS1, and forms intermediate-length glucan chains (DP 13- 22) (Craig et al., 1998; Umemoto et al., 2002; Zhang et al., 2004). It was shown that the loss of SS2 activity (for instance by mutation) has altered chain length distribution since the amount of shorter glucan chains (DP 8) were increased while the medium length glucan chains were decreased (DP 12-30) (Morell et al., 2003). For the continuous synthesis of longer glucan chains, (more than 25 glucosyl residues) SS3 is required (Zhang et al., 2005). However, its suggested function is the synthesis of long chains that run between two or more clusters. In addition to this function, it was revealed that SS3 also provides an overlapping function with other SSs isoforms (Szydlowski et al., 2011). Regarding the role of SS4 in chain length distribution is not yet identified, but it has a unique function related to the initiation, morphology, and accumulation of starch granules (Rolda´n et al., 2007; Zhang et al., 2008; Crumpton-Taylor et al., 2013). Furthermore, another study showed that SS3 is also required for the initiation of starch granules together with SS4. It was observed that plants which lack the *ss4/ss3* double mutant do not synthesize starch granule (Szydlowski et al., 2009). However, in Arabidopsis *ss4* mutant, a remarkable decrease reveals in the number of starch granules compared to the wild type plants (Rolda´n et al., 2007; Crumpton-Taylor et al., 2012; Malinova et al., 2017).

1.4.3 Starch branching enzymes (SBEs) E.C. 2.4.1.18

Starch branching enzymes (SBEs) belong to the amylase superfamily of enzymes (glycoside hydrolase) family 13 (GH13) (CAZy; Stam et al., 2006). It is also called

glucanotransferase that produces the branching structure of amylopectin by generating α 1, 6 linkages through cleavage of internal α 1, 4 glycosidic bonds glucan chain and transfers the cut chain to the position of the C6 hydroxyl of glucosyl residue in the same or another linear chain to create a new branch point. However, SBE has two classes, class I or (family B) which is found in higher plants as a single isoform (SBEI) with the exception of Arabidopsis (Dumez et al., 2006) and class II or (family A) (SBE II) with two isoforms, SBE IIa and SBE IIb (Burton et al.,1995; Sun et al., 1998). However, Arabidopsis has three types of SBEs (SBE1, SBE2 and SBE3). All of the three types are expressed in leaves, but only SBE2 and SBE3 are required for the synthesis of normal starch, while SBE1 has no apparent function in the metabolism of starch (Dumez et al., 2006). Furthermore, SBEs act on different glucan chains length as a substrate.While *in vitro* study, it was revealed that SBEI preferentially transfers longer chains (DP≥ 16) compared to SBEII which showed that it transferred short glucan chains (DP≤ 12). Thus, SBEI exhibits a higher affinity toward amylose while SBEII has a higher affinity with amylopectin (Takeda et al., 1993; Guan and Preiss 1993; Guan et al., 1997; Rydberg et al., 2001; Nakamura et al., 2010; Li et al., 2017). On the other hand, genetic studies revealed that maize *sbeI* mutant has normal amylopectin chain length profile compared to wild-type while in *sbeII b* mutant there is a distinct alteration in starch structure noticed in the frequency of amylopectin branches (Hedman and Boyer 1982; Blauth et al., 2002; Regina et al., 2010). Recently, Sawada et al. (2018) confirmed the distinct roles of the three SBEs isoforms (BEI, BEIIa, and BEIIb) cooperatively in the synthesis of amylopectin through their study on developing rice endosperm. The authors examined whether all three isoforms contribute to form the fine amylopectin structure through the suppression of their activities. They found a remarkable impact of the loss of BEIIb on amylopectin fine structure, while analysis of the chain length distribution revealed a reduction in the short chains with a DP 6-13. On the other hand, loss of SBEI alone does not affect the amylopectin synthesis, whereas a clear effect was when both SBE1 and SBEIIb were inhibited. Additionally, there was a marked reduction in the DP 11-12 intermediate chains in the *sbe1/sbeIIb* line compared to the *sbeIIb* line. This indicates the role of the SBEI in the synthesis of intermediate amylopectin chains. Interestingly, it was suggested that the role of the SBEIIa is compensated for the role of the SBEI rather than that of SBEIIb. While his roles was confirmed through the analysis of the amylopectin

structure from the *sbeI/sbeIIa/sbeIIb* line in comparison to the amylopectinn structure from *sbeI/sbeIIb* line by its formation of chains with a DP 11-13.

Furthermore, there is evidence that SBEs form complexes with other starch biosynthetic enzymes (Liu et al., 2009; Tetlow et al., 2004). For instance, it has been revealed in wheat endosperm that is a protein complex formed by an interaction of SBEIIb, SBEI, and plastidial phosphorylase (Tetlow et al., 2004). Furthermore, it was reported in Arabidopsis that all starch synthase isoforms (SSI-SSIV) have the ability to functional interact with SBEs and form branched glucans (Brust et al., 2014).

1.4.4 Starch debranching enzymes DBEs E.C. 3.2.1.41

Starch debranching enzymes (DBEs) belong to the glycoside hydrolase family 13 (CAZy) (Lombard et al., 2013). These enzymes which are involved in hydrolyzing α 1, 6 glycosidic bonds in starch granule and release linear glucose chains play an important role in the evolution of crystalline amylopectin. DBE enzymes can be divided into two types: isoamylases (ISAs E.C.3.2.1.68) and pullulanase (PUI) or limit-dextrinase (LDA E.C.3.2.1.41). Furthermore, the genetic study revealed that Arabidopsis contains three isoforms of isoamylases (ISA1, ISA2 and ISA3) which are encoded in plant genomes as debranching isoforms (Hussain et al., 2003). Functionally, it was found that ISA1 and ISA2 play an important role in starch granule synthesis. The studies showed that ISA1 and ISA2 are interacted together to form a hetero-oligomeric enzyme complex (Hussain et al., 2003; Panpetch et al., 2018). Thus, the authors suggested that this complex involves in the debranching soluble glucan chains during starch biosynthesis. Moreover, a reverse-genetic approach in Arabidopsis identified that the loss of ISA1 or ISA2 led to reduced starch content and accumulation of water-soluble polysaccharide (Phytoglycogen) thereby influenced amylopectin structure (Delatte et al., 2005; Wattebled et al., 2005). In contrast, ISA3 is thought to have a specific function in debranched starch during its degradation (Streb et al., 2012). Thus, in Arabidopsis *isa3* mutant has *starch-excess* (*sex)* phenotype at the end of both the light and the dark phases including alteration of amylopectin structure (Wattebled et al., 2005).

1.5 Disproportionating enzyme D-enzyme E.C. 2.4.1.25

Disproportionating enzyme (D-enzyme) is a α 1, 4 glucanotransferase that catalyzes the hydrolysis of α 1, 4 glycosidic bonds of unbranched malto-oligosaccharides (maltotriose

metabolism), transferring two glucosyl units to the nonreducing end of another glucan (glycogen or amylopectin) or free glucose and releasing glucose or a glucan chain, depending on the cleavage site (Takaha et al., 1993; Bresolin et al., 2006).

In plants, it has been discovered that there are two types of disproportionating enzyme (DPE) the first one located in the plastid named DPE1 (Critchley et al., 2001) and the second located in the cytoplasm called DPE2 (Chia et al., 2004). The mutants study identified the role and function of DPE1 and DPE2 in starch metabolism.

In potato, it was concluded that DPE1 and DPE2 have individual but essential roles in starch metabolism since lacking DPE1 led to an accumulation of slightly more starch and high levels of maltotriose than control while in case of lacking DPE2 there were more maltose and large amounts of starch (Lutken et al., 2010). In Arabidopsis, *dpe1* mutant also showed a reduction in starch degradation at night and accumulation of maltotriose (Critchley et al., 2001). Furthermore, it was identified that Arabidopsis DPE2 gene is necessary for maltose metabolism as the mutant of this gene exhibited a plants dwarf phenotype and accumulated a large amount of maltose and a lower sucrose amount compared to the wild type (Lu and Sharkey, 2004). The authors hypothesized that knocking out DPE2 blocks the conversion from maltose to sucrose. Additionally, Fettke et al. (2006) provides evidence that DPE2 can use the cytosolic heteroglycans as a substrate further to maltose.,while, the analysis of the physical and chemical parameters of heteroglycans from DPE2-deficient mutants, such as the size distribution or the monomer patterns and the priming efficiencies for glycosyltransferases demonstrate a significant difference from those of wild type.

Furthermore, the functional role of DPE1 in starch biosynthesis was revealed in wheat endosperm. To identify that DPE1 has the ability to elongation maltooligosaccharides which is generated by debranching enzymes and starch phosphorylase, the wheat DPE1-enzymeincubate with maltoheptaose in addition to glycogen and starch. Analysis DPE1-enzyme activity revealed that it is able to use maltoheptaose as a doner. The indication of the chain elongation reaction had occurred when a strong signal was detected by using iodine staining. In addition, based on immunoblot experiments with the highly specific polyclonal antibody against DPE1, it was reported that DPE1 is able to produce glycosyl

when the partially purified extracts containing DPE1-enzyme are incubated with maltotriose (Bresolin et al., 2006).

1.6 Alpha glucan phosphorylase

Alpha glucan phosphorylase enzyme (EC 2.4.1.1) belongs to the glycosyltransferase family (GT35). These enzymes are important for carbohydrate metabolism in prokaryotes and eukaryotes. Alpha glucan phosphorylase participates in the transferring of glucosyl residue from glucose-1-phosphate (G-1-P) to the nonreducing end of α 1,4 D-glucan chains by reversible reaction releasing of orthophosphate (Pi) or a degradative (phosphorolysis) reaction, whereby (Pi) is utilized to produce glucose-1-phosphate (G-1-P) through the removal of glucosyl residue from an α 1, 4 linked glucan chain (Kadokawa, 2018) (Fig 1.8).

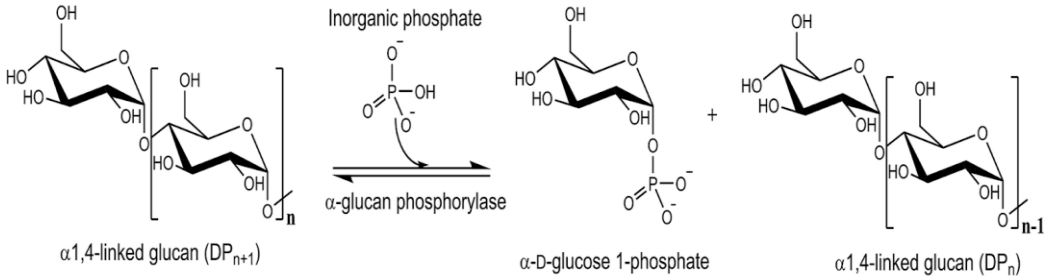

Fig.1.8: Schematic diagram for the typical reversible reactions catalyzed by alpha-glucan phosphorylase. The glucose molecule is liberated from the non-reducing end of the glucose polymer to form α-D-glucose-1-phosphate (Ubiparip et al., 2018).

Alpha glucan phosphorylase is considered one of the central enzymes which play an important role in carbohydrate metabolism in a wide diversity of organisms and tissues (Newgard et al., 1989). An in-plant tissue, α-glucan phosphorylase, commonly called starch phosphorylase is an important allosteric enzyme in starch metabolism. Higher plants have two isoforms of starch phosphorylase: a plastidial phosphorylase named Pho1, Pho L, and PHS1 which has low affinity towards the highly branched carbohydrates such as starch and glycogen (because it carries a 78 amino acid insertion in the middle of its sequence near the glucan-binding site) and high affinity towards the low molecular weight linear glucan such as malto-oligosaccharides (Mori, et al., 1993; Young

et al., 2006). The second isoform is cytosolic phosphorylase named Pho2, PhoH, and PHS2 which prefers highly branched glucan as a substrate (Yu et al., 2001). Functionally, genetic studies identified the role of PHS1 isoform in transitory starch turnover in Arabidopsis since a PHS1 mutant revealed accumulated slightly more starch compared to the wild type (Malinova et al., 2014). Furthermore, it has been proposed that PHS1 also acts in starch biosynthetic in *Chlamydomonas reinhardtii* (Dauvillée *et al.*, 2006). It was demonstrated that starch phosphorylase is required for the synthesis of normal polysaccharide granules as mutants display a significant decrease in amounts of starch during storage with formation and accumulation of abnormally shaped granules. Additionally, this revealed the altered chain-length distribution of amylopectin and increased amylose content.

In rice, the loss of PHS1 results reduced starch content with altered starch granule characteristics and shrunken endosperm when plants are grown at low temperatures (Satoh et al., 2008). The authors suggested that the production of longer malto-oligosaccharides by PHS1 may work as a primer for SSs thereby helping to initiate starch synthesis.In *in vitro* experiment; Cuesta-Seijo et al. (2017) also elucidated the role of PHS1 in the starch synthesis of barley endosperm.

1.7 Starch degradation

Several studies identified many enzymes that are involved in starch degradation using forward and reverse genetic approaches. The starch degradation process is necessary for optimal growth. However, during the night, transitory starch is degraded at a more-or-less constant rate leading to remobilizing of all of the starch which synthesized the previous day. The main products for this process are maltose and glucose. The released sugars are imported from the plastidial to the cytosol by the maltose transporter MALTOSE EXCESS 1 (MEX1) and glucose translocator (pGlcT), respectively (Cho et al., 2011). These products are later used to further metabolism during the night (Zeeman et al., 2007; 2010).

In Arabidopsis leaves, the starch degradation pathway occurs under two types of hydrolytic enzyme, exoamylolytic activity of β-amylases, which cleaved α 1, 4 glycosidic bond and debranching enzyme isoamylase, which cleaved α 1, 6 linkages (Smith and Zeeman 2020). To increase the accessibility of amylolytic enzymes to the granule

surface, starch needs to be previously phosphorylated /dephosphorylated (Kötting et al., 2009). However, starch phosphorylation is a crucial process for starch metabolism. Phosphorylation cycle of the starch granule (Fig. 1.9) is an essential path for its subsequent degradation (Nashilevitz et al., 2009; Kötting, et al 2009).

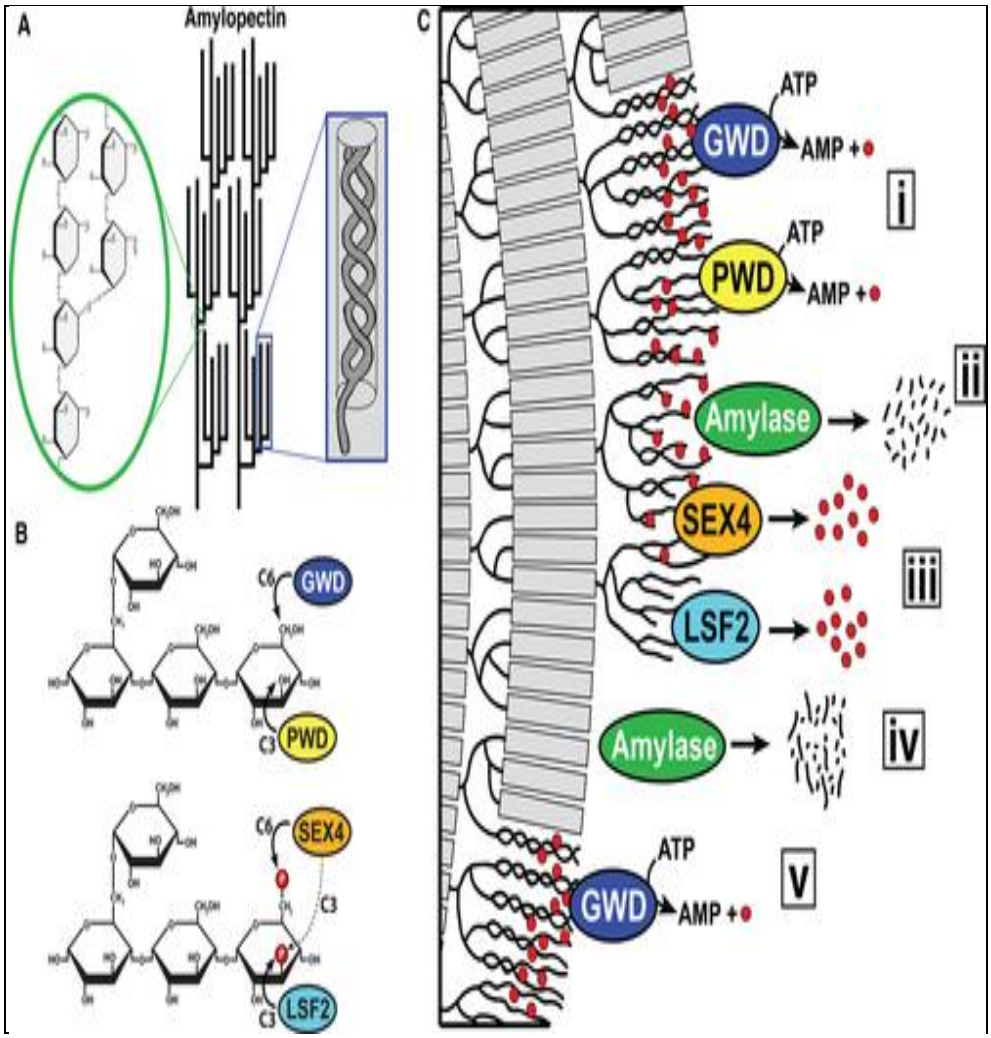

Fig.1.9: Reversible phosphorylation of the plant starch granule. (A) Amylopectin is a glucose polymer and the main component of the starch. It is formed from α1, 4glycosidic linked glucose chains with α1, 6 branches that are clustered at regular intervals (green inset). Adjacent amylopectin chains form double helices (blue inset) that expel water, contributing to the water insolubility of starch. (B) Amylopectin glucans are phosphorylated and dephosphorylated by four enzymes. GWD phosphorylates glucans at the C6 position, followed by phosphorylation at the C3 position by PWD. SEX4 dephosphorylates the C6 and C3 positions, with a preference for the C6 position, and LSF2 exclusively dephosphorylates the C3 position. (C) Reversible phosphorylation in starch degradation. (i) GWD and PWD phosphorylate amylopectin helices (grey bars), causing them to unwind. (ii) Amylases, particularly β-amylase, are able to access and degrade the glucan chains, but β-amylase is unable to hydrolyze glucans past a phosphate group (red circles). (iii) SEX4 and LSF2 dephosphorylate the exposed glucan chains, allowing further degradation (iv). (v) The process continues with phosphorylation on the next layer of amylopectin helices within the starch granular lattice (Meekins et al., 2016).

In Arabidopsis, a small enzyme family was identified as an important enzyme for starch degradation. This family includes Glucan-water dikinase (GWD1 EC 2.7.9.4; At1g10760) (Ritte et al., 2002), Phosphoglycan, water dikinase (EC 2.7.9.5; At5g26570) (Kötting et al., 2005). Both are localized in the chloroplast stroma and GWD2 (At4g24450) not targeted to the chloroplast (Glaring et al., 2007). During amylopectin degradation, glucan water dikinase (GWD) catalyzing the formation of phosphate groups monoesterified at the C-6 position of individual glucosyl residues. Followed by phosphorylation at the C-3 position of a pre-phosphorylated or not pre-phosphorylated amylopectin chain by phosphoglucan water dikinase (PWD), but with low efficiency leading to disrupt the double helices of crystalline lamellae (Fig. 1.10) (Baunsgaard et al., 2005; Kötting et al., 2005; Blennow and Engelsen 2010; Hejazi et al., 2008, 2014). Kozlov et al. (2007) confirm that phosphorylated starch granules caused the changes in granule surface. These changes lead to reducing the crystal stability which allows accessing amylolytic degradation enzymes (Edner et al., 2007; Hansen et al., 2009; Blennow and Engelsen, 2010).

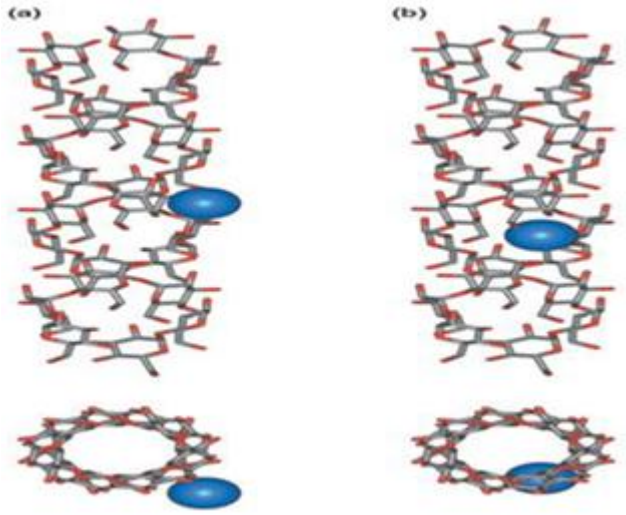

Fig.1.10: Crystalline domain of a starch molecule phosphorylated at the C-3 (a) C-6 (b) position from. (Blennow et al., 2002)

Both GWD and PWD use ATP as a dual phosphate donor. They transfer the β-phosphate group to a small proportion of glucosyl residues on the granule surface and $_{\gamma}$-phosphate group to water.

In Arabidopsis leaves, the ratio of C3- to C6-bound phosphate is about 1: 5, while about 1 of 2,000 glycosyl residues in the starch granule is phosphorylated (Yu et al., 2001; Haebel et al., 2008; Santelia et al., 2011). However, depending on plant origin the concentration of phosphate esters is different and typically very low. For instance, potato starch is highly phosphorylated containing up to 33 nmol phosphate/mg starch (Hoover, 2001) while cereals consist of lowest concentration ≤1 nmol/mg (Lim et al., 1994). Further, based on different techniques like mass spectrometry or quantitative ^{31}P-NMR, it was revealed that the C6 position of glycosyl residues in glucan was the most frequently used phosphorylation site compared with the C3 position (Ritter et al., 2006; Haebel et al., 2008; Nitschke et al., 2013).

Although phosphate esters are present in small quantities, they have an impact on the starch physicochemical properties (Yoneya et al., 2003; Carmona-Garcia et al., 2009) and starch physiological function (Hejazi et al., 2012a). Thus, it was found in potato that the gelatinisation enthalpy of starches with a high degree of phosphorylation was lower than that of starches with a lower degree of phosphorylation (Muhrbeck and Eliasson, 1991). Further, Lorberth et al. (1998) found in potato tuber starch that removal of phosphate lead to a low paste viscosity while in cereal endosperm starch, the increasing of phosphate results in a higher paste viscosity (Zeeman et al., 2010).

Furthermore, structurally GWD1 and PWD enzymes have C-terminal catalytic domain, a short conserved sequence containing the Phosphohistidine residue (Mikkelsen et al., 2004) and N-terminal carbohydrate-binding domains (CBM) that vary between the different dikinases (Fig. 1.11).

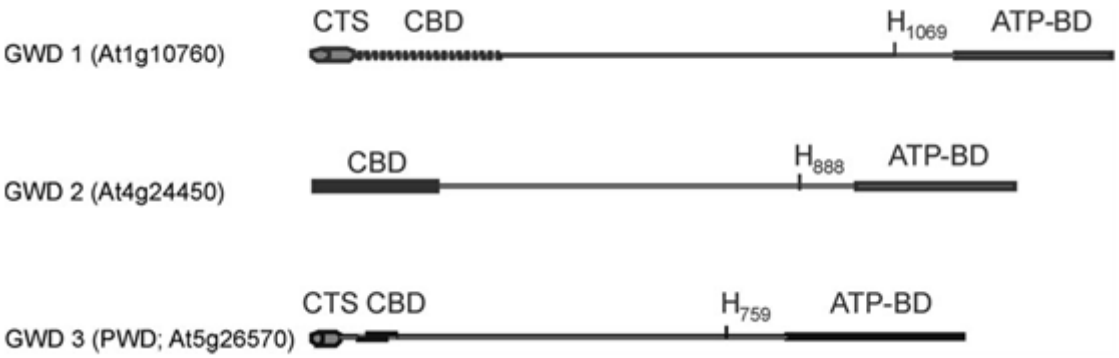

Fig.1. 11: Schematic presentation of the domains of the three glucan-related dikinases from *Arabidopsis thaliana* (L): CTS, chloroplast transit peptide located at the N-terminus, CBD, carbohydrate-binding domain, ATP-BD, ATP binding domain at the C-terminus. The position of the conserved histidine residue that is subjected to autophosphorylation is also indicated (H) (Fettke et al., 2009).

While GWD1 possesses two functionally (CBM45s): CBM45-1 located after the chloroplast transit peptide and CBM45-2 found in the centre of the sequence (Glaring et al., 2011) (Fig.1. 12), PWD has a single CBM20 at the N-terminal with only one functionally binding site1 which lakes the sequence for binding site2 (Christiansen et al., 2009a).

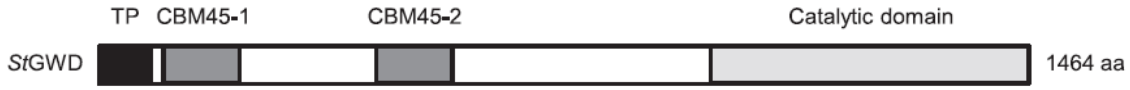

Fig.1.12: Domain structure of *Solanum tuberosum* α-glucan, water dikinase (*St*GWD). Showing the chloroplast transit peptide (TP, black), tandem CBM45s (grey) and the catalytic domain (light grey). The size of the proteins is given in amino acids (aa) (Glaring et al., 2011).

However, both GWD and PWD are important for normal rates of starch degradation, while lack of GWD function results in a strong *starch excess* (*sex1*) phenotype (Yu et al., 2001). Furthermore, the properties of starch granules surface from GWD-deficient plants differs from that of WT. Also, it was found that the isolated starch granules from the *sex1-8* null mutant have short glucan chain residues located at the granule surface which impede the activity of other starch degrading enzymes (Mahlow et al., 2014). In contrast, *pwd* mutant plants reveal a lack of detectable phosphate in C3-bound phosphate (Ritte et al., 2006). Therefore, the starch excess phenotype was also observed in the PWD deficient plants.

In addition, to analyse the role of GWD and PWD in starch phosphorylation, it was also found in *in vitro* study that GWD2 has the ability to phosphorylate glycosyl residue at the C6 position. *gwd2* mutant does not show a *sex* phenotype compared to the wild type. Therefore, it is improbable to have a role in starch degradation (Glaring et al., 2007).
Takeda and Hizukuri (1981) found that β-amylase activity is impeded when a phosphate group is a bind to glucan since it cannot degrade past a phosphate group. Therefore, removal of the phosphate groups, at both the C6 and C3 positions is necessary for proper starch metabolism.

Earlier studies showed that Arabidopsis contains two chloroplastic phosphoglucan phosphatases enzymes that are essential for dephosphorylation, SEX4 enzyme (Starch Excess 4) (EC 3.1.3.48; At3g52180) (Niittylä et al., 2006) and LSF2 enzyme (Like Sex

Four 2) (At3g01510) (Santelia et al., 2011). Both enzymes belong to the protein tyrosine phosphatase (PTP) superfamily (Gentry et al., 2007). Structurally, both enzymes contain a chloroplast targeting peptide, dual-specificity phosphatase (DSP) domain, and unique C-terminal (CT) motif. However, unlike SEX4, LSF2 does not possess a carbohydrate-binding module domain (CBM) (Santelia et al., 2011; Meekins et al., 2013). Functionally both of which are related to the starch and glycogen phosphatase metabolism. Nonetheless, in plants, both enzymes catalyze the removal of the phosphate group from starch granules; thereby generating unphosphorylated substrates for amylases (Gentry et al., 2007; Kötting et al., 2009; Santelia et al., 2011). Thus, it has been shown that SEX4 preferentially dephosphorylates the C6-position, while LSF2 mainly dephosphorylates the C3-position of glucosyl residue (Hejazi et al., 2010; Santelia et al., 2011).

Thus, it was shown that the *sex4* mutant has a *starch excess* phenotype, as a result of a reduced rate of starch degradation thereby accumulation of starch (Niittylä et al., 2006; Kötting et al., 2009; Hejazi et al., 2010). Whilst, Santelia et al. (2011) found that *lsf2* mutant has high levels of C3 phosphate but no starch excess phenotype while the *sex4 lsf2* double mutant displays a clear increase in starch excess, which was higher than that of *sex4* single mutant. On the other hand, in a recent study in potato by Samodien et al. (2018), it was suggested that repression of either SEX4 or LSF2 inhibited leaf starch degradation since they found in both cases significantly increased in the amount of phosphate bound to the starch at C6 position and C3 position in both lines repressed in *st*SEX4 and *st*LSF2, respectively. Additionally, the size of starch was reduced and alterations in glucan chain length distribution compared to wild type were observed.

Besides SEX4 and LSF2, there is another enzyme encoded in Arabidopsis called LSF1 (*Like SEX Four 1*) (At3g01510), that shows similarity to both enzymes, but it has no phospho-glucan phosphatase activity. It is located in the chloroplasts and binds to the surface of starch granules. It is likely that it is required for normal starch degradation since the *lsf1* mutant has a starch excess phenotype (Comparot-Moss et al., 2010). Interestingly, *lsf1* mutant has the same levels of C3 and C6 phosphate to wild-type, thus LSF1 might have a regulatory role rather than catalytic function.

Glucan phosphorylation/dephosphorylation is suggested to disrupt the crystalline arrays of amylopectin double helices, facilitating the action of hydrolytic enzymes. β-amylase is an exo hydrolytic enzyme that attacks the non-reducing ends of α 1, 4 glycosidic bond glucan chains to produce β-maltose. The maltose is transported to the cytosol where it is undergoing further conversions. In Arabidopsis, the genome has nine genes encoding β-amylases isoforms designated (BAM1-9) (Smith et al., 2004; Fulton et al., 2008). Four of which (BAM1-4) located in the chloroplast (Lao et al., 1999, Fulton et al., 2008). Moreover, it has been shown that BAM1 and 3 have been implicated in starch degradation (Lao et al., 1999, Fulton et al., 2008). Further, BAM3 is considered as the dominant enzyme in starch degradation. The *bam3* mutant has reduced levels of maltose at night thereby exhibits starch excess phenotype, by contrast, *bam1* mutant do not show this effect. Whereas, in *bam1 bam3* double mutant, there was increased severity of the starch excess phenotype indicated that both enzymes have an overlapping function during starch degradation (Fulton et al., 2008).

For complete degradation of glucan chains by β-amylase action, theα 1, 6 linkages residues at the branch points of the amylopectin molecule limit the progression. Therefore, debranching enzymes (DBEs) are necessary for hydrolysing the branch points, thereby releasing linear glucans. However, the Arabidopsis genome contains two genes encoded DBEs as isoamylases with three isoforms (ISA): ISA1, ISA2, ISA3 and limit dextrinase (LDA) also known as pullulanase (Hussain et al., 2003; Delatte et al., 2006). Functionally, it was shown that only ISA3 and LDA have a role in starch degradation (Streb et al., 2008; 2012). Furthermore, ISA3 was considered being the major debranching enzyme involved in starch degradation at night.

In Arabidopsis, Delatte et al. (2006) identified that *At*ISA3 removes the short branches at the surface of the starch granule. While they found in the *Atisa3* mutant a slower rate of starch degradation, more leaf starch and many very short glucan chains at the starch surface compared to wild type. On the other hand, they confirm the role of *At*ISA3 during the elimination of a second debranching enzyme, LDA. However, *Atlda* mutants have normal starch content. Whereas, the *Atisa3/Atlda* double mutant showed a severely *starch-excess* phenotype, a slower rate of starch degradation and accumulation soluble

branch oligosaccharides than *Atisa3* single mutants or wild type, suggesting an overlap in the function of both enzymes.

Furthermore, it was found in most reserve tissues that α-amylases enzymes (AMYs) (endohydrolytic enzymes) hydrolyses the internal linear α 1, 4 linked glycosyl residues. In the Arabidopsis genome, it was identified as the gene which encods three α-amylase-like proteins (*At*AMY1, *At*AMY2, and *At*AMY3) (Stanley et al., 2002). However, only AMY3 has a predicted transit peptide (Yu et al., 2005). Furthermore, AMY3 does not consider a part of the starch degradation process since the loss of AMY3can compensate for other enzymes, but its activity makes a clear impact on starch metabolism where other degradation enzymes are missing. For instance, lack of AMY3 in *iso3 lad* background was revealed to enhance the starch excess phenotype compared to double mutants (Streb et al., 2012). Furthermore, Kötting et al. (2009) showed that *amy3 sex4* double mutants have a starch excess phenotype stronger than *sex4* mutant alone.

On the other hand, the residual maltotriose and malto-oligosaccharides that are produced by beta-amylase and released in the plastidial stroma can be metabolized by the glucanotransferase enzyme (DPE1). DPE1 releases glucose from maltotriose (Critchley et al., 2001) and α-glucan phosphorylase (PHS1) releases G1P from the non-reducing end of malto-oligosaccharides (Setup and Schächtele, 1981). Figure1. 13 shows the main enzymes responsible for starch degradation in Arabidopsis leaves.

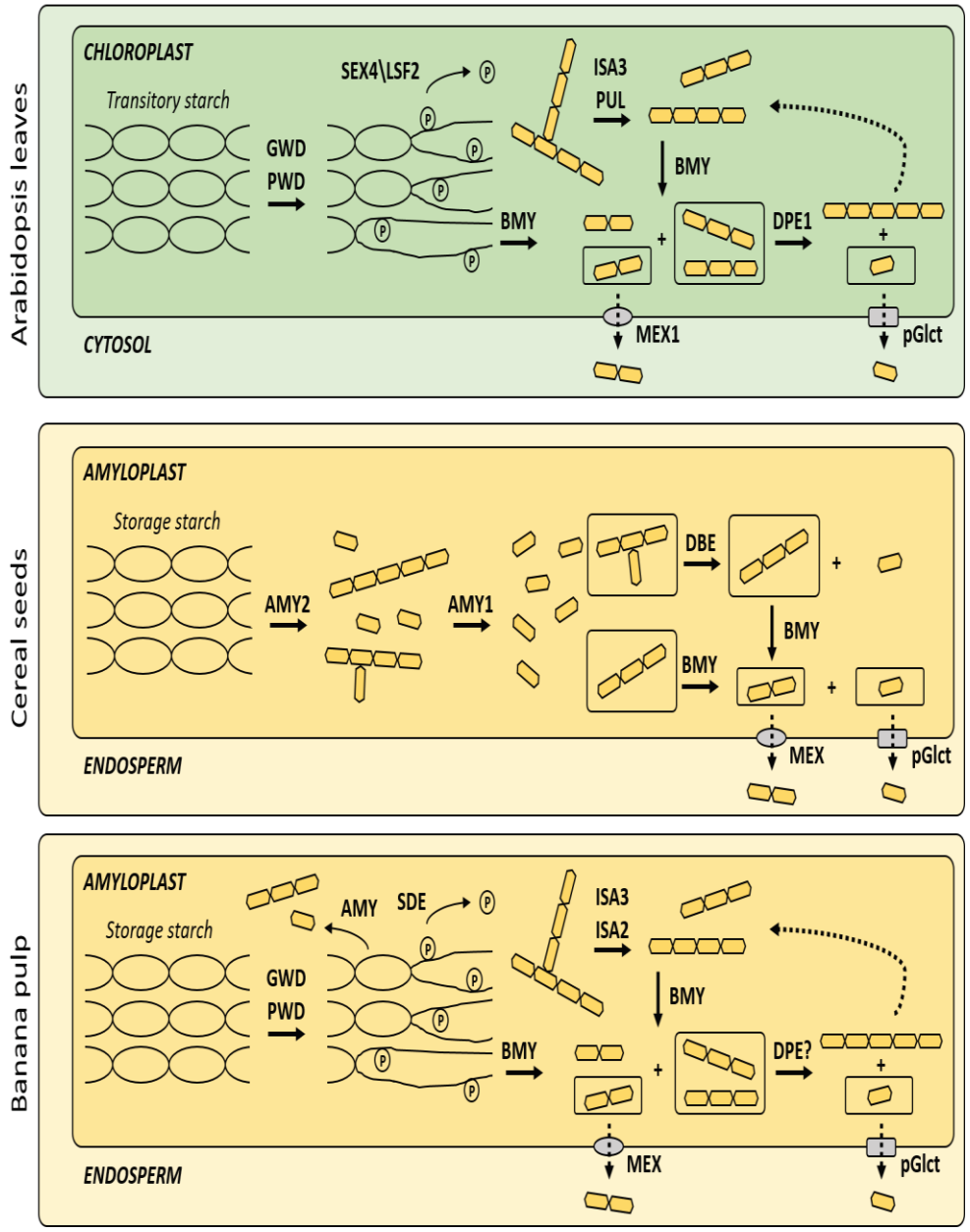

Fig.1.13: Starch degradation in Arabidopsis leaves. GWD, Glucan, water dikinase; PWD, Phosphoglucan, water dikinase; ISA, isoamylase-like protein sub-family; PUL, limit dextrinase family; BMY, β-amylase; DPE1, starch-disproportionating enzyme 1; MEX1, maltose excess transporter 1; pGlcT, plastidic glucose translocator; AMY, α-amylase, corresponding to (Cordenunsi-Lysenko et al., 2019).

1.8 Metabolism of starch

In chloroplasts, there is an extremely complex and organized harmony of various enzymes necessary for the synthesis and degradation of starch. Additionally, they are present in diverse isoforms (Fig. 1.14). However, the reactions of these enzymes are mainly regulated in a specified way for transitory starch biosynthesis during active photosynthesis and mobilization at night (MacNeill et al., 2017).

To understand the nature and regulation of starch synthesis and degradation pathways, it should know the roles of some biochemical reactions in the control of starch metabolism like redox regulation (Skryhan et al., 2018). For instance, so many enzymes were shown to be activated under reducing conditions. For example, it was found in *vitro* experiments that glucan water dikinase (GWD), starch phosphatase, starch synthase1 and α-amylase (BAM1) enzymes revealed increased in their action under reduction conditions (Mikkelsen et al., 2005; Sokolov et al., 2006; Skryhan et al., 2015). Furthermore, other biochemical reactions such as protein phosphorylation, protein-protein interactions and allosteric regulation by metabolites are also involved in the control of starch metabolism (Kötting et al., 2010; White-Gloria et al., 2018).

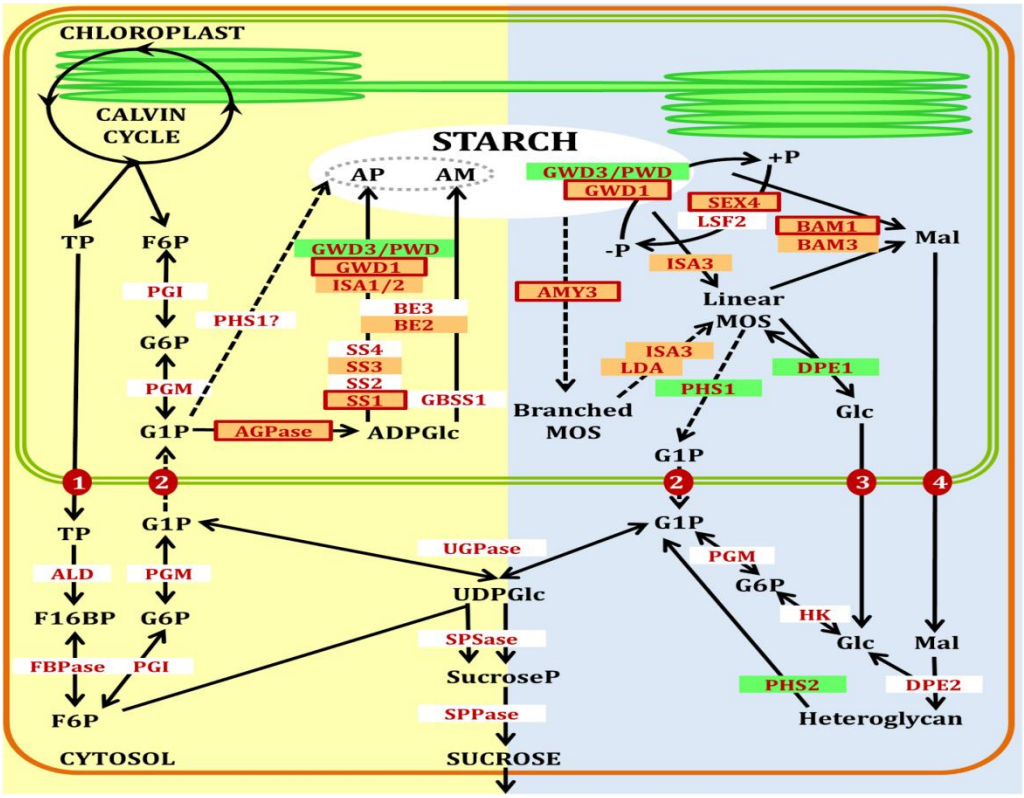

Fig.1.14: Illustrative scheme of the pathway of starch metabolism in *Arabidopsis thaliana* leaves. AM, amylose; AP, amylopectin; TP, triosephosphate; F6P, fructose-6-phosphate; G6P, glucose-6-phosphate; G1P, glucose-1-phosphate; ADPGlc, ADP-glucose; MOS, maltooligosaccharides; Mal, maltose; Glc, glucose; F16BP, fructose-1,6-bisphosphate; UDPGlc, UDP-glucose; SucroseP, sucrose-phosphate; ALD, aldolase; FBPase, fructose-1,6-bisphosphatase; PGI, phosphoglucose isomerase; PGM, phosphoglucomutase; AGPase, ADP-glucose pyrophosphorylase; SS, soluble starch synthase isoforms; GBSS, granule-bound starch synthase; BE, branching enzyme; ISA, isoamylase; LDA, limit dextrinase; PHS, α-glucan phosphorylase; GWD1, glucan water dikinase; PWD, phosphoglucan, water dikinase; SEX4 and LSF2, phosphoglucan phosphatases; BAM, β-amylase; AMY, α-amylase; DPE, disproportionating enzyme; FBPase, fructose-1,6-bisphosphatase; UGPase, UDP-glucose pyrophosphorylase; SPSase, sucrose-phosphate synthase; SPPase, sucrose phosphate phosphatase; HK, hexokinase. Transporters are shown as red filled circles: (1) triose-phosphate/phosphate translocator (TPT); (2), G1P translocator; (3) plastidial glucose transporter (pGLT); (4) maltose transporter (MEX1) (Stitt and Zeeman, 2012)

1.9 The biological function for complex formation of starch metabolic enzymes

Recent genetic and biochemical evidence revealed that starch metabolism pathway is achieved through the formation of complexes between numerous starch synthesising and degrading enzymes as well as the affinity of these complexes towards amylose and amylopectin. Further to the role of the phosphorylation enzymes in this path.

It was found that the complex formation of starch metabolism enzymes affects on amylopectin clusters formation. In maize wild type amyloplast, it was found that SSIIa is interacting with SSI and SBIIb to form a trimeric complex that involved in amylopectin synthesis (Liu et al., 2012). Therefore, the differences in the composition or function of these protein complexes will affect the amylopectin structure. Thus, Miura et al. (2018) tested the effect of SSIIa in this trimeric complex in developing rice seed. The authors prepared a mutant line designated as EM204 (*ssIIa)*. However, analysis of soluble proteins revealed that the loss of *ssIIa* leads alterations in the trimeric protein complex compared to trimeric complexes in wild type. Further, amylose content of *ssIIa* was higher than that in wild type. Also, it had a higher content of amylopectin short chains (DP ≤ 12) compared to SSIIa active line.

Furthermore, it was reported that the synthesis of amylose and amylopectin during developing rice endosperm affected by SSIIIa and/or SBIIb. However, ssIIIa*/sbIIb* double mutant revealed a significantly fewer amylopectin short chains (DP) ≤13 compared to wild type,while the number of long chains (DP ≥25) connecting clusters of amylopectin was higher than in the wild type but lower than in *beIIb* single mutant. On the other hand, both *ssIIIa* and *beIIb* single mutant showed higher activity of AGPase and GBSSI than wild type. This partly explains the high level of apparent amylose content of *ssIIIa/beIIb,* which was >1.5 times greater than that of either *ssIIa* or *beIIb* single mutant (Asai et al., 2014).

Interestingly, further suggestions revealed that some of the biological functions for complex formation depend on the phosphorylation mechanism as a post-translational regulatory mechanism thereby affect the physical and functional stability for enzymes during starch metabolism (Tetlow et al.,2004; Tetlow et al.,2008). In wheat endosperm, physical interactions between starch branching enzymes (SBEs) and starch synthases (SSs) were identified by using immunoprecipitation and cross-linking strategies. It was suggested that the catalytic activity and ability of some enzymes (SBEII class) to form physical interactions with other starch-metabolizing enzymes depended on the phosphorylation while incubated with ATP, whereas their catalytic activity reduces by using dephosphorylation alkaline phosphatase (Tetlow et al., 2004). While immunoprecipitation experiments using peptide-specific anti-SBE antibodies revealed

that SBE is capable of forming protein complexes with SBEIIb and starch phosphorylase in a phosphorylation-dependent manner (Tetlow et al., 2004). Moreover, a recent study in Arabidopsis identified that post-translation mechanisms might be regulated by the SS2 activity. However, *In vitro* evidence suggested that chloroplast- localized casein kinase II (CKII) is a strong phosphorylating enzyme for starch metabolism-associated enzymes. Furthermore, it was shown that (CKII) is responsible for phosphorylation Arabidopsis starch synthase II (*At*SS2) at two N-terminal serine residues (S63, S65) in chloroplasts. To investigate this role in *vitro,* a CKII-specific inhibitor, heparin, was used to pretreated recombinant (CKII) and chloroplast extract prior to recombinant (SS2) phosphorylation. This results in a decrease in (SS2) phosphorylation by chloroplast extract with increasing of heparin concentration (Patterson et al., 2018). Interestingly, the catalytic activity of SS2 is not affected by the phosphorylation mechanism in which the truncation of the N-terminal region of SS2 resulted in a 47-fold increase in its activity. On the other hand, although co-immunoprecipitation experiments identified the complex form between the truncated N-terminal *At* SS2 and SBE2.2, the heterodimeric enzyme complex (HEC) formation between them was shown to be ATP- dependent.

1.10 Putative protein-protein interaction within starch granules

Over the last decades, new techniques for detecting protein-protein interactions have continually been developed including protein co-purification, co-immunoprecipitation, cross-linking, and expression library screening in addition to one of the widely used techniques, yeast two-hybrid (YTH), which developed by Fields and Song (1989). Moreover, these techniques allow identifying several putative partners interacting with other proteins in the living cells especially the precise role for several proteins have not yet been clarified.

However, during starch metabolism, more studies referred to the role of protein-protein or multi-protein interaction within starch granules. Starch synthase 4 (SS4) is one of the plastidial enzymes which has the ability of the interaction with other proteins due to the presence of the coiled-coils in his structure (D'Hulst and Merida 2010). However, as SS4 does not possess a CBM binding domain, it was identified that it binds to his suitable substrates through his interaction with PROTEIN TARGETING TO STARCH 2

(PTST2), which has CBM48 domain. Interestingly, it was noted that the N terminal coiled-coils of SS4 are not required for the interaction between both proteins. Further, it was found that SS4 can interact with itself (Seung et al., 2017). The authors supported this idea when they detected an interaction between SS4 monomers in Arabidopsis leaves. Recently, it was reported that Arabidopsis plastidial phosphorylase enzyme (PHS1) interacts directly with the SS4 (Malinova et al., 2018). Furthermore, in rice endosperm starch, it was shown that the plastidial phosphorylase (PHS1) interacts with branching enzyme (SBE) and disproportionating enzyme 1 (DPE1) (Tetlow et al., 2004; Hwang et al., 2016; Nakamura et al., 2017). Also, it was found during the process of starch synthesis, there was specific interaction between (SSs) enzymes and branching enzymes (Brust et al., 2014). Much progress has been made in understanding protein-protein interactions in the starch granule.

1.11 Novel proteins influence starch metabolism

1.11.1 Regulatory proteins in starch synthesis

In addition to starch metabolic enzymes, several novel proteins were recently identified that affect the starch status, nature and structure (Feike et al., 2016; Seung et al., 2015; Peng et al., 2014). These recent proteins investigations are devoid of known catalytic domains, but they can also be involved in starch metabolism as non-catalytic starch binding proteins.

Approximately 15–40% of all eukaryotic genes are encoding proteins that lack primary sequence homology named proteins with unknown functions (PUFs). Furthermore, the unknown proteins were termed proteins with obscure features (POFs). Little is known about the functional role of these genes (Gollery et al., 2006, 2007; Luhua et al., 2008). Among these genes, QQS (qua-quine starch) is predicted to encode a protein that consists of only 59 amino acids with no known sequence homolog or predicted structural motifs. This gene revealed a potential novel regulator of starch biosynthesis in which the reduction of QQS expression showed excess leaf starch content at the end of the illumination phase of a diurnal cycle (Li et al., 2009). Other proteins were identified as delivery proteins that play important role in targeting starch biosynthesis enzymes during starch metabolism thereby regulating the dynamics of biological function for these

enzymes. These proteins contain a carbohydrate-binding module 48 (CBM48); thus, they may act as a starch-binding protein involved in starch synthesis (Peng et al., 2014; Seung et al., 2015). In Arabidopsis, there are three members of PROTEIN TARGETING TO STARCH (PTST) all of which contain coiled-coils and CBM48 domains present in the C-terminus (Lohmeier-Vogel *et* al., 2008; Seung et al., 2015, 2017). PTST1 was the first protein which was identified as a starch interacting protein-containing CBM48 (Lohmeier-Vogel et al., 2008) possessing predicted N-terminal coiled-coil motifs (Seung et al., 2015). It was shown that GRANULE BOUND STARCH SYNTHASE (GBSS) is actively targeted to starch granule after a direct interaction with PTST1 through its own coiled-coil motifs. The latter then interacts with starch via its CBM48 domain by which this interaction aids GBSS to bind to starch granule (Seung et al., 2015). Further, it was found that Arabidopsis lacking PTST1 has amylose-free starch, but phenotypically was similar to Arabidopsis lacking GBSS. On the other hand, structurally, it was identified that both PTST2 and PTST3 are homologous to the PTST1 protein. It was suggested that PTST2 and PTST3 proteins have a role in the initiation of starch granule (Seung et al., 2017). Both proteins contain CBM48 and coiled-coil motifs similar to that in the PTST1, but in the phylogenetic tree, they are closer to each other than to PTST1. The proposed function of PTST2 and PTST3 are the binding of glucan and then delivering maltooligosaccharides to starch synthase 4 (SS4) during granule starch initiation. However, it was evident that Arabidopsis *ptst2* mutant has zero or one large granule in most chloroplasts while chloroplasts in *ptst3* mutant revealed a minor reduction in granule number compared to the wild-type, whereas in *ptst2 /ptst3* double mutant has a fewer granules in the chloroplast compare to *ptst2* single mutant (Seung et al., 2017). Furthermore, there was other evidence suggested that PTST2 interaction with SS4 and PTST3 when targeted immunoprecipitation experiments revealed that SS4 and PTST3 co-purified with PTST2 (Seung and Smith 2018). By the same experiments, more proteins that are involved in starch granule initiation were discovered (Seung et al., 2018). They found that PTST2 also co-purifies with two plastidial coiled-coil proteins named MAR BINDING FILAMENT-LIKE PROTEIN (MFP1) and MYOSIN-RESEMBLING CHLOROPLAST PROTEIN (MRC). Their results showed that both proteins are required for normal starch granule initiation in Arabidopsis chloroplast.

Recently a yeast-2-hybrid screen reported in Arabidopsis revealed that there is new protein having a role in starch priming that physically interacts with SS4 named PROTEIN INVOLVED IN STARCH INITIATION (PII1) (Vandromme et al., 2018). The genetic studies found that Arabidopsis *pii1* mutant has one starch granule per plastid larger than wild type.

On the other hand, it was found that the rice Floury Endosperm 6 (FLO6) gene encodes an unknown protein with a C-terminal carbohydrate-binding module (CBM) ortholog of PTST2 (Peng et al., 2014). This study suggested that the (FLO6) has a regulatory role in starch synthesis and compound granule formation through direct interaction with isoamylase 1 (ISA1) which lead to target it to bind to starch. Furthermore, it was noted that the lacking of FLO6 results in the decreasing of starch content and the changes of morphology and amylopectin structure of starch granules.

1.11.2 Regulatory proteins in starch degradation

Very recent discovery identified several types of non-enzymatic proteins that are devoid of the known catalytic domain in the Arabidopsis chloroplast. Two of these proteins are involved in the regulation of starch degradation as plastidial starch-binding proteins named Early Starvation 1 (ESV1) and its homolog Like ESV1 (LESV) (Feike et al., 2016; Helle et al., 2018; Malinova et al., 2018). However, ESV1 and LESV proteins were analyzed by matrix-assisted laser desorption/ionization mass spectrometry. Using peptide fingerprinting, ESV1 protein composed of 426 amino acids (Fig 1.15) and a band with an apparent molar mass of ~50 kDa as the product of the At1g42430 gene.

1 MSEMAASSAI SLLDIKLRRF GVGASNHELR LTKWFKGDQAGAPTRRFTCF
51 ADMLAPIRRS EKSEERRFDQ KMSAHGAGIK TSSSAVPFAS PKSRFLSKQE
101 KFYPRCTPRL TGPQSRDTPP KRDTGIANEK DWGIDLLNENVNEAGTNEDG
151 SSWFRESGHD LGDNGYRCRW SRMGGRSHDG SSEWTETWWE KSDWTGYKEL
201 GVEKSGKNSE GDSWWETWQE VLHQDEWSNL ARIERSAQKQ AKSGTENAGW
251 YEKWWEKYDA KGWTEKGAHK YGRLNEQSWW EKWGEHYDGR GSVLKWTDKW
301 AETELGTKWG DKWEEKFFSG IGSRQGETWH VSPNSDRWSR TWGEEHFGNG
351 KVHKYGKSTT GESWDIVVDE ETYYEAEPHY GWADVVGDST QLLSIQPRER
401 PPGVYPNLEF GPSPPPEPDL PPDQPQ

Fig.1.15: The amino acid sequence of ESV1. The protein consists of 426 amino acids. (www.arabidopsis.org)

Although the programmes TargetP and ChloroP (Emanuelsson et al., 1999, 2000) predicted that ESV1 is devoid of chloroplast transit peptide (cTP), the plastidial localization of the protein was predicted by (Bayer et al., 2011) using a proteomic approach compared to the pea EST database. Further, the plastidial localization of Arabidopsis ESV1 was confirmed by (Feike et al., 2016). The authors used fluorescent tag protein experiments and transiently expressing ESV1 in leaves of *N. sylvestris* as C-terminal fusion to YFP. They found the ESV1-YFP fluorescence was associated with discrete bodies seemed to be as starch granules inside the chloroplast. Furthermore, in Arabidopsis leaves, it was also confirmed by mass spectrometry analysis and using fingerprinting that the first (1-58) amino acid of ESV1which is located in N- terminal was missing as transit peptide for entry into plastid (Chapter 4). However, ESV1 protein structure predicted has a proline and tryptophan-rich region and other aromatic amino acid residues at the C-terminus end. Tryptophan is an essential aromatic amino acid and one of the four of the highly conserved residues which are typically directly involved in glucan interactions (Christiansen et al., 2009). Previously, the role of individual tryptophan residues in the granule starch binding domain of *A. niger* glucoamylase 1 (G1) was investigated which has two binding sites (Williamson et al., 1997). While they mutated two tryptophans, (W590) and (W563), which are located in the binding site 1, in addition to mutating a third conserved tryptophan (W615) which is located in the C terminus of the SBD; there was a higher affinity for ligand in wild type than the mutant.

Furthermore, the reduction of stability of the third variant (W615) indicates the structural role of this tryptophan.

The high occurrence of tryptophan in the ESV1 sequence indicated that the protein has starch binding properties. However, in Arabidopsis lacking ESV1 display affects starch degradation at night. This is results in alteration of starch granule morphology by altering matrix organization; thus, accessibility of starch polymers to starch degradation enzymes while the overexpressing ESV1 revealed starch-excess phenotype (Feike et al., 2016). New biochemical evidence supported this finding (Malinova et al., 2018). The authors suggested that ESV1 are capable of altering glucan structures of native starches thereby impacting the action of two enzymes that regulate the initiation of starch degradation, GWD and PWD.

On the other hand, it was recognized a homolog to ESV1, Like-ESV1 (LESV) protein in the same way as ESV1 protein (Feike et al., 2016). This protein has the highest sequence similarity to ESV1 since it has 38% identical amino acid sequences, especially the tryptophan residue region. LESV protein was encoded in Arabidopsis by At3g55760 gene as the unknown starch binding protein. The protein is composed of 578 amino acids (Fig 1.16) and a band with a predicted molar mass of ~66 kDa.

1 MALRLGVSIG AALGSSHWDD GQRVRQRDFS ASVNFTAPVT SRRSLRGSRT
51 GVRILRVSNE GRESYLDMWK NAVDREKKEK AFEKIAENVV AVDGEKEKGG
101 DLEKKSDEFQ KILEVSVEER DRIQRMQVVD RAAAAISAAR AILASNNSGD
151 GKEGFPNEDN TVTSEVTETP KNAKLGMWSR TVYVPRSETS GTETPGPDFW
201 SWTPPQGSEI SSVDLQAVEK PAEFPTLPNP VLEKDKSADS LSIPYESMLS
251 SERHSFTIPPFESLIEVRKE AETKPSSETL STEHDLDLIS SANAEEVARV
301 LDSLDESSTH GVSEDGLKWW KQTGVEKRPD GVVCRWTMIR GVTADGVVEW
351 QDKYWEASDD FGFKELGSEK SGRDATGNVW REFWRESMSQ ENGVVHMEKT
401 ADKWGKSGQG DEWQEKWWEH YDATGKSEKW AHKWCSIDRN TPLDAGHAHV
451 WHERWGEKYD GQGGSTKYTD KWAERWVGDG WDKWGDKWDE NFNPSAQGVK
501 QGETWWEGKH GDRWNRSWGE GHNGSGWVHK YGKSSSGEHW DTHVPQETWY
551 EKFPHFGFFH CFDNSVQLRA VKKPSDMS

Fig.1.16: The amino acid sequence of LESV. The protein consists of 578 amino acids. (www.arabidopsis.org)

Chloroplast location of this protein was suggested by (Peltier et al., 2006; Kleffmann et al., 2004) when they used the chloroplast proteome analysis to identify many proteins that are of unknown function in Arabidopsis chloroplast. Later Feike et al. (2016) confirmed that it when the ChloroP program identified 56- amino acids in the N-terminal as chloroplast transit peptide (cTP). Like ESV1, LESV protein was found in association with starch granules, overexpression of LESV increased the number of granules, but these granules were highly variable in size, shape and smaller than granules of wild type whereas *lesv* mutant displays a less amylose content than wild-type plants (Feike et al., 2016).

Furthermore, it has been hypothesized that some protein inhibitors entrapped within the starch matrix may have a direct role in regulating starch metabolism (Helle et al. 2018).

1.12 The aims of the study

The work aims to study how the protein-glucans and protein-protein interaction are regulated during starch metabolism. Starch synthesis and degradation undergo different mechanisms including the interaction between starch itself and the chloroplasts proteins and, further, the interaction between these proteins.

The information about the role of plastidial proteins in the control of starch degradation is not clear. So far, there have been unknown mechanisms by which these proteins participate in controlling starch degradation. Therefore, the aim of the study was to provide an understaning of how proteins are used in the regulation of starch metabolism pathway.

Glucan water dikinase (GWD) and phosphoglucan water dikinase (PWD) are the key enzymes responsible for initiating the starch degradation process. Phosphorylation of glucan doubles helices at the granule surface by their activity rendering the starch structure less ordered, hence, facilitating the accessibility of hydrolytic enzymes to start the starch breakdown.

Recently, two non-catalytic proteins namely EARLY STARVATION 1 (ESV1) and its homology LIKE EARLY STARVATION 1 (LESV) were identified. It was supposed that both proteins are involved in regulating starch degradation by modulating the organization of the starch structure, thereby affecting the glucan accessible to the hydrolytic enzymes. To confirm the functional role of both proteins in regulating and adjusting the rate of starch degradation, biochemical assay was used to analyze their location and specific binding to the starch structure (amylose and amylopectin) and their influences on the GWD and PWD-mediated phosphate incorporation using ^{33}P-β-ATP with starch from various sources. Their effects were also analyzed on the hydrolysing enzymes as they act downstream of the two dikinases enzymes, isoamylase (ISA), beta-amylase (BAM) and alpha-amylase (AMY). Additionally, it was tested if there was a protein-protein interaction between ESV1 and LESV or between each one with GWD and PWD that would regulate the phosphorylation process using crosslinking assay or between GWD and PWD using yeast two-hybrid assay.

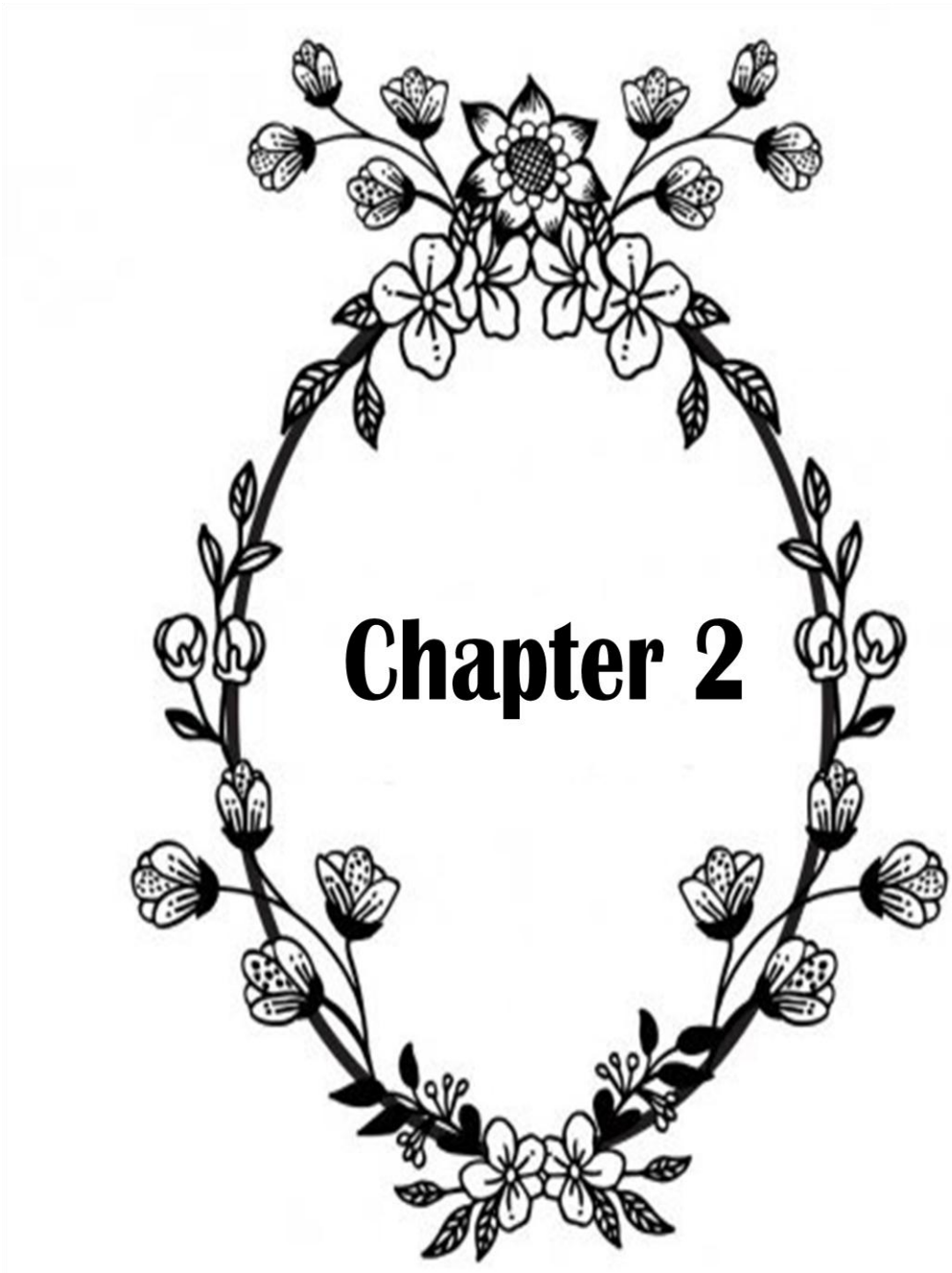
Chapter 2

2. Materials and Methods

2.1 Materials

2.1.1 Plant material and growth conditions

Arabidopsis thaliana (Col-0) and Arabidopsis *sex 1-8* mutant were cultivated as described by Mahlow et al., (2014); Malinova et al., (2017) in a growth chamber under controlled conditions (12 h light, 22°C/12 h dark, 17°C for Arabidopsis *sex 1-8* mutant and 12 h light, 20°C/12 h dark, 16°C for *Arabidopsis thaliana* (Col-0)) and approximately 100 µmol quanta m^{-2} s^{-1}. Six-week-old rosette leaves were harvested after 10 h in the light, directly frozen in liquid nitrogen and stored at -80 °C until use; relative humidity throughout the light/dark cycle was kept at 60% unless stated otherwise. Potato and maize *waxy* and *amylose extender* mutant starches were purchased from ICN Biomedicals (https://www.mpbio.com) and National Starch (http://www.nationalstarch.com), respectively.

2.1.2 Starch isolation

Starch granules were isolated from Arabidopsis wild-type or *sex 1-8* mutant leaves (Malinova et al., 2014). Rosettes from several plants (at least more than 20) were harvested and immediately frozen in liquid nitrogen. Subsequently, leaf material was ground to a fine powder in a frozen state using a precooled mortar. Soluble compounds were extracted from 0.5 g FW each in 1.5 ml 0.7 N perchloric acid (30 min at 4°C). Following centrifugation (10 min at 15,000 *g*), each supernatant was adjusted to pH 5.5 by adding 335 µl 3.38 M KOH containing 0.675 M KCl and 0.675 M MES. Precipitated potassium perchlorate was removed by centrifugation (10 min at 20,000 *g*). Each supernatant was loaded onto a 1 ml column of mixed bed resin (AG 501–x8 [D] Resin, Bio-Rad) to remove salts. Neutral compounds were eluted from the column by adding 5 ml of water. Each eluate was divided into several aliquots that were dried using a speed vac.

2.1.3 Chemicals

All the chemicals used in the experiments were obtained from Sigma Aldrich, Canada, unless otherwise specified. [B-^{33}P]ATP 3000 Ci mmol^{-1}) was purchased from Hartmann Analytic (Germany, https://www.hartmann-analytic.de).

2.1.4 Enzymes

Beta-amylase (Barley) was ordered from Sigma Aldrich (https://www.sigmaaldrich.de). Alpha-amylase (Bacillus amyloliquefaciens) and isoamylase (Pseudomonas *sp*) enzymes were ordered from MEGAzyme (https://www.megazyme.com). For the expression and purification of GWD and PWD from potato (*Solanum tuberosum L.*); and ESV1 from Arabidopsis, proteins were expressed without transit peptide using pET23b vector (Novagen) and the *E. coli* strain BL21 (DE3) in the same protocol performed to the expression and purification of LESV.

2.2 Methods

2.2.1 Preparation of *E.coli* LB21 competent cells

To prepare electrocompetent *E.coli*, 100 ml LB medium was incubated containing 1.5 ml of overnight culture at 37 °C and grew to OD600 of 0.5. After that, the bacterial cells were centrifuged at 2,000 g, 4 °C for 10 min. The cell pellet was washed 2 times with sterile ice-cold water. Finally, the washed pellet was resuspended in 150 µl 10 % [v/v] glycerol in water and aliquots (each 50 µl) were transferred to a new 1.5 ml tube and stored at -80 °C.

2.2.2 Preparation of *E.coli* DH5 α competent cells

E.coli DH5α strain was streaked from a glycerol stock onto LB agar plate and allowed to grow at 37 °C overnight. A single colony from the plate was inoculated in 2 ml LB medium and incubated overnight at 37 °C and 200 rpm to allow bacterial growth. Following incubation, 1 ml of the primary culture was inoculated in a flask containing 100 ml of LB medium and kept at 27 °C, 200 g. The culture was grown to OD600 of 0.35-0.4. Following this, culture was transferred to an ice bath for incubation (15 min). Subsequently, culture was transferred to sterile ice-cold conical tubes. Cells were harvested by centrifugation at 3,000 rpm for 10 min at 4 °C. After decanting the

supernatant, the cells pellets were resuspended in 60 ml of cold Inoue solution [55 mM $MnCl_2$ $4H_2O$, 15 mM $CaCL_2$ $2H_2O$, 250 mM KCl, 10 mM PIPES/KOH (0, 25 M, pH 6,7)] and incubated on ice for 15 min. The cells suspension was once again subjected to centrifugation at 3,000 rpm for 10 min at 4 °C. After discarding the supernatant, the cells pellets were resuspended in 0, 5 ml DMSO (RT) and incubated for 10 min on ice. The cell suspension was finally dispensed as 50 µl aliquots into sterile ice-cold 1.5 ml microfuge tubes, flash-frozen in liquid nitrogen and stored at -80 °C.

2.2.3 Preparation of agarose gel electrophoresis

Agarose solution 1% [w/v] was prepared in 1X TAE buffer (2M Tris/HCl (pH8); 0, 05 M EDTA; 1 M acetic acid) and dissolved completely by boiling. Agarose solution was allowed to cool to 50-60 °C, followed by addition of ethidium bromide (1 mg/ml, Roth). Molten agarose was poured into the casting tray and allowed to solidify for 30 min at room temperature. The comb was removed from the solidified agarose gel and the gel was placed in a running tank containing 1X TAE buffer. DNA samples were prepared by adding 6X loading buffer (40% [v/v] Glycerol; 0,25% [w/v] Bromophenol blue; 0,25% [w/v] xylene cyanol) to a final concentration of 1X and subsequently loaded onto the agarose gel, it used 1kb DNA ladder as a marker ladder (1µg/µl, Invitrogen). Electrophoresis was carried out at constant voltage (96 V) for 30 min; the gel was visualized under UV light.

2.2.4 Preparation of SDS-PAGE

The separating gel used for SDS-PAGE contained 1, 5 M Tris-HCl pH 8.8; 7.5% or 9% [w/v] acrylamide (Rotiphoresegel 30% (37,5: 1), Roth); and 10% [w/v] SDS. Gel polymerisation was started by addition of 10% [w/v] ammonium persulfate (APS, Sigma-Aldrich) and 0.05% [v/v] tetramethylethylenediamine (TEMED, Biorad). The stacking gel contained 5% [w/v] acrylamide, 0.5 M Tris-HCl, pH 6.8; 10% [w/v] SDS; 10 % [w/v] of APS and 0.05 % [v/v] of TEMED. Electrophoresis of gels was carried in a running buffer (0,25mM Tris; 1% [w/v] SDS and 192 mM glycine) at room temperature, 250 V, and 30 mA for 30 min and then at 60 mA until the required separation was achieved.

2.2.5 Western blot

The transfer of proteins to PVDF membrane (Thermo Scientific) was carried out using the Trans-Blot SD transfer apparatus (Bio-Rad) according to the manufacturer's instructions. Blotting was performed overnight at 12 V at room temperature. Then the blot was incubated for one hour at room temperature in blocking solution TBST (100 mM Tris, pH 7.5, 150 mM NaCl, 0.1 % [v/v] Tween 20) containing 3% [w/v] dried milk powder. After that, blots were incubated for one hour with primary antibodies at a 1:1000 (v/v) dilution in blocking solution. Then the blot was washed six times for five min in TBST. The secondary antibody (anti-mouse, conjugated to alkaline phosphatase) was used in a 1:10,000 dilution in blocking solution and then blot was incubated with it for one hour at room temperature. The membrane was washed in TBST as before. To visualise alkaline phosphatase activity, BCIP®/NBT reagent (Sigma-Aldrich) was used.

2.2.6 Detection of Like-Early Starvation 1 protein LESV in *Arabidopsis thaliana*

For protein extraction, leaves from individual 2-weeks-old rosettes of Arabidopsis plant were harvested, immediately frozen in liquid nitrogen, and subsequently broken using a driven blender. The frozen homogenate was suspended in extraction buffer (100 mM HEPES-NaOH, pH 7.5, 1 mM EDTA, 5 mM dithioerythritol, 0.5 mM phenylmethylsulfonyl fluoride, and 10 % [v/v] glycerol). After filtration of the homogenate through a mesh 100 (Sigma-Aldrich, St. Louis MO, USA), the suspension was centrifuged at 7500 g for 12 min, 4°C. The supernatant was rejected and the green pellet was carefully suspended in the isolation buffer and differential centrifugation step was repeated. After centrifugation, the supernatant was removed and the pellets were collected and then resuspended in isolation buffer. The protein concentration of the suspension was determined using a BCA protein assay kit, the indicated amounts of protein were denatured by adding 3-fold concentrated SDS-containing buffer and heating (5 min at 95°C) and loaded onto an SDS-PAGE gel.

2.2.7 Sequence identification of Like-Early Starvation 1 protein LESV in *Arabidopsis thaliana* genome

The sequence of LESV protein was identified in the *Arabidopsis thaliana* genome using the database "Tair" (https://www.arabidopsis.org/). (Fig. 2. 1)

Fig 2.1: The sequence of LESV (AT3G55760.1, 1737 bp)

```
   1 ATGGCTTTGC GTTTAGGTGT TTCTATAGGG GCAGCTTTGG GTTCCTCTCA
  51 TTGGGACGAC GGACAACGAG TACGACAACG TGACTTCTCC GCTTCTGTGA
 101 ATTTCACCGC ACCGGTTACG AGCCGGAGGA GCTTAAGGGG TAGTAGAACC
 151 GGTGTGAGGA TTCTTAGGGT TTCAAATGAA GGACGCGAAT CGTACCTCGA
 201 TATGTGGAAG AACGCTGTTG ATCGCGAGAA GAAAGAGAAG GCCTTTGAAA
 251 AAATTGCAGA GAATGTTGTA GCTGTTGATG GTGAGAAGGA GAAAGGAGGA
 301 GACTTGGAGA AGAAGAGCGA TGAGTTTCAG AAGATCCTCG AGGTTTCCGT
 351 TGAGGAAAGA GATCGGATTC AGCGAATGCA GGTCGTTGAT CGTGCCGCTG
 401 CCGCAATCTC CGCAGCTAGA GCTATTCTCG CCTCTAACAA TTCCGGCGAC
 451 GGCAAAGAAG GATTCCCAAA TGAAGACAAC ACTGTCACAA GTGAAGTCAC
 501 AGAGACACCG AAAAATGCTA AACTTGGAAT GTGGAGCAGA ACAGTGTATG
 551 TGCCACGGTC AGAAACTTCA GGGACTGAGA CACCAGGACC AGATTTTTGG
 601 TCATGGACAC CTCCTCAAGG TAGTGAAATT AGTTCTGTGG ACTTGCAGGC
 651 TGTGGAAAAG CCTGCTGAGT TTCCAACTTT GCCAAATCCT GTATTGGAGA
 701 AAGATAAATC AGCGGATTCT CTTTCGATAC CATATGAGAG TATGCTTTCT
 751 TCTGAAAGAC ATAGCTTTAC TATCCCGCCT TTTGAGTCTT TGATTGAGGT
 801 TCGAAAAGAG GCTGAGACGA AGCCTAGCTC CGAGACTTTA TCGACAGAAC
 851 ATGACCTTGA TCTCATATCT TCAGCAAACG CGGAAGAAGT AGCTCGTGTT
 901 CTTGATAGTT TGGATGAATC TTCAACGCAT GGAGTTAGCG AAGATGGATT
 951 GAAGTGGTGG AAGCAAACGG GTGTGGAGAA AAGACCTGAT GGTGTGGTTT
1001 GCAGGTGGAC AATGATACGT GGGGTTACTG CTGATGGTGT TGTTGAGTGG
1051 CAAGATAAGT ATTGGGAGGC TTCTGATGAT TTTGGGTTCA AGGAACTTGG
1101 TTCTGAGAAA TCAGGACGTG ATGCCACTGG AAACGTGTGG CGTGAGTTCT
1151 GGAGAGAGTC AATGAGCCAG GAGAATGGTG TTGTGCATAT GGAGAAAACT
1201 GCAGACAAAT GGGGAAAGAG TGGACAAGGT GATGAATGGC AAGAGAAATG
1251 GTGGGAGCAT TACGATGCTA CCGGAAAATC AGAAAAATGG GCTCATAAGT
1301 GGTGCAGCAT TGACCGCAAC ACGCCTCTTG ACGCTGGCCA CGCTCATGTC
1351 TGGCACGAGA GGTGGGGAGA GAAGTATGAC GGGCAAGGCG GAAGCACAAA
1401 GTACACAGAC AAGTGGGCGG AACGGTGGGT AGGTGACGGT TGGGACAAAT
1451 GGGGAGACAA ATGGGACGAG AACTTTAACC CGAGCGCTCA AGGAGTGAAA
1501 CAAGGTGAGA CTTGGTGGGA AGGGAAGCAC GGCGACAGAT GGAACCGAAG
1551 CTGGGGAGAA GGTCACAACG GATCAGGATG GGTTCACAAA TACGGAAAAA
1601 GCAGCAGCGG TGAACACTGG GACACACATG TACCACAAGA AACTTGGTAT
1651 GAGAAGTTCC CTCACTTTGG CTTCTTCCAC TGTTTTGACA ACTCTGTTCA
1701 GCTCCGAGCC GTTAAGAAGC CTTCTGATAT GTCCTAG
```

2.2.8 Cloning of Arabidopsis LESV protein

LESV sequence was cloned from *Arabidopsis thaliana* mRNA by generating first-strand cDNA for use in two-step Reverse Transcription Polymerase Chain Reaction (RT-PCR).

Primer design for PCR cloning of LESV sequence (DNA) was conducted using DAN as a template for PCR. Restriction enzymes analysis of LESV sequence was formed to find restriction enzymes that do not cut in the LESV sequence. EcoRI and NotI were the restriction enzymes used in this case (Table 2.1).

Table 2.1: primers with restriction enzymes

Primer with EcoRI **GAATTC**ATGGCTTTGCGTTTAGGTGTTT
Primer with NotI **GCGGCCGC**GGACGTATCAGAAGGCTTC

After thawing, reagents were mixed, briefly centrifuged, and kept on ice. After that, the reaction components were added into a sterile, nuclease-free tube on ice in the indicated order (Table 2.2):

Table 2.2: Reaction components to prepare cDNA

Template RNA	Poly (A) RNA	0,1 pg-500 ng	2 µl
Primer	Oligo (dT)18(#SOBI)	100 pmol	1 µl
dNTP Mix, 10mM each (#RolgII)		0,5 mM final concentration	1 µl
Water, nuclease-free			10,5 µl
5XRT Buffer			4 µl
Thermo Scientific™RiboLock RNase Inhibitor (#EO0381)		20 U	0,5 µl
Maxima Reverse Transcriptase		200 U	1 µl
Total Volume			20 µl

Gently mixed and centrifuged briefly then incubate for 30 min at 50 C°. For the transcription of GC-rich, the reaction temperature was increased to 65 ° C for 2 min. It used 2 µl of the reaction mix to perform PCR using Q5 Hot Start High-Fidelity DNA polymerase (BioLabs, https: //www.neb. com) in a 50 µl volume (Table 2.3). It was assembled all reaction components on ice and quickly transferred the reaction to a thermocycler pretreated to the denaturation temperature (95 ° C)

Table 2.3: PCR components using Q5 Hot Start High-Fidelity DNA polymerase

Components	**50µl Reaction**	**Final concentration**
5X Q5 Reaction Buffer	10 µl	1X
10 mM dNTPs	1 µl	200 µM
10 mM Forward Primer	2,5 µl	0,5 µM
10 mM Reverse Primer	2,5 µl	0,5 µM
Template DNA	2 µl	< 1,000ng
Q5 Hot Start High-Fidelity DNA polymerase	0,5 µl	0,02 U/µl
Nuclease Free Water	31,5 µl	

Gently mixed the reaction then transferred PCR tubes to a PCR machine (programme conditions) (Table 2.4) and begin thermocycling.

Table 2.4: Thermocycling for PCR:

STEP	**TEMPERATURE**	**TIME**
Initial Denaturation	98 C°	30 second
30 Cycles	98 C° 60 C° 72 C°	10 second 30 second 30 second
Final Extension	72 C°	2 minutes
Hold	4-10 C°	

It was added 0, 5 µl of Dream *Taq* polymerase to the blunt-ends of DNA fragments that have been amplified. This step was done for two minutes before the end of the thermocycling.

2.2.9 Agarose-gel electrophoresis

After the end of the thermocycling, the PCR product was purified by 1% [w/v] agarose gel electrophoresis.

2.2.10 DNA-Extraction from agarose gel (GFX PCR DNA and GEL Band Purification Kit)

After the PCR DNA was illustrated, the band was excised from the gel using appropriate equipment [Vilberd Normad Transillminator], and then purified using Illustra GFX PCR DNA and Gel Band Purification Kit (GE Healthcare). After that, 30 µl of DNA-free water (Promega) was run through the column to elute the DNA and its concentration was estimated by the Nanodrop 2000 spectrophotometer.

2.2.11 Ligation of DNA fragments

T4 DNA Ligase was used to ligate the DNA of LESV into the vector (pGEM-T Easy vector). Ligation was performed using the protocol for pGEM-T and pGEM-T Easy Vector System [Promega]. The reaction shown in (Table 2.5) was assembled in a sterile microcentrifuge tube.

Table 2.5: Ligation reaction for TA cloning

Component	**Standard reaction (volume)**
2X Rapid Ligation Buffer, T4 DNA Ligase	5 µl
pGEM-T Easy Vector (50 ng)	1 µl
PCR Product	3 µl
T4 DNA Ligase (3Weiss units/µl)	1 µl
The final volume	10 µl

The reactions were mixed by pipetting and incubated at room temperature for one hour. The reactions were then incubated overnight at 4 °C to increase the number of transformation.

2.2.12 Transformation of plasmid DNA in competent *E.coli* cells

Fifty µl of the competent *E. coli* DH5α cell suspension were placed in chilled microcentrifuge tubes kept on ice for cooling. After that, 2 µl of the ligation reaction was added to the competent *E. coli* DH5α cells.

The cells were mixed by gently flicking the tube and then incubated on ice for 30 minutes. The cells were then heated and shocked for 40 seconds at 42 C°and immediately placed back on the ice for 2 minutes. After that, 300 µl SOC media [0, 5% [w/v] Yeast extract; 2% [w/v] Tryptone; 10 mM NaCl; 2,5 mM KCl, 10 mM $MgCl_2$; 10 mM $MgSO_4$; 20 mM glucose] was added to cells and the tube was incubated for 1 hour at 37 C°, with shaking (~1500 rpm). Using a sterile glass spreader, 50 µl 2% [w/v] X-Gal and 50 µl 0,2 M IPTG (Isopropyl α-D-1-thiogalactopyranoside) was spread on an LB agar plate [10g/l Typtone; 5 g/l Yeast extract; 10 g/l NaCl; 15% Agar] containing 100 mg/ml of Ampicillin. After that, 100-150 µl of the cells were spread on the LB-agar plate and incubated overnight at 37 C°. After that, the plate was removed from the incubator to screen blue-white colonies. Blue colonies contained plasmid vectors without the insert, while white colonies contained plasmid vectors with insert.

2.2.13 Colony PCR

Colony PCR was used to check for insertion of the correct DNA following ligation. To do that, it picked well-isolated colonies to inoculate 5 µl of sterile water in a PCR tube. Part of the colonies transferred to agar plate to prepare a master plate and to 5 ml LB media containing 100 mg/ml ampicillin for overnight culture and miniprep. A master mix containing the reaction in the order listed (Table 2.6) was assembled in one sterile tube on ice and then 5 µl of colonies lysate was added. These were run according to the PCR programme shown in (Table 2.4).

Table 2.6: Reaction components for master mix

Reaction	Volume
10X PCR Reaction Buffer	1 µl
dNTP-Mix 2,5 mM	0,8 µl
Forward Primer [EcoRI] 10 mM	0,1 µl
Reverse Primer [NotI] 10 mM	0,1 µl
Taq DNA Polymerase 5 U/µl	0,25 µl
Sterile Nuclease-Water to	5 µl

The reaction was then analysed on a 1% [w/v] agarose gel.

2.2.14 Plasmid preparation (Miniprep)

The colony PCR was used to identify positive colonies containing the desired insert. A single positive colony was picked up from a master plate, incubated in 5 ml LB media with 100 mg/ml Ampicillin at 37 C° overnight. After that, the 5 ml of bacterial culture was transferred into a 50 ml falcon tubes and centrifuged for 5 minutes at room temperature and 1800 rpm. The medium was completely removed. To purify the plasmid, miniprep was performed according to the manufacturer's instructions (QIAprep Spin Miniprep Kit (250)). To elute the plasmid 30 µl of DNA-free water (Promega) was run through the column.

2.2.15 Restriction with endonucleases

The insert of DNA was checked by restriction digestion. The restriction cutting mix was prepared according to (Table 2.7), mixed briefly, centrifuged and then incubated for 30 minutes at 37 C°. The reaction was then inactivated by heating at 80 C° for 5 minutes. After the restriction, the digests were analyzed on agarose gel 1% [w/v] to determine the size of the fragments.

Table 2.7: Restriction cutting mix

Component	Volume
Nuclease-free water	3 µl
10X Fast digest green buffer	1 µl
Plasmid vector	5 µl
Fast digest Not I	0,5 µl
Fast digest EcoRI	0,5 µl
Total volume	10 µl

2.2.16 Quantification of DNA

To calculate the amount of DNA in a sample, a Nanodrop 2000 was used. The quantity of DNA was calculated based on its absorbance at 260 nm.

2.2.17 Sequencing

Sequencing was done in LGC genomics (https://shop.lgcgenomics.com/). 20 µl of the 100 ng/µl DNA was sufficient for one reaction. The primers used for sequencing were T7pro and SP6-20 (Table 2.8).

Table 2.8: Primers used for sequencing

Name	Sequence
T7pro	TAATACGACTCACTATAGGG
SP6-20	ATTTAGGTGACACTATAG

2.2.18 Subcloning of LESV sequence into pET23B expression vector

2.2.18.1 Restriction digestion for cutting the target sequence and vector

For subcloning of the LESV sequence from plasmid pGEM-T Easy vector carrying LESV sequence into pET23b vector, two DNA oligodeoxyribonucleotides, 5′ sense primer, containing an EcoRI-Restriction site GAATTC and 3′ antisense primer, containing a NotI-Restriction site GCGGCCGC were synthesized.

In the separated tube, the plasmid vector (pET23b) and LESV sequence were digested with EcoRI and NotI restriction enzymes in a microcentrifuge. The following mixture (Table 2.9) was set up for each digesting reaction.

Table 2.9: Mixture of digesting reaction

Reaction	Volume
Nuclease-free water	3 µl
10X fast digest green buffer	1 µl
Plasmid vector pET23b or DNA of LESV	5 µl
Fast digest EcoRI	0,5 µl
Fast digest NotI	0,5 µl
Total volume	10 µl

Thereafter the reaction was incubated at 37 C° for 30 minutes then 5 minutes at 80 C° to inactivate the reaction. The reaction was then run on a 1% [w/v] agarose gel. Both bands were purified from 1% [w/v] agarose gel and extracted by GFX PCR DNA and Gel Band Purification kit.

2.2.18.2 Ligation of LESV sequence into pET23b expression vector

To ligate the LESV sequence fragment into the pET23b vector, 2:1 of insert DNA termini to vector was used. The reaction shown in (Table 2.10) was assembled in a sterile microcentrifuge tube and incubated at 4C° overnight.

Table 2.10: Component reaction of ligation of LESV sequence into pET23b Vector

Reaction	Volume
pET23b(+) vector (15 ng/µl)	3,3 µl
10X Ligase buffer for T4-DNA-Ligase	2 µl
T4-DNA Ligase [5U/µl]	2 µl
Insert-DNA (2:1)	3 µl
Water	9,7 µl
Total volume	20 µl

After that, the plasmid pET23b was transferred into electrocompetent *E.coli* BL21 [DB3] cells. For transformation, 50 µl *E.coli* BL21 competent cells were thawed on ice. 5 µl of the ligation reaction was added and transferred to chilled electroporation cuvette (2 mm) and immediately electroporated using an electro impulse ["Micropulser" programme: EC2]. At room temperature, 300 µl of SOC media was added to the cuvette immediately after electroporation and transfer to sterile tubes and cells were incubated on LB agar plates with 100 mg/ml ampicillin.

2.2.18.3 Minipreparation

Colonies were initially screened by PCR. A single colony of *E.coli* containing plasmid of interest was grown in 5 ml LB media with 100 mg/ml ampicillin overnight at 37 C°/220 rpm. To purify plasmid, miniprep was performed.

2.2.19 Cloning of LESV without transit peptide (tLESV)

To truncate a putative peptide (Fig 2.2) from full-length LESV primers with EcoRI and NotI were the restriction enzymes used (Table 2.11).

ATGGCTTTGC GTTTAGGTGT TTCTATAGGG GCAGCTTTGG GTTCCTCTCA TTGGGA

Figure 2.2: A putative transit peptide of LESV (Feike et al., 2016)

Table 2.11: Primers with the restriction enzymes for truncate LESV

Name	**Sequence**
EcoRI	**GAATTC**ATGGTTTCAAATGAAGGACGCG
NotI	**GCGGCCGC**GGACGTATCAGAAGGCTTC

For PCR 0, 5 µl of the plasmid (pET23b) containing DNA of LESV was used.. After that PCR product was purified by agarose gel electrophoresis and then gel extraction (GFX PCR DNA and Gel Band Purification Kit). 4µl of the DNA of truncate LESV was

inserted into 2 µl of the pET23b plasmid vector (the ratio was 2:1) and then the mixture of ligation was incubated at 4 C° overnight.

After that, 5 µl of the ligation mixture was transformed into 50 µl *E.coli* BL21 (D3+) and then incubated at 37 C° overnight. After that, some of the positive colonies were selected to colony PCR. The correct plasmid size was preparation (Miniprep) and was confirmed by DNA sequencing. The plasmid was kept in -20 C° until use.

2.2.20 Expression and small scale purification of LESV and tLESV in *E.coli* BL21 cells

Here, 2 µl of plasmid was added to 50 µl of competent cells (*E.coli* BL21). The cells transferred to chilled electroporation cuvette (2mm) and immediately electroporated using an electro impulse ["Micropulser" programme: EC2]. After that, 300 µl of SOC media was added to the cuvette then transferred to a new sterile tube. The tube incubated at 37 C° for 1 hour with shaking at 1200 rpm. After incobating, 100-200 µl of cells were spread on the LB agar plates with 100 mg/ml ampicillin and incubated overnight at 37 C°. On the next day, a single colony was picked from the plate and incubated in 5 ml LB media with 100mg/ml ampicillin at 37 C° overnight. From the overnight incubation 2, 5 ml of culture was transferred to big flasks containing 500 ml LB media with 100 mg/ml ampicillin. The flasks were incubated at 37 C° with shaking at 225 rpm until optical density 600 (OD600) reached 0,6-0,8. One flask was inducedwith IPTG final concentration 1mM or without IPTG as a control. Both flasks were incubated at 18 C° with shaking at 225 rpm overnight. The culture was centrifuged at 6000g for 10 minutes at 4 C°. The medium was discarded and the cells were kept. After that, the cells were resuspended in extraction buffer [20 mM NaH_2PO_4/ NaOH (pH 7,4); 500 mM NaCl; 20 mM imidazole; 1 mM DTE; 0,4 mM PMSF; 0,4 mM benzamidine; 0,4 mM amino Capron acid], then subjected to sonication (SONOPULS HD 2070) for 2 minutes with pulse 3, 65% energy. The cells suspension were centrifuged (centrifuge"3K30" Rotor: 19776-H) for 12 minutes and 20000 g at 4C°. The supernatant was collected in new tubes and the cells pellets were also kept. After that, 20 µl of samples containing the supernatant and cell pellets were mixed with 10 µl 3X SDS sample buffer and heated for 3 minutes at 95 C° and 1200 rpm by (Thermomixer "Compact"). And then, 20 µl of samples were run on two different sets of 7, 5% SDS-PAGE. Here, 5 µl of molecular

marker (Thermofisher, PageRuler) was loading alongside samples. One gel was stained by coomassie stain to visualize the protein bands and the other was subjected to immunodetection. Immunodetection was based on the use of the primary antibody against "His-tag" and secondary antibody "anti-mouse". To visualize the protein bands in the PVDF membrane, it was coupled to AP buffer (33 µl of BCIP 50mg/ml in 100% dimethylformamide and 66 µl of NBT in 70% dimethylformamide).

2.2.21 Preparation of glycerol stock for *E.coli* BL21 cells containing the plasmid with the protein of interest

Picked a single colony from the agar plate and inoculated 10 ml LB media with 100mg/ml ampicillin. Incubate it overnight at 37 C° at 220 rpm. After that, added 8ml of the overnight culture to 2ml of 100% glycerol (sterile) in a falcon tube and gently mixed by vortexing or pipetting and divided into aliquots and then frozed (-80 C°).

2.2.22 Expression and purification of recombinant LESV and tLESV (large scale)

After proteins expression in *E.coli* BL21 and harvesting the cells, cell pellets were resuspended in extraction buffer and cells membranes were broken using sonication (3 pul; 67% energy for 2 minutes). The resulting solution was twice centrifuged for 12 minutes at 20000 g at 4 C°. The supernatant was filtered with a 0, 45 µm (Rotilabo-syringe filter, Roth) pore size filter into a plastic tube.

For the loading of the filtered supernatant, 1ml Ni-NTA resin (His TrapFF) (GE healthcare) was washed with 10 ml water then washed with 10 ml 500 mM imidazole-elution buffer [500 mM imidazole/HCl (pH7, 4); 500 mM NaCl; 20 mM NaH_2PO_4] and equilibrated with 10 ml 20 mM imidazole buffer [20 mM imidazole/HCl (pH7, 4); 500 mM NaCl; 20 mM NaH_2PO_4]. After that, sterile filtered supernatant protein lysate was loaded onto the column at a flow rate of 1ml/min. Subsequently, the column was washed with at least 20 column volume of extraction buffer to remove any non-specific protein binders.

Stepwise gradient elution of the His-tagged protein from the His Trap FF crude column was using six different concentrations of the imidazole-elution buffer. It was 1 ml elution buffer for each fraction (Table 2.12).

Table 2.12: Imidazole-elution buffers

Imidazole concentration in mM/HCl (pH7,4)	NaCl in mM	NaH_2PO_4 in mM	Volume in ml
50	500	20	3
75	500	20	2
100	500	20	2
150	500	20	2
250	500	20	3
500	500	20	5

From each fraction 20 µl mixed with 10 µl 3X SDS-sample buffer and heated for 3 minutes at 95 C° and 1200 rpm by thermomixer "Compact" were analyzed by SDS-PAGE.

Elution protein fractions were collected and concentrated by centrifuging (Centrifuge: "3-18K" Rotor; 11180) at 3800 g at 4 C° for 20 minutes in millipore-filter (Amicon Ultra Centrifugal Filter Units, Merck, 50 kDa). Repeat the centrifugation with buffer exchanged HEPES-Buffer (100mM HEPES/NaOH (pH7, 5); 2 mM EDTA; 5 mM DTE; 0,4 mM PMSF; 10% [v/v] glycerol). The proteins were collected and divided into aliquots and then frozen at -80 C°.

2.2.23 Measuring proteins concentration

Bradford assay was performed in 1 ml of a solution containing 1x Bradford solution diluted from 5x stock (Bio-Rad) and 1or 2 µl of protein solution. Samples were incubated for 10 minutes. The absorbance of the solution was read at 595 nm using a spectrophotometer "Cary 100 Bio.

2.2.24 Protein sample preparation for mass spectrometry

Protein bands were excised from the gel and destained in 1 ml acetonitrile and 40% 50 mM NH_4HCO_3 during approximately 30 min with a change of destaining buffer in between. Gel pieces were dehydrated in 50 µl acetonitrile during 5 min and dried in speed vac. Volume from 4 ng/µl trypsin sequencing-grade were reconstituted in pre-cooled 50 mM NH_4HCO_3 and 20 µl of this solution was used for dehydration of the gel

pieces on the ice during 30 min and subsequently incubated overnight at 37 °C. The resulting peptides were extracted by washing the samples with 30 µl water at 37 °C for ~ 30 min under continuous agitation. The supernatant was transferred to the new tube and again 20 µl acetonitrile was added to the samples and left in the RT for 3 min. The solution was transferred to the previous supernatant. The samples were acidified with 20 µl 5 % formic acid at 37 °C for 20 min. The supernatant was combinded with the previous supernatant and 20 µl acetonitrile was added to the samples and left in the RT for 3 min and collected the supernatant to the previous one. The extracts were finally dried in a vacuum concentrator and dissolved in a solution of 8 µl 0.1% formic acid and 2 µl acetonitrile. For mass spectrometric analysis, 0, 3 µl samples and 0,3 µl HCCA matrix were placed on the matrix plate and left to dry. Peptides were analyzed by mass spectrometry with MALDI-TOF (Matrix-Assisted Laser Desorption Ionization-Time-Of-FlightBruker Microflex) and Tandem mass spectrometry using MALDI-LTQ MS (Thermo Scientific). Mascot database search was conducted using either Peptide Mass Fingerprint or MS/MS ions source with a peptide tolerance set to 0.6 Da for the former and 0.6 MS/MS tolerance for the latter. One missed cleavage was allowed for the search and no fixed or variable modifications.

2.2.25 Glucan Binding Assay

2.2.25.1 Detection of tLESV binding to different glucans

For the binding assay, 50 mg for each potato starch or amylose and maize wild-type starch or amylopectin or 20 mg for each Arabidopsis wild-type, *sex 1-8* starches, and maltodextrin were washed five times with water.

The starch pellets were resuspended in 100 µl of binding buffer [50 mM HEPES/KOH pH 7.4, 1 mM EDTA, 6 mM MgC_2, 2 mM DTE, 0.4 mg ml^{-1} bovine serum albumin (BSA)] and incubated with 15 µg of tLESV for 15 min at 30 C° under continuous agitation. After that, the samples were centrifuged for 2 min at 14000 g, and then the pellets were washed once with a binding buffer. All the pellet fractions dissolved with 100 µl water. And then, 20 µl of each sample mixed with an SDS sample buffer and was heated for 3 min at 95 C° and 1200 rpm by thermomixer “Compact”.

The bound protein was analyzed by SDS-PAGE using 9% [w/v] separation gel then transferred to nitrocellulose (0.2 μm pore size) followed by western blotting. To determine the strong binding of tLESV to the starch, 20 mg of Arabidopsis wild-type or maltodextrin b-type and 50 mg of potato tuber or amylose were washed five times with water and once with binding buffer. The pellets were resuspended in 100 µl of binding buffer and incubated with 15 µg of tLESV for 15 min at 30 C° under continuous agitation. After that, the samples were centrifuged for 2 min at 14000 g, the supernatant was collected as a first wash (W1), and the pellets were washed one time with binding buffer and collected as a second wash (W2). Both fractions mixed with SDS sample buffer. The pellets were washed twice with equal volume of SDS sample buffer (final concentration 1X) and collected as (E1) and (E2). All the fractions were heated for 3 min at 95 C°. After that, 20 µl of each sample was loaded on 9% [w/v] SDS-PAGE followed by anti-His immunodetection.

2.2.25.2 tLESV interaction to the starch granules after isoamylase and beta amylase-mediated removal of surface glucan chains

Here, 50 mg of potato or 30 mg of Arabidopsis *sex1-8* starches were washed five times with water. The starches were resuspended in 100 µl of incubation buffer (10 mM Na-acetate, 2 mM DTE, 7 U isoamylase) or (5 mM citric acid, 20 U of beta-amylase). As controls, starches were also incubated in the absence of both enzymes overnight at 37 ^{o}C with continuous agitation. After that, the samples were centrifuged and the pellets were washed (1 ml each) twice with 2% [w/v] SDS and 10 times with water. The starch pellets were resuspended in 100 µl of binding buffer [50 mM HEPES/KOH pH 7.4, 1 mM EDTA, 6 mM $MgCl_2$, 2 mM DTE, 0.4 mg ml-^{1}bovine serum albumin (BSA)] and incubated with 10 µg of tLESV for 30 min at 30 ^{o}C under continuous agitation. After that, the samples were centrifuged and the supernatant was collected. The starch pellets were washed (100 µl each) twice with the binding buffer and transferred to the supernatant (total volume 300 µl). The starch pellets were resuspended with a 300 µl binding buffer. Volume from 20 µl of each sample mixed with an SDS sample buffer and was heated for 3 min at 95 ^{o}C. The bound protein was analyzed by 9% [w/v] SDS-PAGE followed by anti-His immunodetection.

2.2.26 Dikinases enzyme assays

2.2.26.1 α-Glucan, water dikinase (GWD) binding assay

For all GWD assays, the phosphate incorporation into starch was proportional to enzyme concentration. Here, 30 mg for each Arabidopsis wild-type or *sex 1-8* starches and 50 mg for each potato and maize wild-type, *waxy*, and *amylose extender* starches were resuspended in incubation buffer (50 µl total volume) containing 50 mM HEPES/KOH pH 7.4, 1 mM EDTA, 6 mM $MgCl_2$, 2mM DTE, 0.4 mg ml^{-1} bovine serum albumin (BSA), 1 µCi [β-^{33}P]ATP. The reaction was started by adding 0.2 µg of recombinant *St*GWD and 0.2 µg of tLESV (or as indicated). In control, both *St*GWD and tLESV or only tLESV were omitted. Samples were incubated under continuous agitation two times at 30°C. Aliquots of the reaction mixture were mixed with SDS (final concentration 2% [w/v] SDS). Starches were washed three times with 2% [w/v] SDS and three times with water (1 ml each wash) and finally resuspended in 1 ml water. After mixing with 3 ml of scintillation liquid (Beckman Coulter, USA), the incorporation of ^{33}P was determined by scintillation counting (Scintillation counter "LS6500", Beckman Coulter, USA). To test whether the short glucan chains at the starch granules surface effect GWD-mediated phosphorylation in the presence and absence of LESV, the starch granules were pretreated overnight with isoamylase.

2.2.26.1.1 Autophosphorylation of GWD

Either 1 µg of *St*GWD was incubated alone or in combination with 1 µg of tLESV in 50 mM HEPES/KOH pH 7.4, 1 mM EDTA, 6 mM $MgCl_2$, 2 mM DTE, 10 µM ATP, 1 µCi [β-^{33}P] ATP (10 µl total volume) for 30 min at 30°C. As controls, BSA and tLESV (1 µg each) were incubated under identical conditions. In all reactions, the amount of BSA was adjusted to 3 µg total proteins in the reaction. The reaction was stopped with 0.1 N NaOH, and 1 µl of each reaction was spotted onto a nitrocellulose membrane. The membrane was washed (10 times with ice-cold water, 5 min each wash), and the radioactivity was monitored by phosphorimaging (Phosphorimager "FLA-3000") with BAS reader and AIDA programme.

2.2.26.2 Phosphoglucan water dikinase (PWD) binding assay

For PWD binding assay, Arabidopsis wild-type or *sex 1-8,* potato was used and also maize *waxy* or *amylose extender* starches. Starches were pretreated for 1 hour with 0,6 µg of *St*GWD and 5 mM ATP as described above, but the [β-^{33}P] ATP was omitted. The reaction was stopped by the addition of 2% [w/v] SDS. Starches were washed 10 times with water to eliminate *St*GWD. After that, the prephosphorylation-starches were resuspended in the incubation buffer as described in *St*GWD assay. The reaction was started by adding 0.2 µg of recombinant *St*PWD and 0.2 µg of tLESV. The incorporation of ^{33}P was determined in the same way as the *St*GWD assay.

2.2.27 Starch-hydrolytic enzymes assay

2.2.27.1 Beta-amylase and alpha-amylase digestion of starch granules

For this assay, 50 mg of maize WT starch was washed 5 times with water and 1 time with binding buffer [50 mM HEPES/KOH pH 7.4, 1 mM EDTA, 6 mM $MgCl_2$, 2mM DTE, 0.4 mg ml^{-1} bovine serum albumin (BSA)]. The starch pellets were resuspended in 100 µl of binding buffer and incubated with 10 µg of tLESV for 30 min at 30 °C under continuous agitation. The samples were centrifuged and the starch pellets were washed (1 ml each) twice with 2% [w/v] SDS and three times with water. The pellets were resuspended in 50 mM sodium phosphate pH 6.9, 2 mM DTE and 10 U alpha-amylase (AMY) or in 5 mM citric acid pH 5,5 and 20U beta-amylase (BAM) (final volume 100 µl) overnight at 37 C° with continuous agitation. As controls, starches were also incubated in the absence of BAM or AMY enzymes under otherwise identical conditions. Released glucans were separated by centrifugation for 10 min at 14000 g at room temperature. The supernatants were collected and determined using the reducing end assay.

2.2.27.2 Reducing ends of sugar assay

The reducing ends of sugars for the samples were measured by using the bicinchoninic acid/copper-based assay (BCA). Here, 1 ml of a sample containing solution with BCA in tubes were prepared as (500 µl deionized water- xµl sample) with 500 µl 1:1 BCA reagent which consists of solution A: 5 mM BCA; 512 mM $NaCO_3$; 288 mM $NaHCO_3$ and solution B: 5 mM $CuSO_4$; 12 mM L-Serin. All the samples were incubated for 15 minutes at 99 C°. Tubes were then cooled to room temperature on ice for 5 minutes.

Directly, the absorbance was measured at 560 nm (Fluorescence Spectrometer "Spectrophotometer FP-8500"). Maltose concentration released by BAM was determined by reference to a standard curve (y= 0, 0161x+0, 0312) generated with known amounts of maltose. By inserting the samples absorbance value, the concentration of the reducing end of the samples was determined.

To measure the glucans which were released by AMY enzyme, 50 µl from each sample (diluted 1:5) it was hydrolysed with 50 µl 4 M TFA for 2 hours at 99 C° under continuous agitation. The samples were dried by speed vac centrifuge then dissolved with 100 µl water. The sample was prepared (as mentioned above). Determine the glucose concentration by inserting the samples absorbance value in the glucose standard curve (y =4, 7714x-0,054) generated with known amounts of glucose.

2.2.27.3 Isoamylase digestion of starch granules

Native starch granules (5 mg of Arabidopsis wild-type or *sex1-8*, and 50 mg of maize wild-type, maize *waxy*, and potato tuber) were resuspended in incubation buffer (see above) with 15 µg of tLESV for 1 hour at 30°C and centrifuged for 2 min at 1500 g, and the supernatant was then discarded. Starches were washed three times with 2% [w/v] SDS and three times with water (1 ml each wash).

The starch pellets were resuspended in 10 mM Na-acetate buffer, pH 5.5, 2 mM DTE and digested with 7 U isoamylase (final volume 100µl) overnight at 37 °C with continuous agitation. The samples were centrifuged for 10 min at 1500 g and then the supernatant was heated for 5 min at 95°C and filtered through a 10 kDa filter unit. The filtrate was used for determination of the chain length distribution using a capillary electrophoresis apparatus equipped with laser-induced fluorescence detection (CE-LIF).

2.2.27.4. Capillary electrophoresis system (CE)

The capillary electrophoresis experiment was achieved using PA-800 plus electrophoresis apparatus equipped (SCIEX) with LIF detector (Beckman Coulter Inc, Karata, CA, USA) containing N-CHO capillary. The wavelength of detection was set at 200 nm. An uncoated fused-silica capillary of 50 µm i.d. and 50 cm total length (40 cm was used to the detection window). For each use, the capillary was washed with CE running buffer [25 mM $C_2H_2LiO_2$/AH pH 4, 75; 0, 4% [w/v] Poly Ethylenoxid] and with water at 30 psi

for 3 minutes for each. Also prior to each run, the capillary was rinsed with water, then running buffer at 30 psi for 30 seconds each. The temperature of the capillary cartridge was maintained at 25°C. The sample injection was 0, 5 psi, for 20 seconds. The separation was for 25 minutes at 30KV and 25°C. Data was collected and analysed by using MDQ 23 Karat software from Beckman Coulter.

2.2.27.5 Preparation of samples for CE analysis

1, Aminopyrene-3,6,8-trisulfonic acid (ATPS) solution was prepared at a concentration of 0,2 M in 1,2 M citric acid. All the filtrate samples and maltodextrin standard (maltodextrin stock solution was prepared in water at a concentration of 100 mg/ml) were dried in a centrifugal vacuum evaporator. And then, 1 µl of ATPS solution, 1 µl of 1,2 citric acid, 2 µl 1 M Natriumborhydrid ($NaBH_3CN$) were added to dry samples and incubated in (Hybridizer) for 90 minutes at 55°C. The reaction was stopped by the addition of 96 µl water. The samples were stored at -20°C until use.

2.2.27.6 Samples running in CE

From each sample 100 µl was transferred into vail capillary electrophoresis. After the capillary was effectively conditioned as mentioned above, maltodextrin standard was running individual to ensure proper peak assignment then the sample was run in the same manner.

2.2.28 Crosslinking of proteins

Proteins were prepared for cross-linking using buffer free of DTE. Fractions of tLESV and ESV1 or each protein with *St*GWD and *St*PWD were incubated with 50 mM DTSSP cross-linker (prepared by dissolving 10 mg DSP (ProteoChem) in 495 µl of dry DMF solvent using a (1:20) molar excess approach (proteins to crosslinker) in 25 mM Na_3PO_4 pH 7, 4 at room temperature for 5 minutes (total volume was 200 µl with 5 mM final concentration of DTSSP). The cross-linking reaction was quenched by the addition of 200 mM Tris-HCL pH 8. The sample was filtered through (10 kDa) Millipore. The concentrated cross-linked samples were analyzed using native PAGE or SDS-PAGE.

2.2.29 Yeast two-hybrid analyses

Yeast two-hybrid technique was performed according to Nitzsche et al., (2014). The target DNA sequence of *St*GWD and *St*PWD were amplified by a polymerase chain reaction from Arabidopsis cDNA using the primers [Table 2.13]. The resulting fragments were inserted into the pGEM-T-Easy vector according to the manufacturer's instructions (Promega, https://WWW.promega.de) and verified by sequencing. For yeast two-hybrid analysis, fragments were recombined into Gateway®-compatible versions of the GAL4-DNA binding domain vector pGBT-9 and the activation domain vector pGAD424. Yeast two-hybrid techniques were performed according to the yeast protocols handbook and the Matchmaker GAL4 Two-hybrid System 3 manual (both Clontech, Heidelberg, Germany). To prepare the yeast strain Y190, 8 ml YPAD medium (20 g peptone (Difco); 10 g yeast extract; 20 g glucose; 100 mg adenine hemisulfate; 15 g agar) were incubated containing 2 µl of the yeast strain Y190 at 30 °C at 220 rpm. The following day 50 ml YPAD media were incubated containing 2-4 ml of overnight culture for 3-4 hour at 30°C, 220 rpm. The yeast cells were harvested by 3500 rpm centrifugation for 5 min. The cell pellets were washed with 25 ml MilliQ by centrifugation for 5 min. The cell pellets were resuspended with 1 ml 100 mM LiAc and transferred to 1, 5 ml tube and centrifuged at 13000 rpm for 10 s. After that ca. 100 µl 100 mM LiAc the cell pellets were resuspended and aliquots (each 50 µl) were transferred to a new 1, 5 ml tube. To transformation of the bait and prey plasmid into the yeast strain Y190, the cell pellets were resuspended with 240 µl of 50% PEG; 36 µl of 1M LiAc; 5 µl of carrier-DNA; 2,5 µl of each bait and prey; and 74 µl MilliQ (total volume 350 µl). The mixture was mixed for 1 min and incubated for 30 min at 30 °C following 20 min at 42 °C and centrifugated at 13000 rpm for 10 s. The cell pellets were resuspended with 400 µl MilliQ and 200 µl of cells suspension was spread on SCAD-trp/-leu plate (for 600 ml: 4 g of yeast nitrogen base (Difco); 12 g glucose; 0,4 g amino acids mix; 60 g adenine hemisulfate; 10 g agar/4 mM 3AT) and incubated for 2-3 days at 30 °C.

Direct interaction of the two proteins was investigated by cotransformation of the respective plasmids in the yeast strain Y190, followed by selection of transformants on medium lacking leu and trp at 30°C for 2-3 days and subsequent transfer to SCAD medium lacking leu, trp as a control and leu, trp, and his (supplemented with 25 mM 3-Amino-1, 2, 4-triazole (3-AT)) or with membrane to test the growth selection and the

activity of *lacZ* for the interacting clones. To test the activity of *lacZ*, it was placed Whatman filter paper in petri dishes and then it immersed with 2 ml of lac-Z buffer (10 g 60,68 mM Na_2HPO_4; 6,24 g 40 mM NaH_2PO_4; 0,75 g 10 mM KCl; 0,264 g 1 mM $MgSO_4$, pH 7/ 13,5 µl β-ME/ 167 µl 2% X-Gal in DMF). The membrane of colonies was removed from the plate and immersed it into liquid nitrogen for 10–15 s and placed it onto a filter paper. The plates were incubated for 2-5 hour at 30 °C. Strong activation of the *lacZ* gene will give a blue colour within 1 h. If the *lacZ* gene does not give a blue colour immediately, the filters can be incubated overnight.

Table 2.13: Primers for GWD and PWD cloning

GWD	GWD_FW_1_Seq	TTTgCCAgTACgTggTgCTgTTg	Sequencing GWD PrimStart: 1251bp
GWD	GWD_FW_2_Seq	TgAgggTTTgCTTgAAgCTCgTC	Sequencing GWD PrimStart:2301bp
GWD	GWD_FW_3_Seq	CATCTgAggAgTTCACAAgTgACTTgg	Sequencing GWD PrimStart:3251bp
GWD	GWD_RV_1_Seq	TgACCAAAgAAATACTTggAggggC	Sequencing GWD PrimStart:3220bp
GWD	GWD_RV_2_Seq	CCTCATgTAgTgTCCAAgATCACgC	Sequencing GWD PrimStart:2109bp
GWD	GWD_RV_3_Seq	gCCACATgAATTTTCgTCTTTCCgg	Sequencing GWD PrimStart:1154bp
PWD	PWD_FW_1_Seq	CTCggATTAgggACATAgCCCATCgC	Sequencing PWD PrimStart:1091bp
PWD	PWD_FW_2_Seq	gTCTCACCTTggCgTTAgAgCgCggC	Sequencing PWD PrimStart:2271bp
PWD	PWD_RV_1_Seq	CTATTggAAgATgAggAACCAggC	Sequencing PWD PrimStart:2555bp
PWD	PWD_RV_2_Seq	CACTATATTTTCCTggggTCTCgg	Sequencing PWD PrimStart:1255bp

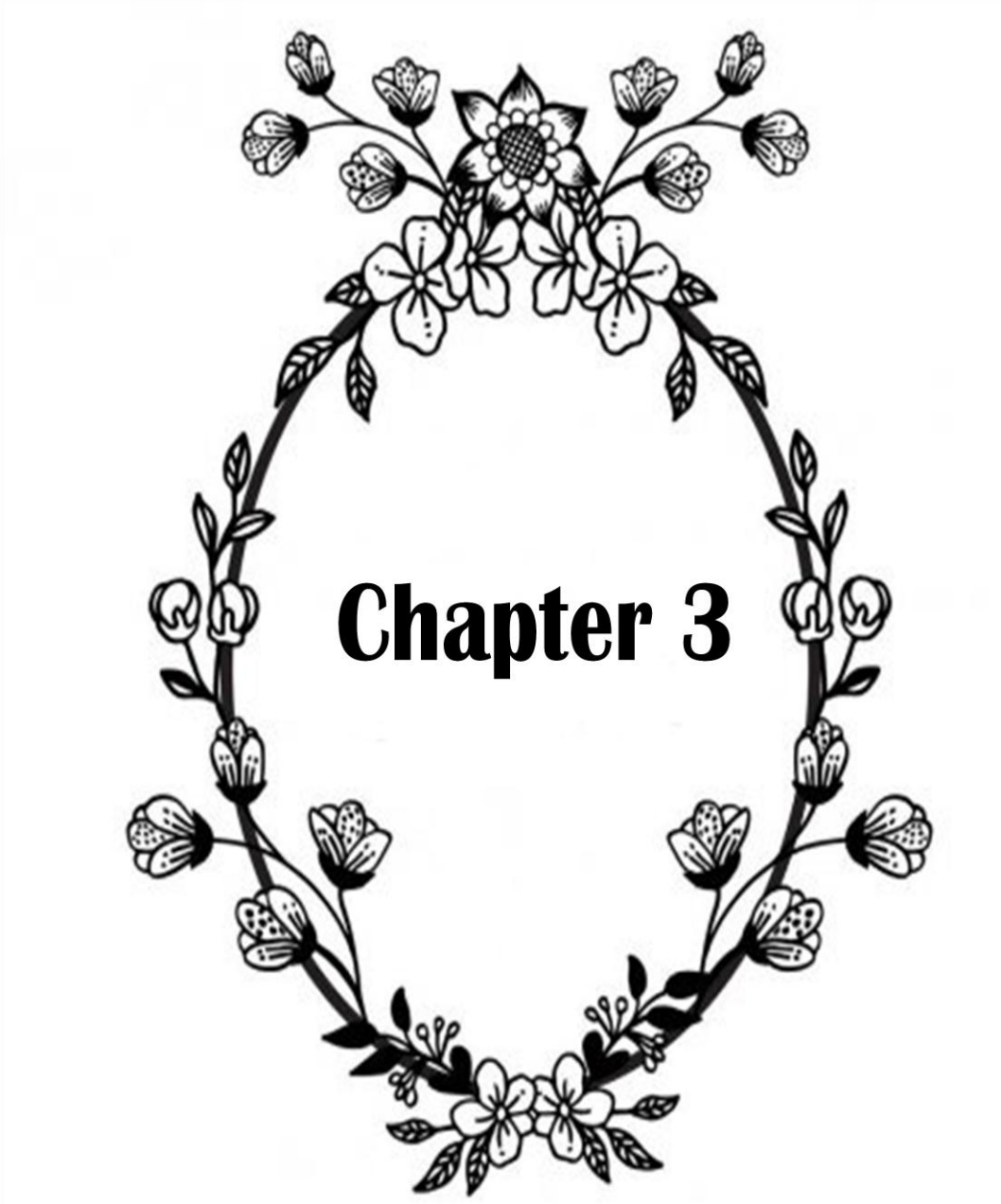
Chapter 3

3 Identify and determine the role of LESV in starch organization

More studies reported that starch granules reveal structural, compositional, and morphological heterogeneity related to the plant source (Jane et al., 1994; Bertoft, 2017; Helle et al., 2019). In addition to lipids, minerals and phosphorus, starch granules also contain minor amounts of proteins (Lindeboom et al., 2004). However, the phosphate groups are one of the important components in starch granules. Most of the phosphate groups are covalently bound to the amylopectin thereby involved in starch turnover (Blennow et al., 1998; 2010). By phosphorylation of double helices of amylopectin, the granule surface will transit to a less ordered state (Hejazi et al., 2009). Hence, the granule surface will be more accessible to glucan hydrolyzing enzymes. Furthermore, dephosphorylation process leads to enhance the rates of starch degradation by hydrolytic enzymes (Kötting et al., 2009). SEX4 is able to remove the phosphate groups from C 3 position and C 6 positions of the glucosyl residues in the amylopectin structure, whereas LSF2 only removes the phosphate group from C 3 positions.

However, proteins are also one of the essential components in starch granules. Most of the proteins that bound to the starch granules act as starch metabolizing proteins (Baldwin et al., 2001). These proteins vary in their association; some proteins are weakly bound, while others bind strongly within the granule. Recently, Helle et al. (2018) identified several families of proteins in the potato genome that are associated with starch. They analyzed the starch bound proteins based on the potato genome annotation using mass spectrometry. They observed that many of these proteins are involved in the starch degradation process. Recently, in Arabidopsis leaves, it was identified that other proteins associated with the starch granule have a role in starch metabolism (Seung et al., 2015; 2017; Feike et al., 2016; Malinova et al., 2018). Two of these proteins named Early Starvation Protein 1 (ESV1) and its homologue Like Early Starvation Protein 1 (LESV) have a role in the control of starch degradation (Feike et al., 2016). Previously it was identified the LESV protein as the unknown starch binding protein encoded by At3g55760 in Arabidopsis genome based on the proteomic study (Edner et al., 2007). Interestingly, this protein eluted with other starch metabolism enzymes like beta amylase1 (BAM1), starch binding 3 (SBE3), isoamylase 3 (ISA3) and disproportion 1

(DPE1). These proteins have an important role during starch degradation. Recently, Helle et al. (2018) confirmed the presence of LESV and ESV1 proteins in potato starch. However, it was supposed through the transgenic study that lacking both proteins involved in adjusting and modulating the matrix organization of starch thereby affected its degradation (Feike et al., 2016). However, in (Chapter 4) it was identified that ESV1 is a starch binding protein able to alter glucan structure. Its binding to starch granules was reflected in the phosphorylation process while it had clear effect in the present of ESV1 on GWD and PWD action at the starch granule surface.

3.1 Results

3.1.1 Characterization of LESV in *Arabidopsis thaliana*

After analysis of the LESV protein from Arabidopsis leaves, the Coomassie-stained gel showed several protein bands (Fig. 3.1). However, the bands which have molecular weight ~60-70 kDa were analyzed by matrix-assisted laser desorption/ionization mass spectrometry using peptide finger-printing. However, MALDI-TOF analysis was successfully determined a protein band with an apparent molar mass of ~65 kDa which identified in a BLAST search (http://www.arabidopsis.org/Blast/index.jsp) as At3g55760 gene, LESV. This data supports the conclusion that LESV is a plastidial protein (Feike et al., 2016).

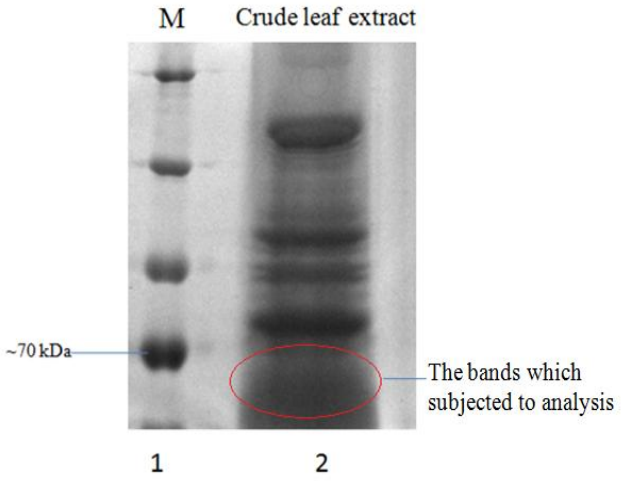

Fig.3.1: SDS-PAGE of chloroplast proteins extracted from the Arabidopsis leaves. Chloroplast proteins from 2-weeksold Arabidopsis leaves were denatured at 95 C° for 3 min. 25 µg of proteins extracted from the sample was loaded on the [7.5 %] SDS gel. Proteins were analyzed under constant 250 V until the bromophenol blue reached the bottom of the gel. After the separation of proteins, the bands were visualized with Coomassie stain. Lane 1: M, protein markers; lane 2: the fraction of the chloroplast proteins.

3.1.1.1 Amplification of the full-length sequence of LESV

To amplified LESV sequence, it was extracted cDNA from mRNA of Arabidopsis and used as a template for PCR amplification. By using forward primer [**GAATTC**ATGGCTTTGCGTTTAGGTGTTT] and reverse primer [**GCGGCCGC** GGAC GTA TCA GAA GGC TTC] a DNA fragment with the correct size was amplified (Fig. 3.2). The product of PCR was extracted (Fig. 3.3) from agarose gel and ligated into a pGEM-T-Easy vector. Later the plasmid was a transformation in the chemical competent *E.coli* DH5 α cells and these bacteria were cultured overnight.

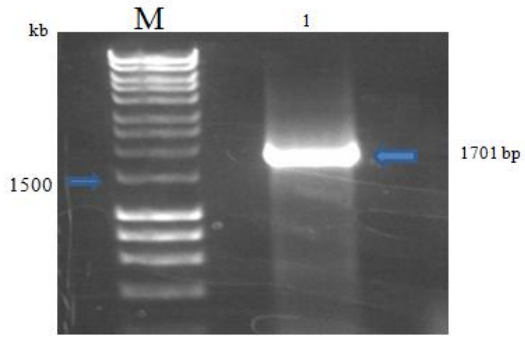

Fig.3.2: PCR amplification of the full-length sequence of LESV. Using cDNA as a template prepared from mRNA of leaves of Arabidopsis. 50 µl of PCR-amplified DNA was run on a 1% [w/v] agarose gel. Lane M, 1-kb DNA ladder; 1, the expected DNA band of LESV.

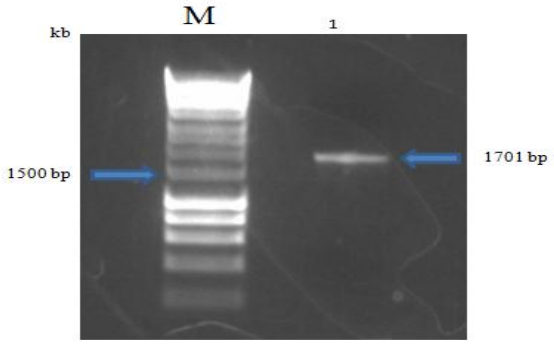

Fig.3.3: The results of PCR after DNA extraction from 1% [w/v] agarose gel. The band excised from the gel then purified using Illustra GFX PCR DNA and Gel Band Purification Kit. M, 1-kb DNA ladder; 1, the expected DNA band of LESV.

3.1.1.2 Gain the pGEM-T-Easy-LESV plasmid

After transformation, the pGEM-T-Easy plasmid was gained from the overnight culture by picking 10 positive individual colonies. An agarose gel electrophoresis was performed

to screen the products (Fig 3.4). After that, the three colonies (5, 8, and 9) were selected for mini preparation and restriction analysis.

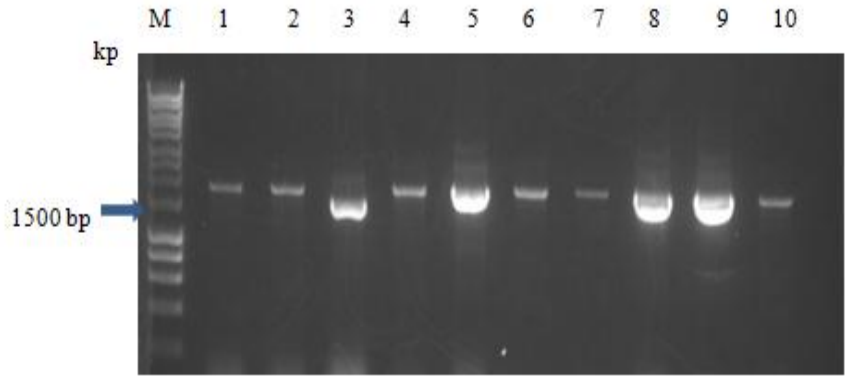

Fig.3.4: Colony PCR results for LESV sequence. The colony PCR product for LESV in pGEM-T Easy vector was running on 1% [w/v] agarose gel. Lane M, 1-kb DNA ladder; lanes 1-10 showing the positive clones with correct insert.

3.1.1.3 Restriction analysis from pGEM-T Easy-LESV

The restriction analysis was performed and confirmed by sequencing (LGC Genomics, Berlin). Figure 3.5 shows that the 3 transformations selected for restriction analysis have the correct insert.

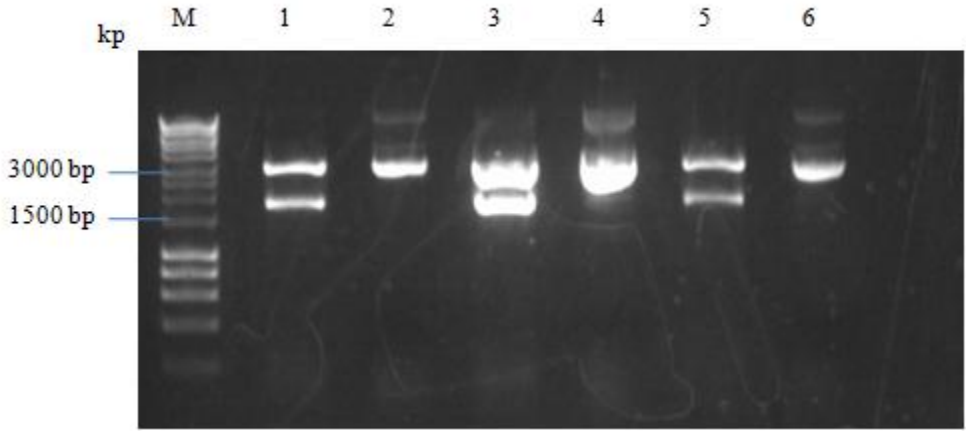

Fig.3.5: Restriction digestion analysis of the pGEM-T Easy-LESV. In the three samples 1, 3, and 5 for the white colonies 5, 8, 9 respectively, the pGEM-T Easy plasmid is present at 3000bp as expected compared with the samples 2, 4, and 6 which used an empty pGEM-T Easy plasmid as a control. PCR products in the samples 1, 3, and 5 indicate a 1701bp fragment for the TP-LESV insert. The samples were run on 1% [w/v] agarose gel. Lane M 1-kb ladder was used as a marker.

3.1.1.4 Ligation of LESV from pGEM-T Easy to pET23b plasmid

To obtain the insert ligate with pGEM-T Easy and enable the ligation of the free insert with pET23b, the restriction of both plasmids is necessary. However, restriction analysis was performed. Following agarose gel electrophoresis (Fig 3.6), the desired DNA (LESV) band and the pET23b plasmid were cut. After that, the ligation was performed. Later, the pET23b-LESV plasmidwas used to be transformed into electroporation competent *E.coli* LB21 cells.

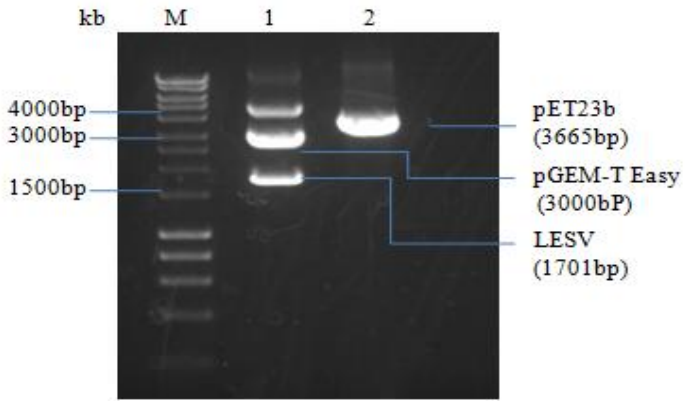

Fig.3.6: Restriction digestion analysis of the pGEM-T Easy-LESV and pET23b plasmid. Lane 1: pGEM-T Easy-LESV and lane 2: pET23b plasmid after digestion by the restriction enzymes digests, *EcoRI* and *NotI*. Lane M 1-kb ladder was used as a marker. The samples were running on 1% [w/v] agarose gel.

3.1.1.5 Preparation of pET23b-LESV

Subsequently, from the overnight culture, 5 individual positive colonies were selected from the agar plate. All the 5 colonies revealed the success of the transformation (Fig 3.7). For further cultivation samples, 1 and 2 were used.

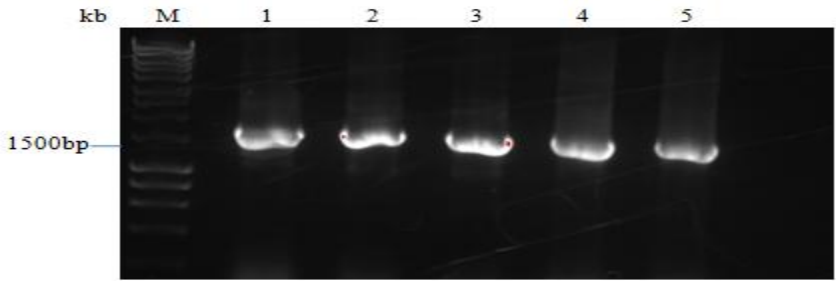

Fig.3.7: Colony PCR products forLESV in pET23b plasmid. Samples were run on 1% [w/v] agarose gel. Lane M, 1-kb DNA ladder; lanes 1-5 showing the positive clones with a correct insert.

3.1.1.6 Small scale expression of LESV

The expression of LESV protein was expressed in *E. coli* BL21 (DE3). This protein was subsequently expressed at 18 C° overnight with 1 mM (final concentration) of IPTG in order to further optimize LESV expression. As a control, *E. coli* BL21 was incubated without IPTG in the same condition. The expression of His-tagged protein was tested by SDS-PAGE followed by immunodetection using anti-His-tag antibodies. As it is shown in (Fig. 3. 8) a clear ~ 66 kDa band of protein was in the supernatant with less concentration in pellets compared to the control.

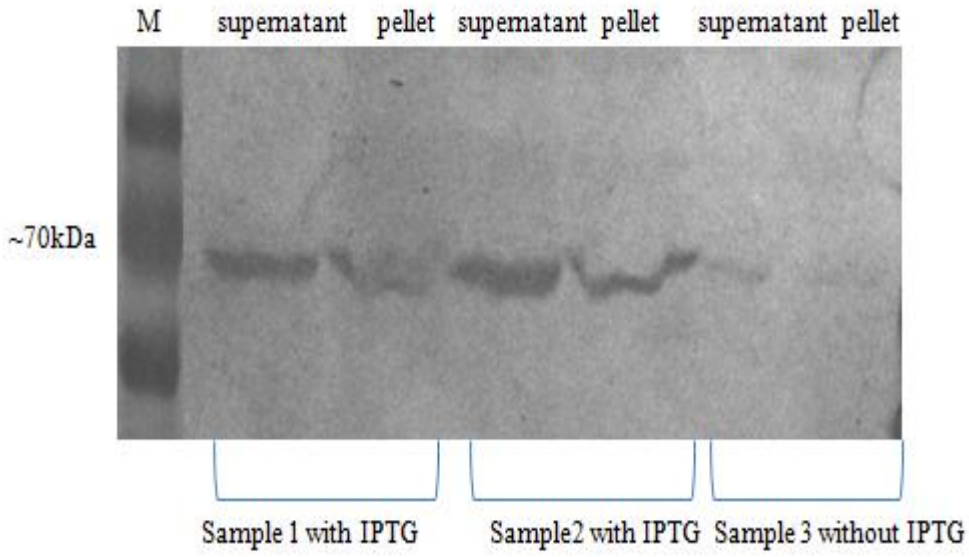

Fig.3.8: Detection of LESV protein expressed in *E.coli LB21* using anti-His immunodetection. The bands were detected in western blot using anti-His antibodies. In sample 1 and 2 (with IPTG), the stronger bands were in the supernatant (soluble) fraction than the pellet (insoluble) fraction compared to the bands of sample 3 (without IPTG) as a control while the expression of protein was very weak. Lane M, protein marker ladder.

3.1.2 Cloning of LESV without transit peptide as truncate LESV (tLESV)

3.1.2.1 PCR amplification

After the restriction analysis of pET23b-LESV and extraction of LESV-DNA from agarose gel, it used as a template for tLESV. PCR amplification of the truncate LESV was performed. Amplification resulted in the desired (1645bp) fragment and the band excised from the gel was then purified using Illustra GFX PCR DNA and Gel Band Purification Kit (Fig. 3.9).

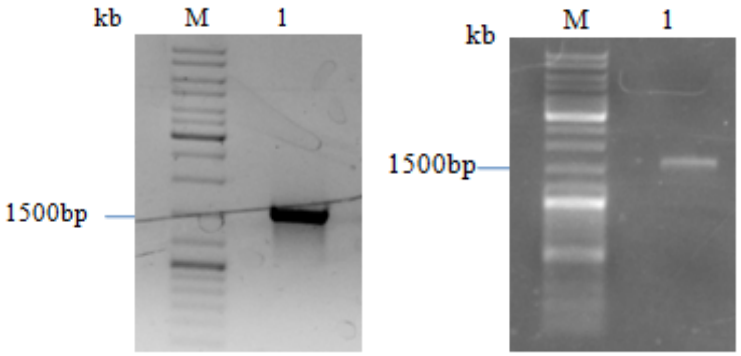

A **B**

Fig.3.9: PCR product of tLESV using LESV as a template and extraction band from agarose gel. The samples were run on 1% [w/v] agarose gel. **A**: lane 1, PCR product of tLESV sequence, the expected size (1645 bp). **B**: lane 1, tLESV-DNA band after the extraction from agarose gel. In both, **A** and **B** lane M, 1-kb DNA ladder.

3.1.2.2 Ligation of tLESV into pET23b plasmid

It was successfully restricted both tLESV fragment and pET23b using Not I and EcoRI resteraction enzymes. After that, it was successfully ligated the tLESV fragment into pET23b. The plasmid was transformed into electroporation competent *E.coli* LB21 cells.

3.1.2.3 Preparation of pET23b-tLESV

From the overnight clture, it was selected 15 individual colonies contained the positive ligation. Twelve colonies revealed the successful transformation (Fig. 3.10). But after restriction digestion, only five colonies revealed the corrected plasmid (Fig. 3.11). For further cultivation samples 3, 5, 9, and 11 were used.

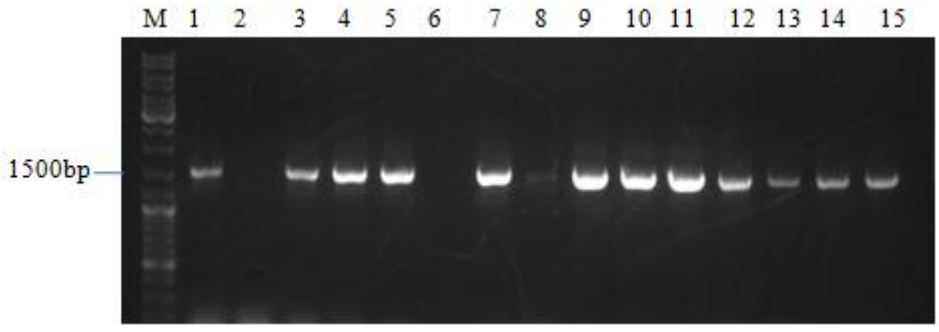

Fig.3.10: Colony PCR products of tLESV. All the samples were running on 1% [w/v] agarose gel. Lane M, 1-kb DNA ladder; lanes 1, 3-5,7, 9-15 showing the positive clones with correct insert; lane 2, 6, and 8 showing negative clones.

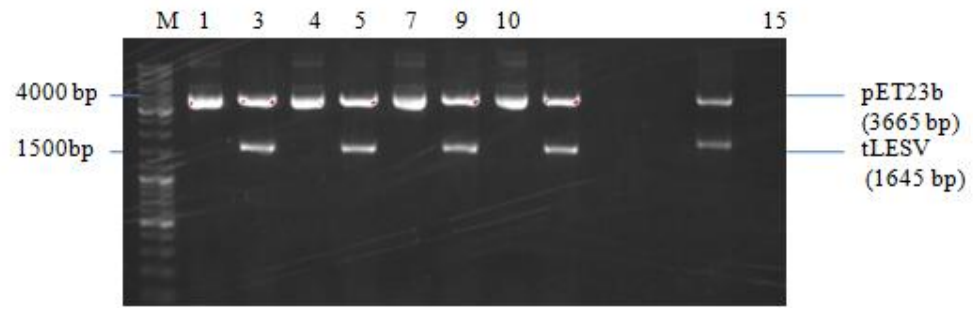

Fig. 3.11: Restriction digestion analysis of the pET23b-LESV clones. All the samples were running on 1% [w/v] agarose gel. Only the samples in lanes 3, 5, 9, 11, and 14 revealed the correct insert.Lane M, 1-kb DNA ladder.

3.1.2.4 Small scale expression of tLESV

The expression of the His-tag protein was performed as LESV. As it is shown in Fig. 3.12 a clear ~ 60 kDa band of protein in soluble and insoluble fractions was detected.

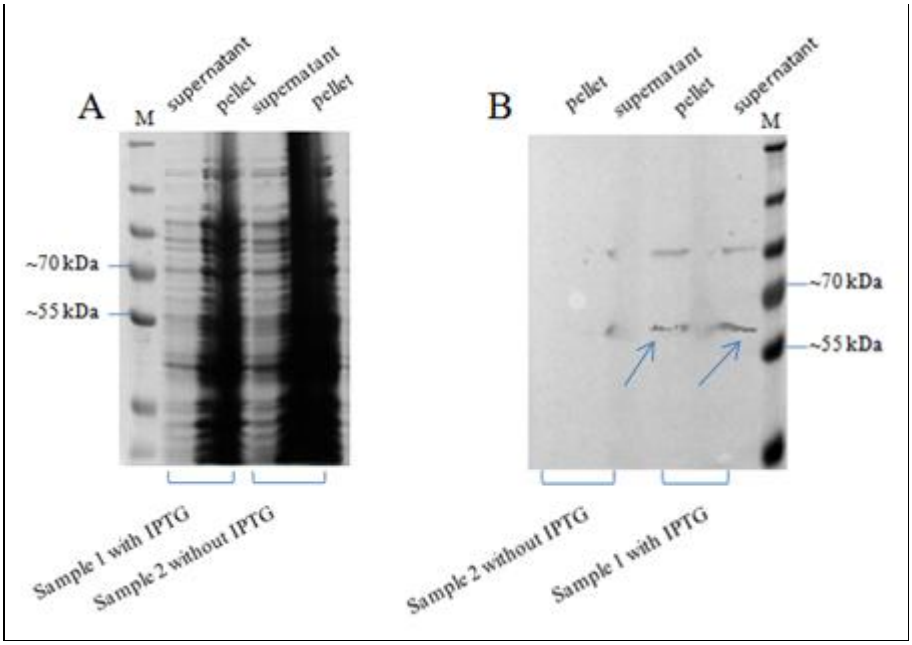

Fig.3.12: Detection of tLESV protein expressed in *E.coli LB21* using SDS-PAGE and blotting followed by anti-His-immunodetection. A: SDS-PAGE separation; B: anti-His-immunodetection analysis; lane M: protein marker ladder. The bands were detected using anti-His antibodies. In sample 1 with IPTG, the bands were in the supernatant (soluble) fraction and the pellet (insoluble) fraction (blue arrows).

3.1.2.5 Large scale expression and purification of LESV and tLESV proteins

After expression of LESV and tLESV proteins, in *E.coli* LB21 (DE3) cells, the culture was extracted and the supernatant fraction was purified using a His-Trap column. The

protein of interest in addition to other non-specific proteins of interest attached to the column. To wash non-specific proteins out of the column washing buffer with 20 mM, imidazole was performed. The first washe by ~ 20 column volume buffer contained 20 mM imidazole and then eluted with buffers containing different concentrations of imidazole started from 50, 75, 100, 150, 250, and 500 mM.

After washing 17 fractions of 1 ml each, they were collected. The fractions were analysed by SDS-PAGE and the slabs gel stained by Coomassie staining to detect the recombinant proteins. Fig. 3.13 A shows the results for LESV fractions and Fig. 3.13 B reveals for tLESV.

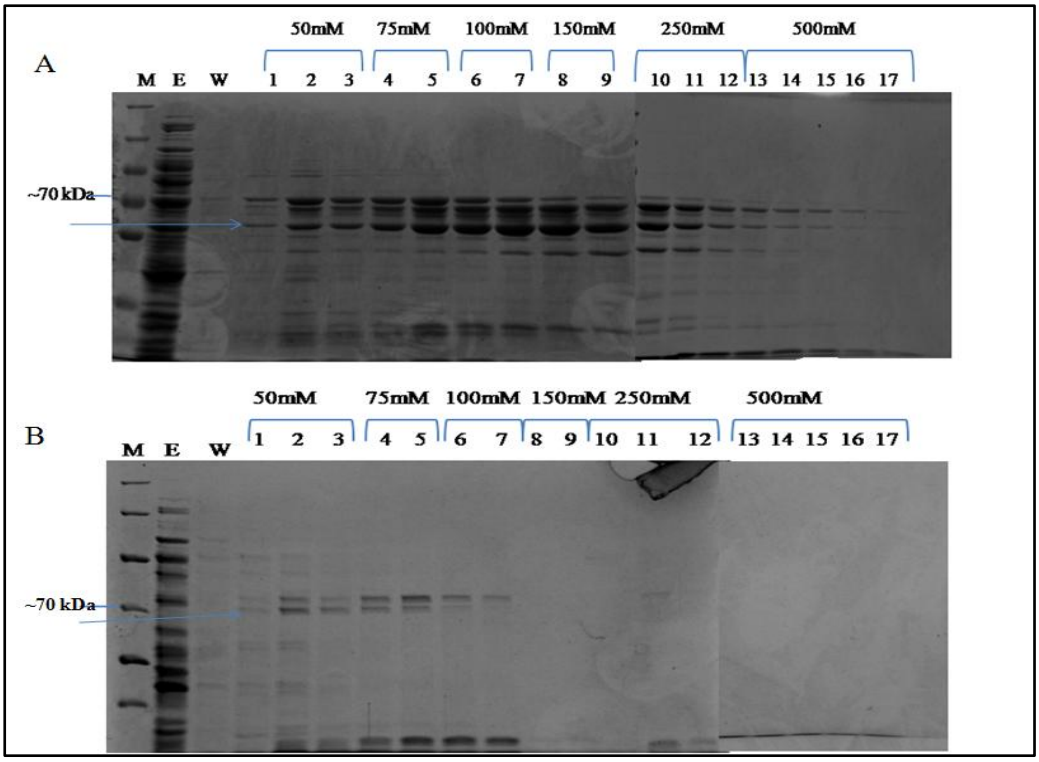

Fig.3.13: SDS-PAGE analysis of the LESV and tLESV proteins fractions, collected from the His-Trap column after elution with different concentrations of imidazole. A: separation of the fractions of LESV; B: separation of the fractions of tLESV. Following lysis, using chromatography on Ni-NTA agarose, the supernatant fractions were run through His column, washed with 50, 75, 100, 150, 250, and 500 mM imidazole gradient and collected in 17 fractions of 1 ml each. The fractions were run on a 7.5% SDS-PAGE, 250 V for 2 hours and stained with Coomassie Brilliant Blue. Lane M, protein marker ladder; Lane E, Flow-through; lane W, washing with 20mM imidazole; lanes with numbers, the gradient of imidazole.

Figure (3.13 A) and (3.13 B) show the SDS-PAGE analysis of the fractions, collected from the His-Trap column after elution with different concentrations of imidazole buffer 50, 75, 100, 150, 250, 500 mM imidazole. The analysis production of both proteins at 18

C° overnight showed that the LESV bands started elution in the first fraction with 50 mM imidazole to the last fraction with 500 mM imidazole, whereas tLESV (Fig. 3.13 B) showed that the tLESV bands started elution with the first 50 mM imidazole fraction until the last 100 mM imidazole fraction.

Several proteins of lower and higher molecular weight have been detected. Maybe the lower molecular mass proteins were degraded products of LESV or tLESV. Bands in the range of ~ 72 kDa were visible in all fractions.

Following a combination of the fractions that showed the protein of interest, the proteins were filtered by 50 kDa filter with HEPES buffer to remove imidazole. After that, it measures the protein concentration and analyzes the purity of protein by SDS-PAGE and blotting followed anti-His immunodetection (Fig. 3.14). Furthermore, the bands of protein were cut from the gel and analysed by the MALDI-TOF to determine the sequence of the protein.

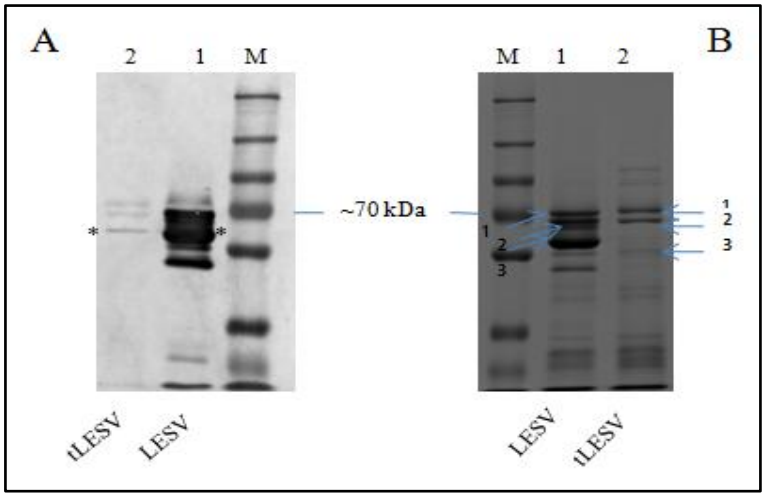

Fig.3.14: Analysis of the LESV and tLESV proteins by SDS-PAGE following blotting and then anti-His immunodetection after purification. A: anti-His immunodetection; B: SDS-PAGE analysis. In both pictures lane 1, the band of LESV with expected size ~66 kDa; lane 2, the band of tLESV with expected size ~60 kDa, Lane 2, protein marker ladder. The stars refer to the size of the expected proteins. The arrows refer to all proteins which were analyzed by MALDI-TOF.

3.1.3 Analysis of LESV and tLESV by MALDI-TOF

Protein detected in SDS-PAGE (Fig. 3.14) was identifie using MALDI-TOF analysis. The peptide mass fingerprinting of protein was observed and subjected to Mascot. However, LESV protein, band 3 was obtained as a result with a score of 97 (Fig. 3. 14

A), while tLESV protein, band 3 was obtained as a result with a score of 108 (Fig. 3. 14 B). These results indicated that the purified LESV or tLESV proteins are from *Arabidopsis thaliana.* Furthermore, the analysis showed that the protein bands 1 and 2 in each lane (LESV, lane 1 and tLESV, lane 2) belong to *E.coli* cells resistance proteins.

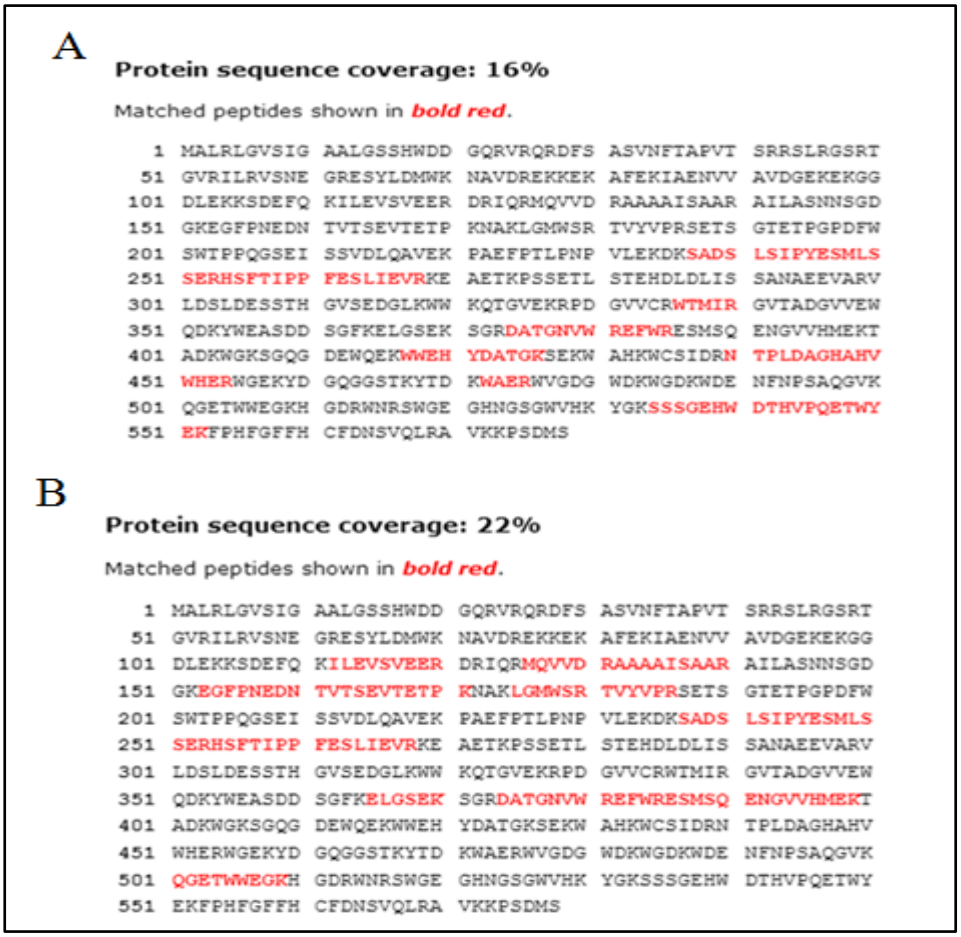

Fig.3.15: MALDI-TOF peptide mass fingerprint spectrometry of the LESV and tLESV proteins. A: the LESV sequence; **B**: the tLESV sequence. The peptide mass fingerprint analysis was made from fragments of purified LESV and tLESV proteins derived through trypsin digestion. The sequence coverage of these fragments was shown in bold red.

However, the binding of both protein forms to starch was analyzed. 30 mg of the native starch granule of Arabidopsis wild-type, Arabidopsis *sex 1-8*, and maize wild-type were incubated with 10 µg of each LESV and tLESVfor 15 min at 30 C°. Following centrifugation, the starch pellets were heat-treated with SDS sample buffer for 3 min at 95 C°. Twenty µl of each sample was loaded on an SDS-PAGE followed by immunodetection using an anti-His antibody (Fig. 3. 16). However, the binding of both protein forms to all the starch types was observed. No difference was detected between them. That means that the presence of the putative of transit peptide did not influence the

protein folding thereby did not alter the binding of the protein to starch. Therefore, for the binding experiments, it only used tLESV (without transit peptide).

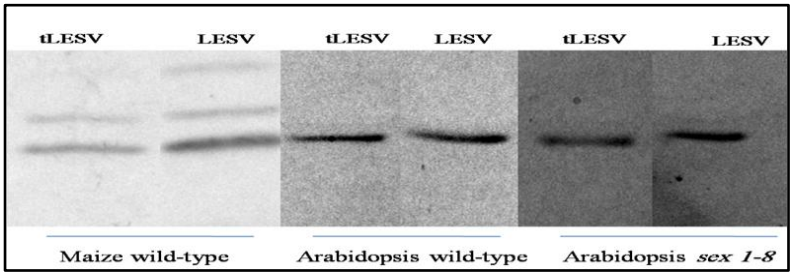

Fig.3.16: Analysis of the binding of LESV and tLESV to different starches. Detection of protein binding using immunodetection anti-His antibodies was performed after analysis of the samples on an [7, 5%] SDS-PAGE and transferred onto a PVDF membrane. The results showed the binding of both forms to Arabidopsis *sex1-8,* Arabidopsis wild-type, and maize wild-type starches.

3.1.4 The binding of tLESV to different starches

However, it was reported that the gene encoded LESV protein was found in the leaves of Arabidopsis as it purified as an unknown protein with other starch- related enzymes like BAM1, SBE3, ISA3, and DPE1 using affinity chromatography on amylose resin (Edner et al., 2007). On the other hand, it was shown in Arabidopsis that the LESV protein has a role in the transitory starch (Feike et al., 2016). For further *in vitro* confirmation of the binding to starch, native starches from various sources like Potato, Arabidopsis wild-type, Arabidopsis *sex 1-8*, in addition to crystalline maltodextrin (B-type allomorph) were analyzed. Starches with 10 µg of tLESV protein were incubated for 15 min at 30 C° followed by washing with the incubation buffer, the starch pellets were heat-treated with SDS sample buffer and analyzed by SDS-PAGE and then transferred onto a PVDF membrane followed by anti-His immunodetection (Fig. 3.17). Immunoblotting mostly revealed that tLESV binds to all starch types. At the same time, it can observe the removal of the protein from starch with the supernatant in all starch types also. These results suggest that the binding of tLESV was not reversible.

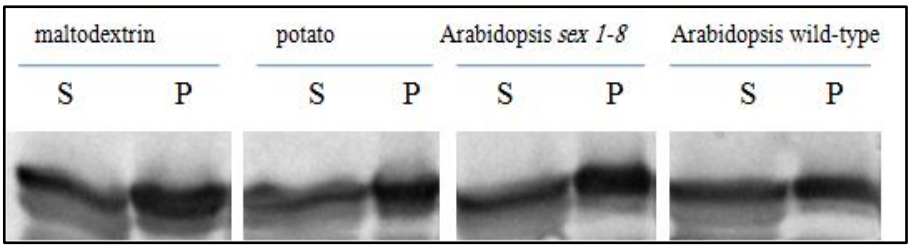

Fig.3.17: Analysis of tLESV binding to different starches. Detection of protein binding by immunodetection using anti-His antibodies, the fractions were subjected to [9%] SDS-PAGE and then transferred onto a PVDF membrane. The results showed the binding of tLESV to Arabidopsis wild-type, *sex1-8,* potato, and maltodextrin in the pellet (P) and supernatant (S).

To determine the effectiveness of the removal of protein from starch, Arabidopsis wild-type, potato starch granules, and crystallized maltodextrin were incubated with tLESV for 10 minutes at 30 C°. Following washing two times with the incubation buffer and was collected as fraction W1 and W2 and denature with SDS sample buffer. The pellets were washed two times with SDS sample buffer (1X final concentration) and collected as E1 and E2. 20 µg of each fraction was loaded on SDS-PAGE and transferred onto a PVDF membrane followed by anti-His immunodetection (Fig. 3.18). The results showed released tLESV after the second wash in the three types of starch, while the release of protein after washing with 2% (w/v) SDS was only shown in Arabidopsis wild-type starch. This indicated that the binding of tLESV to Arabidopsis wild-type starch was stronger than potato and maltodextrin in which his releasing was only after the first wash with 2% (w/v) SDS, while released protein from potato starch and maltodextrin were shown after the second wash with water, or the binding of tLESV to the starch granule surface of Arabidopsis wild-type was more than his binding within the starch in which it was easily released after washing with 2% (w/v) SDS (E1). In contrast, the binding of tLESV to potato and maltodextrin was stronger within the starch in which even using 2% (w/v) SDS, the protein was not released. These results suggest that the binding of protein varies depending on the starch structure properties, which affect the interaction with the protein binding site.

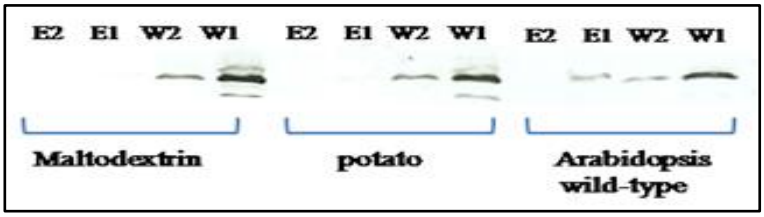

Fig.3.18: Determination of the binding of tLESV to different starches. 20 µg of each fraction was separation on SDS-PAGE [9%] and transferred onto a PVDF membrane followed by anti-His immunodetection. Lane M, protein marker ladder; lanes, W1 and W2, washing with incubation buffer. E1 and E2 washing with SDS sample buffer.

3.1.5 tLESV binds to both amylose and amylopectin

After the detection that the tLESV protein binds to starch, and as the starch granules consist of two polymer types, amylose and amylopectin, it was tried to evaluate the binding of tLESV to the two polymers. The tLESV protein was incubated with amylose from potato and amylopectin from maize. Following electrophoresis and blotting, the binding of tLESV was detected by anti-His immunodetection (Fig 3. 19).

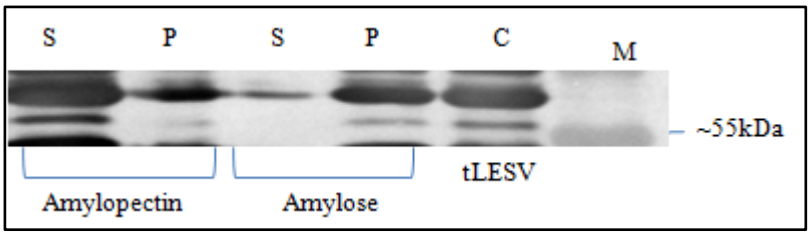

Fig.3.19: Analysis of tLESV binding to amylose and amylopectin. 20 µg of each fraction was run on an [9%] SDS-PAGE followed by anti-His immunodetection. Lane M, protein marker ladder; lane C, tLESV protein as a control; lane P, amylose and amylopectin pellets; lane S, amylose and amylopectin supernatant.

The results showed that the tLESV protein binds strongly to amylose than amylopectin, which is reflected in the lack of most of the protein in the washing fraction. Therefore, to determine the effectiveness of the protein removal by washing it was incubated tLESV with amylose for 15 min at 30 C°. Following washing the starch pellets with incubation buffer, the supernatant was collected as W1 and W2, the pellet was treated twice with SDS sample buffer and collected as E1 and E2. The pellet resuspended with the same volume of incubation buffer. Analyze of the fractions by SDS-PAGE and the binding of

protein were monitored by immunoblotting using anti-His immunodetection (Fig. 3. 20). The result revealed that tLESV binds strongly to amylose since it was not seen after wash with buffer. Even after treating the starches with SDS sample buffer, it observed the protein still binds to the pellet. This result suggests that the long and unbranching glucan structures were probably more preferentially bound by tLESV than the branching and short glucan structures.

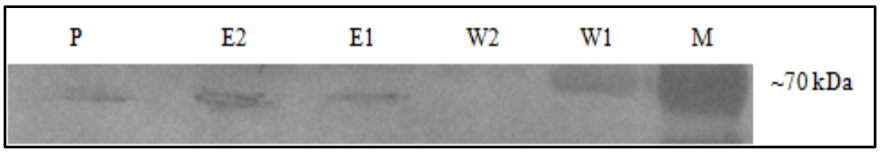

Fig.3.20: Determine the binding of tLESV to amylose. All the fractions were separating on an [9%] SDS-PAGE followed by anti-His immunodetection. Lane M, protein marker ladder; lanes W1 and W2, washing with incubation buffer; lane E1 and E2, washing with SDS sample buffer; lane P, pellet.

3.1.6 Alteration of the starch granule surface does not affect the tLESV binding

However, based on the above results which included the incubation of tLESV with various starch sources, there was variation in the binding of tLESV to these starches reflected in releasing the protein after washing. However, to detect whether the alteration of the starch granule surface will affect the tLESV binding, two starch types were used, Arabidopsis *sex 1-8* starch granules, which have more short glucan chains at the surface (Mahlow et al., 2014), and potato tuber starch. Both starches were treated with isoamylase or beta-amylase enzymes overnight to remove the free glucan chains from the surface of the granules. After centrifugation, the starches were washed one time with an incubation buffer. The pellets were dissolved in the equal volume. 20 µg of each fraction was denatured with SDS sample buffer and separation on an SDS-PAGE followed by anti-His immunodetection (Fig. 3.21 A and B). However, the results did not show differences in the binding of tLESV to starch granules after the removal of the free glucan chains from the surface compared to the controls. This suggests that the alteration of starch structure does not affect the tLESV binding. That means that the binding of tLESV is not limited to the starch granule surface, but it is capable of reaching deeper than the surface.

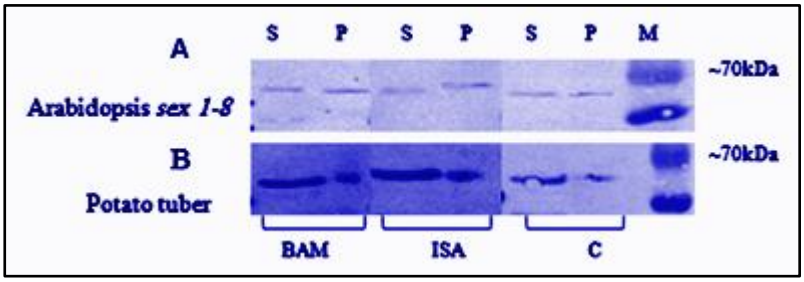

Fig.3.21: Analysis of tLESV binding to Arabidopsis *sex 1-8* and potato tuber starch after treatment with isoamylase and beta-amylase. (A) Arabidopsis *sex 1-8* starch. (B) Potato tuber starch. Both starches were pretreated with isoamylase (ISA) and beta-amylase (BAM) overnight after washing steps the pellets incubated with tLESV. As controls, both starches incubated in the same condition without pretreatment. All fractions were loaded on an SDS-PAGE and transferred onto a PVDF membrane followed by anti-His immunodetection. Lane M, protein marker ladder; P, pellet; S, the supernatant; C, starch as a control; ISA, isoamylase; BAM, beta-amylase.

3.1.7 The presence of LESV and tLESV affects GWD- mediated phosphorylation process

To get insight into the mode of action of tLESV and determine his function through starch metabolism, it was looked at the genetic study for Feike et al. (2016) which found that the lacking and overexpressing of LESV affect starch degradation. On the other hand, it was looked at the action of ESV1 proteins, while it was revealed that it has the ability to alter the starch structure, hence, it affected the phosphorylation process through the starch breakdown (Chapter 4). This process was performed by the activity of GWD and PWD enzymes. The result of the effect of ESV1 on the phosphorylation process leads to speculation that LESV may be capable of affecting the phosphorylation process as both proteins have a similar strucutre. To get a better insight into the effects of Like-Early Starvation 1 protein on the phosphorylation process, the effect of LESV (full length) and LESV truncate of transit peptide (tLESV) was initially examnied on GWD-mediated phosphorylation using recombinant *St*GWD from *Solanum tuberosum*; (EC 2.7.9.4), which has a high affinity to its substrate and exhibits a higher preference for phosphorylating of amylopectin and ^{33}P-β-ATP (1µCi final concentration) was incubated with Arabidopsis wild-type and potato tuber starches in the presence or absence of both LESV and tLESV for two incubation times, 10 and 20 min (Fig. 3.22). As controls, the starches were incubated identically but with the absence of LESV and tLESV or GWD and both protein forms. After the washing steps, the incorporation of phosphate into the starches was measured. It was shown that the incorporation of phosphate in both starches increased over time. On the other hand, in both Arabidopsis wild-type and potato starches

the presence of LESV protein (Fig. 3.22 A) and (Fig. 3.22 C) and of tLESV protein (Fig. 3.22 B) and (Fig. 3.22 D), respectively led to a significant reduction in the GWD-mediated phosphate incorporation. Thus, these results suggest that when both LESV and tLESV proteins binding to starches are capable of altering glucan structures at the starch granule surface in the same mechanism that influences the action of GWD. Therefore, due to the resulting similarity of the effects of both forms on the phosphorylation process by the action of GWD, it was presented only tLESV form for all experiments in this work.

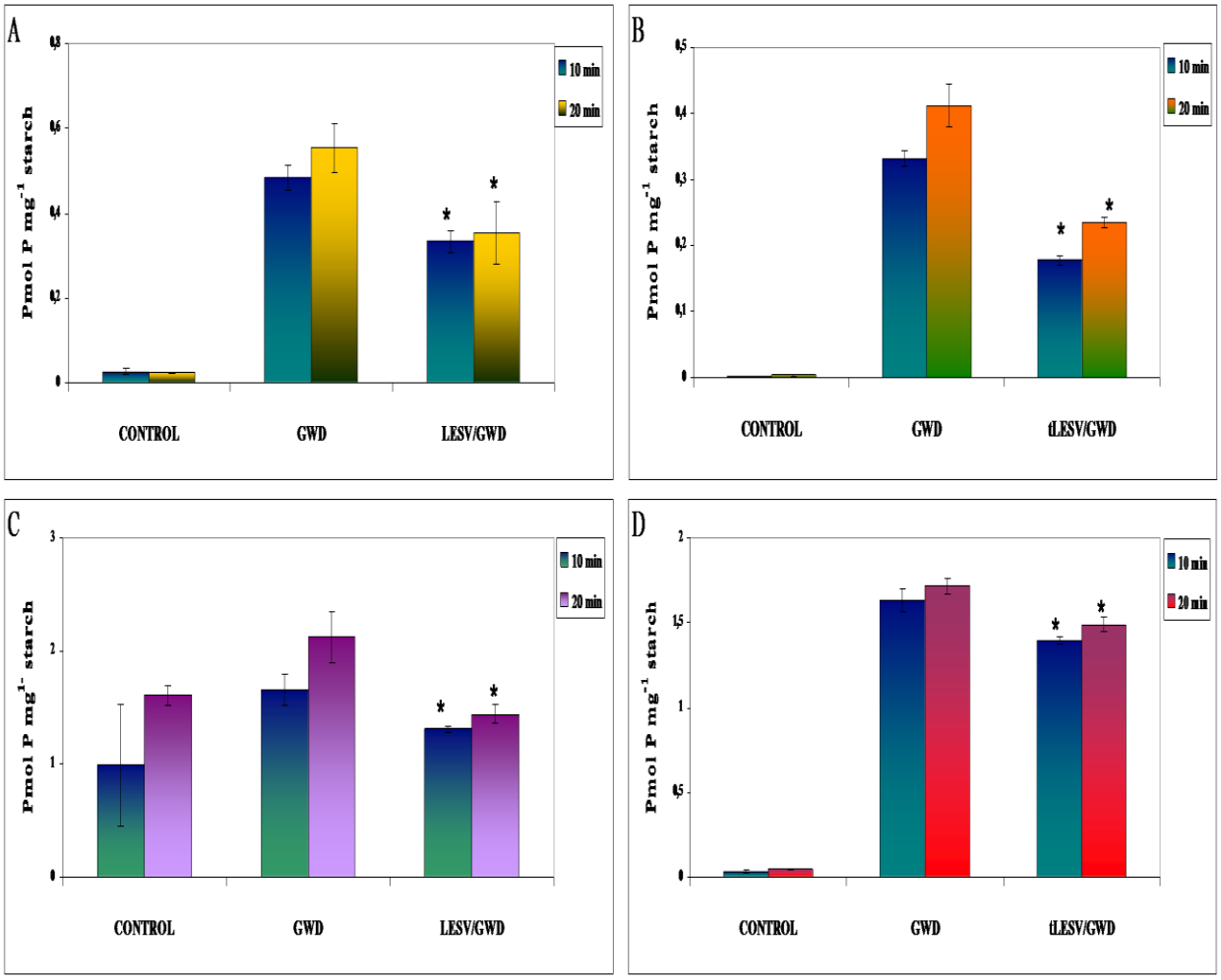

Fig.3.22: Influence of both LESV and tLESV on GWD-mediated phosphorylation of Arabidopsis wild-type and potato starches. Arabidopsis wild-type and potato starches were phosphorylated by *St*GWD and ^{33}P-β-ATP in the presence and absence of both LESV and tLESV forms for two times (10 and 20 min) at 30 C°.As controls, GWD, LESV, and tLESV or both LESV and tLESV were omitted. **A,** Arabidopsis wild-type starch results in the presence of LESV; **B,** Arabidopsis wild-type starch results in the presence of tLESV; **C,** potato starch results in the presence of LESV; **D,** potato starch results in the presence of tLESV. Values are the mean ± standard deviation (SD) (n=3). The asterisk indicates a significant difference (Student's t-test P≤ 0, 05).

3.1.8 tLESV affects the phosphorylation activity of GWD at the different starch granule surface properties

It has been shown that tLESV has an effect on the GWD-mediated phosphate incorporation in Arabidopsis wild-type. To test if the binding of tLESV to the different starch granule surface properties also reveals the same influence on the GWD-mediated phosphate incorporation, it included with Arabidopsis wild-type, Arabidopsis*sex 1-8* native starch granules, which isolated from the GWD- mutant plant. Arabidopsis *sex 1-8* starch granules have different surface properties than the wild-type while they have a higher number of short glucan chains at the granule surface that revealed its impeded GWD activity (Mahlow et al., 2014). However, for both starches it performed a phosphorylation assay. As shown (Fig. 3. 23), both starches revealed a significant reduction in the GWD-mediated phosphate incorporation in the presence of tLESV. Nonetheless, Arabidopsis *sex 1-8* starch granules exhibited less GWD bound to the surface (Fig. 3. 23 B) compared to Arabidopsis wild-type starch granules (Fig. 3. 23 A), while the presence of the short glucan chains at the Arabidopsis *sex 1-8* starch granules surface will reduce the substrate for GWD at the granule surface. Hence, this was reflected in the reduction of glucan phosphorylation. These results suggest that the effect of tLESV on the incorporation of phosphate is not affected by the variation of starch granule properties.

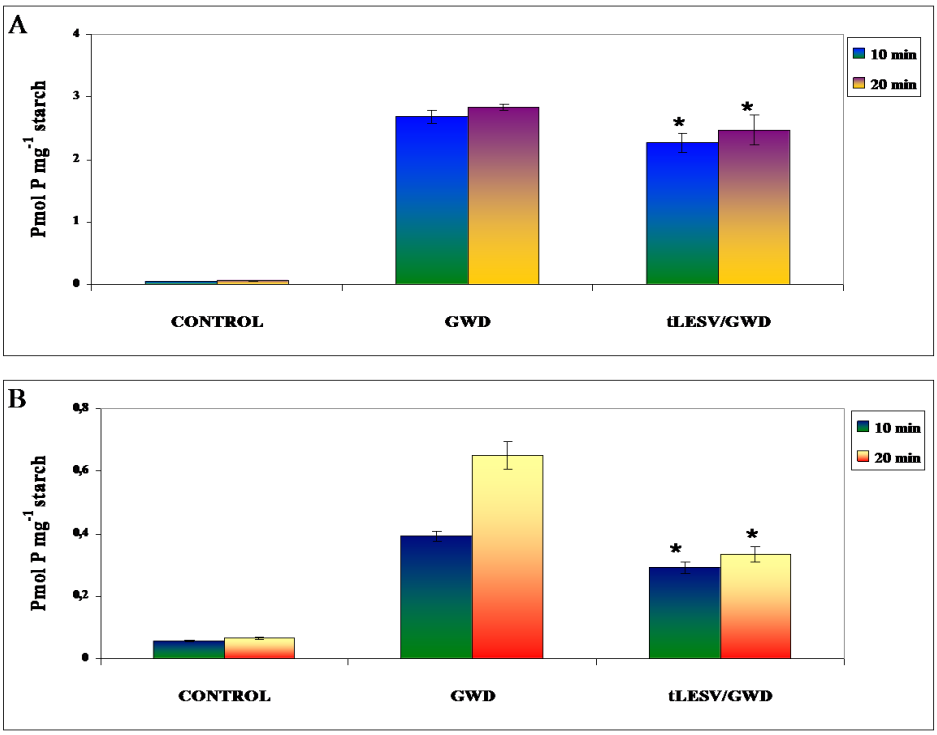

Fig.3.23: Effect of tLESV on the GWD-mediated phosphate incorporation in the Arabidopsis starch granules having different surface properties. A: Arabidopsis wild-type starch. **B:** Arabidopsis *sex 1-8* starch, 30 mg of both starches were phosphorylated by *St*GWD and ^{33}P-β-ATP in the presence and absence of tLESV for two times 10 and 20 min at 30 C°.In control, both GWD and tLESV were omitted. Values are the mean ± standard deviation (SD) (n=3). The asterisk indicates a significant difference (Student's t-test P≤ 0, 05).

However, to confirm the real effect of tLESV on GWD-mediated phosphate incorporation, the activity of LESV was denatured at 95 C° for 3 minutes. After that, the same phosphorylation assay was repeated with Arabidopsis *sex1-8* starch granules (Fig. 3.24). For this assay, 30 mg of Arabidopsis *sex 1-8* starch granules were incubated with *St*GWD and ^{33}P-β-ATP in the presence and absence of both active and inactive forms of tLESV. However, it used a low concentration of the active form of tLESV (0, 04 µg) and 4 fold of the inactive form of tLESV (0,16 µg) to ensure the effects of the active form on the phosphorylation process for two times, 5 and 10 min. As shown in (Fig. 3.24), after measuring the incorporation of phosphate into starch granules, the presence of the active form of tLESV resulted in significantly reduced GWD-mediated phosphate incorporation compared to the inactive form of tLESV which was not affected the incorporation of phosphate to the starch granules. However, the observation suggests that tLESV has a clear effect on the GWD-mediated incorporation phosphate, as with a low

concentration the tLESV was able to alter the glucan structures of starch granules and influencethe GWD- phosphorylation process.

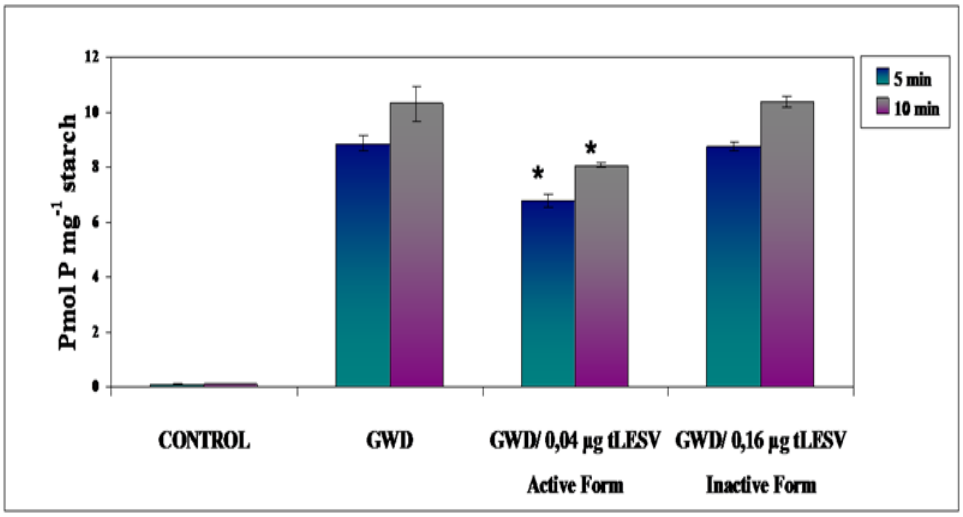

Fig.3.24: Detection of the reduced GWD action by tLESV activity. Arabidopsis *sex1-8* starch granules phosphorylated by constant concentration (0, 1µg) of GWD and ^{33}P-β-ATP in the presence and absence of two forms of tLESV, active tLESV form (low concentration 0, 04 µg) and inactive tLESV form (higher concentration 0,16 µg) for two times, 5 and 10 min at 30 C°,As controls both GWD and both tLESV forms or both forms were omitted. Values are the mean ± standard deviation (SD) (n=3). The asterisk indicates a significant difference (Student's t-test P≤ 0, 05).

3.1.9 Test the effect of tLESV on the autophosphorylation of GWD

Since the action of GWD seems to be affected by tLESV, a closer look onto the autophosphorylation of GWD was tested in order to know whether tLESV has a direct effect on the autophosphorylation activity of GWD, while the autophosphorylation of GWD is considered the first step to use the P-phosphate group of ATP, which is transferred to the conserved histidine in the catalytic sites of the GWD enzyme. In this experiment, the autophosphorylation of GWD by using ATP as a substrate in the presence and absence of LESV was tested (Fig. 3.25). To do so, *St*GWD was incubated with ^{33}P-β-ATP with and without tLESV in the absence of glucan substrate. As controls, bovine serum albumin (BSA), which is a stable and moderately non-reactive protein, was used to determine the quantity of *St*GWD with tLESV vice versa in the samples. However, this experiment revealed clearly that tLESV did not alter the autophosphorylation of GWD since there was no reduction in the turnover of ATP in the presence of tLESV with *St*GWD. Also, there is no possibility that tLESV may have used

ATP as a substrate. The binding of ^{33}P-phosphate to tLESV through the incubation of tLESV with BSA was not observed. These results suggest that tLESV does not work as a competitor with *St*GWD for using ATP, nor does it act as an inhibitor of the action of *St*GWD while the autophosphorylation was not affected. This is evidence that the reduction of GWD-mediated phosphate incorporation in the presence of tLESV is due to the ability of tLESV to change the starch granule surface in a way that affects the GWD-phosphorylation process.

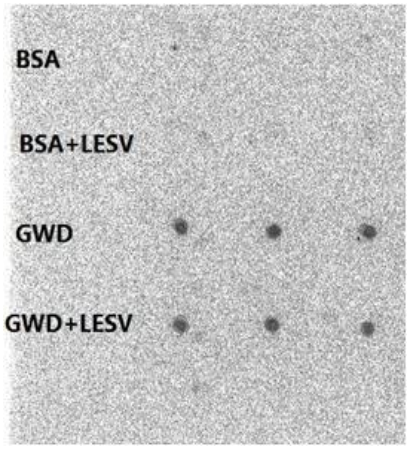

Fig.3.25: Autophosphorylation of GWD in the presence of tLESV. 1µg of tLESV was incubated with 1µg of recombinant *St*GWD and ^{33}P-β-ATP as a phosphate donor in the absence of glucans. The binding of ^{33}P-phosphate to GWD in the presence and absence of LESV was tested. 1µl of each samplewere spotted three times on nitrocellulose membranes.

3.1.10 The correlation between the phosphate incorporation and the amount of tLESV.

While the binding of tLESV at the starch granule surface revealed a significant reduction in the GWD-mediated phosphate incorporated, it was important to test whether the reduction of the incorporation of phosphate into starch was dependent on the ratio of GWD to tLESV. In this assay 30 mg of Arabidopsis *sex1-8* starch was incubated with varying amounts of tLESV (0,08, 0,12, 0,16, and 0,18 µg), a constant amount of *St*GWD (0,1 µg), and ^{33}P-β-ATP (final concentration 1µCi) for two times, 15 and 30 min at 30 C°. However, the result revealed that the GWD-mediated phosphate incorporation into the starch decreasing over time with the increasing the amount of tLESV (Fig. 3.26 A). As

shown in (Fig. 3.26 B) the low amount of 0, 08 µg of tLESV showed a slight reduction in the phosphate incorporation by approximately ~13, 7% after 15 min, while it revealed a significant reduction after 30 min by approximately ~18, 5%. However, the continued increased amount of tLESV led to a significant reduction of the incorporation of phosphate over time. While the amount of 0, 16 µg of tLESV revealed a significant reduction in the incorporation by approximately ~ 20, 1% after 15 min the significant reduction in the incorporation of phosphate goes up to approximately ~26, 2% and ~37% after 15 and 30 min, respectively at an amount of 0, 18 µg of tLESV. On the other hand, the reduction of the incorporation of phosphate was also significant during the comparison between the amounts of protein. However, there was a significant reduction in the phosphate incorporation between the amount of tLESV protein (0, 08 µg and 0, 16 µg) after 30 min and between (0,08 µg and 0,18 µg) over time. Whereas the maximal reduction of the incorporation of phosphate was between the amount of tLESV protein (0, 16 µg and 0, 18 µg), it was significant after 30 min. However, the results suggest that the increase in the amount of tLESV led to reduction but not abolishing the incorporation of phosphate. This means that the binding of tLESV at the starch granule surface will lead to change unknown glucan structures that are preferentially phosphorylated by GWD, hence, this binding will be able to alter the ratio of GWD to tLESV.

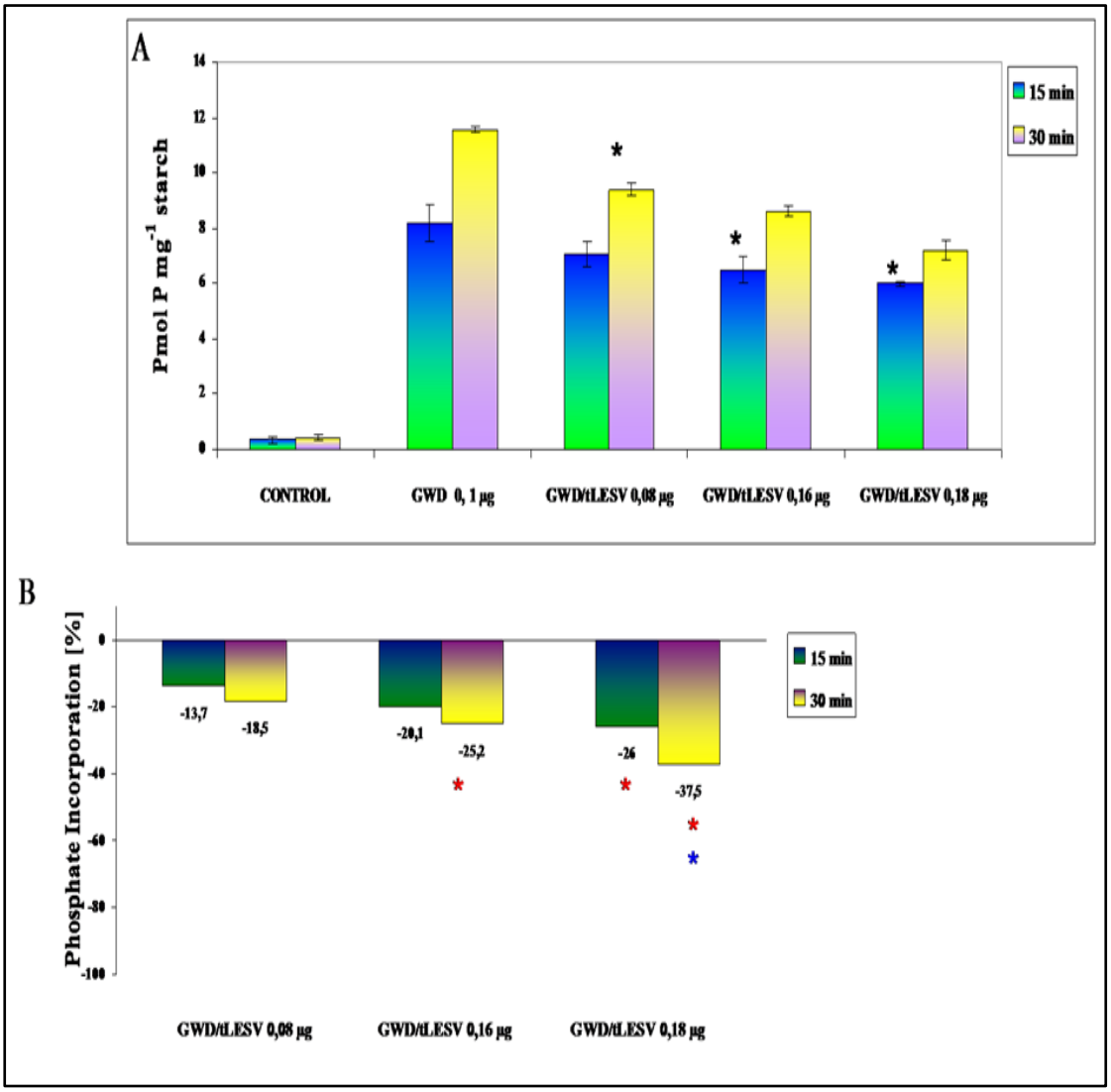

Fig.3.26: Determine the ratio between GWD and tLESV which affect the phosphate incorporation. 30mg of Arabidopsis *sex1-8* starch granules were incubated with a constant amount of *St*GWD (0,1µg) in the presence of varying amounts of tLESV (0,08, 0,16, and 0,18 µg) with ^{33}P-β-ATP. As a control, both *St*GWD and tLESV were omitted. **A**: The ^{33}P phosphate incorporation was measured after two times 15 and 30 min. Values are the mean ± standard deviation (SD) (n=3). The black asterisk indicates a significant difference compared with *St*GWD samples (Student's t-test P≤ 0, 05). **B**: Results for each phosphate of incorporation are expressed as the relative percentage of difference from *St*GWD action value. Values are means of measurements made on 3 replicas. The red asterisk indicates a significant difference between the amount of 0, 08 and 0, 16 µg or 0, 08 and 0, 18 µg. The blue asterisk indicates a significant difference between the amount of 0, 16 µg and 0, 18 µg.

3.1.11 The alteration of the starch granule surface affecting GWD action

The results are shown in Fig. 3. 23 revealed that the GWD-mediated phosphate incorporation revealed a significant reduction in the presence of tLESV in both Arabidopsis wild-type and *sex 1-8* starches. However, both starches have different surface properties.Starch granules of *sex 1-8* have shorter glucan chains at the surface compared to wild-type, which the short glucan chains are accessible to hydrolysing enzymes. However, it was reported that the GWD activity was reduced due to the presence of these soluble glucan chains at the starch granule surface (Mahlow et al., 2014), the results confirmed this finding when it revealed that the incorporation of phosphate by GWD into Arabidopsis wild-type was higher compared to Arabidopsis *sex 1-8* (Fig. 3. 23). On the other hand, the results showed in (Fig. 3. 21) that the alteration of starch structure does not affect tLESV binding. Therefore, it was tested if an alteration of GWD action could be observed in the presence of tLESV after the alteration of the surface structure of these starches. However, it pretreated both Arabidopsis starch forms with isoamylase overnight at 37 C° to remove the free soluble glucan chains from the surface of the starch granule. As controls, the starches were treated identically, but without isoamylase treatment. After that, the reaction was stopped with 2% [w/v] SDS. Following intensive washing, the starch granules was washed and then incubated with ^{33}P-β-ATP and 0,2 µg *St*GWD in the presence and absence of tLESV for two times, 15 and 30 min at 30 C°. The measuring of the GWD-mediated phosphate incorporation into both Arabidopsis starch forms either pretreatment with isoamylase or not showed an increase in the incorporation of phosphate by *St*GWD over time (Fig 3. 27 A and C). In spite of the presence of the increase of the incorporation of phosphate into both starches, there is a difference in the rate of the GWD-mediated phosphate incorporation between them. However, the GWD-mediated phosphate incorporation revealed a significant increase after treatment with isoamylase. Itwas shown that the incorporation of phosphate increased by about 250% and by about 297% after 15 and 30 min, respectively, in Arabidopsis wild-type (Fig 3. 27 B), whereas it was by about 609% and 638% after 15 and 30 min, respectively, in Arabidopsis *sex 1-8* (Fig 3. 27 D). However, a possible explanation for this result that the increase of the incorporation of phosphate in Arabidopsis *sex 1-8* compared to the wild-type refer to the isoamylase-removal of free glucan chains from the Arabidopsis *sex 1-8* starch surfacemaybe, it provides the unknown

glucan structures accessible to *St*GWD that are likely not found in the wild-type starch structure. However, as it was shown that the presence of tLESV resulted in significantly reduced in GWD-mediated phosphate incorporation in both starches. The significant reduction in the GWD-phosphorylation after treatment with isoamylase was revealed after 15 min in Arabidopsis wild-type, whereas it was revealed significantly after 30 min in Arabidopsis *sex 1-8*. Nevertheless, the isoamylase-removal of free glucan chains increased the incorporation of phosphate by *St*GWD by about 169% and 226% in the presence of tLESV after 15 and 30 min, respectively, in Arabidopsis wild-type (Fig 3.27 B), while in Arabidopsis *sex 1-8* the increasing was by 708% and 686% in the presence of tLESV after 15 and 30 min respectively (Fig 3.27 D). These results suggest that it is not only the presence of the free glucan chains at the starch granule surface that affects the GWD-mediated phosphate incorporation but also the presence of tLESV that affects the GWD-phosphorylation process while it was a clear reduction observed in the incorporation of phosphate rate in the presence of tLESV in both starches. Also, the reduction of the GWD-phosphorylation in the presence of tLESV after isoamylase treatment indicates that tLESV is capable of binding to the deep starch layers further to its binding at the granule surface.

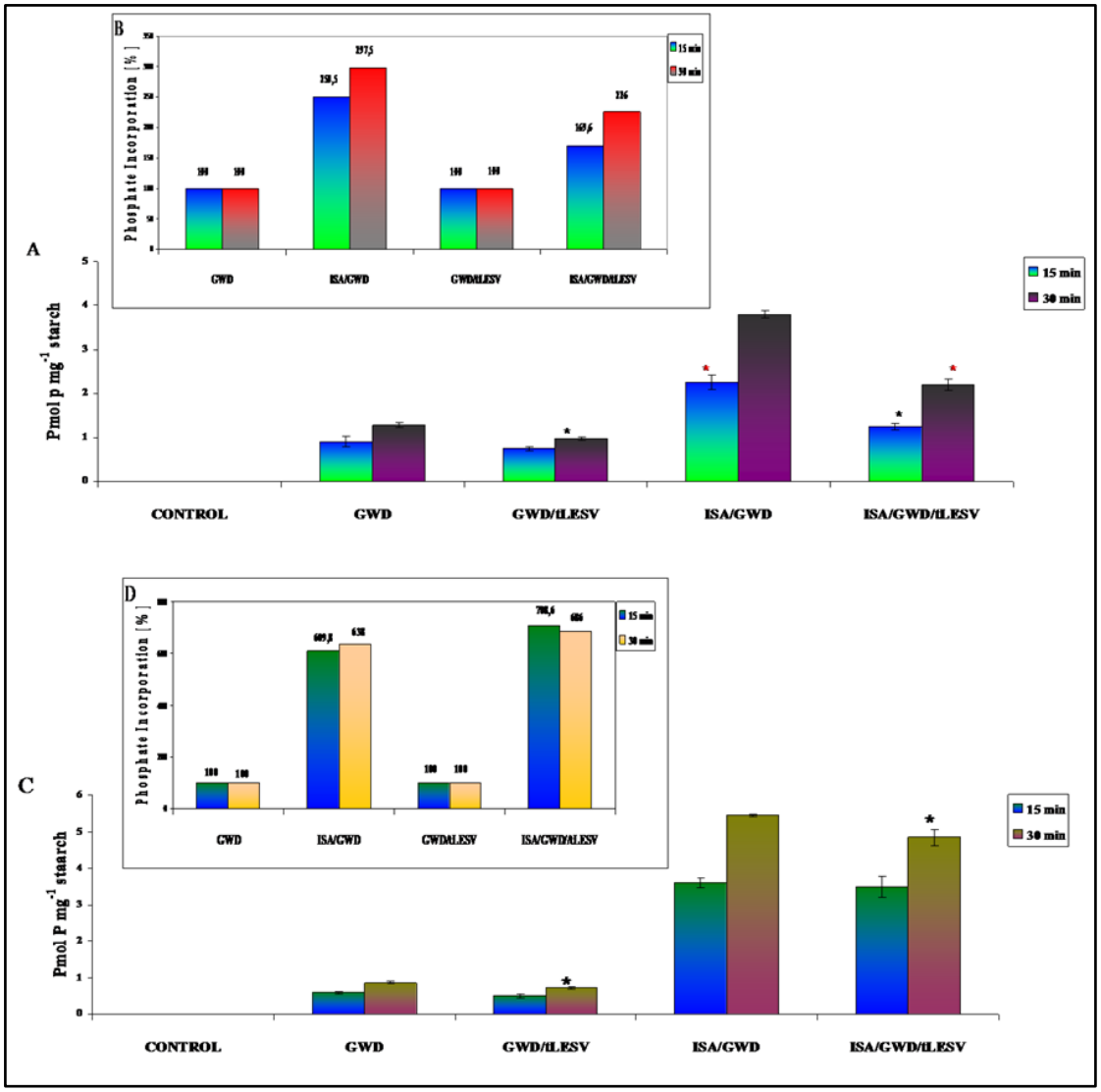

Fig.3.27: Effect of the alteration of starch granule surface on the GWD action. 30 mg of Arabidopsis wild-type or *sex 1-8* starches were resuspended with 7 U of isoamylase overnight at continuous agitation at 37 C°. As controls, starches were incubated in the absence of isoamylase under the same conditions. Following intensive washing, the starches were incubated with 0, 2 µg *St*GWD and ^{33}P-β-ATP in the presence and absence of tLESV at 30 C°. The phosphate incorporation was measured after two times, 15 and 30 min. Values are the mean ± standard deviation (SD) (n=3). The red asterisk indicates a significant difference compared with *St*GWD samples in the presence and absence of isoamylase (IAS).The black asterisk indicates a significant difference compared with *St*GWD samples in the presence and absence of tLESV, (Student's t-test P≤ 0,05). **A** and **C**: Analysis of GWD-phosphate incorporation in Arabidopsis wild-type and sex 1-8 starches, respectively,**B** and **D**: Results for each phosphate incorporation in Arabidopsis wild-type and sex 1-8 starches, respectively are expressed as the relative percentage of difference from *St*GWD action value. Values are means of measurements made on 3 replicas.

3.1.12 tLESV effects the action of GWD in different starch sources

While the effect of tLESV on the GWD-mediated phosphorylation process was detected in Arabidopsis, it was tested if this result is observed in other types of starch. Also, it was

detected if the alterations of the starch granule surface of these starches affect the GWD-phosphate incorporation or affect the influence of tLESV on the GWD action. However, the same Arabidopsis starch phosphorylation assay was used with potato tuber, maize wild-type, maize *waxy*, and maize a*mylose extender* without and with isoamylase pretreated. The ^{33}P phosphate incorporation was measured after 10 and 20 min (Table 3. 1). However, for all starches either with or without isoamylase treatment, the results showed that GWD-incorporation of phosphate increased over time. Further, all starches which were pretreated with isoamylase revealed a significant increase in the GWD-incorporation of phosphate compared to starches that were not treated with isoamylase. However, maize wild-type revealed a greeter increase in the incorporation of phosphate, which was about 431% and 468% in the absence of tLESV and about 477% and 443% in the presence of tLESV after 10 and 20 min, respectively, while maize *amylose extender* showed an increase of about 371% and 370% in the absence of tLESV and about 377% and 222% in the presence of tLESV after 10 and 20 min, respectively. The increase was ~ equal in both potato and maize *waxy* after 10 and 20 min, which was in potato about 121% and 119% and in maize *waxy* was about 120, 9% and 122% in the absence of tLESV and about 113% and 119% and 148% and 149% in the presence of tLESV after 10 and 20 min, respectively. Also for all analysis of starches, the reduction in the GWD-phosphate incorporation was observed in the presence of tLESV either with or without isoamylase treatment. While all the starches without isoamylase treatment revealed a significant reduction in the incorporation of phosphate over time, the starches with isoamylase treatment showed a significant reduction in the incorporation of phosphate after 20 min in both potato and maize wild-type and after 10 min in both maize *waxy* and *amylose extender*. These results suggest that the alteration of the starch granule surface affects the rate of GWD-phosphate incorporation. The difference in the rate of the GWD-phosphorylation reflects the difference of the starch granule surface properties. However, not only the alteration of the surface affects the GWD-phosphorylation but also the presence of tLESV leads to reduction of the incorporation of phosphate. These results may reflect the role of tLESV in regulating the GWD-phosphorylation in starch.

Table 3.1 Effects of tLESV on the GWD-mediated phosphate incorporation in different types of starch without and with isoamylase treatment.

Time	Protein analysis	Starch			
		Potato tuber	Maize WT	Maize *waxy*	Maize *amylose extender*
10 min	Control	0,05±0,02	0,03±0,00	0,08±0,01	0,68±0,01
	GWD	1,50±0,15	0,34±0,01	1,58±0,08	4,03±0,25
	GWD/tLESV	1,39±0,02	0,28±0,02 *	1,04±0,05 *	2,24±0,06 *
	% Phosphate incorporation After treatment with ISA	121,6	431,0	120,9	371,5
20 min	Control	0,07±0,00	0,03±0,00	0,12±0,02	0,70±0,02
	GWD	1,71±0,04	0,40±0,02	1,96±0,22	5,29±0,13
	GWD/tLESV	1,48±0,04 *	0,32±0,02 *	1,28±0,10 *	4,53± 0,3
	% Phosphate incorporation After treatment with ISA	119,1	468,9	122,6	370,8
10 min	ISA/GWD	1,82±0,13 *	1,48±0,34 *	1,91±0,03 *	14,95±1,09 *
	ISA/GWD/tLESV	1,57±0,10 *	1,34±0,28	1,54±0,03 **	8,44 ±1,22 **
	% Phosphate incorporation After treatment with ISA in the presence of tLESV	113,1	477,1	148,3	377,5
20 min	ISA/GWD	2,04±0,05 *	1,88±0,02 *	2,38±0,04 *	19,60±1,70 *
	ISA/GWD/tLESV	1,77±0,05 * *	1,45±0,07 *	1,91±0,37 **	10,04±0,35 * *
	% Phosphate incorporation After treatment with ISA in the presence of LESV	119,4	443,1	149,2	222,0

All values are given in pmol P mg^{-1} starch and represent means ± standard deviation (SD) (n=3). The black asterisk (*) denotes significant difference between GWD and GWD/tLESV or between ISA/GWD and ISA/GWD/tLESV. The red asterisk (*) denotes a significant difference between GWD and ISA/GWD or GWD/tLESV and ISA/GWD/tLESV (Student's t-test P≤ 0, 05). As controls, GWD and tLESV were omitted.

3.1.13 tLESV affects the action of PWD-mediated phosphate incorporation in different starches

Phosphoglucan water dikinase (PWD) is a second dikinase enzyme that adds a phosphate group to the C3 position of a glucosyl residue at the starch granule surface. However, in many starches his action coincides after the activity of GWD by transferring the β-phosphate of ATP to the glucan structures thereby unwinds the double-helical structure of these glucans. Although the action of PWD acts as a downstream of GWD, it was identified that PWD is able to phosphorylate the starch granules without prephosphorylation by GWD (Fettke et al., 2009). However, it was tested if the action of

PWD at the starch granule surface was affected by the tLESV. In the first assay, it incubated *St*PWD directly with starch without prephosphorylation by GWD using different starch surface properties, Arabidopsis wild-type and Arabidopsis *sex 1-8* starches with ^{33}P-β-ATP in the presence and absence of tLESV for 10 and 20 min at 30 C° (Fig. 3. 28). For both starches the result revealed a significant reduction in the PWD-mediated phosphate incorporation over time (Fig. 3. 28 A and B). Although the incorporation of phosphate in Arabidopsis *sex 1-8* starch was a minor, it was significant. These results suggest that PWD is able to phosphorylate yet unknown glucan structures independently. These structures do not need to be pre phosphorylated by GWD regardless of the type of granule surface property.

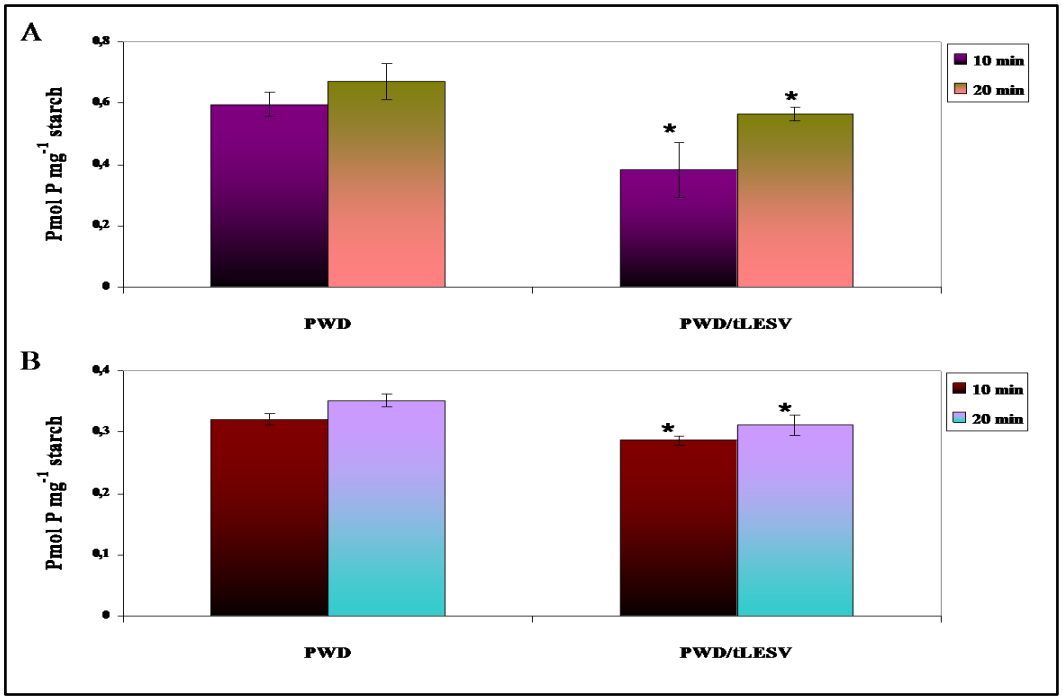

Fig.3.28: Effect of tLESV on PWD-mediated phosphate incorporation without pre phosphorylation by GWD. 30 mg of starch was incubated directly with 0,2 µg of *St*PWD with ^{33}P-β-ATP in the presence and absence of tLESV for two times, 10 and 20 min at 30 C°. As controls both *St*PWD and tLESV were omitted. Values are the mean ± standard deviation (SD) (n=3). The asterisk indicates a significant difference compared with *St*PWD samples in the presence and absence of tLESV, (Student's t-test P≤ 0, 05). **A**: Arabidopsis wild-type starch; **B**: Arabidopsis *sex 1-8*.

In a second assay, it was tested if the PWD-phosphorylation was affected after prephosphorylation by GWD in the presence and absence of tLESV. For this test, it incubated Arabidopsis wild-type starch with non-labelled ATP and 0, 6 µg of *St*GWD

enzyme for one hour at 30 C° as a prephosphorylation. The reaction stopped with 2% [w/v] SDS. Following intensive washing with water, the starch granules were incubated with ^{33}P-β-ATP and 0,2 µg of *St*PWD in the presence and absence of tLESV for two times, 10 and 20 min at 30 C°. As controls both *St*PWD and tLESV were omitted. The measure of the phosphate incorporation showed that the PWD-phosphorylation increased over time. Further, the presence of tLESV led to a decrease in the PWD-phosphate incorporation over time. While the significant decrease in the incorporation of phosphate was observed after 10 min (Fig. 3. 29). However, this suggests that the alteration of the starch granule surface by GWD action may provide glucan structures to PWD. Maybe, these glucan structures are similar to that glucan structures which were phosphorylated by PWD independently without prephosphorylation by GWD. Maybe, these structures are also bound by tLESV. Thus, the binding of tLESV to these structures is involved in the organization of the PWD-phosphorylation process.

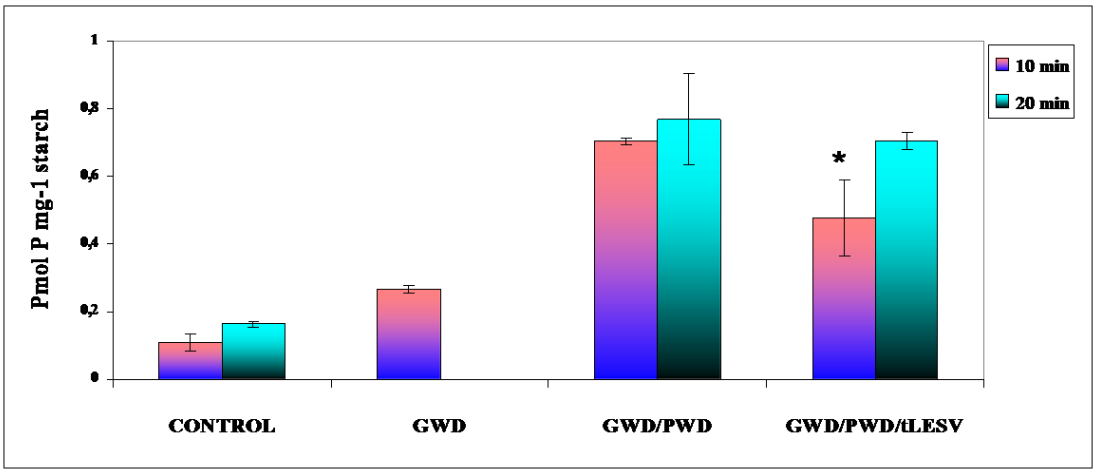

Fig.3.29: Effect of tLESV on PWD activity. 30 mg of Arabidopsis wild-type starch was prephosphorylated with non-labelled ATP and 0, 6 µg of *St*GWD at 30 C° for one hour. Following intensive washing, the starch granules were incubated in the same condition with 0, 2 µg of *St*PWD and ^{33}P-β-ATP in the presence and absence of 2 µg of tLESV for two times, 10 and 20 min at 30 C°. As controls both *St*PWD and tLESV were omitted. Values are the mean ± standard deviation (SD) (n=3). The asterisk indicates a significant difference compared with *St*PWD samples in the presence and absence of tLESV, (Student's t-test P≤ 0, 05).

However, it was also tested if this result could be observed in other starches. Furthermore, it was detected if the alteration of PWD action could be observed after the alteration of a starch granule surface. It was also tested whether the alteration of the starch granule surface affects the influence of tLESV on PWD-mediated phosphate

incorporation. For this assay, it used three types of starch each one of it had different starch granule surface properties. Arabidopsis *sex 1-8*, potato tuber, and maize *amylose extender*. All these starches were treated with isoamylase to remove the free glucan chains from the surface of the granules overnight at 37 C°. As controls, these starches were incubated in the same conditions but without isoamylase pretreated. The reaction stopped with 2% [w/v] SDS. Following washing intensively with water, the starch granules were prephosphorylated with non-labelled ATP by *St*GWD for one hour at 30 C°. The reaction was stopped with 2% [w/v] SDS and followed with intensive washing with water. After that, the starch granules were incubated with *St*PWD and ^{33}P-β-ATP in the presence and absence of tLESV. As controls, the starches were incubated identically but with *St*PWD and tLESV omission. As shown in (Table 3. 2), the incorporation of phosphate into all starches was increasing over time. This increase was significant after isoamylase treatment in the presence and absence of tLESV in all starches. However, the PWD-mediated phosphate incorporation varied among the starches after isoamylase treatment. Maize *amylose extender* revealed greater in the phosphate of incorporation in the absence of tLESV which was about 333% and 313% after 10 and 20 min, respectively, whereas in Arabidopsis *sex 1-8* and potato, it was about 188% and 248% after 10 min and 185% and 199% after 20 min, respectively. This indicates that the PWD-phosphorylation process was much higher at the long glucan structures. Therefore, it is hypothesized that in addition to the role of GWD in generating glucan structures that were used as a substrate by PWD (Fettke et al., 2009), maybe, maize *amylose extender* contains unknown soluble glucan structures that are preferentially phosphorylated by PWD (Hejazi et al., 2009, 2012). However, the presence of such glucan structures cannot be excluded in other types of starch.

On the other hand, a clear significant reduction has been observed in the incorporation of phosphate in the presence of tLESV with or without isoamylase treatment. However, the results suggest that the alteration of the starch granule surface structures due to the action of GWD affects the PWD action and also affects the influence of tLESV on PWD action. The results also suggest that tLESV is involved in the organization of the PWD-phosphorylation process.

Table 3.2 Effects of tLESV on PWD-mediated phosphate incorporation in different types of starch without and with isoamylase treatment

Time	Protein analysis	Starch		
		Potato tuber	Arabidopsis *sex 1-8*	Maize *amylose extender*
1 h	Prephosphorylation/GWD	0,08 ± 0,01	0,53 ± 0,02	1,64 ± 0,19
10 min	Control	0,01 ± 0,00	0,10 ± 0,02	0,28 ± 0,01
	GWD/PWD	0,47 ± 0,02	2,42 ± 0,08	2,71 ± 0,16
	GWD/PWD/tLSV	0,45 ± 0,01	1,00 ± 0,00 *	2,51 ± 0,08
	% Phosphate incorporation After treatment with ISA	248,2	188,7	333,7
20 min	Control	0,03 ± 0,00	0,16 ± 0,00	0,30 ± 0,00
	GWD/PWD	0,74 ± 0,00	2,81 ± 0,15	3,10 ± 0,05
	GWD/PWD/tLSV	0,64 ± 0,01 *	1,24 ± 0,05 *	2,68 ± 0,07 *
	% Phosphate incorporation After treatment with ISA	199,7	185,2	313,2
10 min	ISA/GWD/PWD	1,18 ± 0,09 *	4,56 ± 0,03 *	9,03 ± 0,49 *
	ISA/GWD/PWD/tLESV	0,59 ± 0,06 * *	4,27 ± 0,07 * *	7,16 ± 0,22 * *
	% Phosphate incorporation After treatment with ISA in the presence of tLESV	131,6	423,3	284,8
20 min	ISA/GWD/PWD	1,48 ± 0,09 *	5,21 ± 0,08 *	9,72 ± 0,15 *
	ISA/GWD/PWD/tLESV	0,96 ± 0,06 * *	4,71 ± 0,02 * *	7,70 ± 0,23 * *
	% Phosphate incorporation After treatment with ISA in the presence of tLESV	149,4	379,2	287,0

All values are given in pmol P mg^{-1} starch and represent means ± standard deviation (SD) (n=3). The black asterisk (*) denotes significant difference between GWD/PWD and GWD/PWD/tLESV or between ISA/GWD/PWD and ISA/GWD/PWD/tLESV. The red asterisk (*) denotes a significant difference between GWD/PWD and ISA/GWD/PWD or GWD/PWD/tLESV and ISA/GWD/PWD/tLESV (Student's t-test P≤ 0, 05). As controls, PWD and LESV were omitted.

3.1.14 tLESV did not affect the action of isoamylase

Based on the results available, tLESV possesses a high binding to the starch granule structures. However, phosphorylation of the starch granule surface by GWD and PWD is affected by the presence of tLESV. As it is known, PWD enzyme has a consecutive mode of action with GWD to add a phosphate group to the highly ordered structures at the starch granule surface thereby disrupts it to allow access to the hydrolysis enzymes, as beta-amylase and isoamylase. Therefore, it was tested if the binding of tLESV to the starch granule surface effects on the isoamylase action during releasing the glucan chains from the starch granule surface. Thus, different starches were incubated (Arabidopsis wild-type, Arabidopsis *sex 1-8*, maize wild-type) with 15 µg of tLESV for one hour at 30 C°. The reaction was stopped with 2% [w/v] SDS. Following intensive washing with

water to remove the 2% [w/v] SDS from the samples, the starch granules were incubated with 7 U of isoamylase overnight at 37 C°. As controls, the starches were incubated with isoamylase identically, but without tLESV. Following centrifugation of samples, the releasing glucans were collected and heated for 5 min at 95 C° and filtered through a 10 kDa filter unit. To determine the glucan length distribution, the released glucans were dried and labelled with APTS and separated by CE-LIF. However, for all starches, the released-glucans pattern by isoamylase revealed a slight increase in the short glucan chains in the presence of tLESV (Fig. 3. 30), it was significantly increased in DP 13 in Arabidopsis wild-type (Fig. 3. 30 A), whereas in Arabidopsis *sex 1-8*, it was in DP ≥ 11 (Fig. 3. 30 B), and in maize wild-type, it was in DP ≥ 7 (Fig. 3. 30 C). As it is known that the A chains are the shortest glucan chains (degree of polymerization 13-15) located at the outer layer of the granule surface. Perhaps these glucans were unstable; therefore, the binding of tLESV for these glucans may alter their structure, hence, could be accessible by isoamylase. On the other hand, it was shown that the beta-amylase action was affected by tLESV, while it revealed a clear reduction in the maltose released in the presence of tLESV (Chapter 5). As it is known that beta-amylase degrades only the outer chains of amylopectin (Izydorczyk and Edney 2003). These results suggest that the binding of tLESV increases the stability of the outer glucan chains accessible to the hydrolysis enzymes.

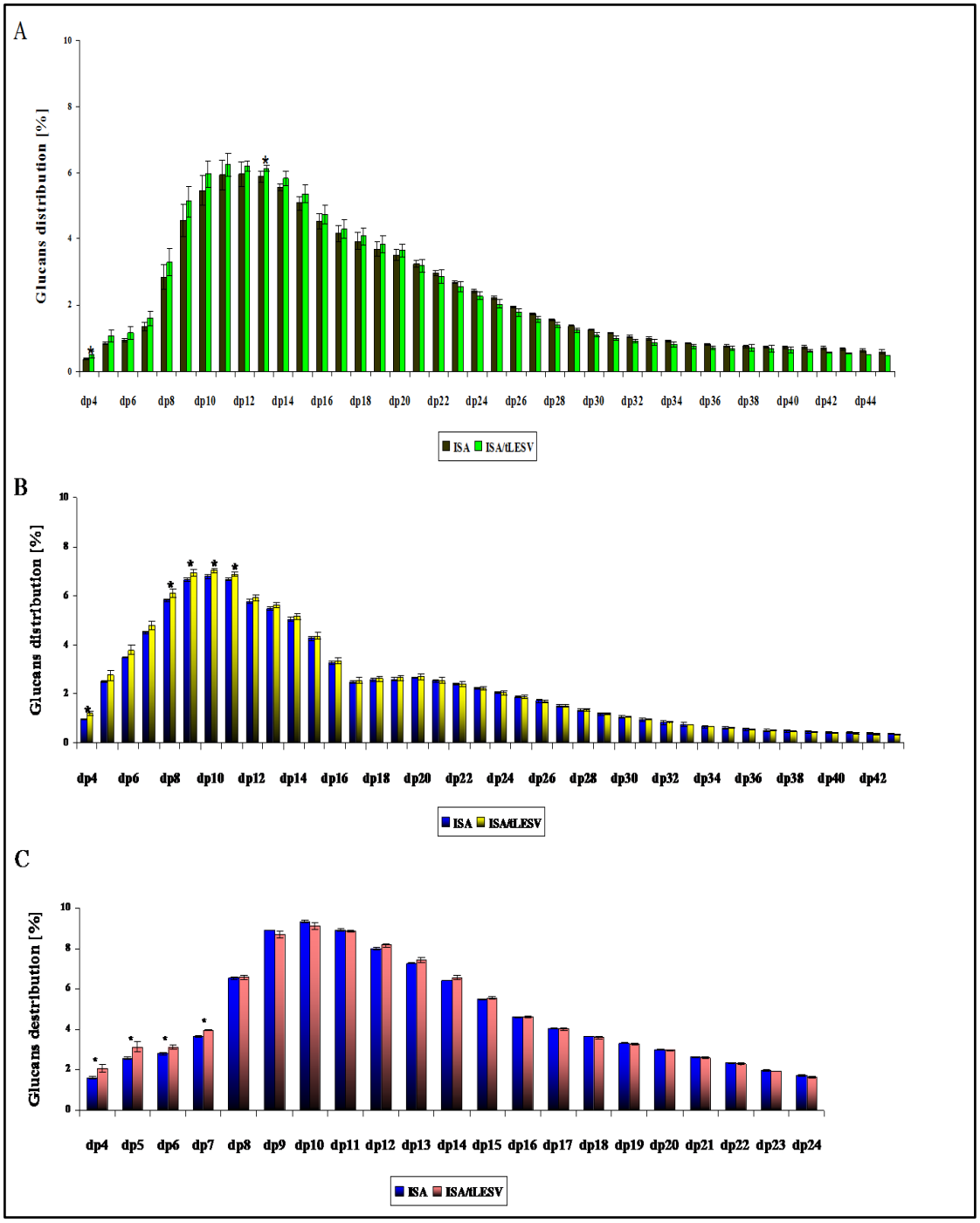

Fig.3.30: Determination of the glucan chains length distribution released by isoamylase (ISA) in the presence and absence of tLESV using CE-LIF. Native starch granules were incubated with 2 µg of tLESV for 1 hour at 30 C°. As controls, the starches were incubated in the same condition, but without tLESV. Following centrifugation, the starch pellets were incubated with isoamylase (ISA) overnight at 37 C° to release the free glucan chains from the starch granules surface. A, Arabidopsis wild-type; B, Arabidopsis *sex 1-8;* C, maize wild-type.

However, it was also tested if the total release of the glucan chains from the starch granule surface is dependent on the ratio of isoamylase and tLESV. For this test, the same

previous assay was repeated using the amount of tLESV from 2 to 6 µg with the constant of isoamylase (7 U) and three types of starch, maize wild-type, maize waxy, and potato tuber. After separating the glucan chains distribution of the starches and calculating the total glucan chains released by isoamylase in the presence of the three amount of tLESV, significant differences was not revealed in the total glucans released in the presence of the different amount of tLESV compared to the total glucan chains released by isoamylase alone (Fig.3. 31). These results suggest that tLESV does not alter the accessible glucan chains at the starch granule surface by isoamylase especially the inner branched. While the increased release of the short glucan chains by isoamylase in the presence of tLESV was very minor, it did not affect the total glucan chains released. However, the same results showed with alpha-amylase while the presence of tLESV did not affect the release of glucan chains by it (Chapter 5).

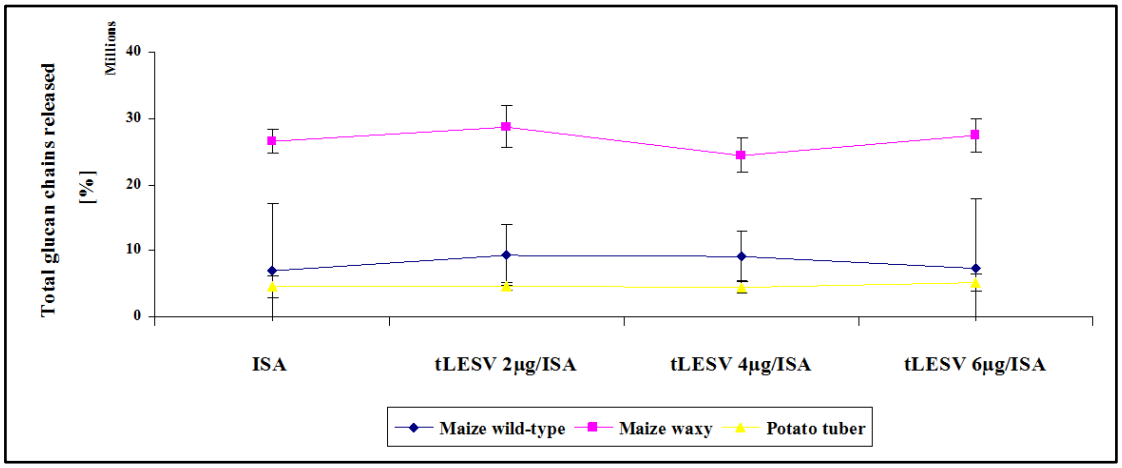

Fig.3.31: Total glucan chains released by isoamylase (ISA) of different starches after being pretreated with a different concentration of tLESV. 50 mg of maize wild-type, maize waxy, and potato tuber were pretreated with 2, 4, and 6 µg of tLESV for 1 hour at 30 C°. As controls, the starches were incubated in the same condition, but tLESV was omitted. Following centrifugation, the starch granules were incubated with 7 U of isoamylase (ISA) overnight at 37C°. Following, labelling of glucan was released with APTS, glucan chains length distributions were monitored using (CE-LIF).

3.2 Discussion

As previously reported, Like-Early Starvation 1 (LESV) protein has been identified as a starch binding protein by using an Arabidopsis forward genetic screen in which the abnormal levels of this protein lead to altering the starch granule structure (Feike et al., 2016). However, recent proteomic studies in addition to the fluorescent-tagged protein experiments identified that the LESV protein is located inside the chloroplast (Edner et

al., 2007; Feike et al., 2016; Helle et al., 2018). Further, in this study, it was confirmed and characterized LESV in *Arabidopsis thaliana* leaves after loading the crude extract of leaves containing the proteins on an SDS-PAGE. Following, the bands of proteins were analyzed by MALDI-TOF. Using BlastP search, the data revealed that the sequence was encoded by At3g55760 in Arabidopsis as a LESV protein. However, a clear 56-amino acid N-terminal as a chloroplastidial transit peptide was predicted using the ChloroP program. As it is known a transit peptide is responsible for targeting the protein encoded by a nuclear into plastidial. Although, mass spectrometry data revealed that it is very likely that the first 56-amino acid act as a transit peptide, it is critical to determine that. Generally, transit peptides are cleaved from the protein. Therefore; they will logically be constructed in protein tagged with the sequence processing information. Two forms of Like-Early Starvation 1 protein were generated and purified, the full-length sequence of protein including the transit peptide which pointed to it as LESV and a truncated sequence of protein without transit peptide which pointed to it as tLESV. However, it was detected whether the presence of the transit peptide with the protein has a different effect than the truncate form on the protein action. Therefore, it included the study of the two protein forms to analyze the binding of both proteins to the starch granules and to detect their effect on the phosphorylation process through starch degradation. The results of both protein forms tests did not reveal differences in their binding to starch. Also the measure of the phosphate incorporation into starch granules in the presence of both protein forms revealed a similar significant reduction in the incorporation of phosphate. Thus, the presence of the 56-aa is not altering the folding of protein thereby did not change the activity of protein. Therefore, it presented only the data of tLESV (truncated form) to explain his role in starch metabolism.

The tLESV protein is associated with different types of glucan

Along with the recent other proteins detected which are associated with starch granules and involved in starch metabolism and its regulation, Like-Early Starvation 1 (LESV) protein is considered one of these proteins. However, in addition to the previous suggestions which referred to the chloroplastidial localization for LESV (Edner et al., 2007, Feike et al., 2016), it confirmed the plastidial localization of LESV in Arabidopsis by loading the crude extract of leaves which contain the proteins on an SDS-PAGE. The appearance of the protein band confirmed the location of protein within the chloroplast

and the protein-glucan interaction experiments confirmed that the tLESV is capable to associate with starch granules with different surface properties. Despite, the variations of the starch granule surface properties and the morphological differentiation of the granules of different starches, tLESV can bind into the surface of these starches in the same mechanism with a variation in the level of his association to these starches. However, it was shown that it is the irreversible binding of tLESV protein to the starch granule, while after incubation of the starches with tLESV it released the amount of the protein by incubation in 2% [w/v] SDS. Further, the starch-tLESV protein associated state revealed that tLESV is binding to deeper layers than the starch surface; while the removal of the soluble glucan chains from the starch surface did not affect the binding of tLESV. However, the binding between the starch and tLESV also refers to the direct protein-starch interaction. Some of starch-related enzymes may interact with a cofactor to reach the starch granules. For instance, granule-bound starch synthases (GBSSs) interacts with Protein Targeting to Starch 1 (PTST1) to transport them to the granules (Seung et al., 2015).

The strength of the binding of the protein to the different starches depends on the starch granule structure. However, the starch of different sources reveals variation in their chemical composition and structural components (Tester, Karkalas, & Qi, 2004). Therefore, the release of protein after washing by 2% [w/v] SDS from Arabidopsis wild-type, potato, and maltodextrin reflects the strength of variation of the binding of tLESV to these starches, hence, determining the affinity of the binding of tLESV to the structures of these starches. Although some starch-related enzymes bind to the starch granule surface and the others enter within the starch granule, tLESV revealed his ability to bind to the surface of starch granules and enter the glucan structure too. This explains the binding of tLESV to the starch structures after removing the free glucan chains from the starch granules surface.

Furthermore, tLESV revealed that it can bind to amylose and amylopectin, but it showed stronger binding to amylose than amylopectin. This suggests that the binding affinity of tLESV to amylose is high, whereas the binding affinity to amylopectin is low. Therefore, his binding to amylose was probably reversible, while it was irreversible with amylopectin. Thus, it can see the release of the amount of protein after washing by 2% [w/v] SDS.

tLESV effects GWD and PWD-mediated phosphate incorporation in different glucans

Phosphorylation process is one of the important mechanisms that occur naturally during starch metabolism. The starch-phosphorylating enzymes, alpha-glucan water dikinase (GWD) and phosphoglucan water dikinase (PWD) play a central role in starch degradation. However, phosphorylation by both enzymes disrupts the crystalline structure of the starch granule surface rendering it more accessible to the hydrolytic enzyme (Hejazi et al., 2008; 2009). It has been shown that GWD acts preferentially on highly ordered structures at the starch granule surface, while PWD acts downstream of GWD and phosphorylates glucan structures formed by the action of GWD (Hejazi et al., 2009; 2012). However, it was shown that PWD activity is not restricted to phosphoglucans when Fettke et al. (2009) revealed that PWD is also able to use neutral alpha-glucan chains. However, it was proposed that LESV acts prior to the start of starch degradation (Feike et al., 2016). Therefore, it was tested whether tLESV is capable to affect the GWD and PWD-phosphorylation process. However, it used different types of starch to test if the activity of GWD and PWD show different effects during starch phosphorylation in the presence of tLESV. To get this point, the effect of tLESV on both dikinases was followed. However, the results clearly showed significant effects of tLESV on the GWD and PWD-mediated phosphate incorporation for all types of starch. Both dikinases revealed the same effect on the phosphorylation of starch by the presence of tLESV, while the GWD and PWD-mediated phosphate incorporation revealed a significant reduction in the presence of tLESV. However, it seems apparent that an increase in the GWD and PWD-phosphorylation process in the absence of tLESV may make the modulation of phosphorylating activity uncontrol thereby affect the rate of starch degradation. Therefore, it is reasonable that the presence of tLESV alters the starch structures in a way that renders the phosphorylation less effective to control the degradation of starch. Although the two dikinases showed the same effect on the starch-phosphorylation process in the presence of tLESV, this does not mean that both dikinases act on the same substrate. Meanwhile, the incubation of PWD without prephosphorylation by GWD with tLESV revealed a significant reduction in the incorporation of phosphate. These results refer that tLESV is capable of binding to

different glucan structures which are used as substrates by two dikinases independently. Further to use PWD the same substrate that is used by GWD.

While GWD acts on highly ordered structures and PWD acts on more soluble glucans structures at the starch granule surface, GWD was also found to bind to soluble glucans, such as maltodextrin. Therefore, the starch granule surface properties have more effect on the phosphorylation process (Chen et al., 2017). However, Mahlow et al. (2014) observed that the short soluble glucan chains at the starch granule surface reduced the rate of GWD-mediated phosphorylation. Furthermore, it was observed that the rate of the incorporation of phosphate by both dikinases varied after starch granule surface alteration by the treatment with isoamylase. However, it was detected that the total phosphorylation increased significantly after isoamylase-mediated removal of short glucan chains from the starch granule surface for all types of starch. While the presence of these glucan chains obstructs are the GWD activity (Mahlow et al., 2014). However, the presence of tLESV also showed a significant reduction in the phosphorylation process by GWD and PWD after the alteration of the starch granule surface. This result indicated that not only the short glucan chains at the starch granule surface affect the phosphorylation process but also the presence of tLESV has a role in limiting the rate of phosphate incorporation. However, it was observed that the ratio of the binding of tLESV at starch granule surface led to reducing of the GWD activity, this is implying that maybe the binding of tLESV to the glucan structures changed the shape of the substrate which is preferentially phosphorylated by GWD thereby affectsthe incorporation of phosphate. While the continuation of the reduction in phosphate incorporation into starch increased with the increase of the amount of tLESV (Fig. 3. 27), changes in the ratio of GWD/tLESV may indicate that the increase of tLESV protein improved organization of GWD-phosphorylation process. It is unclear whether the same equilibria are found in *in vivo*.

Further, the other indication of the role of tLESV to reduce the incorporation of phosphate through the alteration of the granule surface indicates that there is not a competition between tLESV and GWD on the phosphate as a substrate while the autophosphorylation of GWD was not affected by the presence of tLESV. On the other hand, maybe the structural alterations by tLESV protect the starch granule surface from attacking hydrolysis enzymes in an uncontrolled way. Although the presence of tLESV resulted in a slight increase in the short glucan chains, it did not affect the total released

glucan. Also a significant reduction was observed in the action of beta-amylase in the presence of tLESV. However, the decrease in the action of beta-amylase may be linked to a decrease in the action of GWD that is influenced by a change in the starch granule structure resulting from the binding of tLESV. It has been shown that the activity of GWD increases the hydrolytic activity of the plastidial beta-amylase (Edner et al., 2007). In contrast, there was no change in the action of alpha-amylase was observed (Chapter 5). However, maybe the harmony between the binding of tLESV to starch from a side and the effect of this binding on the GWD and PWD as phosphorylating enzymes and ISA, BAM, and AMY as hydrolysing enzymes from another side will generate a balance in the starch consumption during the dark period.

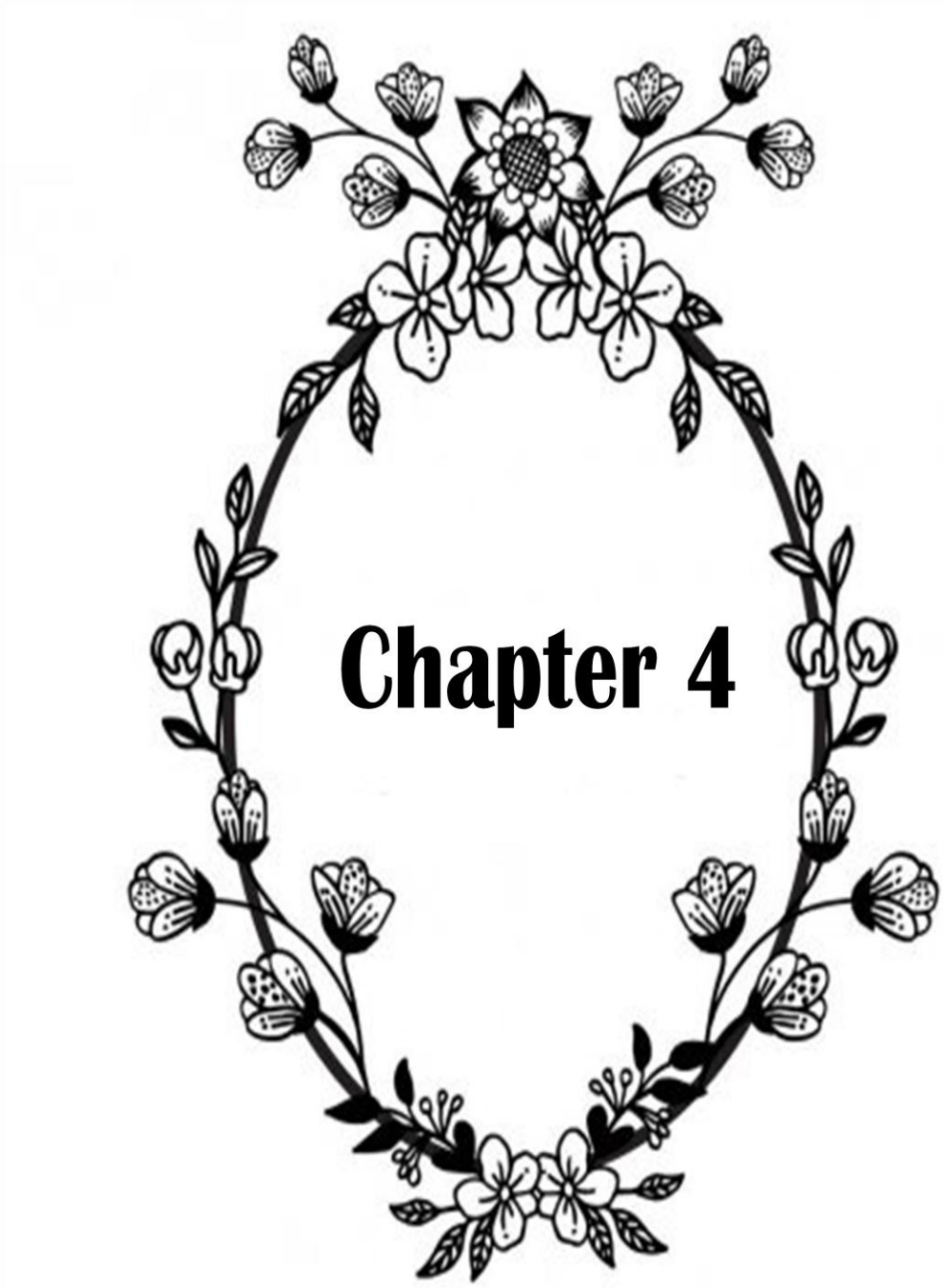
Chapter 4

4. EARLY STARVATION1 specifically affects the phosphorylation action of starch-related dikinases

Irina Malinova, Harendra Mahto, Felix Brandt, **Shadha AL-Rawi**, Hadeel Qasim, Henrike Brust, Mahdi Hejazi and Joerg Fettke. Published in journal of plant physiology (2018)

The experiments related to the binding of ESV1 and tESV1 to Arabidopsis wild-type starch and crystalline maltodextrin, and the binding of ESV1 to amylose were performed by me. The recombinant ESV1 and tESV1 proteins were expressed and purified by me

the plant journal

SEB Society for Experimental Biology

The P lant Journal (2018) 95, 126–137 doi: 10.1111/tpj.13937

EARLY STARVATION1 specifically affects the phosphorylation action of starch-related dikinases

Irina Malinova[†], Harendra Mahto, Felix Brandt, Shadha AL-Rawi, Hadeel Qasim, Henrike Brust[‡], Mahdi Hejazi and Joerg Fettke*

Biopolymer Analytics, Institute of Biochemistry and Biology, University of Potsdam, Karl-Liebknecht-Str. 24–25, 14476, Potsdam-Golm, Germany

Received 27 March 2018; accepted 5 April 2018; published online 22 April 2018.

*For correspondence (e-mail fettke@uni-potsdam.de).

[†] Present address: Max Planck Institute of Molecular Plant Physiology, 14476, Potsdam-Golm, Germany.

[‡] Present address: Plasma Agriculture, Leibniz-Institute for Plasma Science and Technology, 17489, Greifswald, Germany.

SUMMARY

Starch phosphorylation by starch-related dikinases glucan, water dikinase (GWD) and phosphoglucan, water dikinase (PWD) is a key step in starch degradation. Little information is known about the precise structure of the glucan substrate utilized by the dikinases and about the mechanisms by which these structures may be influenced. A 50-kDa starch-binding protein named EARLY STARVATION1 (ESV1) was analyzed regarding its impact on starch phosphorylation. In various *in vitro* assays, the influences of the recombinant protein ESV1 on the actions of GWD and PWD on the surfaces of native starch granules were analyzed. In addition, we included starches from various sources as well as truncated forms of GWD. ESV1 preferentially binds to highly ordered,α-glucans, such as starch and crystalline maltodextrins. Furthermore, ESV1 specifically influences the action of GWD and PWD at the starch granule surface. Starch phosphorylation by GWD is decreased in the presence of ESV1, whereas the action of PWD increases in the presence of ESV1. The unique alterations observed in starch phosphorylation by the two dikinases are discussed in regard to altered glucan structures at the starch granule surface.

Keywords: *Arabidopsis thaliana*, EARLY STARVATION1, glucan, phosphoglucan, starch granule surface, starch phosphorylation, water dikinase.

INTRODUCTION

The growth of most plants is dependent on transitory starch accumulation during the day, when photosynthesis is possible, and starch degradation during the night. Starch is an insoluble polyglucan and consists of two polymers, namely, the branched α-1,4:α1,6-$_D$-glucan amylopectin and the almost unbranched a-1,4-$_D$-glucan amylose. In addition to glucosyl residues, starch contains small amounts of lipids, proteins, and phosphate (Hoover, 2001). Only the phosphate is covalently attached to the starch granule, more specifically to glucosyl residues of the amylopectin. It was shown that starch phosphorylation is transient and predominantly observed during the mobilization of the transitory starch during the dark phase (Ritte *et al.*, 2004). Enzymes that act on and/or bind to starch granules were identified by either incubation with soluble protein extracts and/or direct isolation of native starch granules from *Arabidopsis thaliana* leaves following release of the attached proteins. These proteins were then separated by SDS-PAGE and identified by mass spectrometry. Therefore, using the described method, Ritte and coworkers identified the two plastidial starch-phosphorylating enzymes, namely, glucan, water dikinase (GWD, EC 2.7.9.4; Ritte *et al.*, 2002, 2006) and phosphoglucan, water dikinase (PWD, EC 2.7.9.5; Baunsgaard *et al.*, 2005; Kötting *et al.*, 2005). GWD and PWD selectively

catalyze the formation of C6 and C3 phosphate esters of glucosyl residues, respectively. Both dikinases use ATP as a dual phosphate donor: The terminal γ-phosphate group of ATP is transferred to water, while the β-phosphate group of ATP is transferred to a conserved histidine residue located in the catalytic domain of the enzymes and then to the corresponding hydroxyl group of the glucosyl residue in the amylopectin (Hejazi *et al.*, 2012a). However, additional phospho-transfer reactions have been reported for GWD (Hejazi *et al.*, 2012b).

Glucan, water dikinase shows significant activity towards native starch granules, unlike α-1,4 and α-1,6 hydrolytic enzymes, which preferentially act on soluble glucans (Edner *et al.*, 2007; Fettke *et al.*, 2012a). Crystalline maltodextrins have been shown to be suitable substrates for *in vitro* assays of GWD activity. These crystalline mal- todextrins simulate properties of native starch granules but have been shown to have a much higher degree of crys- tallinity (Hejazi *et al.*, 2008, 2009, 2012a). The rate of phosphorylation of crystalline maltodextrins by GWD was far higher than that observed for any native starch analyzed therefore far and, therefore, it was concluded that GWD preferentially acts on highly ordered crystalline glucan structures. Furthermore, the action of GWD mediates a phase transition of glucan chains on the granule surface from a highly ordered state to a more soluble state (Hejazi *et al.*, 2009). Similar results were obtained when starches of Arabidopsis mutants lacking GWD were analyzed (Mah- low *et al.*, 2014). It was shown that isoamylase-accessible glucan chains on the starch granule surface influence the activity of GWD. Therefore, a greater number of accessible glucan chains at the surface, leads to a less ordered and less crystalline surface, which reduces the action of GWD at the starch granule surface, thereby resulting in a lower phosphorylation rate (Mahlow *et al.*, 2014). Furthermore, it was concluded that accessible glucan chains at the starch granule surface influenced starch morphology (Mahlow *et al.*, 2014).

Glucan, water dikinase is a key enzyme of starch degradation. The GWD-mediated phase transition seems essential for the downstream action of hydrolytic enzymes. Therefore, it has been shown that GWD increases the hydrolytic action of plastidial β-amylases (Edner *et al.*, 2007), however the mechanism how GWD action is regu- lated is obscure (see Hejazi *et al.*, 2012a).

Phosphoglucan, water dikinase acts downstream of GWD and phosphorylates glucan structures formed by the action of GWD (Hejazi *et al.*, 2009, 2012a). However, PWD is also capable of utilizing neutral alpha-glucan chains and, therefore, the action of PWD is not restricted to phospho- glucans (Fettke *et al.*, 2009; Hejazi *et al.*, 2009). Neverthe- less, the exact glucan structures used as substrates by both dikinases remains unknown.

Furthermore, it has been shown that dephosphorylation is also essential for normal transitory starch degradation. In Arabidopsis, there are three phosphoglucan phos- phatases: STARCH EXCESS 4 (SEX4; Kötting *et al.*, 2009), LIKE-STARCH EXCESS FOUR-1 (LSF1; Comparot-Moss *et al.*, 2010) and LIKE-STARCH EXCESS FOUR-2 (LSF2; Santelia *et al.*, 2011). SEX4 and LSF2 are able to remove phosphate esters from starch. As SEX4 dephosphorylates both C6 and C3 in *in vitro* assays (Hejazi *et al.*, 2010), it was concluded that SEX4 acts preferentially on C6 and LSF2 releases C3 phosphate esters during normal starch degradation (Santelia *et al.*, 2011).

To date, for the entire starch phosphorylation/dephos- phorylation cycle (in addition to several other starch- related processes), little or no information is available about regulation. However, recently EARLY STARVA- TION1 (ESV1) protein has been identified by screening mutants with sucrose starvation and abnormal starch turnover during the diurnal cycle (Feike *et al.*, 2016). In the corresponding Arabidopsis mutant, it was shown that the *ESV1* gene is involved in adjusting starch degrada- tion; in the mutant, the transitory starch was seen to be depleted 2 h prior to dawn. The authors suggest that the primary role of ESV1 is not the regulation of starch degradation and hypothesized that ESV1 probably acts prior to the start of starch degradation. However, there was a lack of biochemical evidence to support this hypothesis. We decided to analyze the impact of ESV1 on the start of starch degradation, therefore on the phos- phorylating enzymes, GWD and PWD.

Our finding demonstrates that ESV1 preferentially binds highly ordered starch-like glucan structures. Furthermore, we showed that this protein alters the action of GWD on the starch granule surface and subsequently has an effect also on the action of PWD.

The Plant Journal © 2018 John Wiley & Sons Ltd, The Plant Journal, (2018), 95, 126–137

RESULTS

ESV1 characterization and cloning

To characterize ESV1 from *Arabidopsis thaliana* leaves, transitory starch was isolated under mild conditions. After washing, starch granules were heat treated in SDS sample buffer and centrifuged. The supernatants containing the proteins were loaded on an SDS-PAGE and subsequently analyzed by matrix-assisted laser desorption/ionization mass spectrometry (Figure S1a). Using peptide finger-printing, a protein band with an apparent molar mass of 50 kDa was identified as the product of the At1g42430 gene, *ESV1*. A plastidial localization of the protein was pre- dicted by Bayer *et al.* (2011) using a proteomic approach. Analyses using TargetP (Emanuelsson *et al.*, 2000) and ChloroP (Emanuelsson *et al.*, 1999) did not predict any sig-nificant chloroplastidial transit peptide. However, the plas- tidial localization of ESV1 was confirmed by Feike *et al.* (2016) by transient expression in *N. sylvestris*. Mass spec- trometry analysis revealed a lack of the first 58 amino acids (Figure S1b). Because most nuclear-coded and plastidially localized proteins require a targeting sequence for entry into the plastid, we decided to clone two forms of the ESV1 protein, namely, a full-length ESV1 encoding the entire sequence and a truncated ESV1 (tESV1) that lacks the first 58 amino acids, which most likely represent the putative transit peptide (Figure S1c).

A vector was constructed that allowed the expression of both proteins, each containing a 6xHis tag at the C- terminus, in *Escherichia coli*; the recombinant proteins were purified by a one-step purification using Ni-NTA columns. It should be noted that full-length construct contained a single nucleotide exchange, therefore an ade- nine at position 378 was replaced by a cytosine. However, no alteration in the amino acid sequenced was caused by this exchange (ATA and ATC both coding for Ile).

ESV1 preferentially binds to branched glucans such as native starch

The binding of ESV1 to starch was further confirmed by additional *in vitro* assays. In one assay, recombinant tESV1 was analyzed by native PAGE containing glycogen or soluble starch or lacking α-glucans in the separation gel (Figure 1a). Following electrophoresis and blotting, the tESV1 protein was detected using an anti-His antibody. No inter- action of tESV1 with glycogen was observed; the migration of the protein was unaltered compared with the glucan- free gel. However, a clear retardation was observed when soluble starch was included in the native gel. Similar results were also observed for the full-length ESV1 protein. As the control bovine serum albumin, which does not interact with starch, was analyzed as well. Here no alteration in the migration in the presence or absence of starch in the native gel was observed(Figure 1a).

In a second assay, native starch granules isolated from Arabidopsis and potato were incubated with ESV1 for 10 min at room temperature. Following washing with incubation buffer, the starch granules were treated with SDS sample buffer. All fractions were loaded on a SDS-PAGE and the distribution of ESV1 was monitored by immunoblotting (Figure 1b). In both cases, ESV1 was seen to bind to the starch, but ESV1 could be more effectively removed from the potato starch granules than from the Arabidopsis starch. No difference was observed in the binding of ESV1 to wild-type Arabidopsis starch isolated from the dark or light phase (Figure 1c). Furthermore, we included native starch granules isolated from the GWD- deficient mutant *sex1-8*, as this starch has been described as having altered surface properties compared with the wild-type. Specifically, starch granules of *sex1-8* harbor more, but shorter, glucan chains at the surface that are accessible to hydrolytic enzymes such as iso- and β-amy- lases (Mahlow *et al.*, 2014). However, the binding of ESV1 to starch isolated from *sex1-8* revealed no significant dif- ference compared with the binding of ESV1 to wild-type starch.

Furthermore, we also included crystallized maltodextrins (B-type allomorph) in these experiments. Crystallized mal- todextrins have been shown to simulate the surface prop- erties of native starch granules but show an overall higher degree of crystallinity compared with starches (Hejazi *et al.*, 2009; Hejazi *et al.*, 2012a). As shown in Figure 1(d), ESV1 exhibits stronger binding to crystallized maltodex- trins than to the starches, which is reflected in the lack of the proteins in the first

The Plant Journal © 2018 John Wiley & Sons Ltd, The Plant Journal, (2018), 95, 126–137

washing fractions, therefore only by washing with SDS-containing buffer ESV1 was

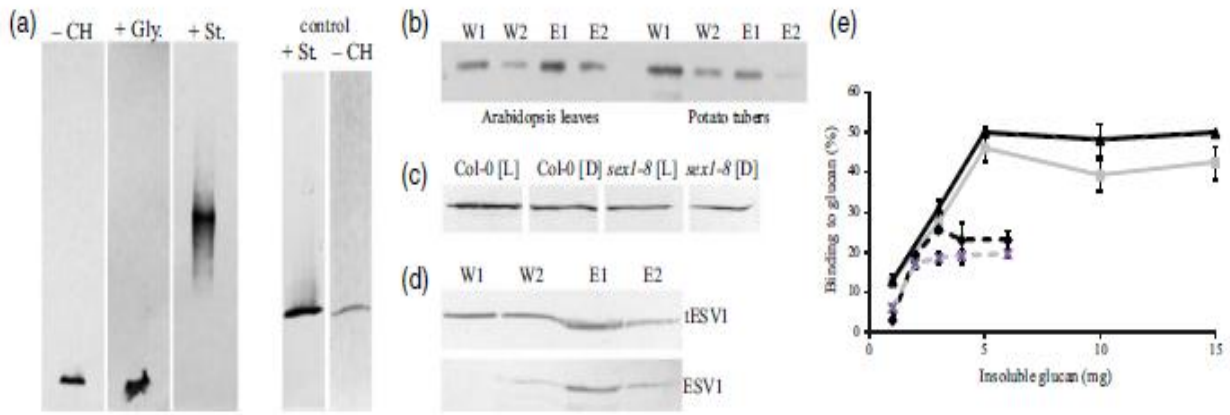

Figure 1. Analysis of ESV1 binding to different carbohydrates.

(a) Separation of tESV1 using native PAGE followed by anti-His immunodetection. Separation gels were supplemented with 0.3% [w/v] glycogen (+Gly), 0.3% [w/v] soluble starch (+ St), or any carbohydrate was omitted (–CH). Here, 2 μg of tESV1 were loaded per lane. As further control 1 μg bovine serum albumin (BSA) were separated using native PAGE. Following western blotting, BSA was stained with Ponceau S.

(b) ESV1 binding to Arabidopsis leaf and potato tuber starch. SDS-PAGE 12% [T] followed by anti-His immunodetection. Here, 20 mg of starches were incubated with 2 μg of ESV1 for 5 min under continuous agitation. Samples were centrifuged and supernatants were collected (fraction W1). Pellets were washed with an equal volume of incubation buffer (fraction W2). Pellets were sequentially washed two times with equal volumes of SDS sample buffer, resulting in fractions E1 and E2, respectively.

(c) Binding of ESV1 to Arabidopsis wild-type and *sex1-8* starches. 6 mg of starches isolated from Col-0 or *sex1-8* leaves harvested at end of the light phase (L) and after 4 h in the dark (D) were incubated with 2 μg of ESV1 for 10 min at 30°C under continuous agitation. Samples were centrifuged and washed twice with incubation buffer. Starch pellets were resuspended in equal volumes of SDS samples buffer, heated at 95°C for 5 min, and volumes equal to 2 μg were loaded on the gel.

(d) ESV1 binding to crystalline maltodextrins. 20 mg of maltodextrins (B-type) were incubated either with 2 μg of tESV1 or with 2 μg of ESV1. Fractions were collected the same way as in (b).

(e) ESV1 and tESV1 binding to Arabidopsis wild-type starch and crystalline maltodextrins. Here, 3 μg of ESV1 and tESV1, respectively were incubated with increasing amounts of the glucan substrate as indicated. Following incubation for 10 min the pellets were washed and the bound protein was determined following SDS-PAGE and western blotting. Black lines represent ESV1; grey lines tESV1; solid lines Arabidopsis wild-type starch; broken line crystalline maltodex- trins.

effectively removed. However, tESV1 exhibited weaker binding to the crystallized maltodextrins than ESV1, which was reflected by the detection of tESV1 in the first washing fraction (Figure 1d).

All observed binding patterns were not related to a specific protein/glucan ratio, as even doubling the amount of ESV1 resulted in the same distribution pattern. Therefore, in the presented experiments, the binding capacity of the starches or crystallized maltodextrins for ESV1 was not limited.

No binding of ESV1 to amylose was observed (Figure S2a). However, as we detected differences in the bind- ing of tESV1 and ESV1 to crystalline maltodextrins (Figure 1d), we analyzed the binding of glucans to Arabidopsis starch and crystalline maltodextrins in greater detail (Figure 1e). For both glucans, we observed a typical binding curve, but tESV1 showed a slightly reduced affinity compared with ESV1. Furthermore, binding of ESV1 and tESV1 plateaued earlier for crystalline maltodextrins but the total portion of proteins bound to crystalline maltodextrins was less. However, all further experiments were performed with both proteins (ESV1 and tESV1) and, as we did not observed any significant difference, we only presented one version for all experiments in this manuscript.

ESV1 alters the phosphorylation activity of the GWD

While the enzymatic activity of ESV1 was not inferable, the strong binding of this protein to crystalline maltodextrins prompted us to take a closer look at the connection between ESV1 and the

The Plant Journal © 2018 John Wiley & Sons Ltd, The Plant Journal, (2018), 95, 126–137

starch-related dikinase GWD. It has been shown that GWD has a much higher activity on crystalline maltodextrins than on any type of starch analyzed to date (Hejazi *et al.*, 2008, 2009).

We performed a phosphorylation assay, using recombi- nant GWD and ^{33}P-β-ATP in the presence or absence of ESV1 and measured the incorporation of phosphate into crystalline maltodextrins (B-type) and Arabidopsis native starch granules. For all experiments we presented two time points of incubation in the linear part of the reaction time course. As shown in Figure 2(a), the incorporation of phos- phate into both substrates increased over time. However, the addition of ESV1 resulted in significantly reduced incorporation of phosphate into native starch granules, whereas the incorporation of phosphates into crystalline maltodextrins was not affected. Also when A-type crystalline maltodextrins were used, no alteration of GWD-mediated phosphate incorporation was detected. However, to test if this result is specific for Col-0 starch, we repeated the assay with starch isolated from various sources (Table 1). For all analyzed starches, a significant reduction of phosphate incorporation was observed, however the amounts clearly differed between the various starches.

We further tested if the observed reduction in phosphate incorporation into starch is dependent on the ratio of GWD and ESV1. To do so, we varied the amount of ESV1 in the assay from 0.3 to 4 μg while keeping the amount of GWD (0.2 μg) constant (Figure 2b). Small amounts of ESV1 resulted in a slight reduction of GWD-mediated phosphate incorporation by approximately 10%, while an increase in the amount of ESV1 used to 2 and 4 μg led to a decrease in incorporation by approximately 40%. Furthermore, the decrease in phosphate incorporation plateaued at approximately 2 μg of ESV1. When the same assay was performed with native *sex1-8* starch granules (Figure 2b), saturation was observed at lower amounts of ESV1 (1 μg). However, the decrease in GWD-mediated phosphorylation is seen to be more than three-fold stronger in Col-0 compared with *sex1-8* starches (Figure 2c).

ESV1 is highly specific in reducing the action of GWD

As depicted in Table 1, our study included wt, *waxy* and *amylose extender* (*ae*) endosperm starches from maize mutants. While *waxy* starches only consist of amylopectin as a result of the absence of granule-bound starch synthase (GBSS1) activity, *amylose extender* starches contain longer glucan chains within the amylopectin and a higher amylose content as the branching enzyme IIb (SBEIIb) is not functional in these mutants (Keeling and Myers, 2010). The incorporation of phosphate by GWD into *waxy* starch was similar to wild-type; in contrast the phosphate incor- poration into *ae* starch was high. No binding of ESV1 to amylose, however, was detected (Figure S2a). We have shown that the action of GWD on the starch granule sur- face is influenced by soluble glucan chains located on the surface, which are accessible to isoamylase. Therefore, a decrease in the number of soluble glucan chains resulted in a strong increase in GWD activity on the surface of the native starch granules (Mahlow *et al.*, 2014). We also tested if an alteration of GWD activity could be observed for these maize starches and if alterations of the starch surface influenced the effect of ESV1 on GWD. Therefore, we pretreated both maize starches with isoamylase overnight to remove free soluble glucan chains from the surface of the starch granules. After the washing steps, the granules were used for a GWD activity assay in the presence or absence of ESV1. As controls, the starches were treated identically but with the omission of isoamylase treatment (Figure 3a). For both maize starches pretreatment with isoamylase resulted in increased phosphorylation by GWD. While *waxy* starch showed a greater increase compared with *ae* starch, both starches still differed in the GWD-mediated phosphate incorporation rate. Therefore, it is not only the glucan chains at the surface of the starch granule that are accessible to isoamlyase treatment, and are responsible for the detected difference. The decrease in GWD-mediated starch phosphorylation in the presence of ESV1, however, sustained for both starches at least during longer incubation.

The Plant Journal © 2018 John Wiley & Sons Ltd, The Plant Journal, (2018), 95, 126–137

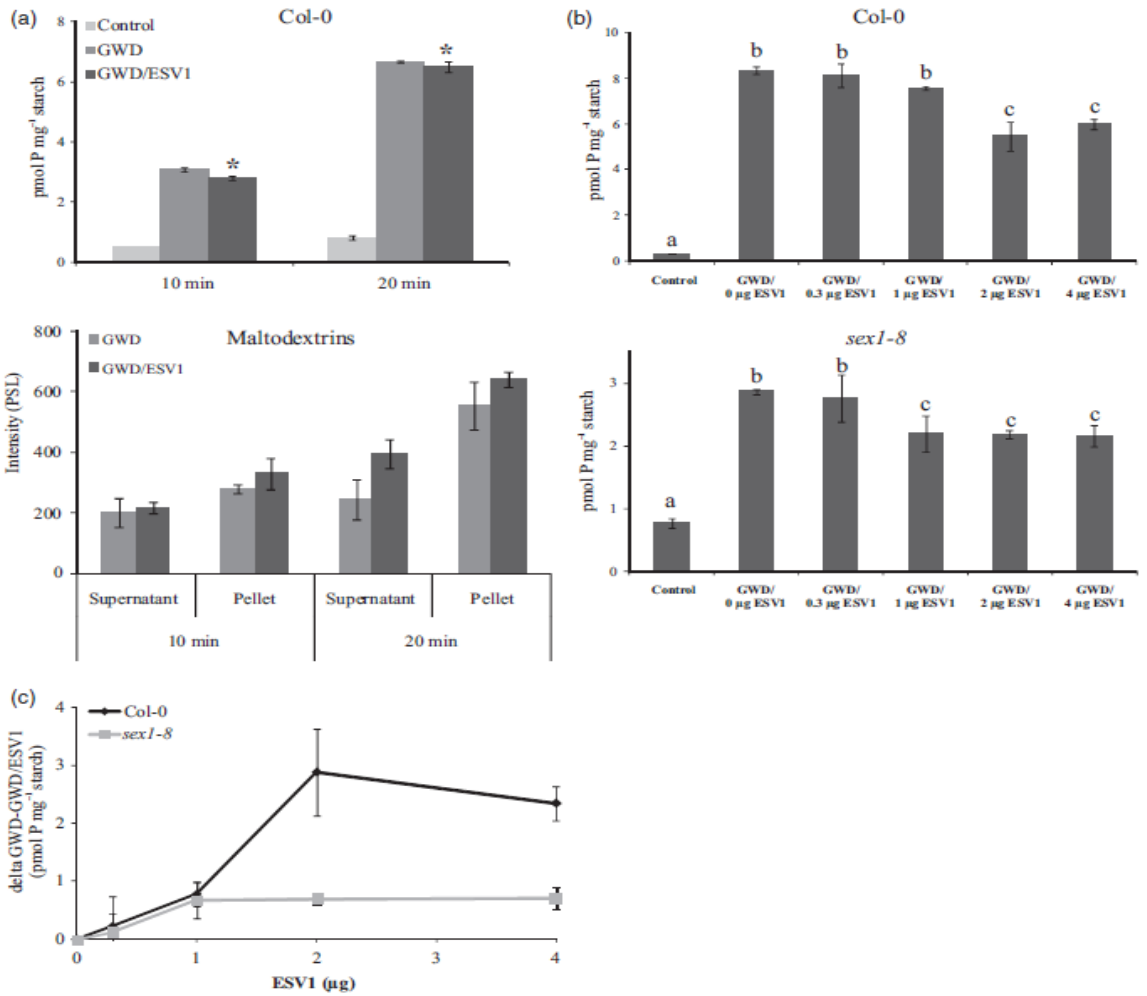

Figure 2. Influence of ESV1 on GWD action.

(a) Phosphorylation of native starches and crystalline maltodextrins by GWD in the presence of ESV1. Here, 8 mg starch granules (Col-0) or 4 mg crystalline maltodextrins were incubated with 0.2 µg GWD, 0.2 µg of GWD/2 µg of ESV1 at 30°C under continuous agitation. The reactions were stopped, and the phosphate incorporation was determined. Values are the means ±standard deviation (SD) (n = 3). Asterisk indicates a significant difference compared with GWD samples (Student's t-test $P \leq 0.01$).

(b) Impact of different ESV1 amounts on starch phosphorylation by GWD. Here, 0.2 µg of GWD and 0–4 µg of ESV1 were applied in the assay; in controls, both GWD and ESV1 were omitted. Samples were incubated for 10 min at 30°C±T values are the means ± SD (n = 3). Letters indicate samples that were not signifi- cantly different ($P \leq 0.05$) according to one-way analysis of variance (ANOVA) with Holm–Sidak post hoc analysis.

(c) Difference plots to compare the influence of ESV1 on GWD-related phosphorylation of Col-0 and *sex1-8* starches. Values of GWD/ESV1 starch phosphoryla- tion were subtracted from GWD starch phosphorylation. Values are means ± SD (n =3).

Additionally, it is possible that the binding of carbohydrate-binding modules at the starch surface influences the activity of GWD and, therefore, the observed alteration of the GWD action is simply a result of an altered structure of the starch granule surface during binding. To test this hypothesis, we generated two truncated versions of GWD, both containing the predicted starch-binding domain, SBDI (1–470 aa) and SBDII (250–470 aa), but differing in size

The Plant Journal © 2018 John Wiley & Sons Ltd, The Plant Journal, (2018), 95, 126–137

Table 1 ESV1 influence on GWD phosphorylation of starches from different sources

	10 min			20 min		
Starch	Control	GWD	GWD/ESV1	Control	GWD	GWD/ESV1
Maize (wt)	0.08 ± 0.03	0.18 ± 0.02	0.14 ± 0.01*	0.08 ± 0.02	0.32 ± 0.02	0.24 ± 0.01*
Maize (ae)	0.02 ± 0.00	1.72 ± 0.16	1.36 ± 0.14*	0.06 ± 0.03	3.49 ± 0.42	2.42 ± 0.50*
Maize (*waxy*)	0.12 ± 0.02	0.17 ± 0.01	0.13 ± 0.01*	0.15 ± 0.03	0.29 ± 0.04	0.25 ± 0.01
Arabidopsis (*sex1-8*)	0.24 ± 0.02	0.74 ± 0.09	0.45 ± 0.05*	0.39 ± 0.04	1.16 ± 0.21	0.53 ± 0.09*
Arabidopsis (Col-0, 2 h dark)	0.38 ± 0.07	3.35 ± 0.48	2.73 ± 0.09*	0.96 ± 0.11	5.48 ± 0.84	4.82 ± 0.07

All values are given in pmol P mg^{-1} starch and represent means ± standard deviation (SD) (n = 3). Asterisk indicates significant difference compared to GWD (Student's t-test $P \leq 0.05$). Control – starches were treated identically but GWD was omitted.

(Figure S3; for further information about the N-terminal starch-binding domain of GWD, please see Hejazi *et al.*, 2012a). Starch binding was confirmed for both truncated GWDs. However, a simultaneous incubation of GWD and the SBDs with wild-type starch did not result in an alteration in GWD action at the starch granule surface compared with the incubation with GWD alone (Figure 3b).

ESV1 influences processes downstream of GWD

It has been shown that a second dikinase, the phosphoglucan, water dikinase (PWD), is also essential for normal starch degradation (Baunsgaard *et al.*, 2005; Kötting *et al.*, 2005). PWD acts downstream of GWD and, therefore, for many starches, prephosphorylation by GWD is required for the action of PWD. To test if the action of PWD at the starch granule surface is also influenced by ESV1, we incubated native starch granules with [β^{33}P]ATP and PWD directly, without GWD-mediated prephosphorylation, in the presence or absence of ESV1 (Figure 4a). A significant incorporation of ^{33}P-phosphate by PWD was observed. Interestingly, a simultaneous incubation with ESV1 resulted in a small but significant decrease in the amount of phosphate incorporated by PWD (Figure 4a). In addition, we tested the effect of prephosphorylation by GWD on the action of PWD in the presence or absence of ESV1. To do so, starch granules were incubated with non–labeled ATP and GWD. Following intensive washing, the starch granules were incubated with ^{33}P-labeled ATP and PWD in the presence or absence of ESV1. The addition of ESV1 resulted in increased PWD-mediated phosphate incorporation (Figure 4b). Furthermore, the observed increase plateaued upon addition of approximately 1 μg of ESV1 (Figure 4c). The observed increase in starch phosphoryla- tion by PWD was also detected for starch isolated from *sex1-8* and *ae* maize (Figure 4b).

In summary, the data point to an alteration of the structure of the starch granule surface specifically and differently used by the two starch-related dikinases. The degree of reduction of the GWD action on the starches is less compared with the degree of increase of phosphorylation via PWD (Figure 4d). We further tested the possibility of detecting these alterations. Therefore, we incubated Col-0 starch with ESV1 for 1 h and then incubated the native starch granules with isoamylase to release the soluble glucans at the surface. As a control, the starch was treated identically but ESV1 was omitted. However, no difference in the released-glucan pattern was observed (Figure S4). Additionally, for larger amounts of ESV1 (2 μg mg^{-1}starch), no alterations of the accessible glucan chains at the starch granule surface were detectable.

ESV1 did not affect the autophosphorylation of the dikinases

As an alteration of the starch phosphorylation was observed for both dikinases in the presence of ESV1, we tested whether ESV1 directly influences the phosphorylation activity of these two dikinases. To do so, we analyzed the autophosphorylation of the dikinases. The autophosphorylation is a consequence of the utilization of the b-phosphate group (and to a lower extent, also the c-phosphate group; see Hejazi *et al.*, 2012b) of ATP, which is transferred to a conserved histidine in the catalytic sites of the enzymes (Ritte *et al.*, 2002). Hence, reduced autophosphorylation is an indication of a reduced turnover of ATP. Therefore, GWD and PWD were incubated with [b^{33}P] ATP and ESV1 in the absence of a glucan substrate. However, the autophosphorylation of the dikinases was not altered in the presence of ESV1 (Figure 5). Similar no significant altered binding of the starch-related dikinases to Arabidopsis wild-type starch was observed in the presence of ESV1 (Figure S2b).

DISCUSSION

We generated and purified two forms of the EARLY STARVATION 1 protein, ESV1 and tESV1. The latter lacked the N-terminal region (1–58 aa), which is usually processed during transport into plastids. However, a clear chloroplastidial transit peptide was not predicted (using ChloroP and TargetP; Emanuelsson *et al.*, 1999, 2000). Mass spectrometry data revealed that it is very likely that the first 58 aa were removed during the import process into the chloroplast. As this processing can be very critical, both ESV1 and tESV1 were included in the analyses, but only slightly differences

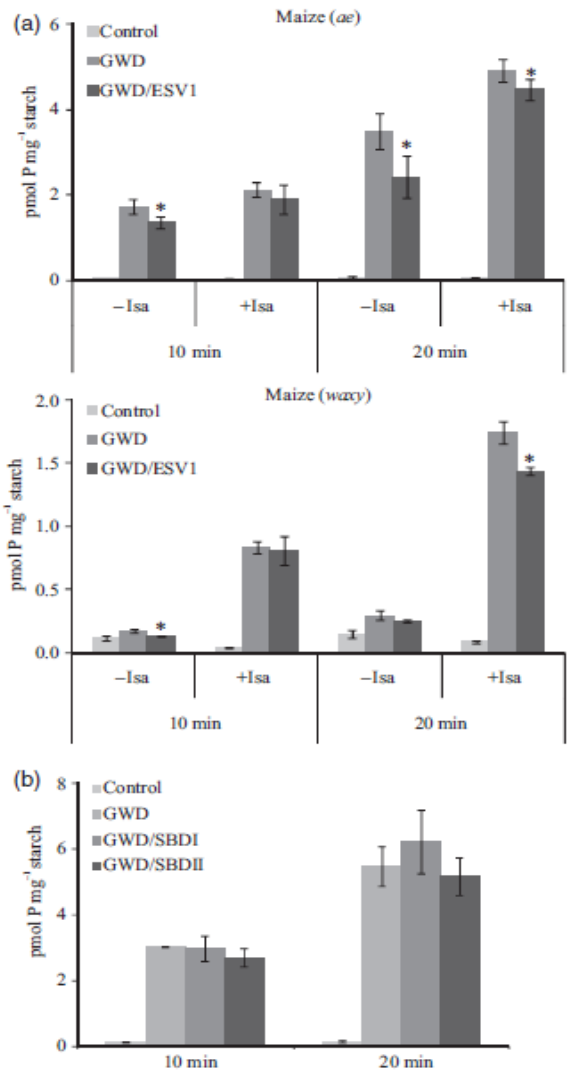

Figure 3. Specificity of the influence of ESV1 on GWD action.
(a) Phosphorylation of maize starch granules following isoamylase digestion. Starch granules isolated from *amylose extender* (*ae*) and *waxy* maize were subjected to isoamylase digestion. As a control, starches were also incubated in the absence of isoamylase under otherwise identical conditions. The starches were resuspended (10 m_M Na-acetate buffer, pH 5.5, 2 m_M DTE) and digested with 12 U isoamylase overnight at 37°C under continuous agitation. The reaction was stopped with SDS, and starch granules were washed 10 times with water. Aliquots of the starches were tested for remaining isoamylase via SDS-PAGE and silver staining. No remaining isoamylase was detected. Starch granules were resuspended and used for GWD (0.3 μg) incorporation assays in the presence or absence of ESV1 (0.3 μg). Values are the means ± standard deviation (SD) (n = 3). Asterisk indicates significant difference compared to GWD samples (Student's t-test $P \leq 0.05$).
(b) Phosphorylation of 8 mg Col-0 starches by GWD in the presence of SBDI and SBDII. Values are the means T SD (n =3).

in glucan binding and enzyme action were observed between the two. It is therefore very unlikely that the N-terminus is massively altering the action of ESV1. Therefore, in this report, we mainly present the data of only one of the proteins (see below) and discuss the function.

ESV1 binds preferentially tordered a-glucan structures similar to starch

As ESV1 was found as a starch-binding protein, we analyzed the specificity of ESV1 for different α-glucans. With regards to soluble α-glucans, no interaction of ESV1 with glycogen was observed, whereas ESV1 was seen to effectively bind solubilized starch. Furthermore, we compared the binding of ESV1 to several insoluble α-glucans; specifically different native starches and starch-like crystalline maltodextrins (Figure 1). Therefore, ESV1 is able to bind to different types of native starch granules (Figures 1–3) although the morphologies and the surface properties of these starches were clearly different. However, when comparing the binding to several starches the available surface should be considered. Interestingly, the binding of ESV1 to native starch granules was not totally reversible. Therefore, after incubation of the starches with ESV1, not all of the protein was released even after washing with 2% SDS (w/v). Therefore, either the binding is very strong, or ESV1 is not only binding the surface of the starch granules but also entering the glucan structure of the starch granules (see below). Furthermore, also soluble starch was bound by ESV1 but no interaction with glycogen was observed (Figure 1a). Therefore, probably the branching structures were important here. However, crystalline maltodextrins did not contain any branches but ESV1 binds strongly to crystalline maltodextrins (Figure 2d; Hejazi *et al.*, 2008, 2009, 2012a). Furthermore, ESV1 was also always detected in the supernatant forming equilibrium between starch bound and unbound state (e.g. Figure 1e). A distribution between starch bound and unbound state of ESV1 is very likely to be observed *in vivo*, also. However, it is unclear whether the equilibria are similar.

ESV1 affects the action of GWD and PWD involved in starch degradation

So far, only the starch-phosphorylating dikinases GWD and PWD have been shown to act preferentially on highly ordered a-glucans, such as crystalline maltodextrins (Hejazi *et al.*, 2008, 2012a), whereas all other enzymes related to starch degradation and synthesis were thought to preferentially act on soluble a-glucans (e.g. Edner *et al.*, 2007; Fettke *et al.*, 2012a; Hejazi *et al.*, 2012a). It was shown that PWD acts downstream of GWD. However, we have also shown that the prephosphorylation of GWD is not necessary for all starches (Fettke *et al.*, 2009; Hejazi *et al.*, 2012a). Furthermore, it is not the phosphorylation event by GWD *per se* that is essential, but rather phosphorylation by GWD generates a yet unknown carbohydrate structure that is used as a substrate by PWD (Fettke *et al.*, 2009; Hejazi *et al.*, 2012a). We tested if ESV1 is able to influence the action of the dikinases at the surfaces of native starch granules (Figures 2–4). Both dikinases were affected by the presence of ESV1 but in an antagonistic manner. Therefore, glucan phosphorylation by GWD was significantly reduced in the presence of ESV1 (Figure 2), whereas the phosphorylating action by PWD, after prephosphorylation by GWD (Figure 4), was increased in the presence of ESV1. Therefore, specific effects of ESV1 on the activities of the two dikinases were observed, which probably reflects the glucan-substrate specificities of the dikinases (see below). However, the observation that the two dikinases were antagonistically influenced by ESV1 excludes other factors e.g. interfering buffer contaminants, enzyme inhibitors, and activators of the dikinases. Furthermore, the influence of ESV1 is rather specific for the dikinases. Therefore, no alterations in the action of all tested other starch-related enzymes were observed. Therefore, ESV1 did not affect the activities of SEX4 (Figure S5a) or isoamylase (Figure S4), two enzymes involved in starch degradation downstream of the dikinase-mediated phosphorylation, or the activities of the main soluble starch synthases of Arabidopsis, AtSS1 and AtSS3 (Figure S5b), at the starch granule surface. For both tESV1 and ESV1 no influence on the activities of other enzymes was detected.

The Plant Journal © 2018 John Wiley & Sons Ltd, The Plant Journal, (2018), 95, 126–137

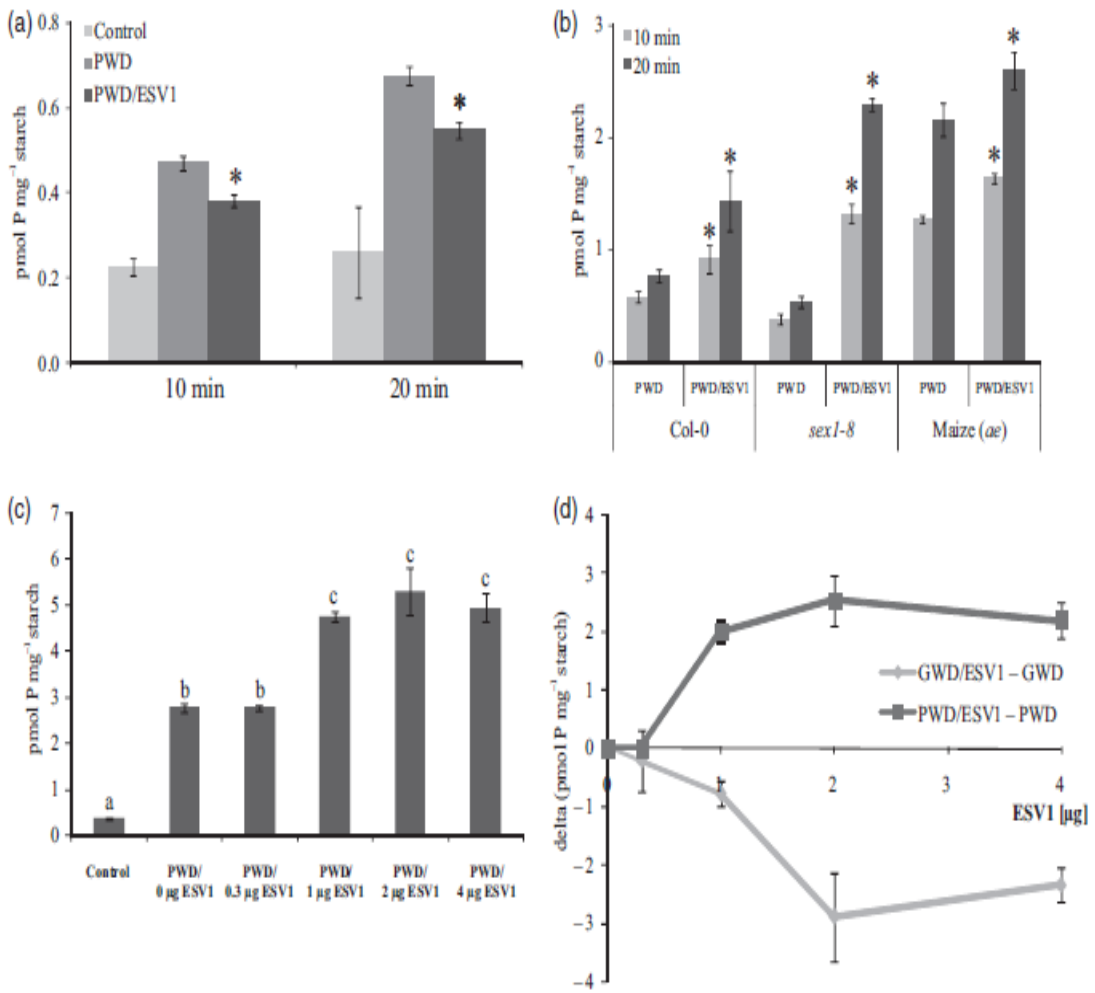

Figure 4. Influence of ESV1 on PWD action.

(a) PWD phosphorylation in the presence of ESV1 without GWD prephosphorylation. Values are the means ± standard deviation (SD) ($n = 3$). Asterisks indicate significant differences compared to PWD samples without ESV1 (Student's t-test $P \leq 0.01$).

(b) PWD phosphorylation of starches from different sources in the presence of ESV1 after GWD prephosphorylation. In the controls, both PWD and ESV1 were omitted, and the values were subtracted. Values are the means ± SD ($n = 3$). Asterisks indicate significant differences compared with PWD samples without ESV1 (Student's t-test $P \leq 0.05$).

(c) Impact of different ESV1 amounts on starch (Col-0) phosphorylation by PWD. 0.2 µg of PWD was used, for controls; both PWD and ESV1 were omitted. Samples were incubated for 10 min at 30°C. Values are the means T SD ($n = 3$). Letters indicate samples that were not significantly different ($P \leq 0.05$) according to one-way analysis of variance (ANOVA) with Holm–Sidak post hoc analysis.

(d) Difference plots to compare the influence of ESV1 on the action of GWD and PWD. Values of dikinase-mediated starch phosphorylation were subtracted from values of dikinase-mediated starch phosphorylation in the presence of ESV1. Col-0 starch was used. Values are the means ±SD ($n = 3$).

Impact of ESV1 on the structure of the starch granule surface

While GWD acts preferentially on highly ordered structures at the starch granule surface (Hejazi *et al.*, 2008, 2012a), the enzyme is also able to bind soluble glucans, such as maltodextrins. However, the soluble glucans could not be phosphorylated by GWD implying that the soluble a-glucans somehow acted as inhibitors (Hejazi *et al.*, 2009, 2012b).

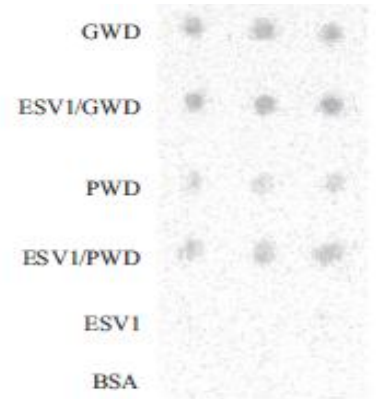

Figure 5. Autophosphorylation of GWD and PWD in the presence of ESV1. Here, 1 μg of GWD and 1 μg of PWD were incubated separately or in combination with 1 μg of ESV1 in 50 m_M HEPES/KOH pH 7.4, 1 m_M EDTA, 6 m_M $MgCl_2$, 2 m_M DTE, 10 μM ATP, 1.3 μCi [β-^{33}P] ATP (10 μl total volume) for 30 min at 30°C. As a control, BSA and ESV1 (1 μg each) were incubated under identical conditions. In all reactions the amount of BSA was adjusted to 3 μg total proteins in the reaction. The reaction was stopped with 0.1 N NaOH, and 1 μl of each reaction was spotted onto a nitrocellulose membrane. The membrane was washed (10 times with ice-cold water, 5 min each wash), and the radioactivity was monitored by phosphor imaging.

It was observed that shorter soluble glucan chains, to be more precise, glucan chains accessible to hydrolyzing enzymes, such as e.g. isoamylase, reduced the rate of GWD-mediated phosphorylation (Mahlow *et al.*, 2014). This reduction of GWD action was also observed with maize and *sex1-8* starches. Therefore, the isoamylase-mediated removal of glucan chains near the surface resulted in a significant increase in total phosphorylation. However, the reduction of glucan phosphorylation in the presence of ESV1 was consistently observed (Figures 2b and 3a). Interestingly, a decrease in the glucan phosphorylation of GWD caused by ESV1 was observed with lower amounts of ESV1 when *sex1-8* starch was used (Figure 2b) compared with when Col-0 starch was used. A possible explanation for this observation could be that the higher number of short glucan chains at the granule surface in *sex1-8* starches (Mah- low *et al.*, 2014) reduces the amount of possible substrate for GWD at the granule surface, and therefore, less GWD is bound to the surface. This would result in an altered ratio of GWD to ESV1 at the starch granule surface. Surprisingly, we observed a stronger binding of ESV1 to crystalline maltodextrins compared with native starch granules, but no significant change in the GWD action on crystalline maltodextrins was detected in the presence of ESV1 (Figure 2a). However, the GWD-mediated phosphorylation of crystalline maltodextrins was much higher compared with that of any known starch; therefore, it is hypothesized that crystalline maltodextrins contain yet unknown glucan structures that are preferentially phosphorylated by GWD (Hejazi *et al.*, 2008, 2010, 2012a). Most likely, ESV1 is not needed to generate or provide such glucan structures for GWD. In fact, ESV1 also binds to these structures, as reflected by the stronger binding. In native starches, these structures were rare, and therefore, the binding of ESV1 to these structures decreased the action of GWD. However, a simple competition for the binding to these glucan structures can be excluded, as we observed no alteration of GWD action in the presence of truncated versions of GWD, SBDI and SBDII (Figure 3b). For both SBDI and SBDII, binding properties similar to GWD were observed, but both SBDs lack the capability to phosphorylate glucans. Another possibility is that ESV1 has an impact on the action of GWD in the proximity of branching points. As crystalline maltodextrins did not contain branching points, ESV1 revealed no effect on the action of GWD.

In the current model of the phosphorylation/dephosphorylation cycle at the surfaces of native starch granules during starch degradation, PWD acts downstream of GWD (Kötting *et al.*, 2005; Hejazi *et al.*, 2012a). PWD acts on more soluble glucan structures at the granule surface (Hejazi *et al.*, 2009, 2012a). Similar to GWD, the combined action of PWD and ESV1 lead to a decrease in phosphorylation compared with the action of PWD alone (Figure 4a). However, a significant increase in PWD-mediated starch phosphorylation was observed in the presence of ESV1 following prephosphorylation by GWD (Figure 4b,c). Not only was this observed with Col-0 starch, but a similar effect was also observed with maize (*ae*) and *sex1-8* starches. The influence of ESV1 on PWD-mediated phosphorylation was significant, especially in the case of *sex1-8*. Therefore, following the logic that ESV1 alters glucan structures, the protein generates or provides glucan structures that are preferred by PWD. Furthermore, these glucan structures were specific for PWD as other starch-

related enzymes, such as starch synthases (AtSS1 and AtSS3) and SEX4, were unaffected by the presence of ESV1. Interestingly, in contrast with PWD, the latter enzymes have a known preference for soluble glucans (Delvallé *et al.*, 2005). However, these alterations of glucan structures were either very minor or were not located on the outer surfaces of the starch granules, as we were unable to detect them during the release of surface near glucan chains using isoamylase (Figure S4) even when using a high amount of ESV1 (2 μg mg^{-1} starch). This observation was in agreement with the incomplete removal of ESV1 from starch granules detected even after washing with buffers containing 2% [w/v] SDS; more than 20% of the ESV1 was still detected as being bound to the starch granules.

The fact that the autophosphorylation of both GWD and PWD was unaltered in the presence of ESV1 (Figure 5) further indicates structural glucan alterations mediated by ESV1. However, these structural alterations did not affect the binding of GWD and PWD to the starch granule surface (Figure S2b).

CONCLUSION

Taken together, the data suggest that ESV1 is a starch-binding protein that is capable of altering glucan structures of native starches and influencing the action of two enzymes that regulate the initiation of starch degradation, GWD and PWD. Overall alterations of the action of GWD and PWD by ESV1 seem little. However, the overall phosphorylation of starch is minor and therefore even small alterations result in important modifications, especially when repeating actions during starch degradation is considered. Likewise a mutant with reduced expression of GWD was reported that revealed a moderate reduction of GWD phosphorylation by 60%. This mutant showed an increased starch content by more than 300% compared with the wild-type (Mahlow *et al.*, 2014).

The observed reduction of GWD action in the presence of ESV1 is also in agreement with the observed increase in the degradation of starches, in ESV1 knock-out mutant, during the dark phase (Feike *et al.*, 2016). Therefore, GWD-mediated phosphorylation in this mutant is expected to be higher because ESV1 is missing, therefore resulting in more rapid starch degradation. However the opposite is expected for PWD. However, it was shown that PWD influences starch degradation to a lesser extent (Kötting *et al.*, 2005; Hejazi *et al.*, 2012a). Interestingly, for double mutants lacking ESV1 and GWD or PWD a decrease in the amount of starch was detected (Feike *et al.*, 2016). Unfortunately, the phosphorylation of the starches isolated from the dou- ble mutants was not determined.

Moreover, a homolog to ESV1, Like-ESV1 (LESV) was also described by Feike *et al.* (2016). However, ESV1 and LESV revealed different impact on starch turnover and it was speculated that ESV1 and LESV have opposite roles in starch granule matrix regulation (Feike *et al.*, 2016). There- fore, a separate analysis of LESV is needed.

EXPERIMENTAL PROCEDURES

[β-^{33}P]ATP (3000 Ci $mmol^{-1}$) was purchased from Hartmann Ana-lytic (Germany, https://www.hartmann-analytic.de). [U-^{14}C] ADPglucose was prepared as described by Fettke *et al.* (2012b). Isoamylase from *Pseudomonas* sp. and 8-aminopyrene-1,3-6-tri- sulfonic acid (APTS) were obtained from Sigma-Aldrich (Germany, https://www.sigmaaldrich.com/germany). For the expression and purification of GWD from potato (*Solanum tuberosum* L.), see Hejazi *et al.* (2012b); PWD from Arabidopsis, see Kötting *et al.* (2005); for starch synthase 1 (AtSS1), see Mahlow *et al.* (2014) and for starch synthase 3 (AtSS3), see Fettke *et al.* (2011a,b). Crystallized maltodextrins were generated as described by Hejazi *et al.* (2009).

The Plant Journal © 2018 John Wiley & Sons Ltd, The Plant Journal, (2018), 95, 126–137

Plant material and growth conditions

Arabidopsis wild-type (Col-0) and *sex 1-8* mutant (Mahlow *et al.*, 2014) were cultivated in a growth chamber under controlled conditions (12 h light and 22°C/12 h dark and 17°C) and approximately 100 μmol quanta m^{-2} sec^{-1}. Six-week-old rosette leaves were harvested after 10 h in the light (or as indicated), directly frozen in liquid nitrogen and stored at — 80°C until use.

Starch isolation

Starch granules were isolated from Arabidopsis leaves as described by Malinova *et al.* (2017). Potato and maize starches were purchased from ICN Biomedicals (https://www.mpbio.com) and National Starch (http://www.nationalstarch.com), respectively.

Cloning of Arabidopsis ESV1

The cloning and expression strategy for ESV1 and tESV1 was similar to that described for AtSS3 by Fettke *et al.* (2011a,b). First-strand cDNA was synthesized using the Maxima First-Strand cDNA Synthesis Kit (Thermo Scientific, https://www.thermofisher. com). The resulting cDNA was amplified by PCR using Q5 Hot Start High-Fidelity DNA polymerase (BioLabs, https://www.neb. com) and primers as indicated in Table S1. The resulting PCR products were subcloned into the pGEM-T-Easy vector (Promega, https://www.promega.de) and successful cloning was verified by sequencing (LGC Genomics, https://www.lgcgroup.com). Subsequently, gene fragments were cloned into the pET23b (Novagen, http://www.novagen.com) expression vector and then transformed into BL21 *E. coli* cells. For heterologous expression, cells were grown in 1 L of LB medium containing 100 μg ml^{-1} ampicillin up to OD = 0.6. The expression was induced by addition of IPTG (1 m_M final concentration), and the cultures were incubated for 16 h at 18°C. Cell harvesting and protein purification were performed as described by Brust *et al.* (2014).

Cloning of SBDI und SBDII

The StGWD plasmid (Ritte *et al.*, 2002) was used as a PCR template to generate the SBDI and SBDII with primer combination containing *Nde*I and *Xho*I restriction sites (Table S1). PCR fragments were subcloned into a pGEM-T-easy vector (Promega). Subsequently, the *Nde*I–*Xho*I fragment was cloned into the expression vector pET23b (Novagen). The constructs were con- firmed by restriction digestion and DNA sequencing. The expression and purification were performed as described above.

Glucan binding assay

For the binding assays, 20 mg of the respective glucans were used (or as stated). The glucans were washed five times with water and resuspended in 50 μl of incubation buffer [50 m_M HEPES/KOH pH 7.4, 1 m_M EDTA, 6 m_M $MgCl_2$, 2 m_M DTE, 0.4 mg ml^{-1} bovine serum albumin (BSA)] and incubated with 2 μg of ESV1 for 10 min at room temperature (RT) under continuous agitation. Then, the samples were centrifuged and washed once with equal volumes of incubation buffer and twice with SDS sample buffer. All supernatants were adjusted to equal volumes, mixed with SDS sample buffer, heated for 5 min at 95°C, and loaded on SDS-PAGE.

PAGE and immunoblotting

Native PAGE and subsequent immunodetection was performed as previously described (Albrecht *et al.*, 1998; Fettke *et al.*, 2005). For SDS-PAGE and immunoblotting, see Mahlow *et al.* (2014).

Enzyme assays

a-Glucan, water dikinase. Starch—For all GWD assays, the ^{33}P incorporation into glucans was proportional to the enzyme concentration. Dried starch (8–10 mg for Arabidopsis starches, 10 mg for maize starches) was resuspended in incubation buffer (100 μl total volume) containing 50 m_M HEPES/KOH, pH 7.4, 1 m_M EDTA, 6 m_M $MgCl_2$, 2 m_M DTE, 0.4 mg ml^{-1} BSA 50 μM ATP, and 1 μCi [β-^{33}P]ATP. The reaction was started by addition of 0.2 μg of recombinant GWD and 2 μg of ESV1 (or as indicated). In controls, either both GWD and ESV1 or only ESV1 were omitted. Samples were incubated under continuous agitation at 30°C. Aliquots of the reaction mixture were mixed with SDS (final concentration 2% [w/v] SDS). Starches were washed three times with 2% [w/v] SDS and three times with water (1 ml each wash) and finally resuspended in 1 ml water. After mixing with 3 ml of scintillation liquid, the incorporation of ^{33}P was

determined by scintillation counting. In some assays, ESV1 was replaced by 40 ng of SBDI or 70 ng of SBDII, but otherwise treated identically.

Crystalline maltodextrins. Here, 4 mg of crystalline maltodextrins were resuspended in an incubation buffer (see above) with 1 μCi [β-^{33}P] ATP, and 2 μg of ESV1. The reaction was started by addition of 0.2 μg of GWD. Samples (50 μl total volume) were incubated at 30°C under continuous agitation. The reaction was stopped sequentially with 20 m_M EDTA (final concentration) on ice. The samples were centrifuged (1000 *g*, 2 min), the pellets were resuspended in incubation buffer, and both pellets and supernatants were adjusted to be of equal volume. All samples were heated at 95°C for 5 min; 3 μL each were used for TLC. The intensities of phosphorylated glucans were measured using phosphor imaging as described by Hejazi *et al.* (2008).

Phosphoglucan, water dikinase

Starches were pretreated for 1 h with GWD and ATP as described above, but the [β-^{33}P] ATP was omitted. The reaction was stopped by addition of 2% [w/v] SDS and the starches were washed 10 times with water to eliminate GWD. For the direct phosphate incorporation via PWD this pretreatment was omitted. The prephosphorylated starches were resuspended in incubation buf- fer (see above) containing 1 μCi [β-^{33}P] ATP and 2 μg of ESV1. The reaction was started by addition of 0.2 μg of recombinant PWD. In controls, either both PWD and ESV1 or only ESV1 were omitted. Samples were incubated under continuous agitation at 30°C. Aliquots of the reaction mixture were mixed with SDS (final concentration 2% [w/v] SDS), washed three times with 2% [w/v] SDS and then washed three times with water (1 ml each). Finally, the starch pellets were resolved in 1 ml of water. Following mixing with 3 ml of scintillation liquid, the incorporation of ^{33}P was determined by scintillation counting.

Isoamylase digestion of starch granules

Next, 10 mg of native starch granules were resuspended in incu- bation buffer (see above) with 2 μg of ESV1 for 1 h at 30°C and centrifuged (1500 *g*, 2 min), and the supernatant was then dis- carded. The starch pellets were resuspended in 10 m_M Na-acetate buffer, pH 5.5, 2 m_M DTE and digested with 12 U isoamylase (final volume 100 μl) overnight at 37°C with continuous agitation. The samples were centrifuged for 10 min at 1500 *g*, and the supernatant was heated for 5 min at 95°C and filtered through a 10 kDa filter unit. The filtrate was used for determination of the chain length distribution using a capillary electrophoresis apparatus equipped with laser induced fluorescence detection (CE-LIF) as described by Malinova *et al.* (2014).

^{33}P-labelling of recombinant proteins

To monitor the autophosphorylation of GWD and PWD in the presence of ESV1, assays were performed as described by Hejazi *et al.* (2012b).

ACKNOWLEDGEMENTS

Authors gratefully thank Dr Sebastian Mahlow for excellent assistance during starch isolation and purification of the recombinant enzymes.

CONFLICT OF INTEREST

The authors declare no conflicts of interest.

FUNDING INFORMATION

The research was supported by DFG (JF1030 2-/1).

AUTHOR CONTRIBUTIONS

I.M. and J.F. planned and designed the research. I.M., F.B., H.B., S. AR., H.Q., H.M., M.H., J.F. performed the experiments and ana- lyzed the data. I.M., H.B, and J.F. wrote the manuscript.

SUPPORTING INFORMATION

Additional Supporting Information may be found in the online ver- sion of this article.

Figure S1. Characterization and cloning of ESV1.

Figure S2. ESV1 did not bind to amylose and did not alter the binding of GWD and PWD to starch.

Figure S3. The deduced amino acid sequence of N-terminal repeated region of StGWD without transit peptide.

Figure S4. Chain length distribution pattern of the starch granule surface glucan chains released by isoamylase.

Figure S5. Impact of ESV1 on SEX4 and on the main soluble starch synthases.

Table S1. Primers used for PCR.

REFERENCES

Albrecht, T., Greve, B., Pusch, L., Kossman, J., Buchner, P., Wobus, U. and Steup, M. (1998) Homodimers and heterodimers of Pho1-type phospho- rylase isoforms in *Solanum tuberosum* L. as relevant by sequence-speci- fic antibodies. *Eur. J. Biochem.* 251, 342–352.

Baunsgaard, L., Lütken, H., Mikkelsen, R., Glaring, M.A., Pham, T.T. and Blennow, A. (2005) A novel isoform of glucan water dikinase phosphory- lates prephosphorylateda-glucans and is involved in starch degradation in Arabidopsis. *Plant J.* 41, 595–605.

Bayer, R.G., Stael, S., Csaszar, E. and Teige, M. (2011) Mining the soluble chloroplast proteome by affinity chromatography. *Proteomics*, 11, 1287– 1299.

Brust, H., Lehmann, T., D'Hulst, C. and Fettke, J. (2014) Analysis of the func- tional interaction of Arabidopsis starch synthase and branching enzyme isoforms reveals that the cooperative action of SSI and BEs results in glucans with polymodal chain length distribution similar to amylopectin. *PLoS ONE*, 9, e102364.

Comparot-Moss, S., Kötting, O., Stettler, M. *et al.* (2010) A putative phosphatase LSF1 is required for normal starch turnover in Arabidopsis leaves. *Plant Physiol.* 152, 685–697.

Delvallé, D., Dumez, S., Wattebled, F. *et al.* (2005) Soluble starch synthase I: a major determinant for the synthesis of amylopectin in *Arabidopsis thaliana* leaves. *Plant J.* 43, 398–412.

Edner, C., Li, J., Albrecht, T. *et al.* (2007) Glucan, water dikinase activity stimulates breakdown of starch granules by plastidial beta-amylases. *Plant Physiol.* 145, 17–28.

Emanuelsson, O., Nielsen, H. and von Heijne, G. (1999) ChloroP, a neural network-based method for predicting chloroplast transit peptides and their cleavage sites. *Protein Sci.* 8, 978–984.

Emanuelsson, O., Nielsen, H., Brunak, S. and Heijne, G. (2000) Predicting subcellular localization of proteins based on their N-terminal amino acid sequence. *J. Mol. Biol.* 300, 1005–1016.

Feike, D., Seung, D., Graf, A. *et al.* (2016) The starch granule-associated pro- tein EARLY STARVATION1 (ESV1) is required for the control of starch degradation in *Arabidopsis thaliana* leaves. *Plant Cell*, 28, 1472–1489.

Fettke, J., Eckermann, N., Tiessen, A., Geigenberger, P. and Steup, M. (2005) Identification, subcellular localization and biochemical characteri- zation of water-soluble heteroglycans (SHG) in leaves of *Arabidopsis thaliana* L.: distinct SHG reside in the cytosol and in the apoplast. *Plant J.* 43, 568–585.

Fettke, J., Hejazi, M., Smirnova, J., Höchel, E., Stage, M. and Steup, M. (2009) Eukaryotic starch degradation: integration of plastidial and cytoso- lic pathways. *J. Exp. Bot.* 60, 2907–2922.

Fettke, J., Malinova, I., Albrecht, T., Hejazi, M. and Steup, M. (2011a) Glu- cose-1-phosphate transport into protoplasts and chloroplasts from leaves of Arabidopsis. *Plant Physiol.* 155, 1723–1734.

Fettke, J., Nunes-Nesi, A., Fernie, A.R. and Steup, M. (2011b) Identification of a novel heteroglycan-interacting protein, HIP 1.3, from *Arabidopsis thaliana*. *J. Plant Physiol.* 168, 1415–1425.

Fettke, J., Fernie, A.R. and Steup, M. (2012a) Transitory starch and its degradation in higher plant cells. In *Essential Reviews in Experimental Biology: Starch: Origins, Structure and Metabolism*, Vol. 5 (Tetlow, I.J., ed). London: SEB, pp. 309–372.

Fettke, J., Leifels, L., Brust, H., Herbst, K. and Steup, M. (2012b) Two carbon fluxes to reserve starch in potato (*Solanum tuberosum* L.) tuber cells are closely interconnected but differently modulated by temperature. *J. Exp. Bot.* 63, 3011–3029.

Hejazi, M., Fettke, J., Haebel, S., Edner, C., Paris, O., Frohberg, C., Steup, M. and Ritte, G. (2008) Glucan, water dikinase phosphorylates

crystalline maltodextrins and thereby initiates solubilisation. *Plant J.* 55, 323–334.

Hejazi, M., Fettke, J., Paris, O. and Steup, M. (2009) The two plastidial starch-related dikinases sequentially phosphorylate glucosyl residues at the surface of both the A- and B-allomorph of crystallized maltodextrins but the mode of action differs. *Plant Physiol.* 150, 962–976.

Hejazi, M., Fettke, J., Kötting, O., Zeeman, S.C. and Steup, M. (2010) The laforin-like dual-specificity phosphatase SEX4 from *Arabidopsis thaliana* hydrolyses both C6- and C3-phosphate esters introduced by starch-related dikinases and thereby affects phase transition of a-glucans. *Plant Physiol.* 152, 711–722.

Hejazi, M., Fettke, J. and Steup, M. (2012a) Starch phosphorylation and dephosphorylation: the consecutive action of starch-related dikinases and phosphatases. In *Essential Reviews in Experimental Biology: Starch: Origins, Structure and Metabolism*, Vol. 5 (Tetlow, I.J., ed). London: SEB, pp. 279–308.

Hejazi, M., Steup, M. and Fettke, J. (2012b) The plastidial glucan, water diki- nase (GWD) catalyses multiple phosphotransfer reactions. *FEBS J.* 279, 1953–1966.

Hoover, R. (2001) Composition, molecular structure and physiochemical properties of tuber and root starches: a review. *Carbohydr. Polym.* 45, 253–267.

Keeling, P.L. and Myers, A.M. (2010) Biochemistry and genetics of starch synthesis. *Ann. Rev. Food Sci. Technol.* 1, 271–303.

Kötting, O., Pusch, K., Tiessen, A., Geigenberger, P., Steup, M. and Ritte, G. (2005) Identification of a novel enzyme required for starch metabolism in Arabidopsis leaves. The phosphoglucan water dikinase. *Plant Physiol.* 137, 242–252.

Kötting, O., Santelia, D., Edner, C. *et al.* (2009) STARCH-EXCESS4 is a laforin-like phosphoglucan phosphatase required for starch degradation in *Arabidopsis thaliana*. *Plant Cell*, 21, 334–346.

Mahlow, S., Hejazi, M., Kuhnert, F., Garz, A., Brust, H., Baumann, O. and Fettke, J. (2014) Phosphorylation of transitory starch by a-glucan, water dikinase during starch turnover affects the surface properties and mor- phology of starch granules. *New Phytol.* 203, 495–507.

Malinova, I., Mahlow, S., Alseekh, S., Orawetz, T., Fernie, A.R., Baumann, O., Steup, M. and Fettke, J. (2014) Double knock-out mutants of *Ara- bidopsis thaliana* grown under normal conditions reveal that the plas- tidial phosphorylase isozyme (PHS1) participates in transitory starch metabolism. *Plant Physiol.* 164, 907–921.

Malinova, I., Alseekh, S., Feil, R., Fernie, A.R., Baumann, O., Schöttler, M.A., Lunn, J. and Fettke, J. (2017) Starch synthase 4 and plastidial phospho- rylase differentially affect starch granule number and morphology. *Plant Physiol.* 174, 73–85.

Ritte, G., Lloyd, J.R., Eckermann, N., Rottmann, A., Kossmann, J. and Steup, M. (2002) The starch-related R1 protein is an alpha-glucan water dikinase. *Proc. Natl Acad. Sci. USA*, 99, 7166–7171.

Ritte, G., Scharf, A., Eckermann, N., Haebel, S. and Steup, M. (2004) Phos- phorylation of transitory starch is increased during degradation. *Plant Physiol.* 135, 2068–2077.

Ritte, G., Heydenreich, M., Mahlow, S., Haebel, S., Kötting, O. and Steup, M. (2006) Phosphorylation of C6- and C3-position of glycosyl residues in starch is catalysed by two distinct dikinases. *FEBS Lett.* 580, 4872–4776.

Santelia, D., Kötting, O., Seung, D. *et al.* (2011) The phosphoglucan phos- phatase like sex Four2 dephosphorylates starch at the C3-position in Ara- bidopsis. *Plant Cell*, 23, 4096–411911

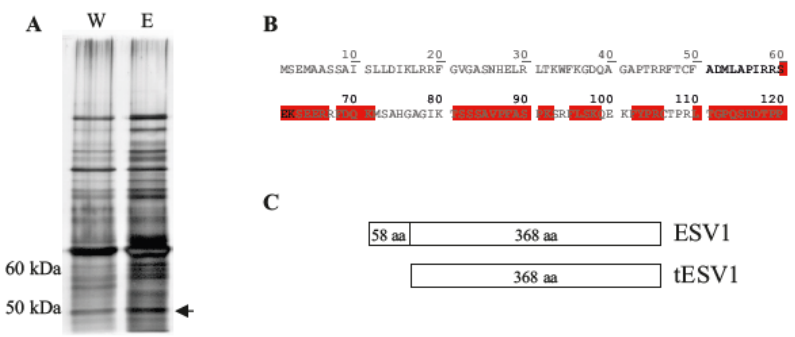

Supplemental Fig. S1. **Characterization of ESV1. A**, Starch-binding proteins resolved by SDS-PAGE 7.5 % [T]. 50 mg of starch granules from leaves of Col-0 were washed twice with 150 µl of SDS sample buffer (W) and granule-bound proteins were eluted by denaturation in 200 µl of SDS sample buffer (E). 25 µl of each fraction were applied per lane. The gel was then silver stained. Starch granules were isolated from Arabidopsis leaves as described by Malinova et al. (2017). Mass spectrometry analysis was performed with a coomassie stained SDS gel similar to that shown as described by Fettke et al. (2011). The arrow indicates ESV1**. B**, Result of mass spectrometric analysis of the first 120 aa of the N terminus of ESV1. red - identified peptides (by peptide finger print and confirmed by ms/ms using MALDI-LTQ). **C,** Schematic representation of ESV1 and tESV1

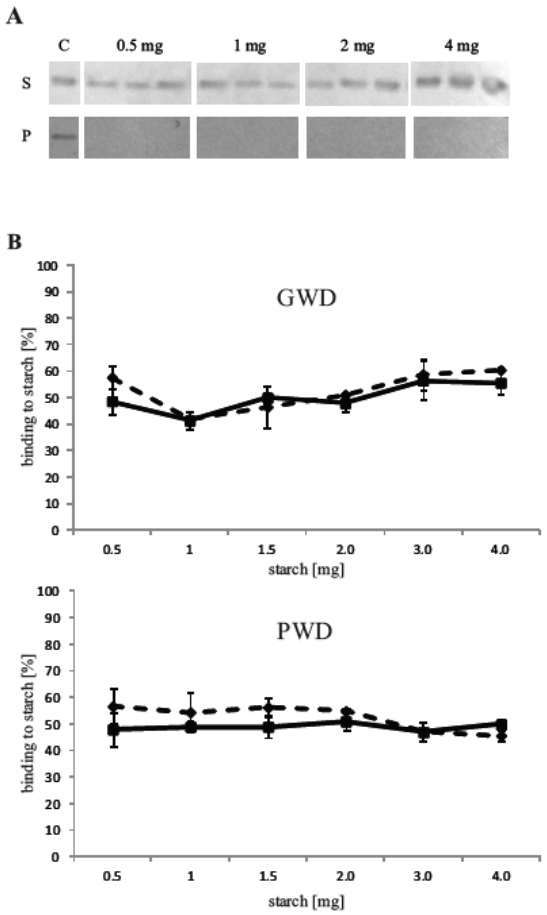

Supplemental Fig. S2. **ESV1 did not bind to amylose and did not alter the binding of GWD and PWD to starch.**

A, 2 µg tESV1 were incubated with increasing amounts of potato amylose as indicated (triplicates). Following incubation for 10 min the pellets were washed and the bound protein was determined following SDS-PAGE and Western blotting. As a control (C) on each SDS gel µg ESV1 were loaded. S - supernatant; P - pellet.

B, Binding of GWD and PWD to starch in the presence of tESV1. The starch was washed five times with water and resuspended in 50 µl of incubation buffer (50 mM HEPES/KOH pH 7.4, 1 mM EDTA, 6 mM MgCl , 2 mM DTE, 0.4 mg 2 ml-1 BSA). Increasing amounts of Arabidopsis wild type starch (as indicated) isolated at the end of the light phase were incubated for 10 min with 3 µg tESV1 and 3 µg GWD and 3 µg PWD, respectively. In controls tESV1 was omitted. The samples were centrifuged and washed once with equal volume of incubation buffer. All samples were adjusted to equal volumes, mixed with SDS sample buffer, heated for 5 min at 95 °C, and loaded on SDS-PAGE following Westernblotting. Solid lines in presence of tESV1; broken lines tESV1 was omitted.

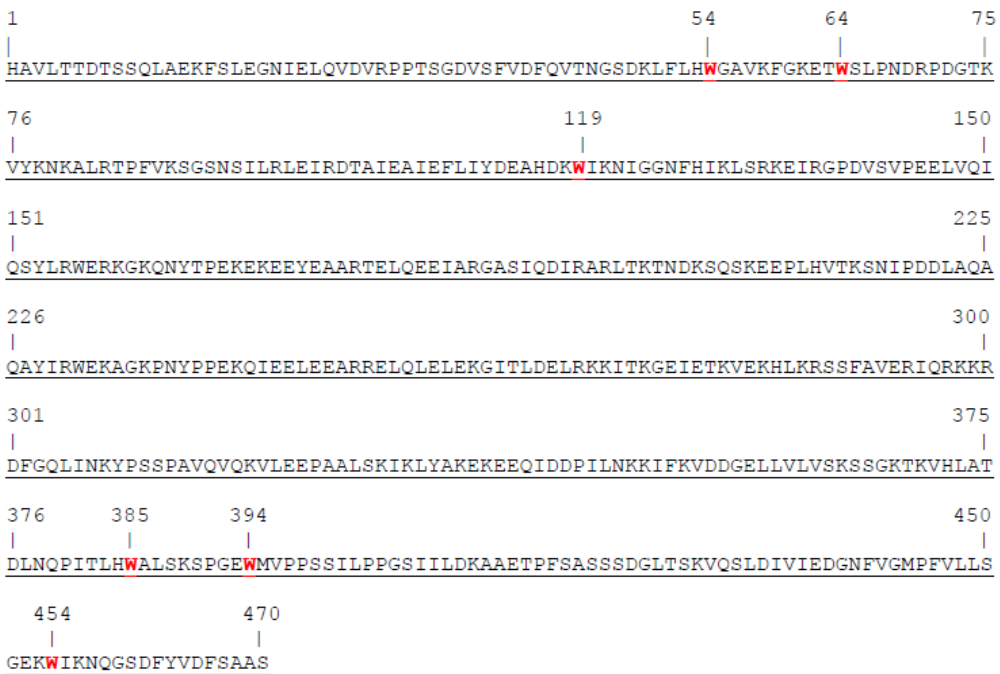

Supplemental Fig. S3. The deduced amino acid sequence of N-terminal repeated region of StGWD without transit peptide. The underlined and double underlined amino acid residues represent the SBDI and SBDII, respectively. The conserved tryptophan residues are shown in red.

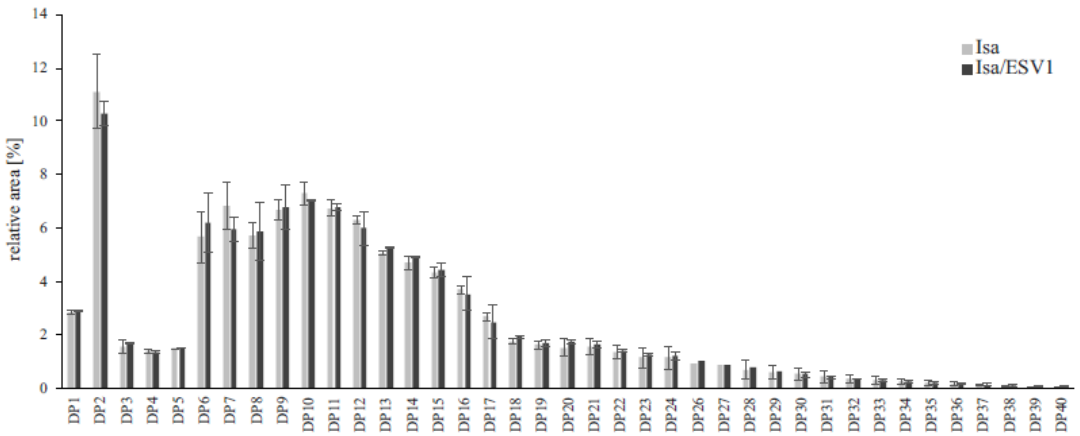

Supplemental Fig. S4. Chain length distribution pattern of the starch granule surface glucan chains released by isoamylase. Starch granules were pre incubated with ESV1. As a control starch was incubated in the absence of ESV1 under otherwise identical conditions

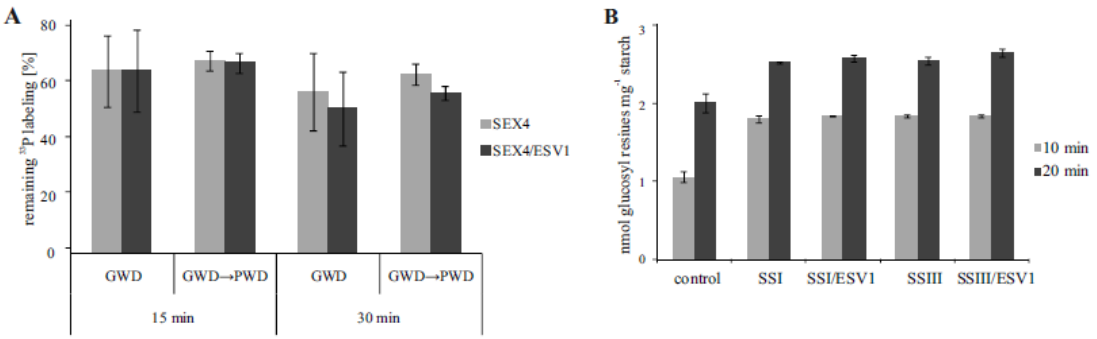

Supplemental Fig. S5. **Impact of ESV1 on SEX4 and the main soluble starch synthases. A**, Dephosphorylation of native starch granules by SEX4. Starch granules (Col-0), were labeled with 33P-ATP and 0.2 µg of GWD for 20 min (GWD) or were incubated with unlabeled ATP and 0.2 µg of GWD for 1 h at 30 °C and then with 0.2 µg of PWD and 33P-ATP for 20 min (GWD->PWD). The phosphorylated starch granules were thoroughly washed, and the 33P labeling was monitored. 33P-labeled starch granules were incubated with 0.3 µg of SEX4 or with 0.3 µg of SEX4 / 2 µg of ESV1 at 30 °C under continuous agitation. The reactions were stopped with 2 % [w/v] SDS, and the granules were washed twice with water. The residual 33P labeling was determined, and the release of labeled phosphate by SEX4 was calculated.
B, Influence of ESV1 on the incorporation of glucosyl residues into Arabidopsis starch granules by the action of Arabidopsis starch synthases 1 and 3. The reaction mixture (final volume 100 µl) contained 8 mg of native starch granules, 0.2 µg of recombinant Arabidopsis starch synthase enzyme, and reaction buffer (0.5 mM ADPglucose, 0.08 µCi [glucosyl-14C] ADPglucose, 0.025 % [w/v] BSA, 200 mM Na-citrate and 10 mM Tricine/NaOH, pH 8.0). Samples were incubated at 30 °C under continuous agitation. Aliquots were sequentially withdrawn, mixed with SDS (final concentration 2 % [w/v]) and washed 7 times with water. Incorporation of 14C-glucosyl residues was quantified by scintillation counting. In controls, either starch synthases and ESV1 or only ESV1 were omitted. 2 µg of ESV1 were used. Values are the means ± SD (n=3). For the control, both SSs and ESV1 were omitted. The incorporation observed in the controls is related to the intrinsic GBSS1 activity (for further information see Keeling and Myers 2010

Table SI. Primers used for PCR. Restriction sites are underlined. All sequences are given in 5' to 3' directions.

Name	Sequence
ESV1-EcoRI	GAATTCGATGAGCGAAATGGCGGCTAGCTC
ESV1-HindIII	AAGCTTTTGTGGTTGGTCAGGGGGTAGG
tESV1-EcoRI	GAATTCGCGCTCTGAGAAGTCAGAGGAACG
SBDI-NdeI	CATATGGTACTTACCACTGATACCTCT
SBDI-XhoI	CTCGAGTTTCCGCAACTCATCAAGGGT
SBDII-NdeI	CATATGGTACTTACCACTGATACCTCT
SBDII-XhoI	CTCGAGGGATGCAGCACTGAAGTCAAC

Chapter 5

5. Early Starvation 1 (ESV1) and its homologue Like-Early Starvation 1 (LESV) between the similarity and functional differences

ESV 1 and LESV have been defined as starch granule binding proteins as well as chloroplast stroma proteins which are involved in the control of starch degradation (chapter 3 and 4). However, the binding of both proteins to the starch granules surface leads to modulate the molecular organization of starch structure in a way affecting negatively the dikinases-phosphorylating enzymes, Glucan water dikinase (GWD) and Phosphoglucan water dikinase (PWD) action, which transfer the phosphate groups to the glucans at the starch granule surface, hence affect the glucans accessibility to the amylolytic enzymes. The results of the analysis of Arabidopsis transgenic plants lacking or overexpressing both proteins revealed that the consumption of starch in these mutants was faster than the wild type. Further, it was shown that both mutants have irregular starch granule shapes (Feike et al., 2016) and that ESV1 and tLESV were involved in the regulation of starch phosphorylation (chapter 3 and 4). Perhaps both proteins share a similar significant function that affects the phosphorylation process. This assumption was based on the finding of Reeck et al. (1987) since they found that proteins which have similar functions are usually homologous and thus have similar sequence. Therefore, based on BlastP search it was found that the Arabidopsis ESV1 and LESV share 146 residues of their amino acid sequence (Fig.5. 1). Furthermore, both proteins share the tryptophan-rich region with the same tryptophan residues number in addition to other aromatic motifs which facilitate interaction of both proteins to glucans. Although both proteins are binding to starch granules as their presence has a clear role during the process of starch degradation, there are more questions about the mechanism common to them to perform this role. For instance, is it possible that the process of organizing the starch structure is achieved by forming a protein complex between ESV1 and LESV? On the other hand, maybe the structural homology between both proteins refers to the functional similarity between them thereby one protein may play a compensatory role to the absence of the other protein during starch metabolism. Moreover, is their action at the same time act in a downstream way? However, in this chapter, using biochemical assays it was an attempt to find an explanation for these questions.

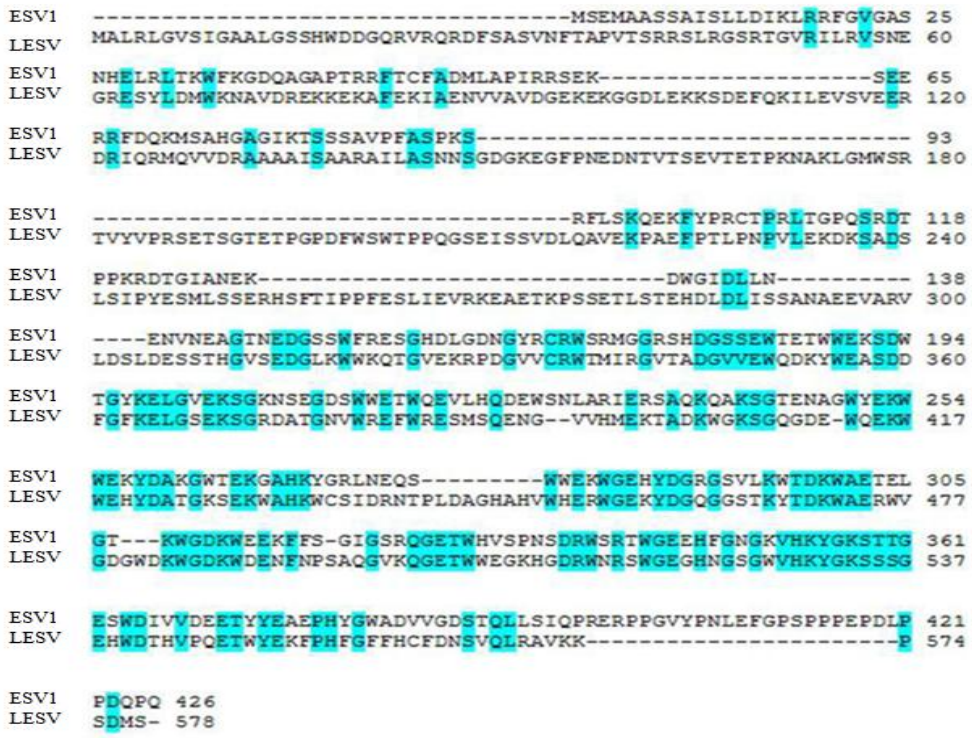

Fig.5.1: Alignment of ESV1 and LESV protein sequences using ClustalW, Amino acids highlighted in green are shared by both proteins.

5.1 Aim of this study

Within the cellular system, proteins rarely work alone. Proteins resort many times to the interaction between them to perform their biological function. Therefore, this work aimed to detect the functional role of ESV1, tLESV, GWD, and PWD using protein-protein interaction analysis. The approach of the study was based on the *in vitro* protein-protein interaction assay between tLESV and ESV1 and the interaction between each protein with GWD or PWD. The second assay was the *in vivo* protein-protein interaction assay between GWD and PWD using a yeast two-hybrid method. In addition, the aim was to analyze the binding of tLESV and ESV1 to starch granule surface and dectectwhether their binding has effects on the phosphorylating-GWD and PWD enzymes and the hydrolysing enzyme (isoamylase, beta-amylase and alpha-amylase)

5.2 Results

5.2.1 Determining the protein-protein interaction between tLESV and ESV1 and between each protein with GWD and PWD enzymes

The high degree of proteins sequence homology plays a role in the determination of the biological functions among these proteins. Detections about protein function in one species will provide comprehension with another protein (Tatusov et al., 1997).

To understand the functional behaviours of tLESV and ESV1 proteins, the functional properties of each one was detected through their binding to starch granules. Furthermore, protein-protein interaction data plays an important role in the attempt to understand the cellular processes. It was, therefore, tested whether protein-protein interaction can be observed between tLESV and ESV1 or between each protein with GWD and PWD phosphorylating enzymes to help us to determine the real function for each one during starch degradation. In order to investigate these interactions, chemical crosslinking was performed among these proteins in solution with DTSSP at a molar ratio of protein to cross-linking equal to 1 to 20 fold molar excess. The mixture was incubated for 5 min at RT and then quenched and denatured. The samples were loaded on a 6% [w/v] SDS-PAGE. The result revealed (data not shown) that no crosslinking reaction occurred between the protein samples which were incubated with DTSSP compared to the controls. This result suggests that the tLESV, ESV1, GWD, and PWD acting independently instead of being coordinated are active. However, it is unclear whether the same result may be observed *in vivo*, especially that some of proteins interactions are transient interactions. Many times, these interactions are brief or weak, so it is difficult to determine such an interaction, especially the information about the structures of tLESV and ESV1 which hasn't beenavailable so far.

To investigate whether the phosphorylation of starch by GWD and PWD is possible to be performing by the complex formation between GWD and PWD, a direct interaction between both enzymes using Y2H experiment was performed. To do this experiment, full-length of *St*GWD and *St*PWD was fused into the DNA binding domain of the GAL4 vector (pGPT9) and used as bait. Also full-length of *St*GWD and *St*PWDwas fused to the DNA activation domain of the GAL4 transcription factor vector (pGAD424) and served

as preys. *St*GWD-bait and *St*PWD-prey or *St*PWD-bait and *St*GWD-prey constructs were transformed into the yeast strain Y190 and then plated on the SCAD medium lacking leucine (-Leu)/ tryptophan (-T) to identify the successful uptake of bait and preyplasmids. To identify the interactions, the growth of yeast cells was plated on the SCAD medium lacking leucine/tryptophan and leucine/tryptophan/histidine or leucine/tryptophan/histidine with a membrane (LacZ). Successfully transformed cells carrying both constructs were not able to turn blue in the β-galactosidase (LacZ) test. Therefore, Y2H analysis had shown that no physical interaction between *St*GWD and *St*PWD was observed in yeast (Fig. 5. 2). However, the failure of activating transcription does not mean that it excludes the true interaction between them in *in vivo*, maybe it is weak to be detected. Anyway, this result indicates that the activity of GWD and PWD is independent during the phosphorylation process of starch. This finding also supports the revealed result that PWD is capable of phosphorylating the native starch granule surface as an independent enzyme without the need to be pretreated by GWD.

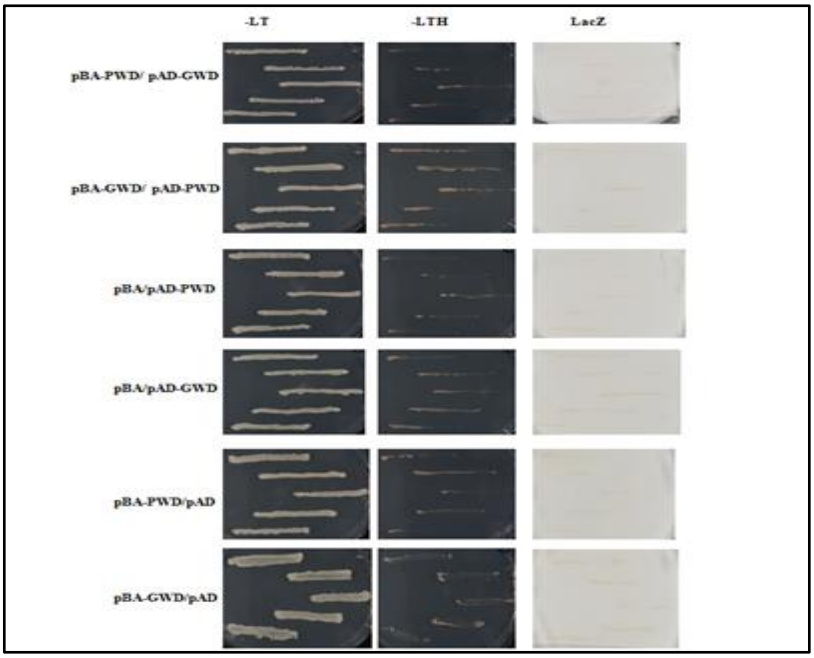

Fig.5.2: Y2H analysis of *St*GWD fused as bait and *St*PWD fused as prey or *St*PWD fused as bait and *St*GWD fused as prey using Y190 strain. Yeast cells transformed with GWD-bait and PWD-prey or PWD-bait and GWD-prey constructs were grown on selective media lacking leucine and tryptophan (–LT) for 3 days at 30 °C to monitor successful uptake of both plasmids. Empty binding domain (pBD) and activation domain (pAD) vectors served as control. **–LT,** yeast growth on medium without Leu and Trp. **–HLT,** yeast growth on medium lacking His, Leu, and Trp, indicating expression of HIS3 reporter gene. **LacZ,** the activity of the lacZ reporter gene was checked after 1 day. Growth on SCAD medium deficient in tryptophan, leucine, and histidine (-LTH) and lacZ test do not show protein interaction.

5.2.2 ESV1 and tLESV reveal different binding to amylose

As it is known, the starch consists of two polymers, almost linear amylose and branched amylopectin. The ratio of them in starch granules is varying depending on the starch source. However, it has been confirmed in chapter 3 and 4 that tLESV and ESV1 were binding to starch granules. Furthermore, there was a higher binding of tLESV to amylose than amylopectin while not observing the binding of ESV1 to amylose. Therefore, to compare the binding of tLESV and ESV1 to amylose, it was repeated the same experiment which was performed with ESV1. However, 2 µg of tLESVwas incubated with different concentrations of potato amylose which varied from 0, 5 to 4 mg for 10 min at 30 C°. Following washing, the pellets were resuspended and denatured and then loaded on a 9% [w/v] SDS-PAGE following immune detectable. As shown in (Fig. 5. 3 B), the binding of tLESV to the starch pellets was clear with increasing the amount of amylose. Also, a very minor amount of the protein can be observed in the supernatant compared to the binding of ESV1 to the starch pellets which were not observed in which all the protein was released in the supernatant (Fig. 5. 3 A). However, the binding of tLESV to both starch structures (amylose and amylopectin) indicates that the tLESV has an affinity to both polymers. That means that tLESV is capable of binding to both long and short glucan chains. While the binding of ESV1 to the amylopectin only suggests that the ESV1 prefers to bind to the short and branched glucan chains. However, it cannot exclude the binding of ESV1 to amylose. Maybe its binding to amylose is transient or weak.

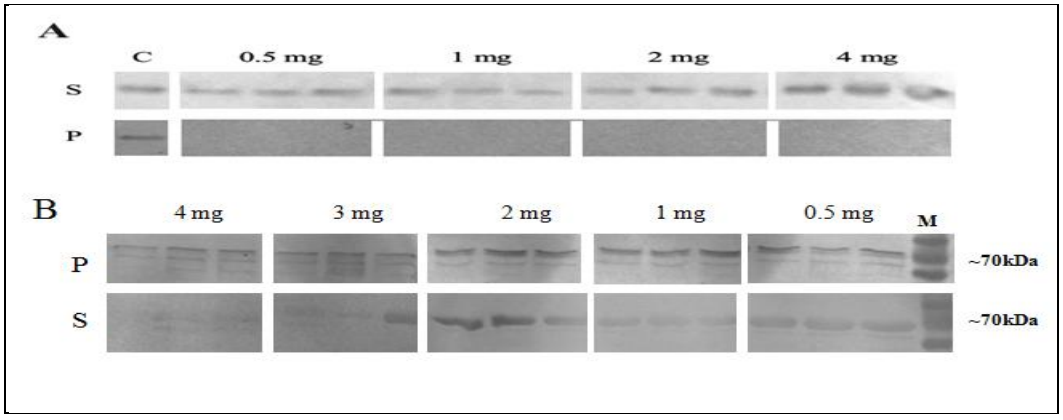

Fig.5.3: Analysis of tLESV and ESV1 binding to potato amylose. (A) ESV1 binding to amylose. (B) tLESV binding to amylose. 2 mg of each protein was incubated with a gradient concentration of potato amylose (0.5-4 mg) as indicated (triplicate) for 10 min at 30 C°. Following washing, all the fractions loaded on [9%] SDS-PAGE, followed by western blotting with an anti-His immunodetection. C, control; S, supernatant; P, pellets; M, protein marker ladder.

5.2.3 tLESV and ESV1 share the influence of the GWD-starch phosphorylation process

Through the results of the study, it can be observed that at the starch granules surface the ESV1 and tLESV have a similar functional role as they reveal a similar effect on the GWD and PWD-phosphorylation process, since the action of GWD and PWD seems to be reduced by the presence of ESV1 and tLESV. On the other hand, GWD and PWD have also similar functional roles as both act as phosphorylating enzymes during starch degradation. Therefore, it is important to look at whether ESV1 and tLESV work together to make an effect on the GWD and PWD-mediated phosphate incorporation. As shown in chapter 3 and 4, the experiments revealed the effects of tLESV and ESV1 independently on the GWD activity in different types of starch.To detect the effects of both proteins together on the activity of GWD, it has been repeated the same previous assay that included incubation of recombinant *St*GWD and ^{33}P-β-ATP with three types of starch, Arabidopsis wild-type, *waxy* maize, which contains high amounts of amylopectin as a result of the mutant of granule-bound starch synthase (GBSS1) action and *amylose extender* maize, which has longer glucan chain and amylopectin with reduced branching point frequency as a result of the lacking of starch branching enzyme IIb (SBEIIb) action in the presence and absence of tLESV and ESV1 separately or together and then measured GWD-mediated phosphate incorporation. However, in all starches, as is expected it was a significant reduction in the GWD-incorporation of phosphate in the presence of both proteins, separate or together (Fig 5.4). As it is shown, also that GWD-mediated phosphate incorporation into Arabidopsis wild-type and *waxy* starches were low (Fig. 5.4 A and B) compared to *amylose extender* starch (Fig. 5.4 C). This observation explains that the difference of the chemical and physical properties of the starch granule surface between the various starch sources is responsible for the diversity of substrates utilized by GWD. On the other hand, it was shown that the effect of tLESV and ESV1 on the phosphate incorporation rate separately was similar to the effect of both proteins together on the phosphate incorporation rate into the waxy and amylose extender starches. Whereas in Arabidopsis wild-type starch it seemed the ESV1 has less effect than tLESV on the GWD activity as the incorporation of phosphate was more in the presence of ESV1 (Fig 5.4 A). A possible explanation of this finding could be that the binding of tLESV to amylose and amylopectin altered the structure of starch in a way that make the ratio between GWD and its substrate at the starch granule surface less than the ratio which is the result from the binding of ESV1 to amylopectin only. However, these

results suggest that the difference between amylose and amylopectin ratio in the different starch sources determines the binding of tLESV and ESV1 to these polymers. Depending on this ratio, the binding of both proteins will lead to create different starch granule surfaces between these starches which are reflected on the GWD-phosphorylation process.

However, *in vitro*, the presence of tLESV and ESV1 always lead to a reduction of the GWD action whether it is separately or together, but it is difficult to detect whether their action is similar *in vivo*. Experimentally it is difficult to determine which protein has more or less activity than the other especially during the incubation of both proteins together. Despite using the same amount of proteins, the impurity of the proteins prevents determining the correct concentration of both. Additionally, there are other factors such as purity of starch, washing steps, protein inhibitors, and functional interference between both proteins that may affect the results. In general, the results showed that tLESV and ESV1 shared the influences on the reduction of the GWD-phosphorylation process.

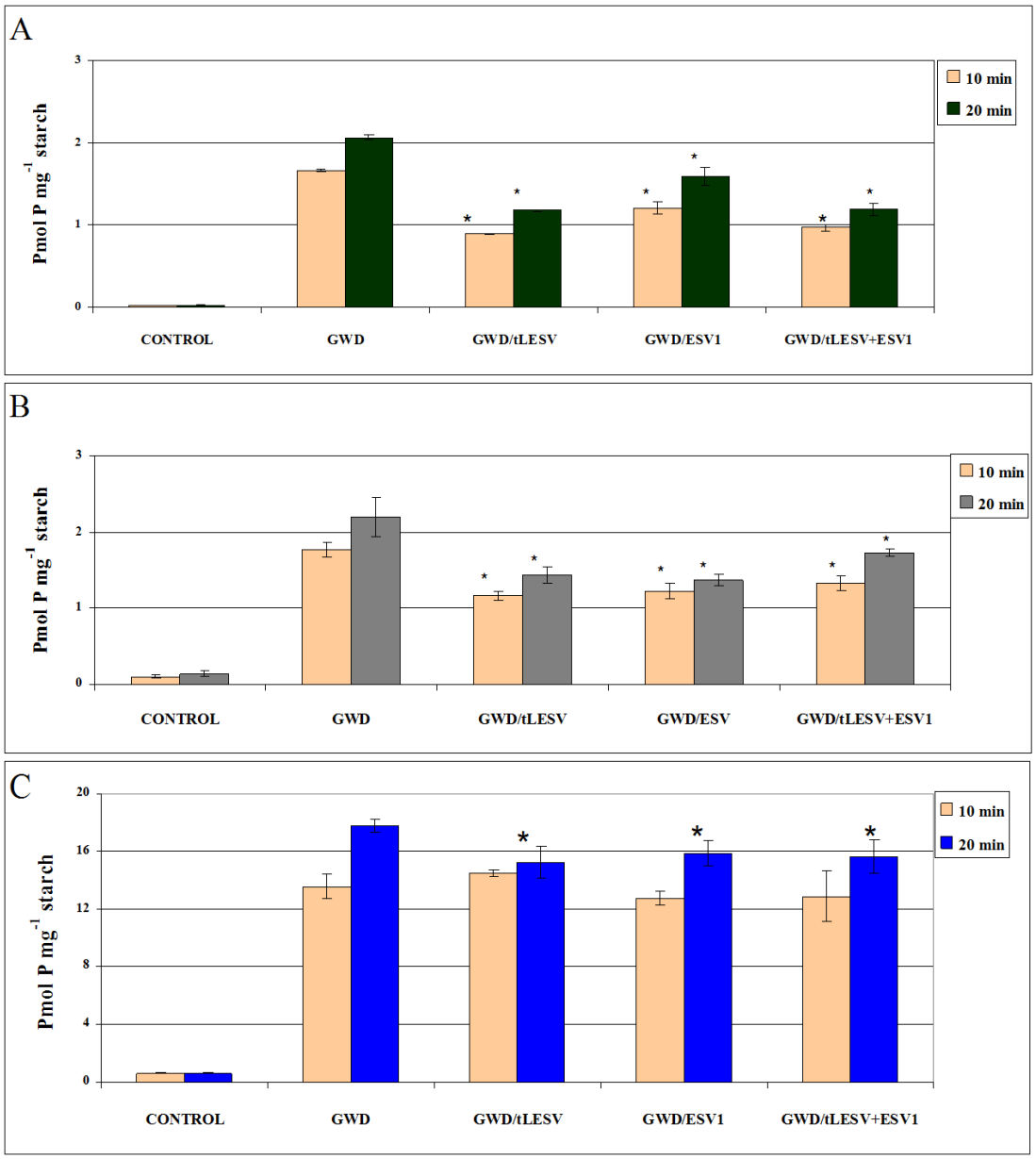

Fig.5.4: Effect of tLESV and ESV1 separately or together on the action of GWD in different glucans. Granules of three types of starch were incubated with *St*GWD and ^{33}P-β-ATP in the presence of tLESV and ESV1 separately or jointly at 30 C°. As controls, starches were incubated in the absence of proteins under otherwise identical conditions. The phosphate incorporation was measured after two times, 10 and 20 min. Values are the mean ± standard deviation (SD) (n=3). The asterisk indicates a significant difference compared with *St*GWD samples in the presence and absence of tLESV and ESV1 separate or together, (Student's t-test P≤ 0, 05). **A**, Arabidopsis wild-type; **B**, maize *waxy*; **C**, maize *amyloseextender*.

5.2.4 Are the tLESV and ESV1 having the same effects on the PWD-phosphorylation process?

Along with GWD, PWD is also essential for normal starch degradation. For many starches, it has been shown that the starch phosphorylating by GWD will provide further

glucan structures that are preferred by PWD thereby acts downstream of GWD and phosphorylates the C3 position of the glucosyl residues (Fettke et al., 2009).

Furthermore, PWD can phosphorylate unphosphorylated starch and hence does not require the previous action of GWD (Fettke et al., 2009). However, referring to the results of Chapter 3 and 4, it has been shown that PWD is capable of phosphorylating the glucan structure directly without prephosphorylation by GWD. A significant reduction was also observed in the rate of phosphate incorporation by PWD in the presence of tLESV and ESV1 when it was incubated directly without prephosphorylation by GWD. However, it repeated the same testing to detect whether tLESV or ESV1 has more effect on the action of PWD at the starch granule surface. To do that, it incubated Arabidopsis *sex 1-8* starch with *St*PWD and ^{33}P-β-ATP directly, without prephosphorylation by GWD in the presence or absence of tLESV and ESV1 for two times, 10 and 20 min at 30 C°. After the measuring of the ^{33}P-phosphate, a significant reduction in the PWD-incorporation of phosphate was observed in the presence of tLESV and ESV1 (Fig. 5. 5). Nevertheless, there was not significant difference observed between tLESV and ESV1 on the effect of the action of PWD. This result suggests that both tLESV and ESV1 bind to the same or similar glucan chains which prefer to phosphorylate by PWD.

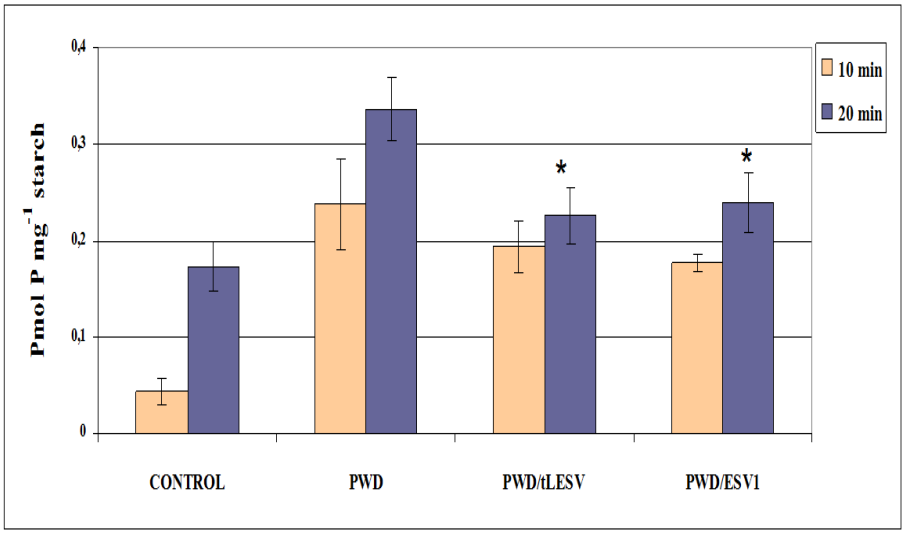

Fig.5.5: Influence of tLESV and ESV1 on PWD action without prephosphorylation by GWD. 30 mg of Arabidopsis *sex 1-8* starch was incubated with PWD and ^{33}P-β-ATP in the presence and absence of tLESV or ESV1 at 30 C°. As controls, starch was incubated in the absence of PWD, tLESV, and ESV1 or both proteins under otherwise identical conditions. The ^{33}P-phosphate incorporation was measured after two times, 10 and 20 min. Values are the mean ± standard deviation (SD) (n=3). The asterisk indicates a significant difference compared with PWD samples in the presence and absence of tLESV or ESV1, (Student's t-test P≤ 0, 05).

On the other hand, it was also observed that there is an antagonist effect for each of tLESV and ESV1 on the action of PWD after prephosphorylation by GWD. Consequently, it was interesting to test the behavior of the action of PWD at the starch granule surface in the presence of both proteins together. For this test, different starches have been incubated (Arabidopsis *sex 1-8*, potato tuber, maize *waxy*, and maize *amylose extender*) with non-labelled ATP and *St*GWD for one hour. After intensive washing, the starch granules were incubated with ^{33}P-β-ATP and *St*PWD in the presence and absence of tLESV and ESV1 alone or together for two times, 10 and 20 min. After measuring the PWD-mediated phosphate incorporation, a significant reduction was found in the action of PWD in the presence of tLESV and ESV1whether separate or together (Fig. 5.6). Surprisingly, the reduction of the action of PWD can be seen even in the presence of ESV1 in all the types of starch and this is different from what was observed in chapter 4. Despite repeating this experiment several times for the different starch types, the same results were observed, therefore, the difference in results can be attributed to several reasons including uncontrolled conditions, contamination, enzyme activity, washing steps, and samples analysis. However, it is difficult to determine which result is correct, especially if it was treated in the same way with both experiments. On the other hand, the effects of tLESV and ESV1 on the PWD-mediated phosphate incorporation were similar either separately or together in potato, maize *waxy*, and maize *amylose extender* (Fig. 5.6 B, C, and D) respectively, while in Arabidopsis *sex 1-8*, it has been seen that the effects of tLESV alone are more than effects of ESV1 alone on the reduction of the phosphate incorporation rate. This result could be attributed to; that tLESV binds preferentially more than ESV1 to yet unknown glucan structures that are also preferentially phosphorylated by PWD, whereas the effects of both proteins together are similar to the effect of ESV1 alone (Fig. 5.6 A) excluding that the ESV1 acts through inhibition of tLESV, but maybe the presence of the impurity of both proteins render the result critical, thereby it is difficult to reflect the correct effects for each protein. On the other hand, it could also attribute the variation of the effects of tLESV and ESV1 on the action of PWD separately or together to the purity of Arabidopsis *sex 1-8* starch, which is extracted in the laboratory if it is compared to the results of their effects on potato, maize waxy, and maize amylose extender as more purity commercial starches. Generally, it is visible that both proteins lead to a reduction of PWD-mediated phosphate incorporation. These results indicated that tLESV and ESV1 are active at the same time and unlikely to act through inhibiting one another and they altered the starch structure before starting the

degradation of starch in a way that limited the phosphate incorporation rate by GWD and PWD.

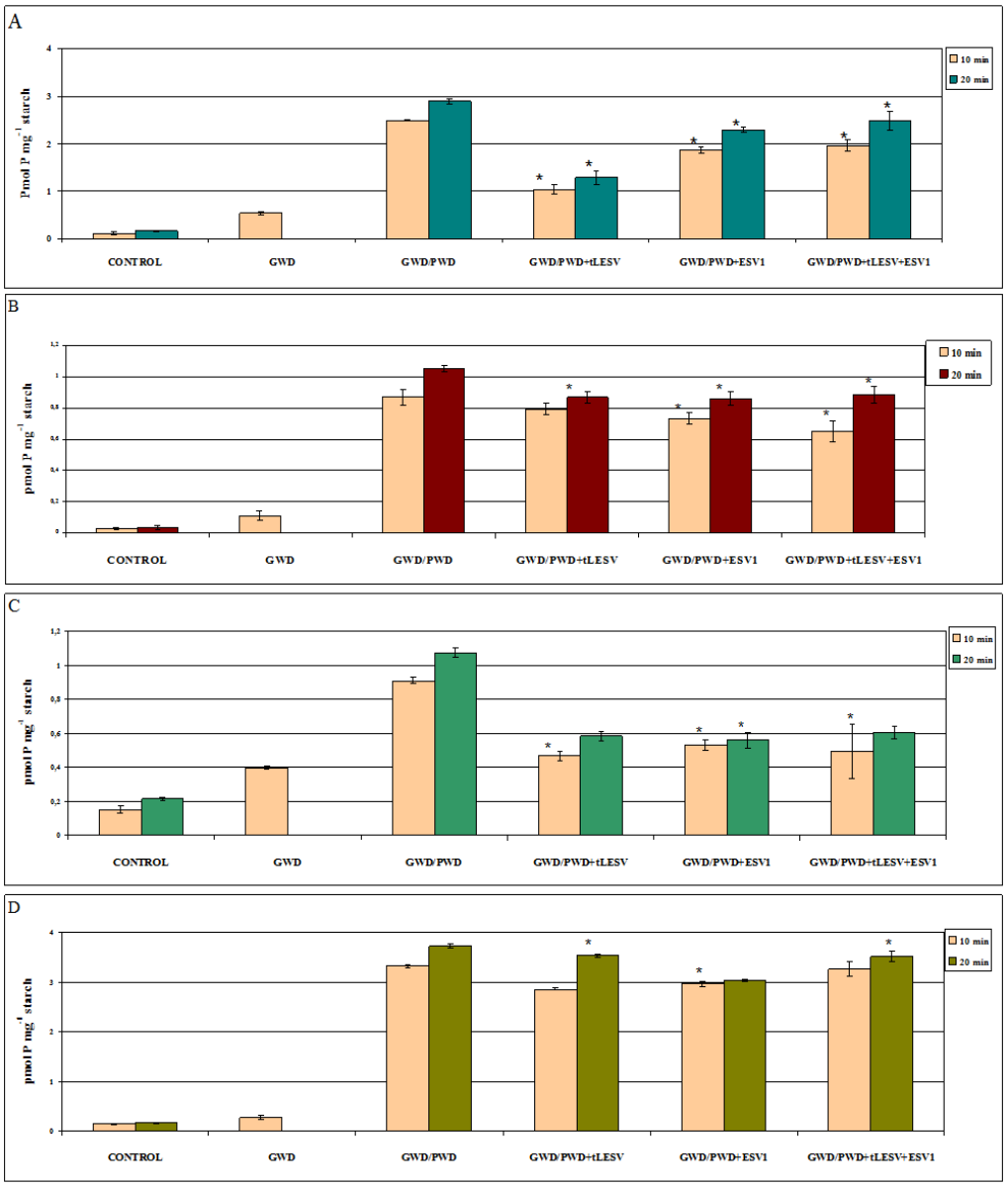

Fig.5.6: Influence of tLESV and ESV1 on the action of PWD for the different starch types after GWD prephosphorylation. Different types of the native starch granules were incubated with non-labelled ATP and *St*GWD for one hour at 30 C°. Following intensive washing, the starch granules were incubated with *St*PWD and ^{33}P-β-ATP in the presence and absence of tLESV or ESV1 separately or together at 30 C°. As controls, starch was incubated in the absence of PWD, tLESV, and ESV1 or both proteins under otherwise identical conditions. The ^{33}P-phosphate incorporation was measured after two times, 10 and 20 min. Values are the mean ± standard deviation (SD) (n=3). The asterisk indicates a significant difference compared with *St*PWD samples in the presence and absence of tLESV or ESV1 separately or together, (Student's t-test P≤ 0, 05). **A**, Arabidopsis *sex 1-8*; **B**, potato tuber; **C**, maize *waxy*; **D**, maize *amylose extender*.

5.2.5 Impact of tLESV and ESV1 on the enzymes involved in starch degradation downstream of the dikinase-mediated phosphorylation, beta-amylase, alpha-amylase, and isoamylase

Beta-amylase, alpha-amylase, and isoamylase are enzymes involved in starch degradation. As shown in Chapter 3 and 4 that tLESV and ESV1 affected the dikinase-mediated phosphorylation. Therefore, to detect whether the reduction of GWD and PWD activity by tLESV and ESV1 proteins might be reflected on the action of hydrolysis enzymes that were required for the starch degradation process. To test that, the native starch granules were preincubated with tLESV or ESV1 or without both proteins as a control for 30 min at 30 C°. After washing steps, the starch granules were incubated with beta-amylase (BAM) or alpha-amylase (AMY) or without both enzymes as a control overnight at 37 C°. After the measuring of glucans released by the action of both enzymes, the results revealed that tLESV and ESV1 affected the action of beta-amylase while it was a significant reduction in the maltose released by BAM in the presence of tLESV and ESV1 (Fig. 5.7 A), no effect was observed on the action of alpha-amylase (Fig. 5. 7 B). However, both BAM and AMY could potentially produce maltose during starch degradation. BAM is an exohydrolase enzyme which can degrade the nonreducing ends of α 1,4–linked glucan chains to produce β-maltose, whereas AMY is an endohydrolase enzyme that acts as a downstream of hydrolysing enzyme (BAM and ISA), and is able to produce an α-maltose or different linear and branched malto-oligosaccharides. Therefore, the effect of tLESV and ESV1 on BAM only confirms that both proteins act before the start of starch degradation. Further, this result suggests that the reduction of dikinases activity in the presence of tLESV and ESV1 will reduce the amount of substrate for BAM at the starch granule surface.

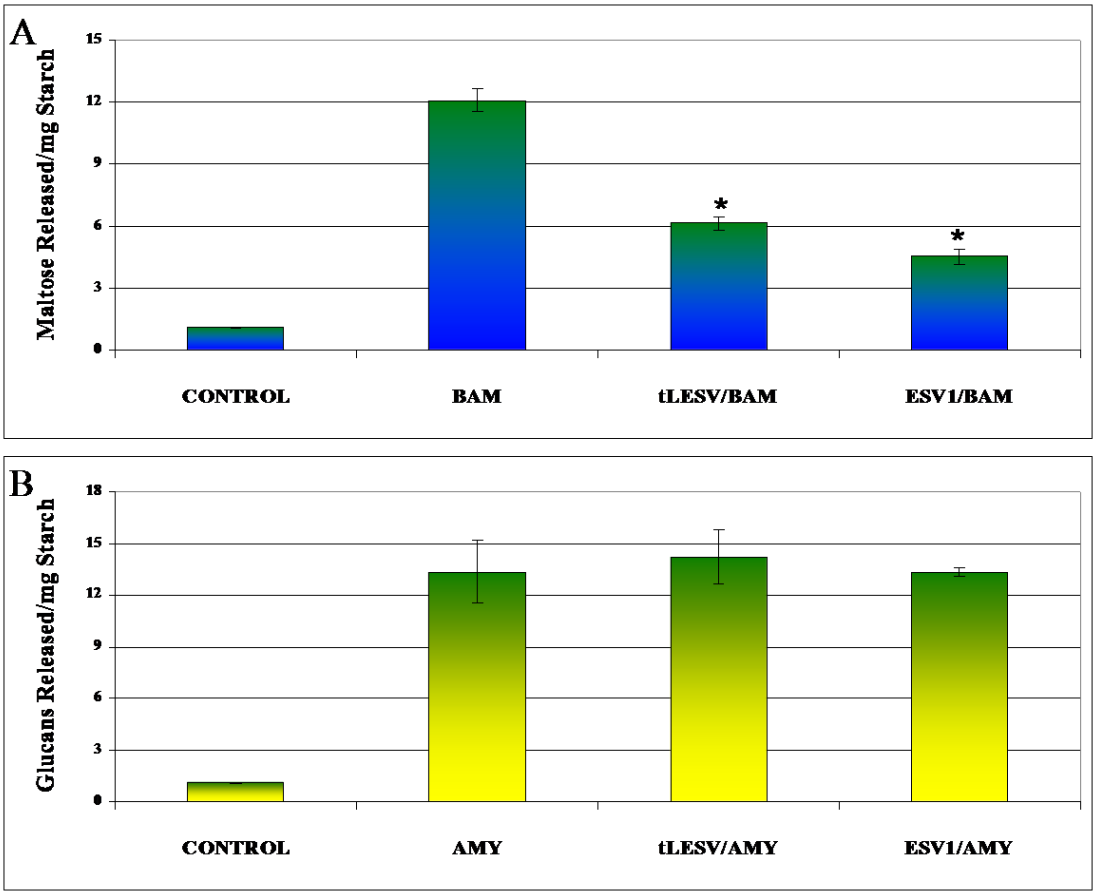

Fig.5.7: Influence of tLESV and ESV1 on beta-amylase (BAM) and alpha-amylase (AMY). Maize wild-typestarch granules were incubated with tLESV or ESV1 for 30 min at 30 C°. As controls, BAM, AMY, and both proteins were omitted. Following washing steps, the starch granules were incubated with (BAM) or (AMY) overnight at 37 C°. Following centrifugation, the released glucans were measured. Values are the mean ± standard deviation (SD) (n=3). The asterisk indicates a significant difference compared with (BAM) or (AMY) samples in the presence and absence of tLESV or ESV1, (Student's t-test P≤ 0, 05). **A**, beta-amylase (BAM); **B**, alpha-amylase (AMY).

On the other hand, the previous results revealed that the presence of tLESV and ESV1 proteins did not affect the glucans released by the action of isoamylase. However, to test whether the presence of both proteins is together at the starch granules have the same effects on the isoamylase action. Therefore, it was repeated the same experiment that included incubation of different starches (Arabidopsis wild-type or *sex 1-8* and maize wild-type) with tLESV or ESV1 separately in addition to incubationof both proteins together for 1 h at 30 C°. As controls, the starches were incubated without proteins under the same conditions. Following washing steps, the native starch granules were incubated with isoamylase to release the soluble glucan chains at the surface overnight at 37 C°. However, the results showed that in Arabidopsis wild-type, the effect of

tLESV on the chains length distribution was intangible as it was limited to DP 13 (Fig. 5. 8. 1A), whereas the significant effects of ESV1 were slight as it was limited to DP 8-12 (Fig. 5 8. 1B) and the significant effects of both proteins together were limited on DP 15-20 (Fig. 5. 8.1 C). In Arabidopsis *sex 1-8* the effect of the chains length distribution was only limited to tLESV. Its significant effects appeared on the DP 4-11 (Fig. 5. 8 2A), whereas the effects of ESV1 were not observed either alone or together with tLESV on the chain length distribution (Fig. 5. 8. 2B and C). In the case of maize wild-type, the significant effect of tLESV was observed on the DP 3-7 (Fig. 5. 8.3 A), while the effect of ESV1 was significantly on the DP 10-15 (Fig. 5. 8.3 B). The same significant effect on the chain length distribution was observed in the presence of both proteins together (Fig. 5. 8. 3 C). The results suggest that the effects of tLESV and ESV1 whether separately or together on isoamylase were slight since their effects were only limited on the glucan chains.

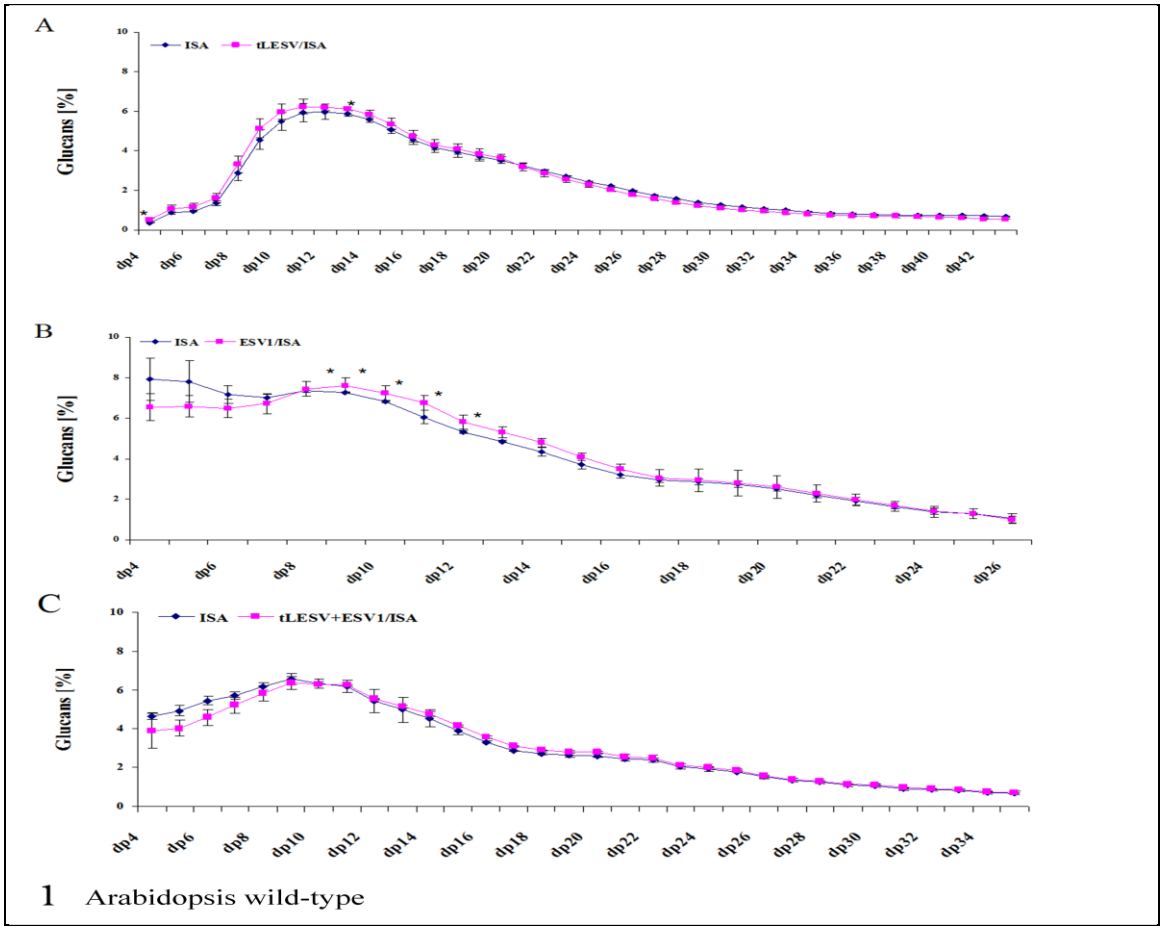

1 Arabidopsis wild-type

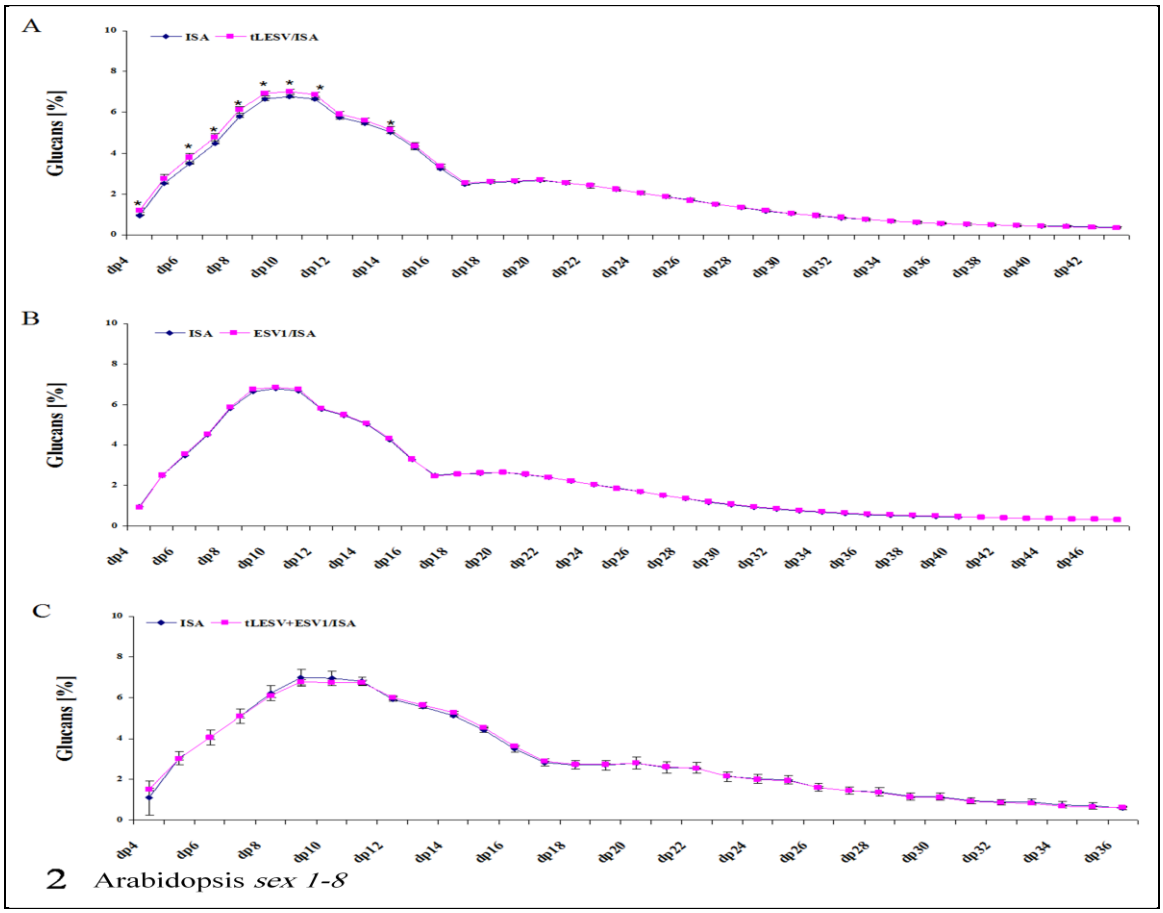

2 Arabidopsis *sex 1-8*

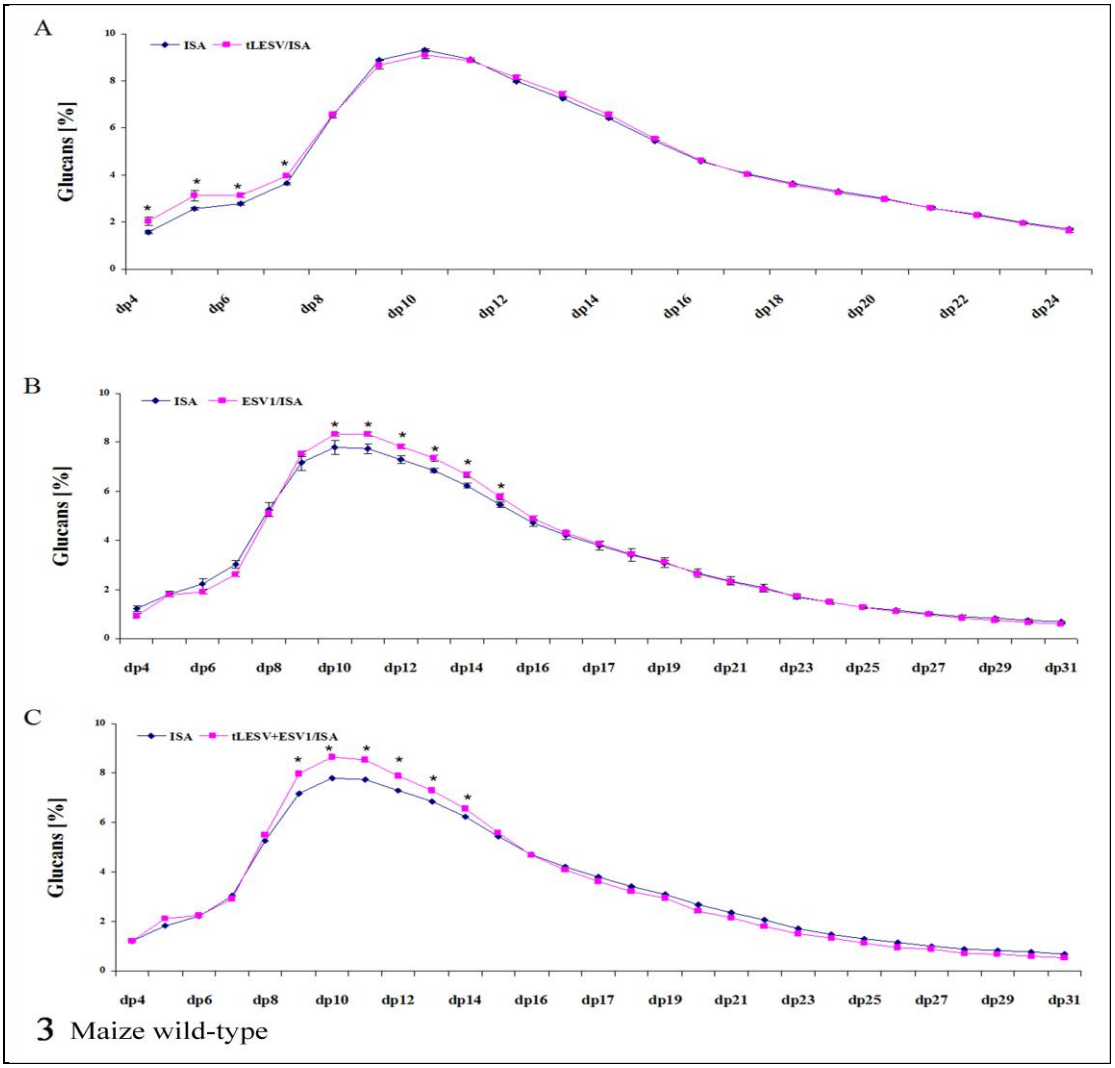

Fig.5.8: Effects of tLESV and ESV1 separately or together on the action of isoamylase. Native starch granules were incubated with tLESV or ESV1 separately or together for 1 hour at 30 C°. As controls, both proteins were omitted and incubated under the same conditions. Following washing steps, the starch granules were incubated with isoamylase overnight at 37 C°. Following, analysis of the chains length distribution of the starch granules surface which are released by isoamylase. **1, A** Arabidopsis wild-type in the presence and absence of tLESV; **1, B** Arabidopsis wild-type in the presence and absence of ESV1; **1, C** Arabidopsis wild-type in the presence and absence of tLESV+ESV1; **2, A** Arabidopsis *sex 1-8* in the presence and absence of tLESV; **2, B** Arabidopsis *sex 1-8* in the presence and absence of ESV1; **2, C** Arabidopsis *sex 1-8* in the presence and absence of tLESV+ESV1; **3, A** maize wild-type in the presence and absence of tLESV; **3, B** maize wild-type in the presence and absence of ESV1; **3, C** maize wild-type in the presence and absence of tLESV+ESV1.

5.3 Discussion

The results of chapter 3 and 4 described the tLESV and ESV1 as starch binding proteins. The binding of both proteins to the starch granule surface is capable of alteration of the starch structure and impacting the starting of starch degradation. It was shown that the

presence of both proteins at the starch granule surface led to reducing the action of GWD and PWD enzymes in a mechanism capable of helping in organizing the phosphate incorporation rate in a way that allows in the modulation of starch degradation. However, from these results, it can be concluded that the presence of both proteins is an important part of the starch degradation system through its association with the starch granules. Therefore, the presence of these findings lead to the importance of studying the mode of action of both proteins together to determine their effects at starch granules using different types of starch.

Detection of protein-protein interactions using crosslinker and yeast two-hybrid assay

Proteins seldom act on their own; therefore, most proteins tend to be associated with other proteins or biomolecules to perform their molecular functions. The interaction of the protein with its partner plays an important role in facilitating the detection of the functions of a protein by giving the information on the biophysical environment in which the protein does its functions. On the other hand, depending on the sequence of amino acids, the protein structure is determined. However, the protein structure dictates the biochemical function of it; therefore, proteins that share a similar amino acid sequence usually perform a similar biochemical function (Alberts et al., 2002).

However, it was mentioned before that tLESV and ESV1 shared functionally important amino acids. Consequently, it is likely that both proteins may perform a similar function. Nonetheless, some of the amino acids in tLESV and ESV1 are highly conserved like aromatic amino acid residues which are arranged in motifs (Feike et al., 2016). It was proposed that the repetition of these motifs mediated binding to several glucans or maybe this binding contributes to the reaction of long glucan chains in many contact areas. Therefore, these findings lead to suppose that functional or structural similarity between both proteins may allow the interaction between them.

The present study determines if there are complex formations resulting from the interactions between tLESV and ESV1 or between each of them with the dikinases-GWD and PWD at the starch granule surface. However, using chemical cross-linking, the results of the protein-protein interactions did not detect the physical interactions between tLESV and ESV1 or between each one of them with the dikinases. In solution, the

interactions of proteins, which are often transient, with added crosslinkers require a traditional biological environment such as inside living cells. This environment is difficult to maintain in vitro. Typically, the cross-linking method used to identify the transient interactions by the formation of covalent bonds between two proteins leads to stabilizing the transient interaction. It could be the bonds were broken before both proteins moved relatively to each other. The phosphorylation process during starch degradation is an obscure process that relies on the action of GWD and PWD at the starch granule surface. However, analysis of starch phosphorylation by PWD without prephosphorylation by GWD provided a test of whether the interaction between both dikinases is required for normal starch degradation. These data were suggestive of no physical interaction between them. On the other hand, it could be the GWD-PWD interactions were not strong enough to be detected by using chemical cross-linking. Transient or weak protein-protein interaction is harder to detect than more strong or stable interactions. Therefore, yeast two-hybrid system was used to detect whether a complex formation between GWD and PWD could occur to perform the phosphorylation of starch. Y2H analysis of *S. cerevisiae* Y190 cells with GWD and PWD present in pGAD and pGBT vectors was performed, but did not show the activation of the HIS3 reporter gene. These results suggest that these proteins may not possess the mechanism which helps them to have physical interaction among them despite localizing all these proteins in the chloroplast. However, some proteins interact if there is a need for this interaction within the same compartment, therefore, most likely both binding proteins and two dikinases did not interact because there are no biological reasons found for that, especially the conditions in vitro or in vivo (in yeast) do not represent the real environment for the presence of these proteins to confirm that. However, the failure of the detection of these interactions does not mean that it can abolish the possibility that these proteins physically interact, even if there should be no biological function of this interaction. On the other hand, the stability of a protein is regulated by the interaction with other protein or by localization of other protein in the same area or maybe by its localization. Therefore, the binding of these proteins to the starch granules may increase their stability thereby no need to interact with other proteins. This may explain there is no interaction occurring among the proteins, but the absence of starch in the interaction of in *in vitro* or *in vivo* (yeast) prevents the investigation of such a reaction. However, another element to predict the protein complex formation is the biological state of proteins. Therefore, not all possible protein interactions occur at any of the same time, perhaps, for

the interaction between these proteins to occur, they need or depend on some conditions like protein modification and presence of cofactors or other binding partners. However, it was found that the presence of some proteins was necessary for the action of starch-related proteins. For instance, the PROTEIN TARGETING TO STARCH (PTST1) protein is important for the localization of GBSS on the starch granule which contains coiled-coils (Seung et al., 2015), while typically the proteins containing coiled-coils are involved in protein-protein interactions (Mason and Arndt, 2004). Indeed, although both *lesv* and *esv1* mutants showed the same effects on the starch content (Feike et al., 2016), there is no evidence that the protein-protein interaction occurs between LESV and ESV1 or the phosphorylating enzymes.

The variance in the binding of tLESV and ESV1 to amylose starch

The result presented demonstrates the variance in the association of tLESV and ESV1 with amylose and amylopectin. It was clear that tLESV preferentially binds to the soluble glucan chains like amylose more than the branched glucan chains like amylopectin, while ESV1 preferentially binds to the amylopectin in which no binding to amylose was observed. Starch granules contain both crystalline parts which contain mostly the amylopectin and the amorphous parts which consist of the main part of amylose and longer, internal chains of amylopectin (Bertoft et al., 2017). However, about 30% of the mass of starch granule is considered as crystalline and about 70% as amorphous regions (Ismail et al., 2013).

These findings suggest that tLESV may bind preferentially to the amorphous regions, but it cannot exclude its binding to the crystalline parts as its binding to amylopectin was observed too. While the binding of ESV1 to amylopectin only suggests that it may bind preferentially to the crystalline regions. However, a possible explanation for the binding of tLESV to amylose could be to involveand increase the amylose stability especially during his crystallinity while the interior of the loose helical amylose chains is hydrophobic that it can bind to hydrophobic molecules like aromatic compounds and lipids, so the binding between amylose and these molecules may lead to lose some amylose stability, while ESV1 may preferentially bind to amylopectin as branching polymer, so a possible explanation that the binding of ESV1 to maize amylose extender which has less branching points of amylopectin due to missing the starch branching

enzyme IIb (SBE IIb) could be by the binding of ESV1 at these branching points. On the other hand, the binding of ESV1 to maltodextrin which does not contain branching points supports the belief that it is also able to bind to different glucans far from contact points. Although the binding of ESV1 to amylose was not observed in *in vitro*, it cannot exclude that this binding could occur in *in vivo*, however, probably the binding has been transient or not stable which is not easy to recognize in *in vitro*. However, the variation in the binding to starch granules for both proteins reflects the importance of their presence together to work as one mechanism that contributes to the regulation of the starch structure during the degradation process.

tLESV and ESV1 shared the influence of the phosphorylation process

Phosphorylation of amylopectin is mediated by dikinases, the glucan, water dikinase (GWD) and the phosphoglucan water dikinase (PWD). This process was repeatedly observed during starch metabolism. By the collaborative action of both enzymes, the crystalline structure of the starch surface disrupts to a less order state to facilitate the process of starch degradation (Mahlow et al., 2016). Anyway, it is known that PWD act downstream of GWD, but it was confirmed that the prephosphorylation by GWD is not necessary for all starches (Fettke et al., 2009; Hejazi et al., 2012a). However, the result also revealed that the action of PWD was observed at the starch granule surface without the need to prephosphorylation by GWD. This suggests that its action on the independent glucan structures.

The previous results revealed variation in the binding of tLESV and ESV1 to starch granules structure. However, by the presence of both proteins at the glucan structures, the GWD and PWD-mediated phosphate incorporation rate was affected in a variance way that was reflected in the phosphorylation process. For normal starch degradation, the modulation of the level of starch phosphorylation reflects the control of the rate of starch degradation, therefore, the compartment for the work of GWD and PWD should be organized in such a way in whichthe phosphorylation process is modified in proportion to the action of the hydrolysing enzymes to maintain a linear level of degradation commensurate with the plant's need for the sugars.

To investigate the effect of the presence of tLESV and ESV1 proteins separately or together on the phosphorylation process, different starches were incubated with *St*GWD or *St*PWD with or without prephosphorylation by *St*GWD in the presence and absence of both proteins separately or together using a biochemical assays approach. However, both dikinases were affected by the presence of tLESV and ESV1 separately and together which is indicating that both proteins are considered fundamental components that participate in the organization of the phosphorylation process during starch degradation. This means that the presence of tLESV and ESV1 influencesthe action of GWD and PWD separately as the binding of both proteins to the starch granules affect the rate of the phosphorylation process whether the phosphorylation process is accomplished by the GWD alone or with PWD alone or it is performed by both enzymes. However, it was shown that the binding of phosphate is more evenly distributed between the crystalline region and amorphous lamellae. Moreover, the amorphous parts are more enriched in C6-bound phosphate than C3-bound phosphate (Nakamura, 2015). Therefore, most likely the binding of tLESV and ESV1 to the glucans structures located in both regions lead to reduced bound phosphate to these structures thereby reducing the glucans disruption.

Although the GWD and PWD-mediated phosphate incorporation revealed a significant reduction in the presence of tLESV and ESV1 whether separately or together regardless of the who has the most influence, there is doubt about the influence of PWD in the presence of ESV1 where a significant decrease in the glucan phosphorylation by PWD was observed during incubating it with ESV1 without prephosphorylation by GWD ,while the rate of its activity increased during incubating it with ESV1 after GWD-prephosphorylation (Chapter 4), but after the repetition of the experiments, it found the reduction in the PWD-phosphate incorporation in the presence of ESV1 whether with or without prephosphorylation by GWD (Chapter 5). However, it is difficult to determine what is the correct result for the action of PWD that is likely to be observed in *in vivo* when the PWD activity acts downstream of GWD in the presence of ESV1, while it can happen that an enzyme action in *in vivo* is not the same action in *in vitro*. Maybe, because one of the reaction components is an unstable, or the way of administration does not allow the enzyme to be able to react or something else. Therefore, if it speculates that the reduction of the action of PWD after prephosphorylation by GWD in the presence of ESV1 is the correct behavior, this means that ESV1 may bind to the unknown glucan structures which could be used as a substrate by PWD. Maybe the binding of ESV1 to the

glucan structures is rendering it not suitable to the PWD action by unknown mechanism while PWD acts preferentially on more soluble glucan structures at the granule surface (Hejazi et al., 2009; 2012). On the other hand, if the action of PWD increased after prephosphorylation by GWD in the presence of ESV1 was a correct behavior, that means that the binding of ESV1 to the starch granules altered the glucan structures in a way that allow to generate glucan structures that are preferred by PWD. However, these results suggest that tLESV and ESV1 work before the two dikinases, GWD and PWD, while their binding to the starch granules leads to organize and prepare the starch structure to both dikinases to perform the phosphorylation process moderately.

Influence of tLESV and ESV1 on the starch-hydrolysis enzymes

To complete the starch degradation, the action of the hydrolysis enzymes is required. It was shown that the phosphorylation process which was performed by the action of dikinases disrupted the glucan double helices rendering the glucan chains at the surface more accessible to these enzymes. To determine whether tLESV and ESV1 affected the action of the hydrolysis enzymes, native starch granules were incubated with beta-amylase (BAM), alpha-amylase (AMY), and isoamylase (ISA) after treatingof these granules with tLESV and ESV1. However, the action of BAM was affected by the presence of both proteins. It was shown a significant reduction in the action of BAM, whereas the reduction of the action of BAM was reflected in the released of glucans. While the release of maltose from starch granules revealed a significant reduction in the presence of tLESV and ESV1. However, it was seen that the released glucans by BAM in the presence of tLESV and ESV1 were not abolished, but reduced, indicating that both proteins do not act through inhibition of the BAM action. On the other hand, during the hydrolysis of the free glucan chains at the starch granule surface by the action of BAM, a water molecule will be consumed, so the binding of tLESV and ESV1 to the starch structure may alter the glucan chains that might modulate a water uptake thereby regulate and organize the hydrolysis process by BAM.

However, it was shown that the degradation of starch granule increases significantly by BAMs if they act together with GWD (Edner et al., 2007). Therefore, it is likely to be observed *in vivo* that the reduction of the action of GWD in the presence of tLESV and ESV1 may be accompanied by a decrease in the action of BAM. On the other hand, no

alteration in the action of AMY was detected. There is no difference between the glucans released by the action of AMY in the presence of tLESV and ESV1 compared to the controls observed. Maybe the nature of the action of AMY as an endoamylolysing enzyme rendered it unaffected by the alteration of starch granule surface structure which resulted from the binding of both proteins. But, because of the mode of action of AMY was downstream of BAM, it cannot exclude the effect of tLESV and ESV1 on the action of AMY after their effect on the action of BAM *in vivo*. However, this result suggests that the binding of both proteins was before starting the degradation process by BAM, in which no effect was observed on AMY which acts downstream of BAM.

Furthermore, in the previous results a slight alteration in the isoamylase action was observed in the presence of tLESV or ESV1 whether separately or together. While it wasshowed a minor shift in the short glucan chains length distribution in Arabidopsis wild-type and maize wild-type in the presence of tLESV or ESV1 separately or together. Perhaps the short branches of glucan chains which are located at the outer layer of the starch granule surface were loose and unstable. Therefore, the presence of these chains in this situation is reflected on the starch granule organization, therefore, the binding of both proteins to these chains may increase their stability thereby increase the effectiveness of isoamylase to attack these chains. This result suggests that the binding of tLESV and ESV1 to the outer short glucan chains may help in pruning the granule surface by isoamylase, thus, maintaining the stability and shape of the starch granule surface.

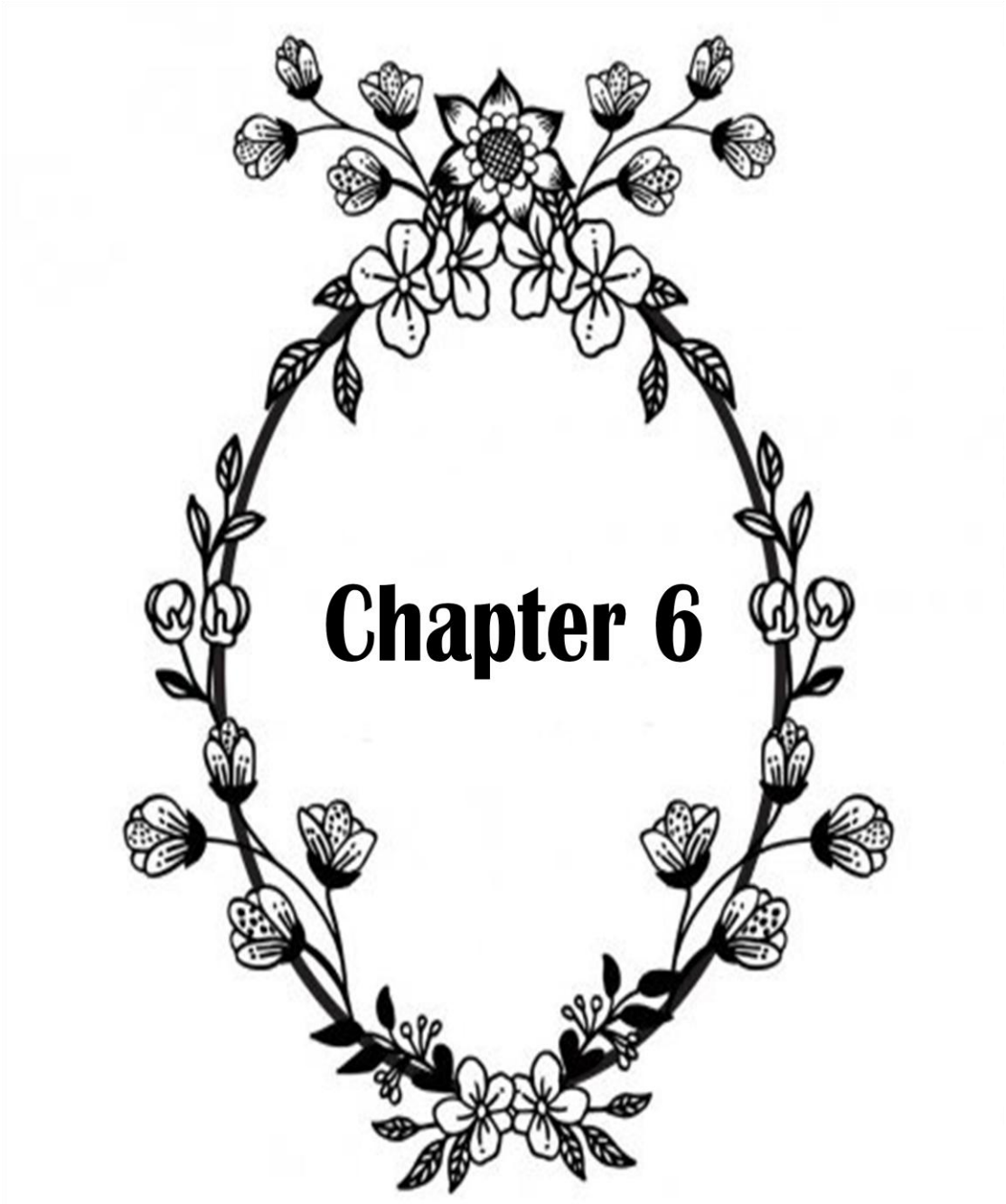

Chapter 6

6. General discussion and outlook

The aim of this work was to identify the mechanisms by which starch degradation is regulated. Using biochemical assays as well as biotechnology approaches, the results revealed the significance of the role of protein-glucan interaction through regulating and adjusting the phosphorylation mechanisms during starch degradation. However, the phosphorylation of starch was reported that it was mediated by GWD and PWD while both enzymes utilize ATP as dual phosphate donors (Mahlow et al., 2016). Whereas GWD acts preferentially on highly ordered structures at the starch granules surface (Hejazi et al., 2008, 2012), it was previously identified that PWD phosphorylated the starch granule only following prephosphorylation with GWD (Kötting et al. 2005). But, in the current study, it was shown that significant incorporation of ^{33}P- phosphate by PWD was observed without GWD-mediated phosphorylation into the starch granules. This result agrees with the finding of Fettke et al. (2009) who has reported that *in vitro*, PWD phosphorylates less ordered starch structures, which are isolated from several transgenic lines that were mutant in some of the starch-synthesis enzymes or such as a commercial maize *amylose extender* without any prephosphorylayion by GWD. Recently, EARLY STARVATION 1(ESV1) and its homology LIKE EARLY STARVATION (LESV) proteins have been identified in Arabidopsis independently by screening mutants with sucrose starvation and abnormal starch turnover during the diurnal cycle (Feike et al., 2016). Furthermore, in this work by SDS-PAGE with MALDI-TOF/MS, it also identified both proteins in the *Arabidopsis thaliana* leaves. Subsequently, using biochemical assays it was detected that both proteins are not only binding to the starch granule surface but also entering the glucan structure of the starch granule. While it found that LESV binds to both amylose and amylopectin, no binding of ESV1 to amylose was observed. Further, the binding of both proteins is capable of altering the starch structure in a way that affects the GWD and PWD-phosphorylation process thereby affecting the hydrolysing enzymes to reach the glucan chains. However, the independent work for each LESV, ESV1 and the two dikinases was detected after protein-protein interactions assays while there was no interaction between LESV and ESV1 or these proteins with the two dikinases enzyme or between the two dikinases themselves were observed.

ESV1 and LESV bind to different types of starch and affect the action of phosphorylating enzymes (GWD and PWD) and hydrolysing enzymes BAM, AMY, and IAS.

The electrophoresis analysis of the leaves crude extract of Arabidopsis showed numerous bands of the proteins. Subsequently, the analysis of MALDI-TOF identified that LESV and ESV1 belong to the Arabidopsis genome, so, it can be understood that both proteins are located in the chloroplast. This result agrees with the findings of Feike, et al. (2016) who they confirmed the plastidial localization of both Arabidopsis LESV and ESV1 proteins by using *in vivo*, YFP fluorescence assay by expressing them as a C-terminal fusion to YFP. Diffuse signal of YFP in the chloroplast stroma indicated the presence of both proteins. However, the BlastP search revealed that the Arabidopsis LESV and ESV1 proteins are encoded by At3g55760 and At1g42430 with ~50 kDa and ~65kDa, respectively. The programmes TargetP or ChloroP predicted a 56-amino acid N-terminal chloroplast transit peptide for LESV, while there is no chloroplast transit peptide predicted for ESV1 (Emanuelsson et al., 1999, 2000). As it reported that the import of most nuclear-encoded proteins into plastids directed by N-terminal targeting signal was called transit peptide (Bruce, 2001; Patron and Waller, 2007). However, the high diversity and lack of a distinct consensus sequence of transit peptides lead to failure in predicting their presence in proteins (Lee et al., 2008). Usually, this region is processed during transport into plastids. This transit peptide (proprotein or prosequence) is removed upon arrival in the plastid (Soll and Schleiff, 2004). Therefore, it was thought that the first 58 amino acids in the ESV1 sequence were removed during the import process into the chloroplast. However, this assumption was supported during two generated and purified forms of ESV1 protein, one was the full length (ESV1) and the other was truncated the first 58 amino acid (tESV1) in which the results of biochemical analysis of both forms revealed only slight or no significant differences in the action of protein between both forms during their binding to the glucan structures. Hence, these results suggest that the N-terminals do not alter the action of the protein; therefore, ESV1 form was adopted in analyzing the data. However, the same finding was observed with LESV protein when it also used two forms of protein, full length (LESV) form and the truncated form which lacks the 56 aa N-terminal (tLESV), while the results of the biochemical analysis revealed that the action of both forms showed the same effect on the binding of

starch and the phosphorylation process. Therefore, the N-terminal also did not alter the folding and action of the LESV, so it was used the tLESV form in analysis of the data. However, the discovery of the LESV and ESV1 as starch binding proteins revealed a strong binding to various starches refers to that both proteins may have surface binding sites (SBSs) while they devoid the carbohydrate-binding modules (CBM) (Feike et al., 2016). For instance, it was reported that in amylolytic enzymes, the CBM and SBSs are important and critical in starch binding (Baroroh et al., 2017). Enhancing the catalytic efficiency of enzymes to degrade the difficult and rigid starch granule crystalline or amorphous form is achieved through the incorporation of the SBS in these enzymes. On the other side, it has already been described that the SBS at the surface of the enzyme is formed by aromatic residues (Baroroh et al., 2017). However, the observation that both LESV and ESV1 structure has a large domain was enriched in conserved tryptophan, phenylalanine and tyrosine residues. Thus, it was speculated that the aromatic acid residues in both proteins have a role in the binding of both proteins to different glucan structures.

In the current study, although LESV and ESV1 bind to various types of starch, there is a disproportion in their binding due to the difference in the morphology and the surface properties of these starches. However, the results revealed that their binding to the starch granule was strong in which even after washing the starch granules with 2% [w/v] SDS, not all of the protein was released. This result also suggests that the binding of both proteins was not limited to the starch surface; they can enter the starch structure too. Further, this result was confirmed after treatment of the starch granules with ISA and BAM to remove the short glucan chains from the surface and then incubate it with both proteins. Analysis of proteins showed that the binding of both proteins to the starches indicates the association of both proteins with deeper layers than the starch granule surface.

On the other hand, through the binding of both proteins to the starches, LESV appears to bind to both polymers, amylose that has already formed long and helical glucan chains and amylopectin that has short and branched glucan chains, while only the binding of ESV1 to amylopectin since it was not observed its binding to amylose. However, it may be expected that these proteins bind to different types of substrates whether at the surface or deeper than the starch granule surface. It was found that the binding of LESV and

ESV1 to the starch, therefore, altered the organization of the glucan structures in a mechanism that led to influence on the phosphorylation process. It is known that starch phosphorylation is an important part of plant metabolism due to its role as a primary process in starch degradation (Lorberth et al., 1998). Further, it was reported that starch phosphorylation leads to increased hydration capacity of the starch granule, thereby rendering it more facilitated and accessible for hydrolyzing enzyme (Yu et al., 2001).
The important role of LESV and ESV1 proteins in the phosphorylation are capable of altering the glucan structures and affect the action of GWD and PWD. It was also shown that the binding of both proteins to the starch granule surface is likely to organize the interaction of the two dikinases, GWD and PWD with the glucan structures to add the phosphate groups during starch degradation, while the presence of both proteins leads to reduce the phosphorylation, but not abolish the incorporation of phosphate into the starch granules. This result clearly suggests that the binding of both proteins is not directly involved in starch degradation.

On the other hand, the presence of both proteins did not affect the autophosphorylation of both GWD and PWD. This indicates that both proteins are not a competition on the substrate with both dikinases, or act on the inhibition of both dikinases enzymes. This result suggests that the binding of both proteins to the starch alters the glycan structures that are preferentially phosphorylated by GWD and PWD thereby they effect indirectly on the phosphorylation process. This finding is also considered another possibility that both proteins effect of starch degradation indirectly.

It was clear that LESV and ESV1 are required for organized soluble and insoluble glucan chains at the starch granule surface and that these glucan chains are necessary for the phosphorylation by GWD and PWD. While GWD acts preferentially on highly ordered structures at the starch granule surface, PWD acts on more soluble glucan (Hejazi et al., 2009, 2012). As the prephosphorylation of GWD is not necessary for all starches (Fettke et al., 2009), it is unlikely to observe the same effect of LESV or ESV1 on the action of GWD and PWD. However, antagonistic results were revealed for the effect of ESV1 on the action of PWD after prephosphorylation by GWD. Despite the increase of the PWD-incorporation of phosphate in the presence of ESV1 after prephosphorylation by GWD (Chapter 4), the reduction of the PWD-incorporation of phosphate in the presence of ESV1 whether separately or together with LESV after prephosphorylation by GWD was

observed (Chapter 5). It is difficult and critical to determine the correct action of ESV1 because little or no information is available about the exact mode of action of this protein so far. Given that LESV, ESV1, GWD, and PWD are required to modulate the phosphorylation process during the degradation of starch, but no interaction between LESV and ESV1 or between each of them with GWD or PWD or between GWD and PWD themselves was detected using crosslinking assays and Y2H system. These results indicate the independent work for each one during the starch degradation process. Given that the binding of both LESV and ESV1 to starch structure showed to act upstream of the process of starch degradation, they were revealed that they both organize the accessibility of glucans at starch granule surface to the two dikinases.

So, to provide more insight into the role of LESV and ESV1 in controlling starch degradation process, the effect of both proteins was tested on starch-related enzymes which act as hydrolysing enzymes, isoamylase, beta-amylase, and alpha-amylase where these enzymes act downstream of the dikinases-mediated phosphorylation. However, it was found that the presence of both proteins whether separately or together had minor effects on the action of isoamylase, while the chain length distribution of starch revealed a slight increase in the short glucan chains. These increases may not appear to lead to the effect of the total of released glucan by isoamylase in the presence of LESV since there was no difference in the total of released glucan was observed.

Furthermore, it was shown that the binding of LESV and ESV1 to the starch granules surface had regulated BAM-glucans interactions after revealing that the presence of LESV and ESV1 did not lead to abolish the action of BAM, but led to reducing it. It may be expected that the binding of LESV and ESV1 to the free glucan chains at the surface leads to modulate these glucans as a substrate to the action of BAM as BAM is considered an exohydrolysing enzyme. In contrast, no alteration in the action of AMY was observed in the presence of LESV and ESV1. However, the mode of action of AMY as an endohydrolysig enzyme may render the enzyme not be affected by the alteration which results from the binding of LESV and ESV1 to the starch surface

Overall, it can be speculated that the degradation process needs a factor to organize it. Without this factor the degradation of starch will be performed in a fast manner thereby it will consume all the starch before the end of the night, so, LESV1 and ESV1 could play this role in organizing this process.

6.1 Conclusion

- LESV and ESV1 are starch binding proteins, both proteins are not only binding the surface of the starch granules but also able to bind to the deeper layers than the starch granule surface.
- LESV and ESV1 revealed a variation in the binding to starch, while LESV was binding to both amylose and amylopectin; ESV1 was only binding to amylopectin.
- The binding of both proteins to starch is an important part of the starch degradation system, their binding to the starch granule surface is capable of alteration of the starch structure.
- The presence of both proteins at the starch granule surface affected the GWD and PWD-mediated phosphate incorporation rate thereby on the phosphorylation process.
- The presence of LESV and ESV1 is more linked to the phosphorylation process than the action of downstream hydration process by hydrolytic enzymes, while it was only detected that the action of BAM enzyme was reduced in the presence of each one compared to IAS and AMY.
- Mode of action of LESV, ESV1, GWD, and PWD was performed in independent mode while no interaction among them was detected.
- PWD was able to phosphorylate starch without prephosphorylation by GWD.

References

- **Adeva-Andany, M. M., González-Lucán, M., Donapetry-García, C., Fernández-Fernández, C., & Ameneiros-Rodríguez, E.** (2016). Glycogen metabolism in humans. *BBA clinical*, *5*, 85-100.
- **Alberts, B., Johnson, A., Lewis, J., Raff, M., Roberts, K., & Walter, P.** (2002). Fibroblasts and their transformations: the connective-tissue cell family. In *Molecular Biology of the Cell. 4th edition*. Garland Science.
- **Alcázar-Alay, S. C., & Meireles, M. A. A.** (2015). Physicochemical properties, modifications and applications of starches from different botanical sources. *Food Science and Technology*, *35*(2), 215-236.
- **Alonso-Casajús, N., Dauvillée, D., Viale, A. M., Muñoz, F. J., Baroja-Fernández, E., Morán-Zorzano, M. T., ... & Pozueta-Romero, J.** (2006). Glycogen phosphorylase, the product of the glgP gene, catalyzes glycogen breakdown by removing glucose units from the nonreducing ends in Escherichia coli. *Journal of bacteriology*, *188*(14), 5266-5272.
- **Asai, H., Abe, N., Matsushima, R., Crofts, N., Oitome, N. F., Nakamura, Y., & Fujita, N.** (2014). Deficiencies in both starch synthase IIIa and branching enzyme IIb lead to a significant increase in amylose in SSIIa-inactive japonica rice seeds. *Journal of experimental botany*, *65*(18), 5497-5507.
- **Baldwin, I. T., Halitschke, R., Kessler, A., & Schittko, U.** (2001). Merging molecular and ecological approaches in plant–insect interactions. *Current opinion in plant biology*, *4*(4), 351-358.
- **Ball, S. G., & Morell, M. K.** (2003). From bacterial glycogen to starch: understanding the biogenesis of the plant starch granule. *Annual review of plant biology*, *54*(1), 207-233.
- **Ballicora, M. A., Iglesias, A. A., & Preiss, J.** (2004). ADP-glucose pyrophosphorylase: a regulatory enzyme for plant starch synthesis. *Photosynthesis Research*, *79*(1), 1-24.
- **Baroroh, U., Yusuf, M., Rachman, S. D., Ishmayana, S., Syamsunarno, M. R. A., Levita, J., & Subroto, T.** (2017). The importance of surface-binding site towards starch-adsorptivity level in α-amylase: a review on structural point of view. *Enzyme research*, *2017*.

- **Batra, R., Saripalli, G., Mohan, A., Gupta, S., Gill, K. S., Varadwaj, P. K., ... & Gupta, P. K.** (2017). Comparative analysis of AGPase genes and encoded proteins in eight monocots and three dicots with emphasis on wheat. *Frontiers in plant science*, *8*, 19.
- **Baunsgaard, L., Lütken, H., Mikkelsen, R., Glaring, M. A., Pham, T. T., & Blennow, A.** (2005). A novel isoform of glucan, water dikinase phosphorylates pre-phosphorylated α-glucans and is involved in starch degradation in Arabidopsis. *The Plant Journal*, *41*(4), 595-605.
- **Bayer, R. G., Stael, S., Csaszar, E., & Teige, M.** (2011). Mining the soluble chloroplast proteome by affinity chromatography. *Proteomics*, *11*(7), 1287-1299.
- **Bertoft, E.** (2017). Understanding starch structure: Recent progress. *Agronomy*, *7*(3), 56.
- **Bianco, R. L., & Rieger, M.** (2002). Roles of sorbitol and sucrose in growth and respiration ofEncore'peaches at the three developmental stages. *Journal of the American Society for Horticultural Science*, *127*(2), 297-302.
- **Blauth, S. L., Kim, K. N., Klucinec, J., Shannon, J. C., Thompson, D., & Guiltinan, M.** (2002). Identification of Mutator insertional mutants of starch-branching enzyme 1 (sbe1) in Zea mays L. *Plant molecular biology*, *48*(3), 287-297.
- **Blennow, A., & Engelsen, S. B.** (2010). Helix-breaking news: fighting crystalline starch energy deposits in the cell. *Trends in plant science*, *15*(4), 236-240.
- **Blennow, A., Bay-Smidt, A. M., Wischmann, B., Olsen, C. E., & Møller, B. L.** (1998). The degree of starch phosphorylation is related to the chain length distribution of the neutral and the phosphorylated chains of amylopectin. *Carbohydrate Research*, *307*(1-2), 45-54.
- **Blennow, A., Nielsen, T. H., Baunsgaard, L., Mikkelsen, R., & Engelsen, S. B.** (2002). Starch phosphorylation: a new front line in starch research. *Trends in plant science*, *7*(10), 445-450.
- **Bresolin, N. S., Li, Z., Kosar-Hashemi, B., Tetlow, I. J., Chatterjee, M., Rahman, S., ... & Howitt, C. A.** (2006). Characterisation of disproportionating enzyme from wheat endosperm. *Planta*, *224*(1), 20-31.

- **Bruce, B. D.** (2001). The paradox of plastid transit peptides: conservation of function despite divergence in primary structure. *Biochimica et Biophysica Acta (BBA)-Molecular Cell Research*, *1541*(1-2), 2-21.
- **Brust, H., Lehmann, T., D'Hulst, C., & Fettke, J.** (2014). Analysis of the functional interaction of Arabidopsis starch synthase and branching enzyme isoforms reveals that the cooperative action of SSI and BEs results in glucans with polymodal chain length distribution similar to amylopectin. *PLoS One*, *9*(7), e102364.
- **Brust, H., Orzechowski, S., Fettke, J., & Steup, M.** (2013). Starch synthesizing reactions and paths: in vitro and in vivo studies. *Journal of applied glycoscience*, *60*(1), 3-20.
- **Burton, R. A., Bewley, J. D., Smith, A. M., Bhattacharyya, M. K., Tatge, H., Ring, S., ... & Martin, C.** (1995). Starch branching enzymes belonging to distinct enzyme families are differentially expressed during pea embryo development. *The Plant Journal*, *7*(1), 3-15.
- **Burwinkel, B., Bakker, H. D., Herschkovitz, E., Moses, S. W., Shin, Y. S., & Kilimann, M. W.** (1998). Mutations in the liver glycogen phosphorylase gene (PYGL) underlying glycogenosis type VI (Hers disease). *The American Journal of Human Genetics*, *62*(4), 785-791.
- **Carmona-Garcia, R., Sanchez-Rivera, M. M., Méndez-Montealvo, G., Garza-Montoya, B., & Bello-Pérez, L. A.** (2009). Effect of the cross-linked reagent type on some morphological, physicochemical and functional characteristics of banana starch (Musa paradisiaca). *Carbohydrate Polymers*, *76*(1), 117-122.
- **Carpenter, M. A., Joyce, N. I., Genet, R. A., Cooper, R. D., Murray, S. R., Noble, A. D., ... & Timmerman-Vaughan, G. M.** (2015). Starch phosphorylation in potato tubers is influenced by allelic variation in the genes encoding glucan water dikinase, starch branching enzymes I and II, and starch synthase III. *Frontiers in plant science*, *6*, 143.
- **Chaikuad, A., Froese, D. S., Berridge, G., von Delft, F., Oppermann, U., & Yue, W. W.** (2011). Conformational plasticity of glycogenin and its maltosaccharide substrate during glycogen biogenesis. *Proceedings of the National Academy of Sciences*, *108*(52), 21028-21033.

- **Chen, Y., Sun, X., Zhou, X., Hebelstrup, K. H., Blennow, A., & Bao, J.** (2017). Highly phosphorylated functionalized rice starch produced by transgenic rice expressing the potato GWD1 gene. *Scientific reports*, *7*(1), 1-10.
- **Chia, T., Thorneycroft, D., Chapple, A., Messerli, G., Chen, J., Zeeman, S. C., ... & Smith, A. M.** (2004). A cytosolic glucosyltransferase is required for conversion of starch to sucrose in Arabidopsis leaves at night. *The Plant Journal*, *37*(6), 853-863.
- **Cho, M. H., Lim, H., Shin, D. H., Jeon, J. S., Bhoo, S. H., Park, Y. I., & Hahn, T. R.** (2011). Role of the plastidic glucose translocator in the export of starch degradation products from the chloroplasts in Arabidopsis thaliana. *New Phytologist*, *190*(1), 101-112.
- **Christiansen, J., Kolte, A. M., & Nielsen, F. C.** (2009). IGF2 mRNA-binding protein 2: biological function and putative role in type 2 diabetes. *Journal of molecular endocrinology*, *43*(5), 187-195.
- **Ciereszko, I., Johansson, H., & KLECZKOWSKI, L. A.** (2001). Sucrose and light regulation of a cold-inducible UDP-glucose pyrophosphorylase gene via a hexokinase-independent and abscisic acid-insensitive pathway in Arabidopsis. *Biochemical Journal*, *354*(1), 67-72.
- **Cobb, B. A., & Kasper, D. L.** (2005). Coming of age: carbohydrates and immunity. *European journal of immunology*, *35*(2), 352-356.
- **Commuri, P. D., & Keeling, P. L.** (2001). Chain-length specificities of maize starch synthase I enzyme: studies of glucan affinity and catalytic properties. *The Plant Journal*, *25*(5), 475-486.
- **Comparot-Moss, S., Kötting, O., Stettler, M., Edner, C., Graf, A., Weise, S. E., ... & Ritte, G.** (2010). A putative phosphatase, LSF1, is required for normal starch turnover in Arabidopsis leaves. *Plant physiology*, *152*(2), 685-697.
- **Cordenunsi-Lysenko, B. R., Nascimento, J. R. O., Castro-Alves, V. C., Purgatto, E., Fabi, J. P., & Peroni-Okyta, F. H. G.** (2019). The starch is (not) just another brick in the wall: The primary metabolism of sugars during banana ripening. *Frontiers in plant science*, *10*.
- **Coutinho, P. M., Deleury, E., Davies, G. J., & Henrissat, B.** (2003). An evolving hierarchical family classification for glycosyltransferases. *Journal of molecular biology*, *328*(2), 307-317.

- **Craig, J., Lloyd, J. R., Tomlinson, K., Barber, L., Edwards, A., Wang, T. L., ... & Smith, A. M.** (1998). Mutations in the gene encoding starch synthase II profoundly alter amylopectin structure in pea embryos. *The Plant Cell*, *10*(3), 413-426.
- **Critchley, J. H., Zeeman, S. C., Takaha, T., Smith, A. M., & Smith, S. M.** (2001). A critical role for disproportionating enzyme in starch breakdown is revealed by a knock-out mutation in Arabidopsis. *The Plant Journal*, *26*(1), 89-100.
- **Critchley, J. H., Zeeman, S. C., Takaha, T., Smith, A. M., & Smith, S. M.** (2001). A critical role for disproportionating enzyme in starch breakdown is revealed by a knock-out mutation in Arabidopsis. *The Plant Journal*, *26*(1), 89-100.
- **Crumpton-Taylor, M., Grandison, S., Png, K. M., Bushby, A. J., & Smith, A. M.** (2012). Control of starch granule numbers in Arabidopsis chloroplasts. *Plant physiology*, *158*(2), 905-916.
- **Crumpton-Taylor, M., Pike, M., Lu, K. J., Hylton, C. M., Feil, R., Eicke, S., ... & Smith, A. M.** (2013). Starch synthase 4 is essential for coordination of starch granule formation with chloroplast division during Arabidopsis leaf expansion. *New Phytologist*, *200*(4), 1064-1075.
- **Cuesta-Seijo, J. A., Nielsen, M. M., Marri, L., Tanaka, H., Beeren, S. R., & Palcic, M. M.** (2013). Structure of starch synthase I from barley: insight into regulatory mechanisms of starch synthase activity. *Acta Crystallographica Section D: Biological Crystallography*, *69*(6), 1013-1025.
- **Cuesta-Seijo, J. A., Ruzanski, C., Krucewicz, K., Meier, S., Hägglund, P., Svensson, B., & Palcic, M. M.** (2017). Functional and structural characterization of plastidic starch phosphorylase during barley endosperm development. *PloS one*, *12*(4), e0175488.
- **D'Hulst, C., & Mérida, Á.** (2010). The priming of storage glucan synthesis from bacteria to plants: current knowledge and new developments. *New Phytologist*, *188*(1), 13-21.
- **Dahiya, A., Saini, R., Saini, H. S., & Devi, A.** (2017). Sucrose metabolism: Controls the sugar sensing and generation of signalling molecules in plants. *Journal of Pharmacognosy and Phytochemistry*, *6*(4), 1563-1572.

- **Darvill, A., Augur, C., Bergmann, C., Carlson, R. W., Cheong, J. J., Eberhard, S., ... & Mohnen, D.** (1992). Oligosaccharins—oligosaccharides that regulate growth, development and defence responses in plants. *Glycobiology*, *2*(3), 181-198.
- **Dauvillée, D., Chochois, V., Steup, M., Haebel, S., Eckermann, N., Ritte, G., ... & Deschamps, P.** (2006). Plastidial phosphorylase is required for normal starch synthesis in Chlamydomonas reinhardtii. *The Plant Journal*, *48*(2), 274-285.
- **Delatte, T., Trevisan, M., Parker, M. L., & Zeeman, S. C.** (2005). Arabidopsis mutants Atisa1 and Atisa2 have identical phenotypes and lack the same multimeric isoamylase, which influences the branch point distribution of amylopectin during starch synthesis. *The Plant Journal*, *41*(6), 815-830.
- **Delatte, T., Umhang, M., Trevisan, M., Eicke, S., Thorneycroft, D., Smith, S. M., & Zeeman, S. C.** (2006). Evidence for distinct mechanisms of starch granule breakdown in plants. *Journal of Biological Chemistry*, *281*(17), 12050-12059.
- **Delvallé, D., Dumez, S., Wattebled, F., Roldán, I., Planchot, V., Berbezy, P., ... & Mérida, Á.** (2005). Soluble starch synthase I: a major determinant for the synthesis of amylopectin in Arabidopsis thaliana leaves. *The Plant Journal*, *43*(3), 398-412.
- **Dong, X., Zhang, D., Liu, J., Liu, Q. Q., Liu, H., Tian, L., ... & Qu, L. Q.** (2015). Plastidial disproportionating enzyme participates in starch synthesis in rice endosperm by transferring maltooligosyl groups from amylose and amylopectin to amylopectin. *Plant physiology*, *169*(4), 2496-2512.
- **Dumez, S., Wattebled, F., Dauvillee, D., Delvalle, D., Planchot, V., Ball, S. G., & d'Hulst, C.** (2006). Mutants of Arabidopsis lacking starch branching enzyme II substitute plastidial starch synthesis by cytoplasmic maltose accumulation. *The Plant Cell*, *18*(10), 2694-2709.
- **Edner, C., Li, J., Albrecht, T., Mahlow, S., Hejazi, M., Hussain, H., ... & Ritte, G.** (2007). Glucan, water dikinase activity stimulates breakdown of starch granules by plastidial β-amylases. *Plant physiology*, *145*(1), 17-28.
- **Emanuelsson, O., Nielsen, H., & Von Heijne, G.** (1999). ChloroP, a neural network-based method for predicting chloroplast transit peptides and their cleavage sites. *Protein Science*, *8*(5), 978-984.

- **Emanuelsson, O., Nielsen, H., Brunak, S., & Von Heijne, G.** (2000). Predicting subcellular localization of proteins based on their N-terminal amino acid sequence. *Journal of molecular biology*, *300*(4), 1005-1016.
- **Emes, M. J., & Neuhaus, H. E.** (1997). Metabolism and transport in non-photosynthetic plastids. *Journal of Experimental Botany*, *48*(12), 1995-2005.
- **Espinosa-Leal, C. A., Puente-Garza, C. A., & García-Lara, S.** (2018). In vitro plant tissue culture: means for production of biological active compounds. *Planta*, *248*(1), 1-18.
- **Fasahat, P., Rahman, S., & Ratnam, W.** (2014). Genetic controls on starch amylose content in wheat and rice grains. *Journal of genetics*, *93*(1), 279-292.
- **Feike, D., Seung, D., Graf, A., Bischof, S., Ellick, T., Coiro, M., ... & Trick, M.** (2016). The starch granule-associated protein EARLY STARVATION1 is required for the control of starch degradation in Arabidopsis thaliana leaves. *The Plant Cell*, *28*(6), 1472-1489.
- **Fettke, J., Albrecht, T., Hejazi, M., Mahlow, S., Nakamura, Y., & Steup, M.** (2010). Glucose 1-phosphate is efficiently taken up by potato (Solanum tuberosum) tuber parenchyma cells and converted to reserve starch granules. *New Phytologist*, *185*(3), 663-675.
- **Fettke, J., Chia, T., Eckermann, N., Smith, A., & Steup, M.** (2006). A transglucosidase necessary for starch degradation and maltose metabolism in leaves at night acts on cytosolic heteroglycans (SHG). *The Plant Journal*, *46*(4), 668-684.
- **Fettke, J., Hejazi, M., Smirnova, J., Höchel, E., Stage, M., & Steup, M.** (2009). Eukaryotic starch degradation: integration of plastidial and cytosolic pathways. *Journal of experimental botany*, *60*(10), 2907-2922.
- **Fields, S., & Song, O. K.** (1989). A novel genetic system to detect protein–protein interactions. *Nature*, *340*(6230), 245-246.
- **Fry, S. C., Aldington, S., Hetherington, P. R., & Aitken, J.** (1993). Oligosaccharides as signals and substrates in the plant cell wall. *Plant Physiology*, *103*(1), 1.
- **Fujita, N., Satoh, R., Hayashi, A., Kodama, M., Itoh, R., Aihara, S., & Nakamura, Y.** (2011). Starch biosynthesis in rice endosperm requires the

presence of either starch synthase I or IIIa. *Journal of experimental botany*, *62*(14), 4819-4831.

- **Fujita, N., Yoshida, M., Asakura, N., Ohdan, T., Miyao, A., Hirochika, H., & Nakamura, Y.** (2006). Function and characterization of starch synthase I using mutants in rice. *Plant physiology*, *140*(3), 1070-1084.
- **Fulton, D. C., Stettler, M., Mettler, T., Vaughan, C. K., Li, J., Francisco, P., ... & Dorken, G.** (2008). β-AMYLASE4, a noncatalytic protein required for starch breakdown, acts upstream of three active β-amylases in Arabidopsis chloroplasts. *The Plant Cell*, *20*(4), 1040-1058.
- **Gentry, M. S., Dowen, R. H., Worby, C. A., Mattoo, S., Ecker, J. R., & Dixon, J. E.** (2007). The phosphatase laforin crosses evolutionary boundaries and links carbohydrate metabolism to neuronal disease. *The Journal of cell biology*, *178*(3), 477-488.
- **George, G. M., Van Der Merwe, M. J., Nunes-Nesi, A., Bauer, R., Fernie, A. R., Kossmann, J., & Lloyd, J. R.** (2010). Virus-induced gene silencing of plastidial soluble inorganic pyrophosphatase impairs essential leaf anabolic pathways and reduces drought stress tolerance in Nicotiana benthamiana. *Plant physiology*, *154*(1), 55-66.
- **Gibbons, B. J., Roach, P. J., & Hurley, T. D.** (2002). Crystal structure of the autocatalytic initiator of glycogen biosynthesis, glycogenin. *Journal of molecular biology*, *319*(2), 463-477.
- **Glaring, M. A., Baumann, M. J., Hachem, M. A., Nakai, H., Nakai, N., Santelia, D., ... & Svensson, B.** (2011). Starch-binding domains in the CBM45 family–low-affinity domains from glucan, water dikinase and α-amylase involved in plastidial starch metabolism. *The FEBS journal*, *278*(7), 1175-1185.
- **Glaring, M. A., Zygadlo, A., Thorneycroft, D., Schulz, A., Smith, S. M., Blennow, A., & Baunsgaard, L.** (2007). An extra-plastidial α-glucan, water dikinase from Arabidopsis phosphorylates amylopectin in vitro and is not necessary for transient starch degradation. *Journal of experimental botany*, *58*(14), 3949-3960.
- **Gollery, M., Harper, J., Cushman, J., Mittler, T., & Mittler, R.** (2007). POFs: what we don't know can hurt us. *Trends in plant science*, *12*(11), 492-496.

- **Gollery, M., Harper, J., Cushman, J., Mittler, T., Girke, T., Zhu, J. K., ... & Mittler, R.** (2006). What makes species unique? The contribution of proteins with obscure features. *Genome biology*, *7*(7), R57.
- **Guan, H. P., & Preiss, J.** (1993). Differentiation of the properties of the branching isozymes from maize (Zea mays). *Plant Physiology*, *102*(4), 1269-1273.
- **Guan, H., Li, P., Imparl-Radosevich, J., Preiss, J., & Keeling, P.** (1997). Comparing the properties ofEscherichia colibranching enzyme and maize branching enzyme. *Archives of Biochemistry and Biophysics*, *342*(1), 92-98.
- **Haebel, S., Hejazi, M., Frohberg, C., Heydenreich, M., & Ritte, G.** (2008). Mass spectrometric quantification of the relative amounts of C6 and C3 position phosphorylated glucosyl residues in starch. *Analytical biochemistry*, *379*(1), 73-79.
- **Hansen, P. I., Spraul, M., Dvortsak, P., Larsen, F. H., Blennow, A., Motawia, M. S., & Engelsen, S. B.** (2009). Starch phosphorylation—Maltosidic restrains upon 3′-and 6′-phosphorylation investigated by chemical synthesis, molecular dynamics and NMR spectroscopy. *Biopolymers: Original Research on Biomolecules*, *91*(3), 179-193.
- **Hayen, S. M., den Hartog Jager, C. F., Knulst, A. C., Knol, E. F., Garssen, J., Willemsen, L. E., & Otten, H. G.** (2018). Non-digestible oligosaccharides can suppress basophil degranulation in whole blood of peanut-allergic patients. *Frontiers in Immunology*, *9*, 1265.
- **Hedman, K. D., & Boyer, C. D.** (1982). Gene dosage at the amylose-extender locus of maize: effects on the levels of starch branching enzymes. *Biochemical Genetics*, *20*(5-6), 483-492.
- **Hejazi, M., Fettke, J., & Steup, M.** (2012). Starch phosphorylation and dephosphorylation: the consecutive action of starch-related dikinases and phosphatases. *Essential Reviews in Experimental Biology: Starch: Origins, Structure and Metabolism, Edited by IJ Tetlow, SEB, London*, *5*, 279-308.
- **Hejazi, M., Fettke, J., Haebel, S., Edner, C., Paris, O., Frohberg, C., ... & Ritte, G.** (2008). Glucan, water dikinase phosphorylates crystalline maltodextrins and thereby initiates solubilization. *The Plant Journal*, *55*(2), 323-334.

- **Hejazi, M., Fettke, J., Kötting, O., Zeeman, S. C., & Steup, M.** (2010). The Laforin-like dual-specificity phosphatase SEX4 from Arabidopsis hydrolyzes both C6-and C3-phosphate esters introduced by starch-related dikinases and thereby affects phase transition of α-glucans. *Plant physiology*, *152*(2), 711-722.
- **Hejazi, M., Mahlow, S., & Fettke, J.** (2014). The glucan phosphorylation mediated by α-glucan, water dikinase (GWD) is also essential in the light phase for a functional transitory starch turn-over. *Plant signaling & behavior*, *9*(7), e28892.
- **Helle, S., Bray, F., Putaux, J. L., Verbeke, J., Flament, S., Rolando, C., ... & Szydlowski, N.** (2019). Intra-Sample Heterogeneity of Potato Starch Reveals Fluctuation of Starch-Binding Proteins According to Granule Morphology. *Plants*, *8*(9), 324.
- **Helle, S., Bray, F., Verbeke, J., Devassine, S., Courseaux, A., Facon, M., ... & Szydlowski, N.** (2018). Proteome analysis of potato starch reveals the presence of new starch metabolic proteins as well as multiple protease inhibitors. *Frontiers in plant science*, *9*, 746.
- **Hii, S. L., Tan, J. S., Ling, T. C., & Ariff, A. B.** (2012). Pullulanase: role in starch hydrolysis and potential industrial applications. *Enzyme research*, *2012*.
- **Hurley, T. D., Walls, C., Bennett, J. R., Roach, P. J., & Wang, M.** (2006). Direct detection of glycogenin reaction products during glycogen initiation. *Biochemical and biophysical research communications*, *348*(2), 374-378.
- **Hussain, H., Mant, A., Seale, R., Zeeman, S., Hinchliffe, E., Edwards, A., ... & Bustos, R.** (2003). Three isoforms of isoamylase contribute different catalytic properties for the debranching of potato glucans. *The Plant Cell*, *15*(1), 133-149.
- **Hwang, S. K., Singh, S., Cakir, B., Satoh, H., & Okita, T. W.** (2016). The plastidial starch phosphorylase from rice endosperm: catalytic properties at low temperature. *Planta*, *243*(4), 999-1009.
- **Izydorczyk, M. S., & Edney, M. J.** (2003). MALT| Chemistry of Malting.
- **Ibrahim, M. F., Kim, S. W., & Abd-Aziz, S.** (2018). Advanced bioprocessing strategies for biobutanol production from biomass. *Renewable and Sustainable Energy Reviews*, *91*, 1192-1204.

- **Ismail, H., Irani, M., & Ahmad, Z.** (2013). Starch-based hydrogels: present status and applications. *International Journal of Polymeric Materials and Polymeric Biomaterials*, *62*(7), 411-420.
- **Jane, J. L., Ao, Z., Duvick, S. A., Wiklund, M., Yoo, S. H., Wong, K. S., & Gardner, C.** (2003). Structures of amylopectin and starch granules: How are they synthesized?. *Journal of Applied Glycoscience*, *50*(2), 167-172.
- **Jane, J. L., Kasemsuwan, T., Leas, S., Zobel, H., & Robyt, J. F.** (1994). Anthology of starch granule morphology by scanning electron microscopy. *Starch-Stärke*, *46*(4), 121-129.
- **Jenkins, P. J., Cameron, R. E., & Donald, A. M.** (1993). A universal feature in the structure of starch granules from different botanical sources. *Starch-Stärke*, *45*(12), 417-420.
- **Kadokawa, J. I.** (2018). Enzymatic preparation of functional polysaccharide hydrogels by phosphorylase catalysis. *Pure and Applied Chemistry*, *90*(6), 1045-1054.
- **Keeling, P. L., & Myers, A. M.** (2010). Biochemistry and genetics of starch synthesis. *Annual review of food science and technology*, *1*, 271-303.
- **Khowala, S., Verma, D., & Banik, S. P.** (2008). BIOMOLECULES:(INTRODUCTION, STRUCTURE & FUNCTION).
- **Kleffmann, T., Russenberger, D., von Zychlinski, A., Christopher, W., Sjölander, K., Gruissem, W., & Baginsky, S.** (2004). The Arabidopsis thaliana chloroplast proteome reveals pathway abundance and novel protein functions. *Current Biology*, *14*(5), 354-362.
- **Kötting, O., Kossmann, J., Zeeman, S. C., & Lloyd, J. R.** (2010). Regulation of starch metabolism: the age of enlightenment?. *Current opinion in plant biology*, *13*(3), 320-328.
- **Kötting, O., Pusch, K., Tiessen, A., Geigenberger, P., Steup, M., & Ritte, G.** (2005). Identification of a novel enzyme required for starch metabolism in Arabidopsis leaves. The phosphoglucan, water dikinase. *Plant physiology*, *137*(1), 242-252.
- **Kötting, O., Santelia, D., Edner, C., Eicke, S., Marthaler, T., Gentry, M. S., ... & Ritte, G.** (2009). STARCH-EXCESS4 is a laforin-like phosphoglucan

phosphatase required for starch degradation in Arabidopsis thaliana. *The Plant Cell*, *21*(1), 334-346.

- **Kozlov, S. S., Blennow, A., Krivandin, A. V., & Yuryev, V. P.** (2007). Structural and thermodynamic properties of starches extracted from GBSS and GWD suppressed potato lines. *International journal of biological macromolecules*, *40*(5), 449-460.
- **Lao, N. T., Schoneveld, O., Mould, R. M., Hibberd, J. M., Gray, J. C., & Kavanagh, T. A.** (1999). An Arabidopsis gene encoding a chloroplast-targeted β-amylase. *The Plant Journal*, *20*(5), 519-527.
- **Lee, D. W., Kim, J. K., Lee, S., Choi, S., Kim, S., & Hwang, I.** (2008). Arabidopsis nuclear-encoded plastid transit peptides contain multiple sequence subgroups with distinctive chloroplast-targeting sequence motifs. *The Plant Cell*, *20*(6), 1603-1622.
- **Li, L., Foster, C. M., Gan, Q., Nettleton, D., James, M. G., Myers, A. M., & Wurtele, E. S.** (2009). Identification of the novel protein QQS as a component of the starch metabolic network in Arabidopsis leaves. *The Plant Journal*, *58*(3), 485-498.
- **Li, C., Powell, P. O., & Gilbert, R. G.** (2017). Recent progress toward understanding the role of starch biosynthetic enzymes in the cereal endosperm. *Amylase*, *1*(1), 59-74.
- **LIM, S. T., KASEMSUWAN, T., & JANE, J.** (1994). by" P-Nuclear Magnetic Resonance Spectroscopy. *Cereal Chem*, *71*(5), 488-493.
- **Lin, B., Hiraiwa, H., Pan, C. J., Nordlie, R. C., & Chou, J. Y.** (1999). Type-1c glycogen storage disease is not caused by mutations in the glucose-6-phosphate transporter gene. *Human genetics*, *105*(5), 515-517.
- **Lindeboom, N., Chang, P. R., & Tyler, R. T.** (2004). Analytical, biochemical and physicochemical aspects of starch granule size, with emphasis on small granule starches: a review. *Starch-Stärke*, *56*(3-4), 89-99.
- **Liu, H., Yu, G., Wei, B., Wang, Y., Zhang, J., Hu, Y., ... & Huang, Y.** (2015). Identification and phylogenetic analysis of a novel starch synthase in maize. *Frontiers in plant science*, *6*, 1013.
- **Liu, P., Yu, L., Liu, H., Chen, L., & Li, L.** (2009). Glass transition temperature of starch studied by a high-speed DSC. *Carbohydrate polymers*, *77*(2), 250-253.

- **Liu, Y., Chen, L., Xu, H., Liang, Y., & Zheng, B.** (2019). Understanding the digestibility of rice starch-gallic acid complexes formed by high pressure homogenization. *International journal of biological macromolecules*, *134*, 856-863.
- **Lohmeier-Vogel, E. M., Kerk, D., Nimick, M., Wrobel, S., Vickerman, L., Muench, D. G., & Moorhead, G. B.** (2008). Arabidopsis At5g39790 encodes a chloroplast-localized, carbohydrate-binding, coiled-coil domain-containing putative scaffold protein. *BMC plant biology*, *8*(1), 120.
- **Lombard, V., Golaconda Ramulu, H., Drula, E., Coutinho, P. M., & Henrissat, B.** (2013). The carbohydrate-active enzymes database (CAZy) in 2013. *Nucleic acids research*, *42*(D1), D490-D495.
- **Lorberth, R., Ritte, G., Willmitzer, L., & Kossmann, J.** (1998). Inhibition of a starch-granule–bound protein leads to modified starch and repression of cold sweetening. *Nature biotechnology*, *16*(5), 473.
- **Loreti, E., Poggi, A., Novi, G., Alpi, A., & Perata, P.** (2005). A genome-wide analysis of the effects of sucrose on gene expression in Arabidopsis seedlings under anoxia. *Plant Physiology*, *137*(3), 1130-1138.
- **Lu, Y., & Sharkey, T. D.** (2004). The role of amylomaltase in maltose metabolism in the cytosol of photosynthetic cells. *Planta*, *218*(3), 466-473.
- **Luhua, S., Ciftci-Yilmaz, S., Harper, J., Cushman, J., & Mittler, R.** (2008). Enhanced tolerance to oxidative stress in transgenic Arabidopsis plants expressing proteins of unknown function. *Plant physiology*, *148*(1), 280-292.
- **Luo, J., Ahmed, R., Kosar-Hashemi, B., Larroque, O., Butardo, V. M., Tanner, G. J., ... & Millar, A.** (2015). The different effects of starch synthase IIa mutations or variation on endosperm amylose content of barley, wheat and rice are determined by the distribution of starch synthase I and starch branching enzyme IIb between the starch granule and amyloplast stroma. *Theoretical and applied genetics*, *128*(7), 1407-1419.
- **Lütken, H., Lloyd, J. R., Glaring, M. A., Baunsgaard, L., Laursen, K. H., Haldrup, A., ... & Blennow, A.** (2010). Repression of both isoforms of disproportionating enzyme leads to higher malto-oligosaccharide content and reduced growth in potato. *Planta*, *232*(5), 1127-1139.

- **MacNeill, D., Stiehl, G. M., Guimaraes, M. H. D., Buhrman, R. A., Park, J., & Ralph, D. C.** (2017). Control of spin–orbit torques through crystal symmetry in WTe 2/ferromagnet bilayers. *Nature Physics*, *13*(3), 300-305.
- **Mahlow, S., Hejazi, M., Kuhnert, F., Garz, A., Brust, H., Baumann, O., & Fettke, J.** (2014). Phosphorylation of transitory starch by α-glucan, water dikinase during starch turnover affects the surface properties and morphology of starch granules. *New Phytologist*, *203*(2), 495-507.
- **Malinova, I., Alseekh, S., Feil, R., Fernie, A. R., Baumann, O., Schöttler, M. A., ... & Fettke, J.** (2017). Starch synthase 4 and plastidal phosphorylase differentially affect starch granule number and morphology. *Plant physiology*, *174*(1), 73-85.
- **Malinova, I., Mahlow, S., Alseekh, S., Orawetz, T., Fernie, A. R., Baumann, O., ... & Fettke, J.** (2014). Double knockout mutants of Arabidopsis grown under normal conditions reveal that the plastidial phosphorylase isozyme participates in transitory starch metabolism. *Plant physiology*, *164*(2), 907-921.
- **Malinova, I., Qasim, H. M., Brust, H., & Fettke, J.** (2018). Parameters of starch granule genesis in chloroplasts of Arabidopsis thaliana. *Frontiers in plant science*, *9*.
- **Mason, J. M., & Arndt, K. M.** (2004). Coiled coil domains: stability, specificity, and biological implications. *Chembiochem*, *5*(2), 170-176.
- **Maughan, R.** (2009). Carbohydrate metabolism. *Surgery (Oxford)*, *27*(1), 6-10.
- **Meekins, D. A., Guo, H. F., Husodo, S., Paasch, B. C., Bridges, T. M., Santelia, D., ... & Gentry, M. S.** (2013). Structure of the Arabidopsis glucan phosphatase like sex four2 reveals a unique mechanism for starch dephosphorylation. *The Plant Cell*, *25*(6), 2302-2314.
- **Meekins, D. A., Vander Kooi, C. W., & Gentry, M. S.** (2016). Structural mechanisms of plant glucan phosphatases in starch metabolism. *The FEBS journal*, *283*(13), 2427-2447.
- **Meyer, K.** (1969). Biochemistry and biology of mucopolysaccharides. *The American journal of medicine*, *47*(5), 664-672.
- **Mikkelsen, R., Baunsgaard, L., & Blennow, A.** (2004). Functional characterization of alpha-glucan, water dikinase, the starch phosphorylating enzyme. *Biochemical Journal*, *377*(2), 525-532.

- **Mikkelsen, R., Mutenda, K. E., Mant, A., Schürmann, P., & Blennow, A.** (2005). α-Glucan, water dikinase (GWD): a plastidic enzyme with redox-regulated and coordinated catalytic activity and binding affinity. *Proceedings of the National Academy of Sciences*, *102*(5), 1785-1790.
- **Mohammadinejad, R., Karimi, S., Iravani, S., & Varma, R. S.** (2016). Plant-derived nanostructures: types and applications. *Green Chemistry*, *18*(1), 20-52.
- **Morell, M. K., Kosar-Hashemi, B., Cmiel, M., Samuel, M. S., Chandler, P., Rahman, S., ... & Li, Z.** (2003). Barley sex6 mutants lack starch synthase IIa activity and contain a starch with novel properties. *The Plant Journal*, *34*(2), 173-185.
- **Mori, H., Tanizawa, K., & Fukui, T.** (1993). Engineered plant phosphorylase showing extraordinarily high affinity for various α-glucan molecules. *Protein Science*, *2*(10), 1621-1629.
- **Muhrbeck, P., Svensson, E., & Eliasson, A. C.** (1991). Effect of the degree of phosphorylation on the crystallinity of native potato starch. *Starch-Stärke*, *43*(12), 466-468.
- **Naguleswaran, S., Li, J., Vasanthan, T., & Bressler, D.** (2011). Distribution of granule channels, protein, and phospholipid in triticale and corn starches as revealed by confocal laser scanning microscopy. *Cereal chemistry*, *88*(1), 87-94.
- **Nakamura, Y., Ono, M., Sawada, T., Crofts, N., Fujita, N., & Steup, M.** (2017). Characterization of the functional interactions of plastidial starch phosphorylase and starch branching enzymes from rice endosperm during reserve starch biosynthesis. *Plant Science*, *264*, 83-95.
- **Nakamura, Y. (Ed.).** (2015). *Starch: metabolism and structure*. Springer.
- **Nakamura, Y., Utsumi, Y., Sawada, T., Aihara, S., Utsumi, C., Yoshida, M., & Kitamura, S.** (2010). Characterization of the reactions of starch branching enzymes from rice endosperm. *Plant and cell physiology*, *51*(5), 776-794.
- **Nashilevitz, S., Melamed-Bessudo, C., Aharoni, A., Kossmann, J., Wolf, S., & Levy, A. A.** (2009). The legwd mutant uncovers the role of starch phosphorylation in pollen development and germination in tomato. *The Plant Journal*, *57*(1), 1-13.

- **Newgard, C. B., Hwang, P. K., & Fletterick, R. J.** (1989). The family of glycogen phosphorylases: structure and functio. *Critical reviews in biochemistry and molecular biology*, *24*(1), 69-99.
- **Nietzsche, M., Schießl, I., & Börnke, F.** (2014). The complex becomes more complex: protein-protein interactions of SnRK1 with DUF581 family proteins provide a framework for cell-and stimulus type-specific SnRK1 signaling in plants. *Frontiers in plant science*, *5*, 54.
- **Niittylä, T., Comparot-Moss, S., Lue, W. L., Messerli, G., Trevisan, M., Seymour, M. D., ... & Zeeman, S. C.** (2006). Similar protein phosphatases control starch metabolism in plants and glycogen metabolism in mammals. *Journal of Biological Chemistry*, *281*(17), 11815-11818.
- **Nishi, A., Nakamura, Y., Tanaka, N., & Satoh, H.** (2001). Biochemical and genetic analysis of the effects ofamylose-extender mutation in rice endosperm. *Plant physiology*, *127*(2), 459-472.
- **Nitschke, F., Wang, P., Schmieder, P., Girard, J. M., Awrey, D. E., Wang, T., ... & Kleinpeter, E.** (2013). Hyperphosphorylation of glucosyl C6 carbons and altered structure of glycogen in the neurodegenerative epilepsy Lafora disease. *Cell metabolism*, *17*(5), 756-767.
- **Okita, T. W., Nakata, P. A., Anderson, J. M., Sowokinos, J., Morell, M., & Preiss, J.** (1990). The subunit structure of potato tuber ADPglucose pyrophosphorylase. *Plant physiology*, *93*(2), 785-790.
- **Orzechowski, S.** (2008). Starch metabolism in leaves. *Acta biochimica polonica*, *55*(3), 435-445.
- **Panpetch, P., Field, R. A., & Limpaseni, T.** (2018). Heterologous co-expression in E. coli of isoamylase genes from cassava Manihot esculenta Crantz 'KU50'achieves enzyme-active heteromeric complex formation. *Plant molecular biology*, *96*(4-5), 417-427.
- **Patron, N. J., & Waller, R. F.** (2007). Transit peptide diversity and divergence: a global analysis of plastid targeting signals. *Bioessays*, *29*(10), 1048-1058.
- **Patterson, J. A., Tetlow, I. J., & Emes, M. J**. (2018). Bioinformatic and in vitro analyses of Arabidopsis starch synthase 2 reveal post-translational regulatory mechanisms. *Frontiers in Plant Science*, *9*, 1338.

- **Peltier, J. B., Cai, Y., Sun, Q., Zabrouskov, V., Giacomelli, L., Rudella, A., ... & van Wijk, K. J.** (2006). The oligomeric stromal proteome of Arabidopsis thaliana chloroplasts. *Molecular & Cellular Proteomics*, *5*(1), 114-133.
- **Peng, C., Wang, Y., Liu, F., Ren, Y., Zhou, K., Lv, J., ... & Jiang, L.** (2014). FLOURY ENDOSPERM 6 encodes a CBM 48 domain-containing protein involved in compound granule formation and starch synthesis in rice endosperm. *The Plant Journal*, *77*(6), 917-930.
- **Pérez, S., & Bertoft, E.** (2010). The molecular structures of starch components and their contribution to the architecture of starch granules: A comprehensive review. *Starch-Stärke*, *62*(8), 389-420.
- **Pfister, B., & Zeeman, S. C.** (2016). Formation of starch in plant cells. *Cellular and Molecular Life Sciences*, *73*(14), 2781-2807.
- **Porowska, H., Paszkiewicz-Gadek, A., Anchim, T., Wolczynski, S., & Gindzienski, A.** (2004). Inhibition of the O-glycan elongation limits MUC1 incorporation to cell membrane of human endometrial carcinoma cells. *International journal of molecular medicine*, *13*(3), 459-464.
- **Posocco, B., Dreussi, E., De Santa, J., Toffoli, G., Abrami, M., Musiani, F., ... & Dapas, B.** (2015). Polysaccharides for the delivery of antitumor drugs. *Materials*, *8*(5), 2569-2615.
- **Qu, J., Xu, S., Zhang, Z., Chen, G., Zhong, Y., Liu, L., ... & Guo, D.** (2018). Evolutionary, structural and expression analysis of core genes involved in starch synthesis. *Scientific reports*, *8*(1), 12736.
- **Reeck, G. R., De Haen, C., Teller, D. C., Doolittle, R. F., Fitch, W. M., Dickerson, R. E., ... & Zuckerkandl, E.** (1987). "Homology" in proteins and nucleic acids: a terminology muddle and a way out of it. *Cell*, *50*(5), 667.
- **Regina, A., Kosar-Hashemi, B., Ling, S., Li, Z., Rahman, S., & Morell, M.** (2010). Control of starch branching in barley defined through differential RNAi suppression of starch branching enzyme IIa and IIb. *Journal of experimental botany*, *61*(5), 1469-1482.
- **Reiter, W. D.** (2002). Biosynthesis and properties of the plant cell wall. *Current opinion in plant biology*, *5*(6), 536-542.

- **Ritte, G., Heydenreich, M., Mahlow, S., Haebel, S., Kötting, O., & Steup, M.** (2006). Phosphorylation of C6-and C3-positions of glucosyl residues in starch is catalysed by distinct dikinases. *FEBS letters*, *580*(20), 4872-4876.
- **Ritte, G., Lloyd, J. R., Eckermann, N., Rottmann, A., Kossmann, J., & Steup, M.** (2002). The starch-related R1 protein is an α-glucan, water dikinase. *Proceedings of the National Academy of Sciences*, *99*(10), 7166-7171.
- **Roach, P. J.** (2002). Glycogen and its metabolism. *Current molecular medicine*, *2*(2), 101-120.
- **Roach, P. J., Depaoli-Roach, A. A., Hurley, T. D., & Tagliabracci, V. S.** (2012). Glycogen and its metabolism: some new developments and old themes. *Biochemical Journal*, *441*(3), 763-787.
- **Robyt, J. F.** (2012). *Essentials of carbohydrate chemistry*. Springer Science & Business Media.
- **Roldán, I., Wattebled, F., Mercedes Lucas, M., Delvallé, D., Planchot, V., Jiménez, S., ... & Mérida, Á.** (2007). The phenotype of soluble starch synthase IV defective mutants of Arabidopsis thaliana suggests a novel function of elongation enzymes in the control of starch granule formation. *The Plant Journal*, *49*(3), 492-504.
- **Ruan, Y. L.** (2014). Sucrose metabolism: gateway to diverse carbon use and sugar signaling. *Annual review of plant biology*, *65*, 33-67.
- **Rydberg, U., Andersson, L., Andersson, R., Åman, P., & Larsson, H.** (2001). Comparison of starch branching enzyme I and II from potato. *European Journal of Biochemistry*, *268*(23), 6140-6145.
- **Samodien, E., Jewell, J., Loedolff, B., Oberlander, K., George, G. M., Zeeman, S. C., ... & Lloyd, J. R.** (2018). Repression of sex4 and like sex four2 orthologs in potato increases tuber starch bound phosphate with concomitant alterations in starch physical properties. *Frontiers in plant science*, *9*, 1044.
- **Santelia, D., Kötting, O., Seung, D., Schubert, M., Thalmann, M., Bischof, S., ... & Allain, F. H. T.** (2011). The phosphoglucan phosphatase like sex Four2 dephosphorylates starch at the C3-position in Arabidopsis. *The Plant Cell*, *23*(11), 4096-4111.
- **Satoh, H., Shibahara, K., Tokunaga, T., Nishi, A., Tasaki, M., Hwang, S. K., ... & Hosaka, Y.** (2008). Mutation of the plastidial α-glucan phosphorylase gene

in rice affects the synthesis and structure of starch in the endosperm. *The Plant Cell*, *20*(7), 1833-1849.

- **Sawada, T., Itoh, M., & Nakamura, Y.** (2018). Contributions of Three Starch Branching Enzyme Isozymes to the Fine Structure of Amylopectin in Rice Endosperm. *Frontiers in plant science*, *9*, 1536.
- **Senoura, T., Isono, N., Yoshikawa, M., Asao, A., Hamada, S., Watanabe, K., ... & Matsui, H.** (2004). Characterization of starch synthase I and II expressed in early developing seeds of kidney bean (Phaseolus vulgaris L.). *Bioscience, biotechnology, and biochemistry*, *68*(9), 1949-1960.
- **Seung, D., & Smith, A. M.** (2018). Starch granule initiation and morphogenesis—progress in Arabidopsis and cereals. *Journal of Experimental Botany*, *70*(3), 771-784.
- **Seung, D., Boudet, J., Monroe, J., Schreier, T. B., David, L. C., Abt, M., ... & Zeeman, S. C.** (2017). Homologs of PROTEIN TARGETING TO STARCH control starch granule initiation in Arabidopsis leaves. *The Plant Cell*, *29*(7), 1657-1677.
- **Seung, D., Schreier, T. B., Bürgy, L., Eicke, S., & Zeeman, S. C.** (2018). Two plastidial coiled-coil proteins are essential for normal starch granule initiation in Arabidopsis. *The Plant Cell*, *30*(7), 1523-1542.
- **Seung, D., Soyk, S., Coiro, M., Maier, B. A., Eicke, S., & Zeeman, S. C.** (2015). PROTEIN TARGETING TO STARCH is required for localising GRANULE-BOUND STARCH SYNTHASE to starch granules and for normal amylose synthesis in Arabidopsis. *PLoS biology*, *13*(2), e1002080.
- **Skryhan, K., Cuesta-Seijo, J. A., Nielsen, M. M., Marri, L., Mellor, S. B., Glaring, M. A., ... & Blennow, A.** (2015). The role of cysteine residues in redox regulation and protein stability of Arabidopsis thaliana starch synthase 1. *PloS one*, *10*(9), e0136997.
- **Skryhan, K., Gurrieri, L., Sparla, F., Trost, P., & Blennow, A.** (2018). Redox regulation of starch metabolism. *Frontiers in plant science*, *9*.
- **Smith, A. M., Denyer, K., & Martin, C.** (1997). The synthesis of the starch granule. *Annual review of plant biology*, *48*(1), 67-87.
- **Smith, A. M., Zeeman, S. C., & Smith, S. M.** (2005). Starch degradation. *Annu. Rev. Plant Biol.*, *56*, 73-98.

- **Smith, S. M., Fulton, D. C., Chia, T., Thorneycroft, D., Chapple, A., Dunstan, H., ... & Smith, A. M.** (2004). Diurnal changes in the transcriptome encoding enzymes of starch metabolism provide evidence for both transcriptional and posttranscriptional regulation of starch metabolism in Arabidopsis leaves. *Plant physiology*, *136*(1), 2687-2699.
- **Smith, A. M., & Zeeman, S. C.** (2020). Starch: A Flexible, Adaptable Carbon Store Coupled to Plant Growth. *Annual Review of Plant Biology*, *71*.
- **Smythe, C., & Cohen, P.** (1991). The discovery of glycogenin and the priming mechanism for glycogen biogenesis. In *EJB Reviews 1991* (pp. 149-155). Springer, Berlin, Heidelberg.
- **Sokolov, L. N., Dominguez-Solis, J. R., Allary, A. L., Buchanan, B. B., & Luan, S.** (2006). A redox-regulated chloroplast protein phosphatase binds to starch diurnally and functions in its accumulation. *Proceedings of the National Academy of Sciences*, *103*(25), 9732-9737.
- **Solfanelli, C., Poggi, A., Loreti, E., Alpi, A., & Perata, P.** (2006). Sucrose-specific induction of the anthocyanin biosynthetic pathway in Arabidopsis. *Plant physiology*, *140*(2), 637-646.
- **Soll, J., & Schleiff, E.** (2004). Protein import into chloroplasts. *Nature Reviews Molecular Cell Biology*, *5*(3), 198-208.
- **Stam, M. R., Danchin, E. G., Rancurel, C., Coutinho, P. M., & Henrissat, B.** (2006). Dividing the large glycoside hydrolase family 13 into subfamilies: towards improved functional annotations of α-amylase-related proteins. *Protein Engineering, Design and Selection*, *19*(12), 555-562.
- **Stanley, D., Fitzgerald, A. M., Farnden, K. J., & MacRae, E. A.** (2002). Characterisation of putative alpha-amylases from apple (Malus domestica) and Arabidopsis thaliana. *BIOLOGIA-BRATISLAVA-*, *57*(SUP/2), 137-148.
- **Steup, M., & Schächtele, C.** (1981). Mode of glucan degradation by purified phosphorylase forms from spinach leaves. *Planta*, *153*(4), 351-361.
- **Stitt, M., & Zeeman, S. C.** (2012). Starch turnover: pathways, regulation and role in growth. *Current opinion in plant biology*, *15*(3), 282-292.
- **Streb, S., & Zeeman, S. C.** (2012). Starch metabolism in Arabidopsis. *The Arabidopsis book/American Society of Plant Biologists*, *10*.

- **Streb, S., Delatte, T., Umhang, M., Eicke, S., Schorderet, M., Reinhardt, D., & Zeeman, S. C.** (2008). Starch granule biosynthesis in Arabidopsis is abolished by removal of all debranching enzymes but restored by the subsequent removal of an endoamylase. *The Plant Cell*, *20*(12), 3448-3466.
- **Sun, C., Sathish, P., Ahlandsberg, S., & Jansson, C.** (1998). The two genes encoding starch-branching enzymes IIa and IIb are differentially expressed in barley. *Plant Physiology*, *118*(1), 37-49.
- **Szydlowski, N., Ragel, P., Hennen-Bierwagen, T. A., Planchot, V., Myers, A. M., Mérida, A., ... & Wattebled, F.** (2011). Integrated functions among multiple starch synthases determine both amylopectin chain length and branch linkage location in Arabidopsis leaf starch. *Journal of experimental botany*, *62*(13), 4547-4559.
- **Szydlowski, N., Ragel, P., Raynaud, S., Lucas, M. M., Roldán, I., Montero, M., ... & Pozueta-Romero, J.** (2009). Starch granule initiation in Arabidopsis requires the presence of either class IV or class III starch synthases. *The Plant Cell*, *21*(8), 2443-2457.
- **Takaha, T., Yanase, M., Okada, S., & Smith, S. M.** (1993). Disproportionating enzyme (4-alpha-glucanotransferase; EC 2.4. 1.25) of potato. Purification, molecular cloning, and potential role in starch metabolism. *Journal of Biological Chemistry*, *268*(2), 1391-1396.
- **Takeda, Y., & Preiss, J.** (1993). Structures of B90 (sugary) and W64A (normal) maize starches. *Carbohydrate Research*, *240*, 265-275.
- **Tatusov, R. L., Koonin, E. V., & Lipman, D. J.** (1997). A genomic perspective on protein families. *Science*, *278*(5338), 631-637.
- **Tester, R. F., Karkalas, J., & Qi, X.** (2004). Starch—composition, fine structure and architecture. *Journal of cereal science*, *39*(2), 151-165.
- **Tetlow, I.** (2018). Starch Biosynthesis in Crop Plants.
- **Tetlow, I. J., Beisel, K. G., Cameron, S., Makhmoudova, A., Liu, F., Bresolin, N. S., ... & Emes, M. J.** (2008). Analysis of protein complexes in wheat amyloplasts reveals functional interactions among starch biosynthetic enzymes. *Plant physiology*, *146*(4), 1878-1891.

- **Tetlow, I. J., Morell, M. K., & Emes, M. J.** (2004). Recent developments in understanding the regulation of starch metabolism in higher plants. *Journal of experimental botany*, *55*(406), 2131-2145.
- **Tognetti, R., Cocozza, C., & Marchetti, M.** (2013). Shaping the multifunctional tree: the use of Salicaceae in environmental restoration. *iForest-Biogeosciences and Forestry*, *6*(1), 37.
- **Ubiparip, Z., Beerens, K., Franceus, J., Vercauteren, R., & Desmet, T.** (2018). Thermostable alpha-glucan phosphorylases: characteristics and industrial applications. *Applied microbiology and biotechnology*, *102*(19), 8187-8202.
- **Umemoto, T., & Terashima, K.** (2002). Research note: Activity of granule-bound starch synthase is an important determinant of amylose content in rice endosperm. *Functional Plant Biology*, *29*(9), 1121-1124.
- **Van Der Maarel, M. J., Van der Veen, B., Uitdehaag, J. C., Leemhuis, H., & Dijkhuizen, L.** (2002). Properties and applications of starch-converting enzymes of the α-amylase family. *Journal of biotechnology*, *94*(2), 137-155.
- **Vandromme, C., Spriet, C., Dauvillée, D., Courseaux, A., Putaux, J. L., Wychowski, A., ... & Wattebled, F.** (2019). PII1: a protein involved in starch initiation that determines granule number and size in Arabidopsis chloroplast. *New Phytologist*, *221*(1), 356-370.
- **Verbančič, J., Lunn, J. E., Stitt, M., & Persson, S.** (2018). Carbon supply and the regulation of cell wall synthesis. *Molecular plant*, *11*(1), 75-94.
- **Voragen, A. G., Coenen, G. J., Verhoef, R. P., & Schols, H. A.** (2009). Pectin, a versatile polysaccharide present in plant cell walls. *Structural Chemistry*, *20*(2), 263.
- **Vrinten, P. L., & Nakamura, T.** (2000). Wheat granule-bound starch synthase I and II are encoded by separate genes that are expressed in different tissues. *Plant physiology*, *122*(1), 255-264.
- **Wang, X. L., Zeng, J., Yang, Y., Xiong, Y., Zhang, Z. H., Qiu, M., ... & Wang, J. Z.** (2015). Helicobacter pylori filtrate induces Alzheimer-like tau hyperphosphorylation by activating glycogen synthase kinase-3β. *Journal of Alzheimer's Disease*, *43*(1), 153-165.
- **Wattebled, F., Dong, Y., Dumez, S., Delvallé, D., Planchot, V., Berbezy, P., ... & D'Hulst, C.** (2005). Mutants of Arabidopsis lacking a chloroplastic

isoamylase accumulate phytoglycogen and an abnormal form of amylopectin. *Plant Physiology*, *138*(1), 184-195.

- **White-Gloria, C., Johnson, J. J., Marrit, K., Kataya, A., Vahab, A., & Moorhead, G.** (2018). Protein kinases and phosphatases of the plastid and their potential role in starch metabolism. *Frontiers in plant science*, *9*, 1032.
- **Williamson, M. P., Le Gal-Coëffet, M. F., Sorimachi, K., Furniss, C. S., Archer, D. B., & Williamson, G.** (1997). Function of conserved tryptophans in the Aspergillus niger glucoamylase 1 starch binding domain. *Biochemistry*, *36*(24), 7535-7539.
- **Wilson, W. A., Roach, P. J., Montero, M., Baroja-Fernández, E., Muñoz, F. J., Eydallin, G., ... & Pozueta-Romero, J.** (2010). Regulation of glycogen metabolism in yeast and bacteria. *FEMS microbiology reviews*, *34*(6), 952-985.
- **Xiao, L., van De Worp, W. R., Stassen, R., Van Maastrigt, C., Kettelarij, N., Stahl, B., ... & van't Land, B.** (2019). Human milk oligosaccharides promote immune tolerance via direct interactions with human dendritic cells. *European journal of immunology*.
- **Yoneya, T., Ishibashi, K., Hironaka, K., & Yamamoto, K.** (2003). Influence of cross-linked potato starch treated with POCl3 on DSC, rheological properties and granule size. *Carbohydrate Polymers*, *53*(4), 447-457.
- **Young, G. H., Chen, H. M., Lin, C. T., Tseng, K. C., Wu, J. S., & Juang, R. H.** (2006). Site-specific phosphorylation of L-form starch phosphorylase by the protein kinase activity from sweet potato roots. *Planta*, *223*(3), 468-478.
- **Yu, T. S., Kofler, H., Häusler, R. E., Hille, D., Flügge, U. I., Zeeman, S. C., ... & Steup, M.** (2001). The Arabidopsis sex1 mutant is defective in the R1 protein, a general regulator of starch degradation in plants, and not in the chloroplast hexose transporter. *The Plant Cell*, *13*(8), 1907-1918.
- **Yu, T. S., Lue, W. L., Wang, S. M., & Chen, J.** (2000). Mutation of Arabidopsis plastid phosphoglucose isomerase affects leaf starch synthesis and floral initiation. *Plant Physiology*, *123*(1), 319-326.
- **Yu, T. S., Zeeman, S. C., Thorneycroft, D., Fulton, D. C., Dunstan, H., Lue, W. L., ... & Tsai, D. L.** (2005). α-Amylase is not required for breakdown of transitory starch in Arabidopsis leaves. *Journal of Biological Chemistry*, *280*(11), 9773-9779.

- **Yu, Y., Mu, H. H., Wasserman, B. P., & Carman, G. M.** (2001). Identification of the maize amyloplast stromal 112-kD protein as a plastidic starch phosphorylase. *Plant Physiology*, *125*(1), 351-359.
- **Zeeman, S. C., Delatte, T., Messerli, G., Umhang, M., Stettler, M., Mettler, T., ... & Kötting, O.** (2007). Starch breakdown: recent discoveries suggest distinct pathways and novel mechanisms. *Functional plant biology*, *34*(6), 465-473.
- **Zeeman, S. C., Kossmann, J., & Smith, A. M.** (2010). Starch: its metabolism, evolution, and biotechnological modification in plants. *Annual review of plant biology*, *61*, 209-234.
- **Zeeman, S. C., Tiessen, A., Pilling, E., Kato, K. L., Donald, A. M., & Smith, A. M.** (2002). Starch synthesis in Arabidopsis. Granule synthesis, composition, and structure. *Plant Physiology*, *129*(2), 516-529.
- **Zeqiraj, E., Tang, X., Hunter, R. W., García-Rocha, M., Judd, A., Deak, M., ... & Sakamoto, K.** (2014). Structural basis for the recruitment of glycogen synthase by glycogenin. *Proceedings of the National Academy of Sciences*, *111*(28), E2831-E2840.
- **Zhang, P., Whistler, R. L., BeMiller, J. N., & Hamaker, B. R.** (2005). Banana starch: production, physicochemical properties, and digestibility—a review. *Carbohydrate polymers*, *59*(4), 443-458.
- **Zhang, X., Colleoni, C., Ratushna, V., Sirghie-Colleoni, M., James, M., & Myers, A.** (2004). Molecular characterization demonstrates that the Zea mays gene sugary2 codes for the starch synthase isoform SSIIa. *Plant molecular biology*, *54*(6), 865-879.
- **Zhang, X., Szydlowski, N., Delvallé, D., D'Hulst, C., James, M. G., & Myers, A. M.** (2008). Overlapping functions of the starch synthases SSII and SSIII in amylopectin biosynthesis in Arabidopsis. *BMC plant biology*, *8*(1), 96.

Further research performed during the PhD study

Acta Physiologiae Plantarum (2019) 41:190
https://doi.org/10.1007/s11738-019-2983-x

ORIGINAL ARTICLE

Do carbohydrate metabolism and partitioning contribute to the higher salt tolerance of *Hordeum marinum* compared to *Hordeum vulgare*?

Wided Medini[1] · Nèjia Farhat[1] · Shadha Al-Rawi[2] · Harendra Mahto[2] · Hadeel Qasim[2] · Emna Ben-Halima[1] · Mouna Bessrour[1] · Farhat Chibani[1] · Chedly Abdelly[1] · Joerg Fettke[2] · Mokded Rabhi[1,3]

Received: 18 November 2018 / Revised: 31 July 2019 / Accepted: 14 November 2019 / Published online: 16 November 2019

Abstract

The aim of the present work was to check whether carbohydrate metabolism and partitioning contribute to the higher salt tolerance of the facultative halophyte *Hordeum marinum* compared to the glycophyte *Hordeum vulgare*. Seedlings with the same size from the two species were hydroponically grown at 0 (control), 150, and 300 mM NaCl for 3 weeks. *H. marinum* maintained higher relative growth rate, which was concomitant with a higher aptitude to maintain better shoot tissue hydration and membrane integrity under saline conditions compared to *H. vulgare*. Gas exchanges were reduced in the two species under saline conditions, but an increase in their water use efficiency was recorded. *H. marinum* exhibited an increase in leaf soluble sugar concentrations under saline conditions together with an enhancement in the transglucosidase DPE2 (EC 2.4.1.25) activity at 300 mM NaCl. However, *H. vulgare* showed a high increase in starch phosphorylase (EC 2.4.1.1) activity under saline conditions together with a decrease in leaf glucose and starch concentrations at 300 mM NaCl. In roots, both species accumulated glucose and fructose at 150 mM NaCl, but *H. marinum* exhibited a marked decrease in soluble sugar concentrations and an increase in starch concentration at 300 mM NaCl. Our data constitute an initiation to the involvement of carbohydrate metabolism and partitioning in salt responses of barley species and further work is necessary to elucidate how their flexibility confers higher tolerance to *H. marinum* compared to *H. vulgare*.

Keywords Cultivated barley · DPE2 · Flexibility · Pho1 · Pho2 · Sea barley

Abbreviations

A	Net CO_2 assimilation
C	Control
E	Transpiration rate
EC	Electrical conductivity
EDTA	Ethylenediaminetetraacetic acid
EL	Electrolyte leakage
g_s	Stomatal conductance
NAD^+	Oxidized form of nicotinamide adenine dinucleotide
PGI	Phosphoglucose isomerase
Pho1	Plastidial phosphorylase isoform
Pho2	Cytosolic phosphorylase isoform
PPFD	Photosynthetic photon flux density
RGR	Relative growth rate
ROS	Reactive oxygen species
S1	150 mM NaCl
S2	300 mM NaCl
WUE	Water use efficiency

Communicated by G. Montanaro.

✉ Mokded Rabhi
mokded.rabhi@gmail.com

[1] Laboratory of Extremophile Plants, Centre of Biotechnology of Borj Cedria (CBBC), P. O. Box 901, 2050 Hammam-Lif, Tunisia

[2] Biopolymer Analytics, University of Potsdam, Potsdam-Golm, Germany

[3] Department of Plant Production and Protection, College of Agriculture and Veterinary Medicine, Qassim University, Buraydah, PO Box 6622, Qassim 51452, Saudi Arabia

Introduction

Salinity is an increasing problem that have been shown to decrease plant growth and crop yields and affect agricultural soil properties (Shahbaz et al. 2012). High salt concentrations (especially toxic ions such as Na^+ and Cl^-) exert

various negative effects on plants, in particular oxidative and osmotic stresses, as well as ionic imbalances (Cardi et al. 2015). The 'osmotic effects' of salinity as referred to by Munns and Tester (2008) appear as early effects resulting from a salt-induced decrease in soil water potential around the root system, reducing, in this way, the plant's ability to take up water, which can lead to cell dehydration (Islam et al. 2007). Salt-induced osmotic effects reduce transpiration rate through stomatal closure, which may affect CO_2 fixation (Maggio et al. 2007; Chaves et al. 2009). The 'ionic effects' of salinity occur after relatively long-term exposure to salt (competitive ion uptake and transport within the plant) following intracellular accumulation of toxic ions of Na^+ and Cl^- within shoot tissues (Munns and Tester 2008; Harris et al. 2010). These effects disturb metabolic processes, photosynthetic efficiency, and plant growth and yield (Jusovic et al. 2018). The degree of damage depends among others on salinity level, exposure duration, and plant species (Munns and Tester 2008; Rozema and Flowers 2008). A variety of physiological and biochemical mechanisms has been evolved by plants to cope with salinity, including but not limited to (i) ion homeostasis (the regulatory mechanisms of ion uptake, transport, accumulation, and compartmentalization), (ii) osmotic adjustment (use of Na^+ and Cl^- in osmotic adjustment and biosynthesis of osmoprotectants and compatible solutes), (iii) reactive oxygen species (ROS) homeostasis (enzymatic and non-enzymatic antioxidant systems), and (iv) stress signaling (phytohormones and signaling molecules) (Gupta and Huang 2014). According to their degree of salinity tolerance, plants were divided into halophytes and glycophytes. Nevertheless, up to now, no clear definition was retained for halophytes (Munns and Tester 2008; Cheeseman 2015).

During the last decades, sea barley (*Hordeum marinum* Huds. or *Hordeum maritimum* With.) has attracted more and more attention as a promising plant at both fundamental and applied levels. This wild barley species was described as an annual facultative halophyte (Hafsi et al. 2007, 2010, 2011a, b; Lakhdar et al. 2008; Yousfi et al. 2010; Alamri et al. 2013; Chalbi et al. 2013; Ferchichi et al. 2018) and its responses to salinity was compared to those of its glycophytic relative *Hordeum vulgare* L. (cultivated barley) in several works (Garthwaite et al. 2005; Yousfi et al. 2010; Chalbi et al. 2013; Ferchichi et al. 2018). Garthwaite et al. (2005) compared the responses to increasing salinity for 16–21 days of eight wild barley species, including sea barley, to cultivated barley. They found that the majority of them showed a higher capacity to 'exclude' Na^+ and Cl^- from their shoots and to maintain higher leaf K^+ than *H. vulgare*. The authors considered the most studied wild barley species more salt-tolerant than cultivated barley and retained the restriction of Na^+ and Cl^- entry to shoots as a criterion of salt tolerance in these species. The subjection of sea barley and cultivated barley to 0, 100, 200, and 300 mM NaCl for 60 h (osmotic shock) confirmed these statements and showed that *H. vulgare* adopted an energy-consuming strategy to combat salt osmotic effect using K^+ and organic metabolites for osmotic adjustment, while *H. marinum* exhibited efficient metabolite management and metabolic nutrient regulation. Sea barley relied on Na^+ for osmotic adjustment at moderate salinity, keeping in this way K^+ and organic metabolites for metabolic purposes and used them only at high salinity (Yousfi et al. 2010). Islam et al. (2007) succeeded to transfer some salt-adaptive mechanisms from *H. marinum* to *H. marinum–Triticum aestivum* amphiploid. Chalbi et al. (2013) stated that sea barley maintained a less affected photosynthetic activity under long-term salinity compared to cultivated barley. They demonstrated also that despite the increase in the unsaturated-to-saturated fatty acid ratio and the double bond index observed in salt-treated *H. vulgare* plants, they showed more affected membrane integrity compared to *H. marinum* plants. Recently, Ferchichi et al. (2018) demonstrated in a metabolomic study that *H. marinum* experienced sequential metabolite and ion accumulation that allowed it a 2–3 week delay in showing stress damage symptoms in comparison with *H. vulgare*.

Triose phosphates produced during carbon fixation are either stored as starch within the chloroplast or transported to the cytosol, where they contribute to sucrose synthesis (Hartman et al. 2017). Contrarily to starch synthesized in cells of storage organs (storage starch that can be stored over seasons and even over years), transitory starch in photosynthetic cells is synthesized and degraded within 1 day–night rhythm (Lu et al. 2005). The function of starch depends on the cell type from which it is derived, as well as on environmental conditions (Thalmann and Santelia 2017). Starch is also considered as a key molecule involved in the responses of plants to abiotic stresses; its remobilization constitutes a source of energy and carbon under potentially limited photosynthesis conditions. In addition, the released soluble sugars were reported to support plant growth and play a key role in osmotic adjustment, as well as in stress signaling (Van den Ende and El-Esawe 2014; Thalmann and Santelia 2017). Several enzymes are involved in starch metabolism, including starch phosphorylase (EC 2.4.1.1)—with its plastidial (Pho1) and cytosolic (Pho2) isoforms—that transfers glucosyl units from glucose-1-phosphate (G-1-P) to glycans containing α-1–4 linked glucan chains (Fettke et al. 2005a, b, 2012) and the transglucosidase DPE2 (EC 2.4.1.25) that transfers glucosyl residues from maltose to a polysaccharide with the release of glucose (Chia et al. 2004; Fettke et al. 2006). Thus, Pho2 and DPE2 are related to the degradation of starch and formation of sucrose in the cytosol, the transport metabolite of most plants. Furthermore, DPE2 also contributes to the release of glucose.

For the plastidial phosphorylase, it has been reported that it contributes to starch metabolism under specific stress conditions such as cold (Orawetz et al. 2016).

Although carbohydrate concentrations were determined in mature leaves of *H. marinum* and *H. vulgare* under saline and non-saline conditions and their relative contribution to osmotic adjustment was estimated (Yousfi et al. 2010; Ferchichi et al. 2018), more importance should be given to their contribution to salt tolerance. This was the aim of the present study, in which we tried to find relationships between carbohydrate metabolism/partitioning and tolerance to moderate and high salinities in a comparative study between *H. marinum* and *H. vulgare*.

Materials and methods

Plant materials and growth conditions

Hordeum marinum seeds were collected in the Sebkha of Soliman (30 km south of Tunis, semi-arid area) and *H. vulgare* (var. Manel) seeds were provided by the National Institute of Agronomic Research of Tunis (INRAT). Seeds of both barley species were disinfected with calcium hypochlorite (2%) and germinated in petri dishes on filter paper moistened with distilled water. To obtain seedlings with the same size in the beginning of treatments, *H. marinum* germination was started 14 days before that of *H. vulgare*. Obtained seedlings were transferred in dark plastic containers filled with a continuously aerated Hewitt's (1966) nutrient solution that was renewed twice a week. This pretreatment period took 40 days and seedlings received quarter strength, then half strength and finally complete nutrient medium. After 40 days for *H. vulgare* and 54 days for *H. marinum*, salt treatments were applied by adding NaCl to final concentrations of 0 mM (C: control), 150 mM (S1), and 300 mM (S2). Both pretreatment and treatment were conducted in a growth chamber with a light/dark temperature regime of 25/20 °C, a relative humidity of 60–80%, a light intensity of approximately 250 µmol photons m^{-2} s^{-1}, and a photoperiod of 12 h. After 21 days of treatment, gas exchange parameters were measured then plants were harvested.

Growth and water content determination

Plants used for growth and water content analyses were cut into shoots and roots, weighed fresh, then oven-dried for 3 days at 70 °C, and weighed dry. Growth was measured as relative growth rate (RGR) as described by Rabhi et al. (2010).

Gas exchange measurements

Gas exchange parameters were measured in both species exposed to 0, 150, and 300 mM NaCl for 21 days of treatment, using a portable Licor gas analyzer (LC pro^+, ADC Bio Scientific Ltd.). Measurements were taken in a greenhouse from the mid-lamina portion of fully expanded attached leaves. The measurements were carried out between 10.00 am and 1.00 pm at the following cuvette conditions: 800 µmol PPFD m^{-2} s^{-1}, 30 °C leaf temperature, 0.35 mbar ambient CO_2 partial pressure, and 26 mbar cuvette H_2O partial pressure. Measured parameters were net CO_2 assimilation (A), stomatal conductance (g_s), transpiration rate (E), and water use efficiency (WUE). The latter was calculated as A/E ratio.

Electrolyte leakage measurements

Electrolyte leakage (EL) was determined in fresh discs of fully expanded leaves through electrical conductivity (EC) measurements according to Dionisio-Sese and Tobita (1998). The leaf discs were immediately put into tubes containing 10 mL MilliQ water each. Their incubation for 2 h in a water bath at 32 °C allowed the determination of the initial electrical conductivity of the solution (EC1) by a Metrohm 712 conductivity meter. After incubation at 121 °C for 20 min and cooling to 25 °C, the final value (EC2) was determined. EL was then calculated as follows:

$$\mathrm{EL}\,(\%) = \mathrm{EC1} \times 100/\,\mathrm{EC2}.$$

Sample preparation for starch and soluble sugar assays

At the harvest, samples from roots and fully expanded leaves were collected at the end of the light period (after 10–11 h of illumination) and frozen in liquid nitrogen then stored at − 80 °C until use. Soluble sugars were extracted in ethanol [80% (v/v)], then resuspended in double distilled water according to a modified method of Caporn et al. (1999). To an aliquot of 40–50 mg frozen material, an ethanol [80% (v/v)] volume of 0.85 mL was added and the mixture was incubated at 80 °C under continuous agitation for 15 min. After centrifugation at 20,000*g* for 10 min, the supernatant was collected. A second extraction was performed in the same way and the two supernatants were combined in a single ethanol extract. The latter was immediately evaporated in speed vacuum and the obtained pellet was resuspended in 200 µL double distilled water for 10 min at 30 °C, then centrifuged for 10 min at 20,000*g*. The concentrations of glucose, sucrose, and fructose were spectrophotometrically

determined in the supernatant through measurements of NAD^+ reduction in the presence of specific enzymes at 340 nm. Four replicates from four different plants were used for each sugar assay. The pellet was used for starch assays.

Soluble sugar assays

A modified method of Caporn et al. (1999) was used for all soluble sugar assays. The assay buffer used to determine glucose concentrations was reconstituted from a reagent kit and contained: 200 mM imidazole/HCl (pH 6.9), 3 mM $MgCl_2$, 5 mM NADP, 11 mM ATP, 0.5 unit mL^{-1} hexokinase, and 25 µL glucose-6-phosphate dehydrogenase suspension (Roche). A volume of glucose assay reagent was added to 5–20 µL sample to a final volume of 600 µL. Then, mixtures were agitated and incubated at room temperature for 15 min. Thereafter, absorbance was read at 340 nm versus deionized water.

For fructose assay, 2 units phosphoglucose isomerase (PGI) was added to the tube previously used for glucose determination. After incubation at room temperature for 15 min, absorbance was measured at 340 nm.

As for the determination of sucrose concentration, a suspension of 100 units invertase was added to the tube previously used for fructose assay. Absorbance was then read at 340 nm after incubation at room temperature for 10 min.

Starch assays

Starch pellet was washed with 1 mL cold double distilled water, centrifuged for 10 min at 20,000*g,* and shortly dried in speed vacuum. Thereafter, it was solubilized for 1 h in 0.5 mL KOH (0.2 M) at 95 °C. A subsequent neutralization was then performed by the addition of 88 µL acetic acid (1 M). After centrifugation for 10 min at 20,000*g*, an aliquot of 50 µL supernatant was mixed with 50 µL starch assay reagent containing 5 units amyloglucosidase, then incubated overnight at 55 °C. Subsequently, the starch content was determined using the hexokinase/glucose-6-phosphate dehydrogenase assay with an incubation of 15 min at room temperature. The absorbance was then measured at 340 nm (Stitt et al. 1989).

Sample preparation for enzyme assays

Frozen samples of roots and fully expanded leaves were homogenated in extraction buffer containing 100 mM Hepes–NaOH (pH 7.5), 1 mM EDTA, 2 mM dithiothreitol, 0.5 mM phenylmethylsulfonyl fluoride, 10% (v/v) glycerol, 0.1% (*w*/*v*) Natriumsulfit, and 0.075% (*w*/*v*) Natriumdisulfit. Homogenates (or crude extracts) were then centrifuged for 12 min at 20,000*g* at 4 °C and the supernatants that are designated as crude extracts were collected. The concentrations of soluble proteins were determined using the microversion of Bio-Rad protein assay (Bio-Rad, Munich, Germany) and bovine serum albumin as standard.

Zymograms

Zymograms were performed according to Fettke et al. (2005b). Crude extracts were run on native PAGE gels. Thereafter, gels were incubated overnight at 37 °C in 100 mM citrate–NaOH (pH 6.5) containing 20 mM substrate. In the case of phosphorylases (Pho1 and Pho2), the substrate was glucose-1-phosphate (Sigma-Aldrich, Munich, Germany) and in the case of transglucosidase (DPE2), the substrate was maltose (Roth, Karlsruhe, Germany). Finally, gels were subjected to iodine staining.

Statistical analysis

Data were subjected to an ANOVA test using SPSS 16.0 software and means were compared according to Duncan's test at 5% level of significance. Gas exchange data were presented as Log2(treated/control) and untransformed means were compared to the control using Student's *t* test at 5% level of significance.

Results

Growth and water content

Under control conditions, *H. marinum* plants showed RGR values of 0.143 and 0.132 day^{-1}, respectively in shoots and roots (Table 1). Both salinity levels decreased shoot RGR in this species by 16–19% and root RGR by 22–29%. As regards *H. vulgare*, shoot and root RGR values under control conditions were, respectively, 0.122 and 0.094 day^{-1}. They decreased with the increasing salinity, keping root/shoot ratio statistically unchanged. The comparison of salt effects on the two barley species on the basis of whole plant RGR showed that S1 treatment reduced RGR of cultivated barley (ca. − 41%) more than did S1 and S2 in sea barley (− 21 and − 17%, respectively). Shoot water content exhibited the same trend as biomass in each species, whereas root water content was maintained constant regardless of the treatment in both of them (Table 1).

Membrane integrity

Membrane integrity was estimated through electrolyte leakage (EL) measurements; an increase in EL means a loss of membrane integrity. In *H. marinum*, EL increased from 6% in the control to about 10% in S1 and S2 treatments (Fig. 1a). In *H. vulgare*, recorded EL values were noticeably higher:

Table 1 Growth and tissue hydration parameters in *H. marinum* and *H. vulgare* plants hydroponically grown for 3 weeks at 0 (C), 150 (S1), and 300 (S2) mM NaCl. Values are means of six replicates ± SE

	C	S1	S2
H. marinum			
Shoot RGR	0.143 ± 0.007a	0.116 ± 0.004b	0.120 ± 0.003b
Shoot WC	4.99 ± 0.18a	3.58 ± 0.09b	3.65 ± 0.05b
Root RGR	0.132 ± 0.004a	0.094 ± 0.002b	0.103 ± 0.003b
Root WC	10.61 ± 1.37a	12.04 ± 0.42a	10.95 ± 0.70a
Whole plant RGR	0.141 ± 0.006a	0.111 ± 0.004b	0.116 ± 0.003b
Root/shoot ratio	0.23 ± 0.01a	0.19 ± 0.01b	0.20 ± 0.01b
H. vulgare			
Shoot RGR	0.122 ± 0.003a	0.074 ± 0.004b	0.041 ± 0.007c
Shoot WC	6.10 ± 0.30a	4.25 ± 0.16b	2.53 ± 0.22c
Root RGR	0.094 ± 0.003a	0.049 ± 0.004b	0.023 ± 0.004c
Root WC	11.87 ± 0.37a	11.48 ± 0.49ab	10.55 ± 0.28b
Whole plant RGR	0.116 ± 0.003a	0.069 ± 0.004b	0.038 ± 0.006c
Root/shoot ratio	0.18 ± 0.01a	0.19 ± 0.01a	0.20 ± 0.02a

RGR relative growth rate (day^{-1}), *WC* water content (mL H_2O g^{-1} DW)

Values of the same row followed by at least one same letter are not significantly different according to Duncan's test at $P \leq 0.05$

they increased from 18% in the control to 39 and 70% in S1 and S2 treatments, respectively (Fig. 1b).

Gas exchange parameters

Net CO_2 assimilation (A), stomatal conductance (g_s), and transpiration rate (E) were significantly reduced by salt treatments in the two studied species (Fig. 2a, b). To mitigate this decrease in photosynthetic activity induced by salinity stress, both species increased their water use efficiency (WUE). Nevertheless, in sea barley, this adaptive response was observed only in S2 treatment.

Starch and soluble sugar concentrations

Figure 3 illustrates sugar concentrations in leaves of the two barley species in C, S1, and S2 treatments. Leaf glucose concentration was maintained unchanged in S1 treatment in both species, but it increased in S2 treatment in *H. marinum* by 64.4% and decreased in *H. vulgare* by 44.9%, in comparison with their controls (Fig. 3a, b). Leaf fructose concentration was maintained constant except in S1-treated plants of sea barley, in which it increased by 54.2% (Fig. 3c, d). The sharpest variation in leaf sugar concentrations was recorded in sucrose in *H. marinum* plants of S2 treatment (ca. + 179.8%) (Fig. 3e). Apart from this peak, no other significant change was observed in sucrose concentration in both species. As regards leaf starch concentration, it decreased only in cultivated barley in S2 treatment (Fig. 3h).

Figure 4 shows sugar concentrations in roots of *H. marinum* and *H. vulgare* in C, S1, and S2 treatments. The two studied species exhibited high root glucose and fructose peaks in S1 treatment (Fig. 4a–d). In S2 treatment, root concentrations of these two soluble sugars were either maintained at the level of the control (case of *H. vulgare*) or markedly decreased (case of *H. marinum*). Root sucrose concentration of sea barley decreased by 30.3% in S1 treatment and by 93.3% in S2 treatment (Fig. 4e). In cultivated barley, root sucrose concentration showed no significant variation (Fig. 4f). As regards root starch concentration, it was doubled in S2-treated plants of *H. marinum* (Fig. 4g), while no other variation was observed in both species.

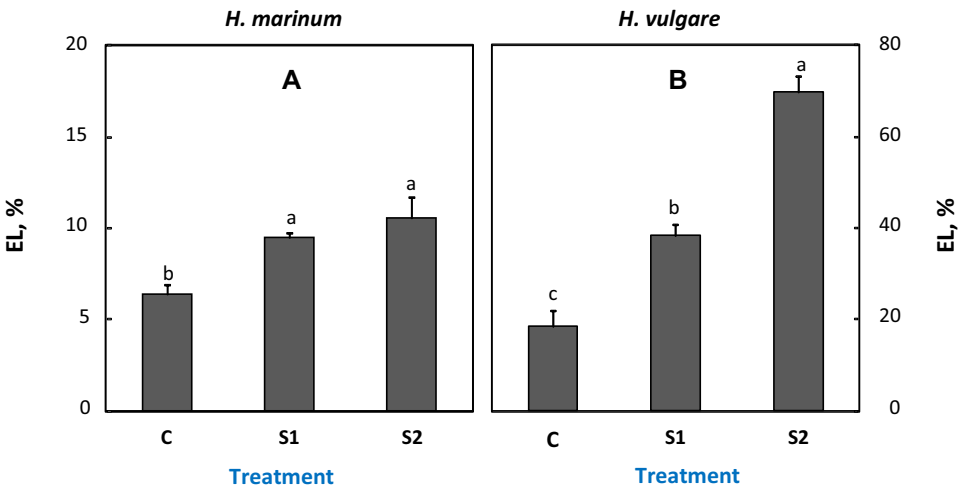

Fig. 1 Electrolyte leakage (EL) in *H. marinum* and *H. vulgare* plants hydroponically grown for 3 weeks at 0 (C), 150 (S1), and 300 mM NaCl (S2). Bars are means of six replicates ± SE. Bars labeled with at least one same letter are not significantly different according to Duncan's test at $P \leq 0.05$

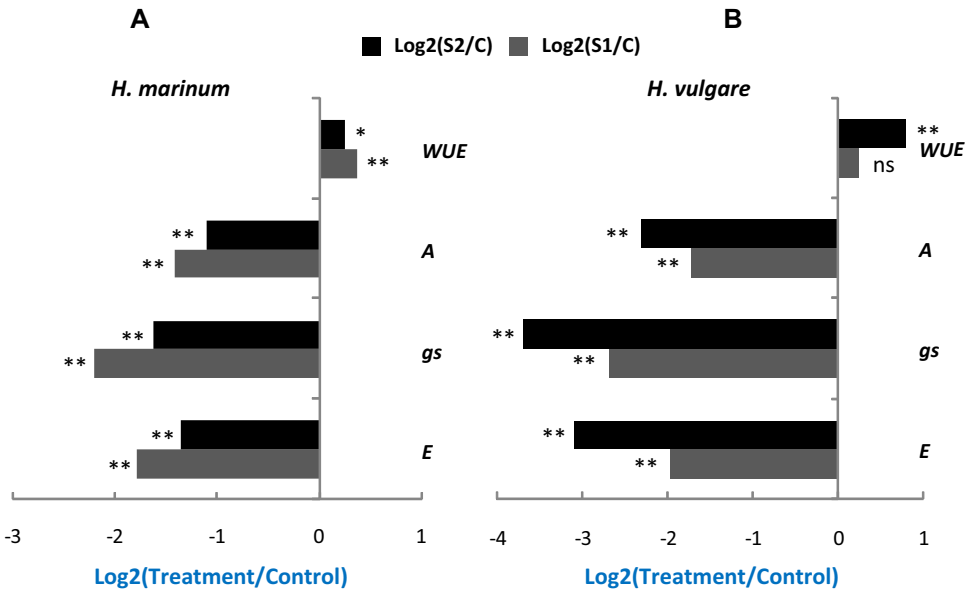

Fig. 2 Net CO_2 assimilation (A), stomatal conductance (*gs*), transpiration rate (E), and water use efficiency (*WUE*) expressed as Log2(treated/control) in *H. marinum* and *H. vulgare* plants hydroponically grown for 3 weeks at 0 (C), 150 (S1), and 300 mM NaCl (S2). Values are means of four replicates. *ns* not significant; $*P \leq 0.05$; $**P \leq 0.01$ according to Student's *t* test

Leaf enzyme activities

DPE2 activity showed contrasting trends in salt-treated plants of *H. marinum* and *H. vulgare*; it noticeably increased (ca. +120%) in S2 treatment in sea barley, and sharply decreased (up to − 82%) in S1 and S2 treatments in cultivated barley (Fig. 5a, b).

Pho1 activity decreased in *H. marinum* by 58% in S2 treatment and increased in *H. vulgare* to threefold and 12-fold the level of the control in S1 and S2 treatments, respectively (Fig. 6a, b). Pho2 activity was maintained unchanged in sea barley and increased under saline conditions by 147–163% in cultivated barley (Fig. 6c, d).

Discussion

H. marinum maintained its RGR at 89–93% of the control level at both high and moderate salinities, while *H. vulgare* was unable to maintain even 60% of its RGR at 150 mM NaCl (Table 1). Similar results were also obtained by Garthwaite et al. (2005) in the two barley species subjected to 150 and 300 NaCl for the same treatment period (3 weeks). In a previous work (Yousfi et al. 2010), some of us showed that since the early 60 h of salt treatment, *H. marinum* was able to maintain its capacity to produce biomass at the level of the control, while *H. vulgare* exhibited reduced shoot and root growth at high salinities (200 and 300 mM). EL data revealed also better membrane integrity in the facultative halophyte (*H. marinum*) compared to the salt-tolerant glycophyte (*H. vulgare*) (Fig. 1). Chalbi et al. (2013) stated that although increased unsaturation in membrane phospholipids is known to maintain membrane fluidity, it did not confer higher salt tolerance to cultivated barley in comparison with sea barley that showed no change in unsaturated–to–saturated fatty acid ratio and double bond index. Garthwaite et al. (2005) attributed this difference in salt tolerance to the higher aptitude of *H. marinum* to avoid leaf invasion by sodium and chloride ions and to maintain higher leaf potassium supply compared to *H. vulgare*.

Photosynthesis was impaired in the two barley species under moderate and high salinities (Fig. 2). Nevertheless, both species increased *WUE* in response to the salt-induced limitation in *A*. Such a response seems to be transitory in *H. vulgare* (it was not recorded after 30 days of treatment), whereas it seems permanent in *H. marinum* (it was observed after 30 days of treatment) (Chalbi et al. 2013). Stomatal closure and the enhanced *WUE* helped the latter maintain its shoot water content above 70% of the control level, whereas the former exhibited decreased shoot water content with the increasing salinity down to 41% of the control. *H. marinum* was found indeed to adapt since the early hours of salt treatment an efficient strategy to cope with the osmotic stress, the first phase of the biphasic salt stress, in comparison with *H. vulgare* that adapted an energy-consuming one (Yousfi et al. 2010). Osmotic adjustment in cultivated barley is ensured by K^+ and organic metabolites (soluble sugars, proline, and free amino acids) at both moderate and high salinities. By contrast, in sea barley, it depends on salinity level: it is ensured by Na^+ at moderate salinity with the involvement of organic metabolites at high salinity (Yousfi et al. 2010). Ferchichi et al. (2018) found that sea barley modulated its osmotic adjustment players with treatment period, too.

The halophyte *H. marinum* exhibited more marked variations in leaf soluble sugar concentrations compared to the glycophyte *H. vulgare* (Fig. 3). The former showed

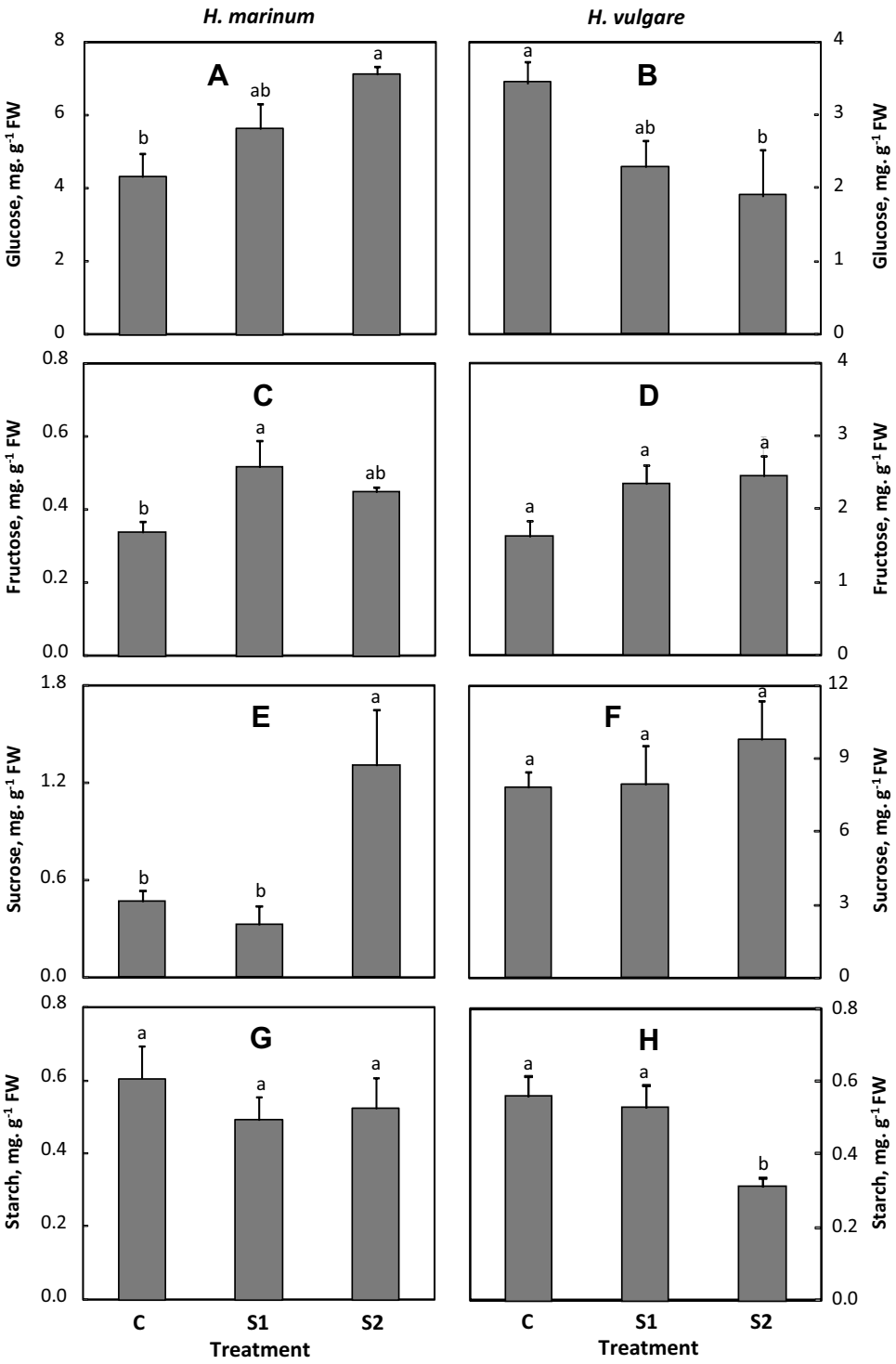

Fig. 3 Concentrations of starch and soluble sugars in fully expanded leaves of *H. marinum* and *H. vulgare* plants hydroponically grown for 3 weeks at 0 (C), 150 (S1), and 300 mM NaCl (S2). Bars are means of four replicates ± SE. Bars labeled with at least one same letter are not significantly different according to Duncan's test at $P \leq 0.05$

an increase in fructose concentration in S1 treatment and those of glucose and sucrose in S2 treatment, while the latter showed no soluble sugar accumulation. According to Ferchichi et al. (2018), leaf soluble sugars did not show an increase in their relative contribution to leaf total osmolality in response to 200 mM NaCl after 15 and 33 days of treatment in both *H. marinum* and *H. vulgare*. In fact, carbohydrate involvement in salt stress responses is not limited to osmotic adjustment. Sugars together with proline can be involved in protein and cell structure stabilization, especially under severe or prolonged stresses. A scavenging role of free radicals was also given to sugars, which protects cells from oxidative stress damages and maintains redox homeostasis (Singh et al. 2015). Furthermore, sugars were found

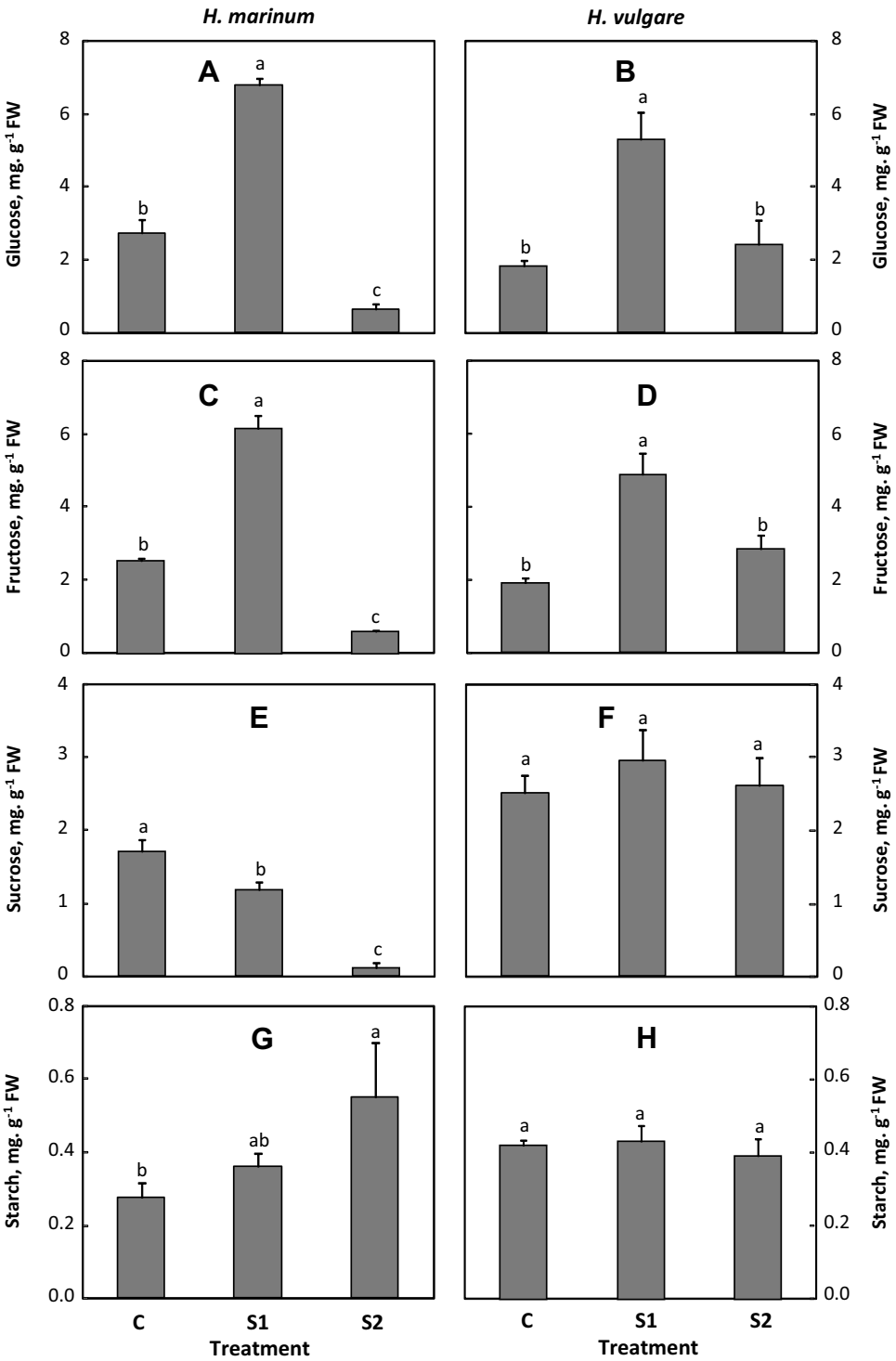

Fig. 4 Concentrations of starch and soluble sugars in roots of *H. marinum* and *H. vulgare* plants hydroponically grown for 3 weeks at 0 (C), 150 (S1), and 300 mM NaCl (S2). Bars are means of four replicates ± SE. Bars labeled with at least one same letter are not significantly different according to Duncan's test at $P \leq 0.05$

to play a key role in stress signaling (Rolland et al. 2006). Comparative proteomics of the halophyte *Thellungiella halophyla* leaves at different salinity levels revealed that the majority of salt-responsive proteins are involved in carbohydrate metabolism; the most affected were starch and sucrose metabolisms that seem crucial for salt tolerance in halophytes (Wang et al. 2013).

Glucose accumulation in leaves of sea barley at 300 mM NaCl was concomitant with an increase in leaf DPE2 activity (Fig. 5). This enzyme is indispensable for transitory starch degradation and maltose metabolism that occur in source leaves at night (Fettke et al. 2006). In cultivated barley, leaf DPE2 activity was substantially reduced under salinity. These results suggest that this enzyme is

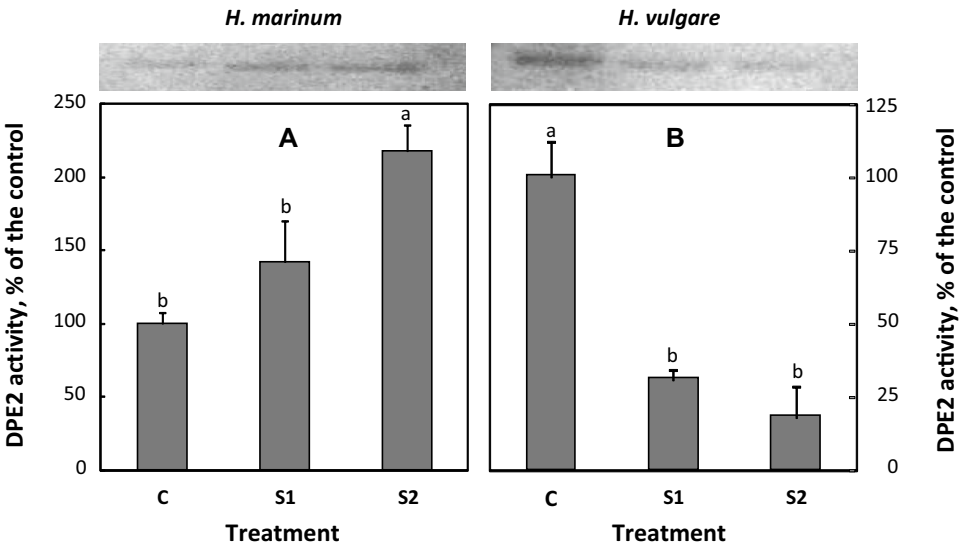

Fig. 5 Zymograms of disproportionating enzyme 2 (DPE2) activity in fully expanded leaves of *H. marinum* and *H. vulgare* plants hydroponically grown for 3 weeks at 0 (C), 150 (S1), and 300 mM NaCl (S2). Bars are means of three replicates ± SE. Bars labeled with at least one same letter are not significantly different according to Duncan's test at $P \leq 0.05$

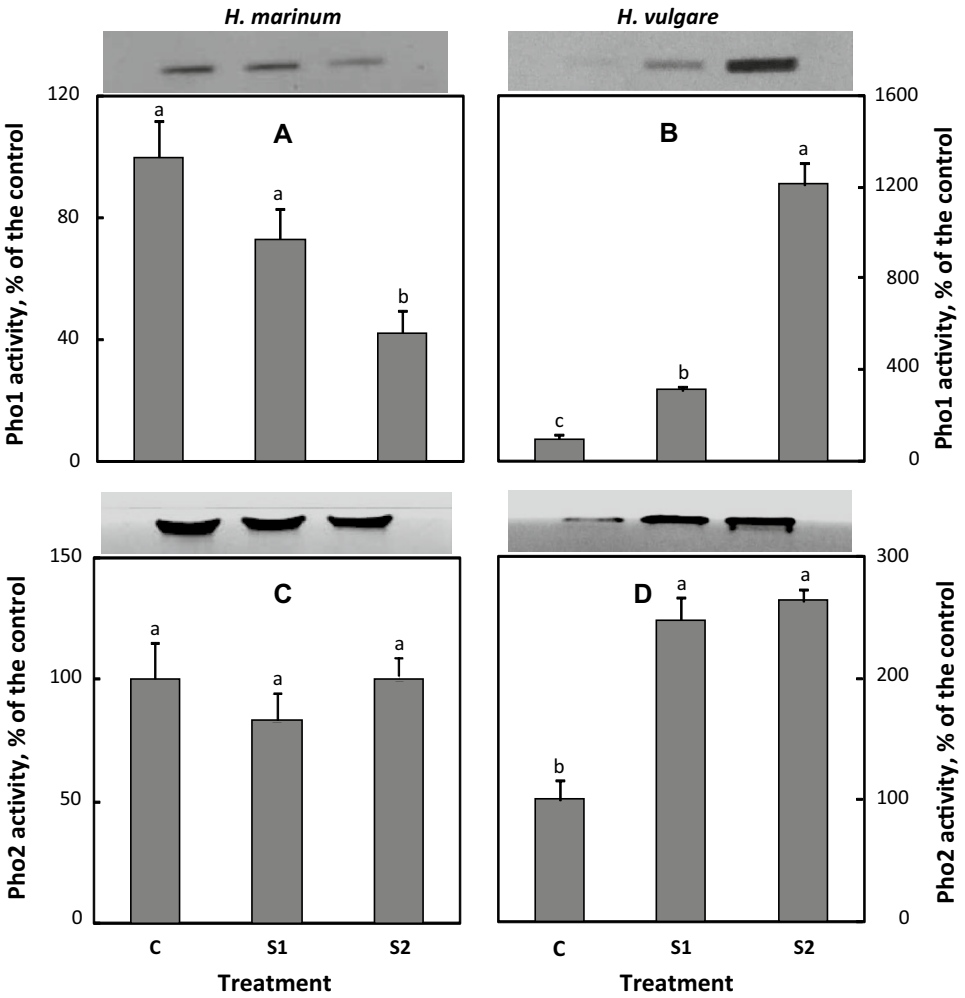

Fig. 6 Zymograms of plastidial (Pho1) and cytosolic (Pho2) α-glucan phosphorylase activities in fully expanded leaves of *H. marinum* and *H. vulgare* plants hydroponically grown for 3 weeks at 0 (C), 150 (S1), and 300 mM NaCl (S2). Bars are means of three replicates ± SE. Bars labeled with at least one same letter are not significantly different according to Duncan's test at $P \leq 0.05$

involved in *H. marinum* responses to high salinity levels through the degradation of starch and the resulting accumulation of soluble sugars. In *H. vulgare*, DPE2 seems not involved and/or damaged by NaCl. As for Pho1 and Pho2, their activities were highly increased in cultivated barley, which suggests a possible role of these enzymes in

the responses of carbohydrate metabolism to salinity. In sea barley, Pho1 activity was markedly decreased by only S2 treatment and Pho2 activity was not modified under saline conditions, which excludes their role in the responsive mechanisms of carbohydrate metabolism to salt stress. Ma et al. (2013) found that the expression of the genes encoding Pho1 and Pho2 (*Pho1* and *Pho2*, respectively) varied with plant species, tissue, development stage, and environmental conditions (abiotic and biotic stresses). These authors stated that the effect of 100 mM NaCl on the expression of *Pho1* and *Pho2* in cultivated barley seedlings depended also on treatment duration. Zeeman et al. (2004) found that Pho1 was involved in leaf responses to a transient osmotic stress, but it was not necessary for starch degradation under non-stressful conditions. However, it was also shown that Pho1 is involved in starch metabolism under standard growth conditions (Malinova et al. 2014). The differential responses of DPE2, Pho1, and Pho2 led to the maintenance of leaf starch concentration at the level of the control at 150 mM NaCl in the two species and a decrease in starch level at 300 mM NaCl in *H. vulgare*.

In roots, cultivated barley exhibited an increase in glucose and fructose concentrations in S1 treatment, while no variation was detected in starch and soluble sugar concentrations in S2 treatment (Fig. 4). These results suggest that root carbohydrate metabolism may play a role in plant responses to S1 treatments, but not to S2 one. As for sea barley roots, a marked accumulation of glucose and fructose was observed at 150 mM NaCl together with a decrease in sucrose concentration, starch level being maintained unchanged. This can be explained by a high capacity of plants to transport sucrose from source (leaves) to sink (roots) organs and a high activity of root invertase and/or sucrose synthase. These two enzymes catalyze sucrose cleavage into glucose and fructose (Koch 2004). At 300 mM NaCl, *H. marinum* showed a substantial decrease in all soluble sugars and a noticeable accumulation of starch. Hence, under these conditions, *H. marinum* accumulated carbohydrates in two different forms depending on plant organ: in leaves, where salt ions are not accumulated at high amounts, carbohydrates are accumulated as soluble sugars, while in roots, where salt ions can be accumulated at high amounts, carbohydrates are stored as starch. Starch is considered as a storage substance that can be mobilized when energy is not sufficiently supplied to cover energy demands (Krasensky and Jonak 2012), while soluble sugars can be immediately used for several purposes (Rolland et al. 2006; Singh et al. 2015). Our data constitute an initiation to the involvement of carbohydrate metabolism and partitioning in salt responses of barley species and further work is necessary to elucidate how their flexibility confers higher tolerance to *H. marinum* compared to *H. vulgare*.

Conclusion

Although carbohydrate metabolism is still in its infancy (Thalmann and Santelia 2017), the differential behaviors of the halophyte *H. marinum* and the glycophyte *H. vulgare* in terms of starch and soluble sugar distribution between source and sink organs, as well as the enzymes involved in starch metabolism can give insights into the importance of sugars in salt tolerance in barley species. This importance is not due to osmotic adjustment, but to other functions that need further investigations. The comparison between sea and cultivated barley species revealed a higher flexibility in carbohydrate metabolism and distribution in the former, which probably contributed to its higher salt tolerance in particular at high salinity levels.

Author contribution statement WM participated in all steps of the work. NF, EB-H, and MB helped in the physiological study. SA-R, HM, and HQ helped in carbohydrate and enzyme assays. FC contributed to data analysis and interpretation. CA was the receipt of the grant as Head of the Laboratory of Extremophile Plants. JF and MR were the supervisors of the work.

Acknowledgements This work was supported by the Tunisian Ministry of Higher Education and Scientific Research (LR10CBBC02) and the University of Potsdam (Germany).

References

Alamri SA, Barrett-Lennard EG, Teakle NL, Colmer TD (2013) Improvement of salt and waterlogging tolerance in wheat: comparative physiology of *Hordeum marinum-Triticum aestivum* amphiploids with their *H. marinum* and wheat parents. Funct Plant Biol 40:1168–1178. https://doi.org/10.1071/FP12385

Caporn S, Brooks A, Press M, Lee J (1999) Effects of long-term exposure to elevated CO_2 and increased nutrient supply on bracken (*Pteridium aquilinum*). Funct Ecol 13(Suppl. 1):107–115. https://doi.org/10.1046/j.1365-2435.1999.00013.x

Cardi M, Castiglia D, Ferrara M, Guerriero G, Chiurazzi M, Esposito S (2015) The effects of salt stress cause a diversion of basal metabolism in barley roots: possible different roles for glucose-6-phosphate dehydrogenase isoforms. Plant Physiol Biochem 86:44–54. https://doi.org/10.1016/j.plaphy.2014.11.001

Chalbi N, Hessini K, Gandour M, Naeit-Mohamed S, Smaoui A, Abdelly C, Ben Youssef N (2013) Are changes in membrane lipids and fatty acid composition related to salt-stress resistance in wild and cultivated barley? J Plant Nutr Soil Sci 176:138–147. https://doi.org/10.1002/jpln.201100413

Chaves MM, Flexas J, Pinheiro C (2009) Photosynthesis under drought and salt stress: regulation mechanisms from whole plant to cell. Ann Bot 103:551–560. https://doi.org/10.1093/aob/mcn125

Cheeseman JM (2015) The evolution of halophytes, glycophytes and crops, and its implications for food security under saline

conditions. New Phytol 206:557–570. https://doi.org/10.1111/nph.13217
Chia T, Thorneycroft D, Chapple A, Messerli G, Chen J, Zeeman SC, Smith SM, Smith AM (2004) A cytosolic glucosyltransferase is required for conversion of starch to sucrose in *Arabidopsis* leaves at night. Plant J 37:853–863. https://doi.org/10.1111/j.1365-313X.2003.02012.x
Dionisio-Sese ML, Tobita S (1998) Antioxidant responses of rice seedlings to salinity stress. Plant Sci 135:1–9. https://doi.org/10.1016/S0168-9452(98)00025-9
Ferchichi S, Hessini K, Dell'Aversana E, D'Amelia L, Woodrow P, Ciarmiello LF, Fuggi A, Carillo P (2018) *Hordeum vulgare* and *Hordeum maritimum* respond to extended salinity stress displaying different temporal accumulation pattern of metabolites. Funct Plant Biol 45(11):1096–1109. https://doi.org/10.1071/FP18046
Fettke J, Eckermann N, Tiessen A, Geigenberger P, Steup M (2005a) Identification, subcellular localization and biochemical characterization of water-soluble heteroglycans (SHG) in leaves of *Arabidopsis thaliana* L.: distinct SHG reside in the cytosol and in the apoplast. Plant J 43:568–585. https://doi.org/10.1111/j.1365-313X.2005.02475.x
Fettke J, Poeste S, Eckermann N, Tiessen A, Pauly M, Geigenberger P, Steup M (2005b) Analysis of cytosolic heteroglycans from leaves of transgenic potato (*Solanum tuberosum* L.) plants that under- or overexpress the Pho 2 phosphorylase isozyme. Plant Cell Physiol 46:1987–2004. https://doi.org/10.1093/pcp/pci214
Fettke J, Chia T, Eckermann N, Smith A, Steup M (2006) A transglucosidase necessary for starch degradation and maltose metabolism in leaves at night acts on cytosolic heteroglycans (SHG). Plant J 46:668–684. https://doi.org/10.1111/j.1365-313X.2006.02732.x
Fettke J, Fernie AR, Steup M (2012) Transitory starch and its degradation in higher plant cells. In: Tetlow IJ (ed) Essential reviews in experimental biology: starch: origins, structure and metabolism. SEB, London, pp 311–374
Garthwaite AJ, Von Bothmer R, Colmer TD (2005) Salt tolerance in wild *Hordeum* species is associated with restricted entry of Na^+ and Cl^- into the shoots. J Exp Bot 56:2365–2378. https://doi.org/10.1093/jxb/eri229
Gupta B, Huang B (2014) Mechanism of salinity tolerance in plants: physiological, biochemical, and molecular characterization. Int. J. Genomics. https://doi.org/10.1155/2014/701596
Hafsi C, Lakhdhar A, Rabhi M, Debez A, Abdelly C, Ouerghi Z (2007) Interactive effects of salinity and potassium availability on growth, water status, and ionic composition of *Hordeum maritimum*. J Plant Nutr Soil Sci 170:469–473. https://doi.org/10.1002/jpln.200625203
Hafsi C, Romero-Puertas MC, Gupta DK, del Río LA, Sandalio LM, Abdelly C (2010) Moderate salinity enhances the antioxidative response in the halophyte *Hordeum maritimum* L. under potassium deficiency. Environ Exp Bot 69:129–136. https://doi.org/10.1016/j.envexpbot.2010.04.008
Hafsi C, Atia A, Lakhdar A, Debez A, Abdelly C (2011a) Differential responses in potassium absorption and use efficiencies in the halophytes *Catapodium rigidum* and *Hordeum maritimum* to various potassium concentrations in the medium. Plant Prod Sci 14:135–140. https://doi.org/10.1626/pps.14.135
Hafsi C, Romero-Puertas MC, del Río LA, Abdelly C, Sandalio LM (2011b) Antioxidative response of *Hordeum maritimum* L. to potassium deficiency. Acta Physiol Plant 33:193–202. https://doi.org/10.1007/s11738-010-0537-3
Harris BN, Sadras VO, Tester M (2010) A water-centred framework to assess the effects of salinity on the growth and yield of wheat and barley. Plant Soil 336:377–389. https://doi.org/10.1007/s11104-010-0489-9
Hartman MD, Figueroa CM, Arias DG, Iglesias AA (2017) Inhibition of recombinant aldose-6-phosphate reductase from peach leaves by hexose-phosphates, inorganic phosphate and oxidants. Plant Cell Physiol 58:145–155. https://doi.org/10.1093/pcp/pcw180
Hewitt EJ (1966) Sand and water culture methods used in the study of plant nutrition. Commonw Bur Hortic Tech Commun 22:431–446
Islam S, Malik AI, Islam AKMR, Colmer TD (2007) Salt tolerance in a *Hordeum marinum–Triticum aestivum* amphiploid, and its parents. J Exp Bot 58:1219–1229. https://doi.org/10.1093/jxb/erl293
Jusovic M, Velitchkova MY, Misheva SP, Börner A, Apostolova EL, Dobrikova AG (2018) Photosynthetic responses of a wheat mutant (Rht-B1c) with altered DELLA Proteins to salt stress. J Plant Growth Regul 37:645–656. https://doi.org/10.1007/s00344-017-9764-9
Koch K (2004) Sucrose metabolism: regulatory mechanisms and pivotal roles in sugar sensing and plant development. Curr Opin Plant Biol 7:235–246. https://doi.org/10.1016/j.pbi.2004.03.014
Krasensky J, Jonak C (2012) Drought, salt, and temperature stress-induced metabolic rearrangements and regulatory networks. J Exp Bot 63:1593–1608. https://doi.org/10.1093/jxb/err460
Lakhdar A, Hafsi C, Rabhi M, Debez A, Montemurro F, Abdelly C, Jedidi N, Ouerghi Z (2008) Application of municipal solid waste compost reduces the negative effects of saline water in Hordeum maritimum L. Bioresour Technol 99:7160–7167. https://doi.org/10.1016/j.biortech.2007.12.071
Lu Y, Gehan JP, Sharkey TD (2005) Daylength and circadian effects on starch degradation and maltose metabolism. Plant Physiol 138(4):2280–2291. https://doi.org/10.1104/pp.105.061903
Ma J, Jiang QT, Zhang XW, Lan XJ, Pu ZE, Wei YM, Liu C, Lu ZX, Zheng YL (2013) Structure and expression of barley starch phosphorylase genes. Planta 238:1081–1093. https://doi.org/10.1007/s00425-013-1953-6
Maggio A, Raimondi G, Martino A, de Pascale S (2007) Salt stress response in tomato beyond the salinity tolerance threshold. Environ Exp Bot 59:276–282. https://doi.org/10.1016/j.envexpbot.2006.02.002
Malinova I, Mahlow S, Alseekh S, Orawetz T, Fernie AR, Baumann O, Steup M, Fettke J (2014) Double knockout mutants of *Arabidopsis* grown under normal conditions reveal that the plastidial phosphorylase isozyme participates in transitory starch metabolism. Plant Physiol 164:907–921. https://doi.org/10.1104/pp.113.227843
Munns R, Tester M (2008) Mechanisms of salinity tolerance. Annu Rev Plant Biol 59:651–681. https://doi.org/10.1146/annurev.arplant.59.032607.092911
Orawetz T, Malinova I, Orzechowski S, Fettke J (2016) Reduction of the plastidial phosphorylase in potato (*Solanum tuberosum* L.) reveals impact on storage starch structure during growth at low temperature. Plant Physiol Biochem 100:141–149. https://doi.org/10.1016/j.plaphy.2016.01.013
Rabhi M, Hajji S, Karray-Bouraoui N, Giuntini D, Castagna A, Smaoui A, Ranieri A, Abdelly C (2010) Nutrient uptake and management under saline conditions in the Xerohalophyte: *Tecticornia indica* (Willd.) subsp. indica. Acta Biol Hung 61:486–497. https://doi.org/10.1556/ABiol.61.2010.4.11
Rolland F, Baena-Gonzalez E, Sheen J (2006) Sugar sensing and signaling in plants: conserved and novel mechanisms. Annu Rev Plant Biol 57:675–709. https://doi.org/10.3389/fpls.2014.00113
Rozema J, Flowers T (2008) Crops for a salinized world. Science 322:1478–1480. https://doi.org/10.1126/science.1168572
Shahbaz M, Ashraf M, Al-Qurainy F, Harris PJC (2012) Salt tolerance in selected vegetable crops. Crit Rev Plant Sci 31(4):303–320. https://doi.org/10.1080/07352689.2012.656496
Singh M, Kumar J, Singh S, Singh VP, Prasad SM (2015) Roles of osmoprotectants in improving salinity and drought tolerance in plants: a review. Rev Environ Sci Biotechnol 14:407–426. https://doi.org/10.1007/s11157-015-9372-8

Stitt M, Lilley RM, Gerherdt R, Heldt HW (1989) Metabolite levels in specific cells and subcellular compartments of plant leaves. Methods Enzymol 174:518–552. https://doi.org/10.1016/0076-6879(89)74035-0

Thalmann M, Santelia D (2017) Starch as a determinant of plant fitness under abiotic stress. New Phytol 214:943–951. https://doi.org/10.1111/nph.14491

Van den Ende W, El-Esawe SK (2014) Sucrose signaling pathways leading to fructan and anthocyanin accumulation: a dual function in abiotic and biotic stress responses? Environ Exp Bot 108:4–13. https://doi.org/10.1016/j.envexpbot.2013.09.017

Wang X, Chang L, Wang B, Wang D, Li P, Wang L, Yi X, Huang Q, Peng M, Guo A (2013) Comparative proteomics of *Thellungiella halophila* leaves from plants subjected to salinity reveals the importance of chloroplastic starch and soluble sugars in halophyte salt tolerance. Mol Cell Proteom 12:2174–2195. https://doi.org/10.1074/mcp.M112.022475

Yousfi S, Rabhi M, Hessini K, Abdelly C, Gharsalli M (2010) Differences in efficient metabolite management and nutrient metabolic regulation between wild and cultivated barley grown at high salinity. Plant Biol 12:650–658. https://doi.org/10.1111/j.1438-8677.2009.00265.x

Zeeman SC, Thorneycroft D, Schupp N, Chapple A, Weck M, Dunstan H, Haldimann P, Bechtold N, Smith AM, Smith SM (2004) Plastidial a-glucan phosphorylase is not required for starch degradation in *Arabidopsis* leaves but has a role in the tolerance of abiotic stress. Plant Physiol 135:849–858. https://doi.org/10.1104/pp.103.032631

OPEN ACCESS
Scholars International Journal of Biochemistry
Abbreviated Key Title: Sch Int J Biochem
ISSN 2616-8650 (Print) |ISSN 2617-3476 (Online)
Scholars Middle East Publishers, Dubai, United Arab Emirates
Journal homepage: https://scholarsmepub.com/sijb/

Original Research Article

Identify the Specificity of Interaction between the Arabidopsis Starch Synthase 4 and the Plastidial Starch Phosphorylase using a Homologous Protein-Animal Rabbit Muscle Phosphorylase a

Hadeel Mohammed Qasim[1], Julia Compart[1], Slawomir Orzechowski[2], Joerg Fettke[1] and Shadha Abduljaleel AL-Rawi[1*]

[1]Biopolymer Analytics, University of Potsdam, 14476 Potsdam-Golm, Germany
[2]Department of Biochemistry, Warsaw University of Life Sciences, -SGGW, 02-776 Warsaw, Poland

DOI: 10.36348/sijb.2019.v02i12.003 | **Received:** 30.11.2019 | **Accepted:** 07.12.2019 | **Published:** 28.12.2019

***Corresponding author:** Shadha Abduljaleel AL-Rawi

Abstract

The starch synthase 4 (SS4) is a key enzyme for initiation of starch granules and regulation of the starch granule number in chloroplasts of higher plants. These enzymes transfer glucosyl residue from ADPglucose to the non-reducing end of a preexisting glucan chain. The presence of a coiled-coil motive in the N-terminus of Arabidopsis SS4 has been involved in mediating some of the protein-protein interactions. Thus, it was also shown that *At*SS4 directly interacts with the plastidial phosphorylase (AtPHS1). However, phosphorylase enzymes are widespread in animals, microorganism, and plants. So far, it was unclear if the observed protein-protein interaction is specific for plant origin phosphorylase enzymes. Therefore, we tested whether or not an animal type phosphorylase, the rabbit muscle phosphorylase a (Pho a), also interacts with AtSS4. Our results show that the protein-protein interaction of AtPHS1 and AtSS4 is specific and cannot archived by Pho a. Furthermore, also a functional interaction between AtSS4 and the Pho a was not detected.

Keywords: Arabidopsis thaliana, plastidial phosphorylase, starch synthase, rabbit muscle phosphorylase, protein interaction, protein crosslinking.

INTRODUCTION

Carbohydrates are one of the main types of biomolecules, playing a vital role in the living organism. The two most abundant storage carbohydrates are starch and glycogen. Starch is a polysaccharide that consists of two polymers amylose and amylopectin in both the glucosyl residues are linked by α 1-4 glycosidic bond with a lesser frequency of α 1-6 linkages in amylose, so it is defined as a major linear glucan, and significant amount in amylopectin [1, 2] Like amylopectin glycogen is a polymer that is exclusively formed by glucose units that are linked by α 1-4 and α 1-6 glycosidic linkage. These linkages formed during the starch and glycogen biosynthesis by the activity of starch synthases (SSs) with branching (BE) and debranching (DBE) enzymes and glycogen synthase (GS) with glycogen branching enzyme (GBE), respectively. However, the formed α 1-6 branches are randomly distributed in glycogen but were ordered in amylopectin.

In addition to the chemical similarities of both glucans, the mode of action of the metabolizing enzymes is also clearly related [3]. For instance, starch phosphorylase (AtPHS1 in Arabidopsis or Pho1 in other plant species) and glycogen phosphorylase (Pho a) have a similar function, as both of them catalysis the reversible exchange of glucosyl units between glucose-1-phosphate (G-1-P) and the non-reducing ends of α 1-4 glucans. In higher plants, PHS1 play a dynamic role in starch metabolism, thus in degradation and synthesis [4-6]. Pho1 plays a crucial role in starch synthesis in plastids of non-photosynthetic storage tissue of higher plants, as the loss of Pho1 caused smaller starch granules and accumulation of a modified amylopectin structure. Recently, more biochemical and genetic studies revealed that PHS1/Pho1 play a key role in the initiation and formation of storage starch. Barley Pho1 was reported to initiation α 1-4 glucan synthesis from G-1-P alone, based on experiments where preparations of enzyme and substrate missing the potential acceptor glucans [7]. In rice, Pho1 can work in starch priming by elongating short glucan chains [6] which can be generated during starch degradation by the activity of α-amylase (AMY3), β-amylase (BAM) and isoamylase

(ISO3) [8]. Besides the plastidial phosphorylase to elongating the short glucan chains, there are several other plastidial enzymes that can act *e.g.* disproportion enzyme (DPE1) which has the ability to release a portion from the non-reducing end of one glucan chain and connect it to another non-reducing end thereby forming short and long glucan chains [9, 10]. Also starch synthases (SSI, SSII and SSIII) are involved in the elongation of α-glucan chains of amylopectin [11]. Recently, a new hypothesis proposes protein-protein or multi-protein complex machinery for starch metabolism, for instance, starch synthase 4 (AtSS4) which possess a coiled-coil motive in its structure led to the interaction with other starch metabolizing proteins [12]. However, AtSS4 is required for granule initiation [13]. Interaction of AtSS4 and AtPHS1 was shown [14]. Thus, we tested the specificity of the interaction of starch synthase 4 with the Arabidopsis plastidial phosphorylase by using a non-plant, phosphorylase- the rabbit muscle phosphorylase a (Pho a).

MATERIAL AND METHODS

Starch granules were isolated from Arabidopsis leaves as described by [15]. Glycogen phosphorylase was purchased from Sigma Aldrich product No.-232-878-8 and the isoamylase (200U/ml) from Megazyme. 8-aminopyrene-1, 3-6trisulfonic acid (ATPS) and sodium Cyanoborhydrid were purchased from Sigma Aldrich.

Cloning, expression, and purification of recombinant AtSS4 and AtPHS1proteins

AtSS4 and AtPHS1 were cloned as described elsewhere [16, 2]. The proteins were expressed without transit peptide using pET23b vector (Novagen) and the *E. coli* strain BL21 (DE3). For expression, cells were grown in 800ml (37C°) Luria-Bertani medium containing 100µg/ml ampicillin. Expression (overnight at 20C°) was induced by addition of isopropyl thio-β-galactoside (IPTG 1mM final concentration) at OD 600nm values between 0.6 and 0.8. Harvesting of the cells and purification of His-tagged protein were performed as described [16]**.** Purified protein fractions were concentrated via ultrafiltration (50kDa; Amicon Ultra; Millipore) in 50mM HEPES/NaOH, pH 7.5, 1mM EDTA, 2mM DTE and 10% (w/v) glycerol. Aliquots were frozen in liquid nitrogen and stored at -80°C until use. Protein concentration was estimated using Bradford assay (SIGMA, Taufkirchen, Germany).

SDS-PAGE, Western blotting, and immune detection

Fractions were analyzed by SDS-PAGE and the proteins were transferred to a membrane see [17]. The membrane was analyzed by antibodies specific against AtSS4 and AtPHS1, respectively.

Protein-Protein Interaction Studies

The interaction between AtPHS1 and AtSS4 by using a cross linker

10mg of a cross linker DTSSP was dissolved in 495µl of dry DMF solvent. The cross linker was used in a 20–fold excess compared to the proteins. The final cross linker concentration was 0.5mM and optimal pH range was from 7 to 9. 40µg of the recombinant plastidial phosphorylase and 200µg of crude extract isolated from Col-0 were incubated with cross linker DTSSP for 5min at 21°C. Quench of any unreacted DTSSP was performed by using 25M of Tris, pH 7.4 and allowed to react for 10-15min, 21°C. Following purification of the recombinant AtPHS1 by using Ni-NTA agarose column and washing 6 times with 1mL of 50mM Imidazole the proteins were eluted by 6 mL 150mM Imidazole. After purification all fractions were transferred to ultrafiltration units (Amicon®, 10kDa Millipore, and Billerica, MA, United States) and centrifuged for 12min at 4°C, 13000rpm. Finally, all fractions were analyzed by SDS–PAGE (7.5%) and incubated with anti–SS4 antibody. In addition, the same procedure was performed but without recombinant plastidial phosphorylase.

Confirm the interaction between AtPHS1 and AtSS4 by using α-amylase

40µg of the AtPHS1 and 200µg protein crude extract were incubated in the presence of 20 units α-amylase for 10min at 37°C. After the incubation the purification were done by using the Ni-NTA agarose as described above.

The interaction between AtPHS1 and both enzymes AtSS1 and AtSS3

250µg crude extract proteins isolated from Col-0 were incubated with 40µg of AtPHS1 and the recombinant protein was isolated by Ni-NTA agarose as described above. The eluting fractions were loaded on native gel. As a control 250µg crude extract were directly loaded on native gel. After electrophoreses the gels were incubated in buffer that contained 50mM Tricin/KOH pH.8, 25mM K-acetate, 5mM DTE, 2mM EDTA, 0.02% (w/v) bovine serum albumin, and 1mM ADPglucose overnight at room temperature and stained with iodine.

The interaction between AtSS4 and Pho a using the cross linker DTSSP, 40µg of AtSS4 and 40µg of Pho a were incubated in presence of the cross linker DTSSP and the recombinant AtSS4 was purified and analyzed by native-PAGE as described above. For washing and elution 9mL 50mM and 9mL 150mM Imidazol were used.

Native-PAGE and phosphorylase activity staining

Native-PAGE followed by phosphorylases activity staining was performed as described by [14].

Glucan synthesizing assay and glucan preparation

0.5mg of native starch granules were resuspended in incubation buffer [50mM HEPES/KOH pH 7.4 ,1mM DTE, 10mM G-1-P] with 10µg of glycogen Pho a or 5µg of starch phosphorylase AtPHS1 alone or in presence of 5µg AtSS4. The samples were incubated for 60min at 30C° under continuous agitation and were centrifuged at 1500g for 2min. The supernatant was then discarded and the starch pellets were resuspended in 10mM Na- acetate buffer, pH 5.5, 2mM DTE, 7 units isoamylase (final volume 100µl over nights at 37°C) under continuous agitation. The samples were centrifuged for 10min at 1500g; the supernatant was heated at 95°C for 5min and were filtrated (10kDa), lyophilized, labeled, and analyzed using CE-LIF as described in [17].

CE-LIF analysis

Chain length distribution analysis of the samples were performed by measuring the ATPS-labeled α 1-4 glucans using a PA-800 (Beckman coulter) equipped with a laser-induced fluorescence detector (LIF). The total length of the N-CHO-coated capillary (i.d., 50µm) was 50cm. The running buffer was a mixture of 25mM Li-acetate (pH 4.75) and 0.4 (w/v) polyethylene oxide. The separation was performed for 25min at 30kV and 25°C.

RESULTS

Conformation of the direct interaction of AtPHS1 with AtSS4

As published in [14] a direct protein-protein interaction was observed for the plant derived plastidial phosphorylase and the starch synthase 4. We therefore test if this interaction is observed also under our experimental conditions. In *E. coli* heterologous expressed AtPHS1, that has a C-terminal 6x His-tag, was incubated with crude extract of Arabidopsis leaves harvested in the middle of the light period. Following incubation for five minutes at 21°C the recombinant AtPHS1 was purified by a Ni-NTA agarose column. The proteins bound to the column were eluted and analyzed using SDS-PAGE, western blotting, and immune detection using a specific antibody against AtSS4. As shown in Figure (1, A) the interaction between AtSS4 and AtPHS1 was confirmed. As control an identical experiment was performed but the recombinant AtPHS1 was omitted. In this control experiment no signal for AtSS4 was observed, excluding any unspecific co-purification of the enzyme by this procedure (Figure 1, A). The co-purification is specific for AtSS4, as no interaction with AtSS1 and AtSS3 was observed (Fig. 1, B).

No protein interaction was observed for the rabbit muscle phosphorylase a with AtSS4

We then test if the rabbit muscle phosphorylase a also interacts with AtSS4. Therefore, we incubated purified rabbit muscle phosphorylase a directly with purified recombinant AtSS4 C-terminal fused to a 6x His-tag. Following incubation for five minutes at 21°C the His-tagged AtSS4 was purified using a Ni-NTA agarose column. The eluted protein fraction was tested for the presence of the rabbit phosphorylase a using a native-PAGE and staining for phosphorylase activity. No phosphorylase was co-purified with AtSS4 (Fig. 1, C). As maybe the interaction of the rabbit muscle Pho a and AtSS4 is much weaker and thus during the purification procedure the phosphorylase is not co-purified, we included the cross-linking by DTSSP. Therefore, we test again first the procedure with both plant derived enzymes and observed again a clear interaction also using the crosslinking protocol (Fig. 1, C). However, using the same procedure for Pho a and AtSS4, we did not observe any phosphorylase activity (Fig. 1, C). Thus, even a very weak protein-protein interaction between these two proteins is very unlikely.

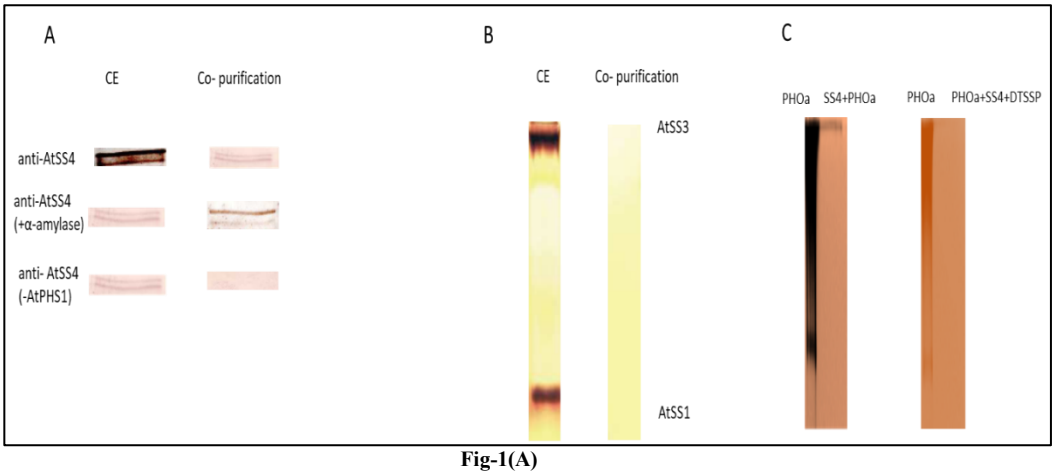

Fig-1(A)

Fig 1(A): The interaction of starch synthase 4 (AtSS4) with the recombinant plastidial phosphorylase (AtPHS1). 40µg C-terminal 6x His tagged recombinant plastidial phosphorylase protein from *Arabidopsis thaliana* expressed in *E.coli* was incubated with 200µg protein crude extract (CE) isolated from Col-0 for 5min at 21°C. Following purification of the recombinant plastidial phosphorylase using Ni-NTA agarose

column, all fractions were analyzed by an antibody specific for AtSS4. In addition, in order to rule out the possibility of the correlation between AtSS4 and AtPHS1 the recombinant plastidial phosphorylase and the protein crude extract (CE) isolated from Col-0 were incubated with 20 units α-amylase for 10min at 37°C. As a control the recombinant plastidial phosphorylase was omitted (AtSS4-AtPHS1). (**B**): 200µg of the crude extract with recombinant plastidial phosphorylase were incubated then purified with the column, the fractions were loaded on native-PAGE and incubated with buffer containing 50mM Tricin/KOH pH 8, 25mM K-acetate, 5mM DTE, 2mM EDTA, 0.02% (w/v) bovin serum albumin and 1mM ADPglucose over night at room temperature and stained with iodine. Thus no co-purification of plastidial phosphorylase with AtSS1 or AtSS3 was observed. (**C**): 40µg of the starch synthase 4 and 40µg of non-plant phosphorylase a from rabbit muscle was incubated with the cross linker DTSSP for 5min at 21°C. Following purification using Ni-NTA agarose column for the recombinant AtSS4, washing, and elution with Imidazole (50 and 150mM) all fractions were loaded on native-PAGE and after electrophoreses incubated for phosphorylase activity staining. Thus, no co-purification of phosphorylase a and starch synthase 4 was observed.

Simultaneous incubation of AtPHS1 and AtSS4 revealed alterations of the glucans accessible by isoamylase at the surface of starch

We did not observe any direct protein-protein interaction for phosphorylase a and AtSS4, thus we analyzed whether or not the proteins functional interact during glucan synthesis. Therefore, we incubated AtSS4 with AtPHS1 or Pho a in presence of glucose-1-phosphate and starch as substrate. As control AtSS4 was omitted. The glucan products were analyzed after 1h incubation in synthesizing direction. Following debranching of the starch surface by isoamylase treatment, the glucans were analyzed by CE-LIF. We observed slightly different glucan distribution patterns for both phosphorylase. Thus incubation with the plant derived AtPHS1 resulted in elongation of short glucan chains compared to the incubation with the animal phosphorylase a. However, for the plant derived phosphorylase a small increase of shorter glucan chains were detected in the presence of AtSS4 that was significant, even very weak. However, the resulting patterns for the animal phosphorylase showed no significant alterations in presence or absence of AtSS4 (Fig. 2). Thus, no evidence for a functional interaction was observed.

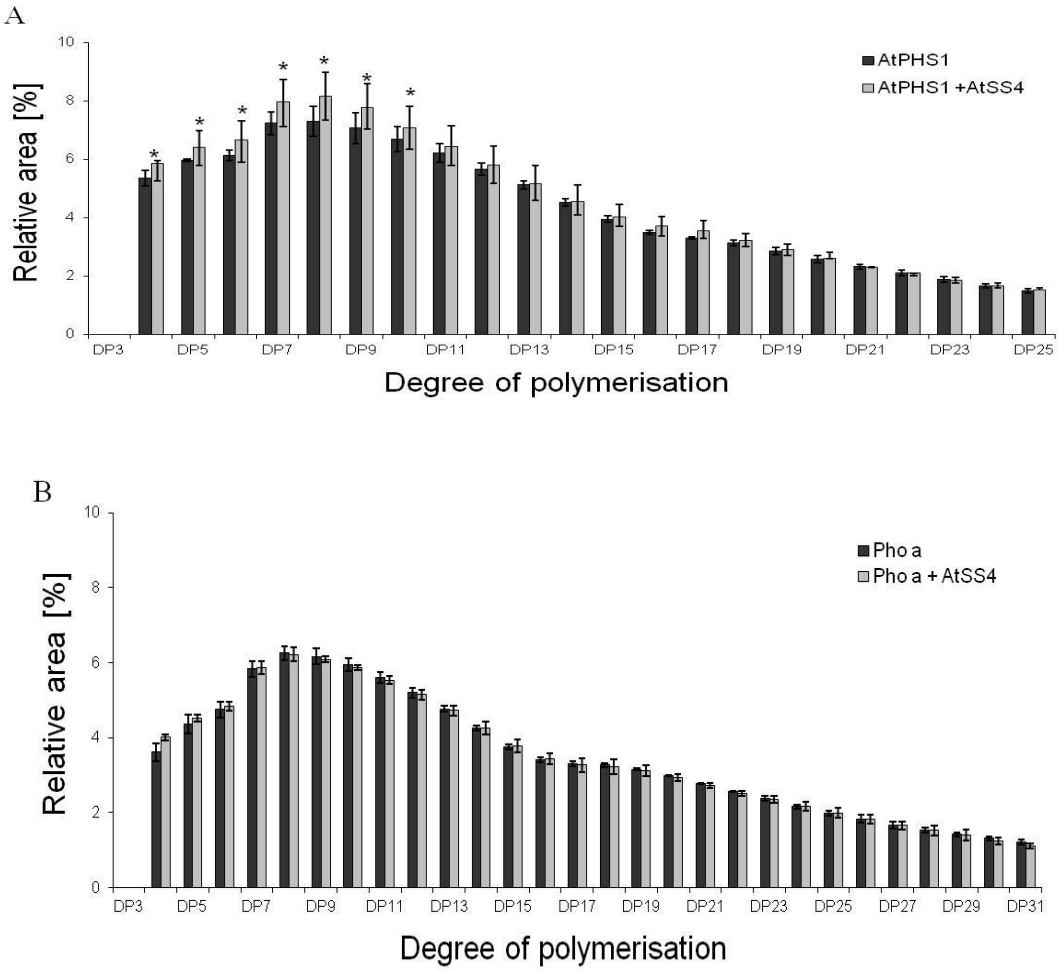

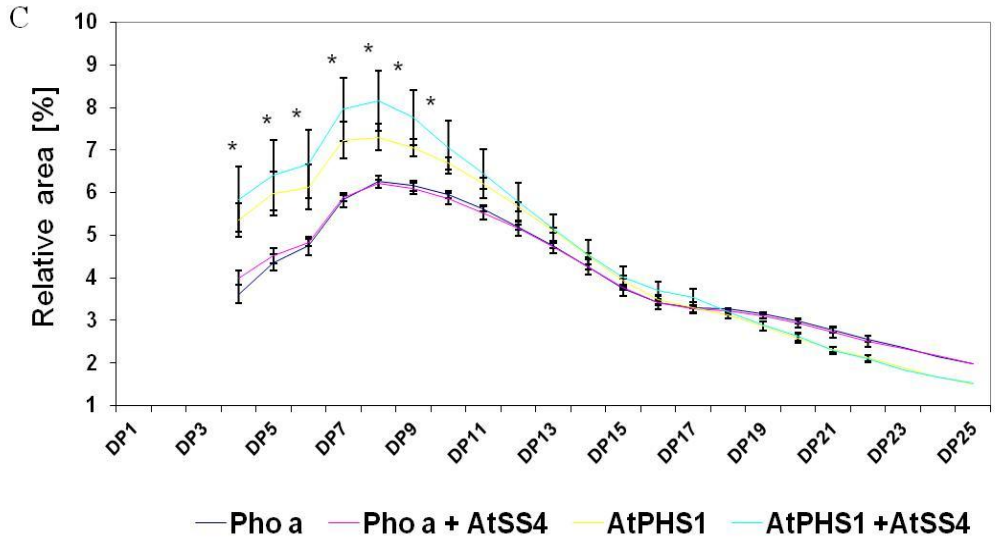

Fig-2

Fig 2: Chain length distribution of Arabidopsis starch formed by the interaction of AtPHS1 or Pho a with AtSS4. (A, B): 5mg Arabidopsis starch were incubated with 10µg Pho a or 5µg AtPHS1 alone as a control or with 5µg AtSS4.The pellets were debranched with isoamylase, glucans were labeled with APTS, and then separated and detected using CE-LIF. Values are the means ± SD (n=3). C: Deference plots to compare the effect of AtSS4 on the action of Pho a and AtPHS1. Values are the means ± SD (n=3) *, $P \leq 0,5$ according to Student's t-test.

DISCUSSION

Recently more biochemical and genetic studies reveal the role of AtSS4. Thus, it was shown that AtSS4 is involved in the process of starch initiation by formation of the priming molecule, but also appeared to be required for other activities during starch synthesis. However, the precise role has not yet been clarified [18]. All classes of SS contain a highly conserved C-terminal end that included the glucosyl transferase catalytic domains (GT5) and (GT1). The N- terminal regions differ in size and amino acid sequence [19]. AtSS4 differs from the other classes in containing two long coiled-coil domains, extended from the (GT5) domain [20, 21].This region is highly conserved and led to the suggestion that it is important for protein-protein interactions [12, 22]. Recently, more evidences revealed that interaction of SS4 with the other proteins is important for granule initiation for instance in Arabidopsis, thus three proteins were identified, belonging to the protein targeting to starch (PTST) family, PTST1, PTST2, and PTST3 [23, 24]. Other results showed that AtSS4 interact with the protein fibrillin1a and 1b (FBN 1a and FBN 1b), respectively which are mainly located in the plastoglobules (PGs) [25]. Furthermore, a protein named PII1 (protein involved in starch initiation) was identified as an interacting protein of AtSS4. Also the *pii1* mutant revealed a reduced number of starch granules compared to the wild type [26]. It was also reported, that AtSS4 interacts with the plastidial starch phosphorylase (AtPHS1) [14]. In the present study we tested whether or not this reported interaction is specific for plant phosphorylase or can this interaction also be observed by non-plant phosphorylases. Therefore, we included the rabbit muscle phosphorylase a. Both proteins share the same biochemical reaction that catalyses the reversible reaction of α 1-4 glucan and inorganic phosphate to glucose-1-phosphate and a glucan reduced in length by one glucosyl unit from the non-reducing end. We analyzed the direct protein-protein interaction and showed that AtSS4 and AtPHS1 interact, as reported by [14]. However, no interaction of AtSS4 and Pho a was observed (Fig.1, C) .As we know all phosphorylases consist of dimers or tetramers of identical subunits. Further, their kinetic and structural properties are also similar but, they differ in their regulation mechanisms which depend on the source of these enzymes [4]. Thus, the presence of specialized interaction between AtSS4 and AtPHS1 can be explained by the origin of these enzymes.

Furthermore, we analyzed if a functional interaction can be detected. Therefore, we incubated both phosphorylases with starch and glucose 1-phosphate (synthesizing reaction), and analyzed the formed product by CE-LIF in presence and absence of AtSS4. However, the significant elongation of short glucan chains in the presence of AtSS4 with AtPHS1 indicates a functional interaction between both proteins (Fig. 2, A). By contrast, no significant alterations were observed in the presence of AtSS4 with Pho a, thus a functional interaction can be excluded (Fig 2, B). However, missing of the functional interaction between AtSS4 and Pho a and the clear detection with AtPHS1 uncover a potential function for AtSS4 with AtPHS1 during starch synthesis. Several studies revealed that

starch phosphorylase has a certain effect during starch synthesis rather than during degradation in higher plants. While, it was shown that the increasing of starch phosphorylase activity coincides with starch accumulation in wheat, developing rice cereal endosperms, and [5, 6, 27].

Our study showed that Arabidopsis plastidial phosphorylase (AtPHS1) specifically interacts with AtSS4 that cannot be replaced by Pho a. However, so far it is unclear whether or not other plant derived phosphorylases can replace the Arabidopsis enzyme and if all animal phosphorylases don't show an interaction with the AtSS4. However, our data support the idea that during starch synthesis the plastidial phosphorylase and the starch synthase 4 interact.

REFERENCES

1. Ball, S.G., Morell, M.K. (2003). From bacterial glycogen to starch: Understanding the biogenesis of the plant starch granule. Annu Rev Plant Biol, 54: 207–233.
2. Fettke, J., Fernie, A. R., Steup, M. (2012). Transitory starch and its degradation in higher plant cells. In: Essential Reviews in Experimental Biol. Vol. 5: The Synthesis and Breakdown of Starch. I.J. Tetlow, ed. The Society for Experimental Biology, London, 309–372.
3. Ball, S., Colleoni, C., Cenci, U., Raj, J. N., Tirtiaux, C. (2011). The evolution of glycogen and starch metabolism in eukaryotes gives molecular clues to understand the establishment of plastid endosymbiosis. Journal of Experimental Botany, *62*, 1775-180
4. Dauville, D., Chochois, V., Steup, M., Haebel, S., Eckermann, N., Ritte, G., Ral, J. P., Colleoni, C., Hicks, G., Wattebled, F., Deschamps, P., d'Hulst, C., Liénard, L., Cournac, L., Putaux, J. L., Dupeyre, D., Ball, S.G. (2006). Plastidial phosphorylase is required for normal starch synthesis in Chlamydomonas reinhardtii. Plant J. 48: 274–285.
5. Schupp, N., Ziegler, P. (2004). The Relation of Starch Phosphorylases to Starch Metabolism in Wheat. Plant Cell Physiol, 45: 1471–1484.
6. Satoh, H., Shibahara, K., Tokunaga, T., Nishi, A., Tasaki, M., Hwang, S. K., Thomas, W., Nanae, O., Naoko, K., Mayumi, F., Yuko, Y., Aya Sato, H., Utsumi, Y., Ohdan, T., Nakamura, Y. (2008). Mutation of the Plastidial a-Glucan Phosphorylase Gene in Rice Affects the Synthesis and Structure of Starch in the Endosperm. The Plant Cell. 20: 1833–1849.
7. Cuesta-Seijo, J. A., Ruzanski, C., Krucewicz, K., Meier, S., Hägglund, P., Svensson, B., Palcic, M. M. (2017). Functional and structural characterization of plastidic starch phosphorylase during barley endosperm development. PLOS One 12, 1–25.
8. Seung, D., Thalmann, M., Sparla, F., Abou Hachem, M., Lee, S. K., Issakidis-Bourguet, E. Svensson, B., Zeeman, S. C., Santelia, D. (2013). arabidopsis thaliana AMY3 is a unique redox-regulated chloroplastic α- amylase. Journal of Chemistry, 288, 33620-33633.
9. Critchley, J. H., Zeeman, S. C., Takaha, T., Smith, A. M., Smith, S. M. (2001). A critical role for disproportionating enzyme in starch breakdown is revealed by a knock- out mutation in Arabidopsis. Plant Journal, 26, 89-100.
10. Kartal, Ö, Mahlow, S., Skupin, A., Ebenhöh, O. (2011). Carbohzdrateßactive enyzmes exemplifz entropic principles in metabolism. Molecular Szstms Biology 7, 542.
11. Brust, H., Orzechowski, S., Fettke, J., Steup, M. (2013). Starch synthesizing reaction and path: in vitro and in vivo studies. Journal of Applied Glycoscience, 60, 3-20.
12. D'Hulst, C., Mérida, Á. (2010). The priming of storage glucan synthesis from bacteria to plants: current knowledge and new developments. New Phytologist, 188, 13-21.
13. Roldán, I., Wattebled, F., Mercedes Lucas, M., Delvallé, D., Planchot,V., Jiménez, S., Pérez, R., Ball, S., D'Hulst, C., Mérida, A. (2007). The phenotype of soluble starch synthase IV defective mutants of arabidopsis thaliana suggests a novel function of elongation enzymes in the control of starch granule formation. Plant Journal, 49,492-504.
14. Malinova, I., Qasim, H. M., Brust, H., Fettke, J. (2018). Parameters of starch granule genesis in chloroplasts of Arabidopsis thaliana. Frontiers in Plant Science, 9, 1-7.
15. Malinova, I., Mahlow, S., Alseekh, S., Orawetz, T., Fernie, A. R., Baumann, O., Steup, M., Fettke, J. (2014). Double knock-out mutants of Arabidopsis thaliana grown under normal conditions reveal that the plastidial phosphorylase isozyme (PHS1) participates in transitory starch metabolism. Plant Physiol. 164, 907–921.
16. Brust, H., Lehmann, T., D'Hulst, C., Fettke, J. (2014). Analysis of the Functional Interaction of Arabidopsis Starch Synthase and Branching Enzyme Isoforms. Reveals that the Cooperative Action of SSI and BEs Results in Glucans with Polymodal Chain Length DistributionSimilartoAmylopectin.PLoSONE9(7):e 102364.
17. Malinova, I., Mahlow, S., Alseekh, S., Orawetz, T., Fernie, A. R., Baumann, O., Steup, M., Fettke, J. (2014). Double knock-out mutants of Arabidopsis thaliana grown under normal conditions reveal that the plastidial phosphorylase isozyme (PHS1) participates in transitory starch metabolism. Plant Physiol, 164, 907–921.
18. Seung, D., Lu, K-J., Stettler, M., Streb, S., Zeeman, S.C. (2016). Degradation of glucan primers in the absence of Starch Synthase 4 disrupts starch

granule initiation in Arabidopsis. Journal of Biological Chemistry, 291, 20718–20728.
19. Leterrier, M., Holappa, L. D., Broglie, K. E., Beckler, D. M. (2008). Cloning, characterisation and comparative analysis of a starch synthase IV gene in wheat: functional and evolutionary implications. BMC Plant Biol. 8, 98–119.
20. Rose,A., Manikantan,S., Schraegle,S., Maloy,M., S tahlberg,E., Meier,I. (2004). Genome- wide identification of Arabidopsis coiled- coil proteins and establishment of the ARABI- COIL database. Plant Physiol, 134, 927– 939.
21. Raynaud, S., Ragel, P., Rojas, T., Mérida, Á. (2016). The N-terminal part of Arabidopsis thaliana Starch Synthase 4 determines the localization and activity of the enzyme. Journal of Biological Chemistry, 291, 10759–10771.
22. Szydlowski, N., Rage, l. P., Raynaud, S., Mercedes, M. L., Roldán, I., Montero, M., Muñoz, F. J., Ovecka, M., Bahaji, A., Planchot, V., Pozueta-Romero, J., D'Hulst, C., Mérida, Á. (2009). Starch granule initiation in Arabidopsis requires the presence of either class IV or class III starch synthases. Plant Cell, 21, 2443– 2457.
23. Seung, D., Soyk, S., Coiro, M., Maier, B.A., Eicke, S., Zeeman, S.C. (2015). Protein targeting to starch is required for localising granule-bound starch synthase to starch granules and for normal amylose synthesis in Arabidopsis. PLOS Biology 13, e1002080.
24. Seung, D., Boude,t J., Monroe, J.D., Schreier, T.B., David, L. C., Abt, M, Lu, K-J., Zanella, M., Zeeman, S. C. (2017). Homologs of protein targeting to starch control starch granule initiation in Arabidopsis leaves. Plant Cell, 29, 1657–1677.
25. Gámez-Arjona, F. M., Raynaud, S., Ragel, P., Mérida, Á. (2014). Starch synthase 4 is located in the thylakoid membrane and interacts with plastoglobule-associated proteins in Arabidopsis. Plant Journal, *80*(2): 305–316.
26. Vandromme, C., Spriet, C., Dauvillee, D., Courseaux, A., Putaux, J.L., Wychowski, A., Krzewinski, F., Facon, M., D'Hulst, C., Wattebled, F. (2019). PII1: a protein involved in starch initiation that determines granule number and size in Arabidopsis chloroplast. New Phytologist 221:356–370.
27. Yu, Y., Mu, H. H., Mu-Forster, C., Wasserman, B. P., George, M. C. (2001). Identification of the maize amyloplast stromal 112-kD protein as a plastidic starch phosphorylase. *Plant Physiol.* 125: 351-359.